GENETIC AND EPIGENETIC INSIGHTS INTO THE DEVELOPMENTAL ORIGINS OF HEALTH AND DISEASE

EDITED BY: Tesfaye B. Mersha, Fasil Tekola-Ayele and Daniel Enquobahrie

PUBLISHED IN: Frontiers in Genetics

frontiers Research Topics

frontiers

ISSN 1664-8714
ISBN 978-2-88974-747-4
DOI 10.3389/978-2-88974-747-4

About Frontiers

Frontiers is more than just an open-access publisher of scholarly articles: it is a pioneering approach to the world of academia, radically improving the way scholarly research is managed. The grand vision of Frontiers is a world where all people have an equal opportunity to seek, share and generate knowledge. Frontiers provides immediate and permanent online open access to all its publications, but this alone is not enough to realize our grand goals.

Frontiers Journal Series

The Frontiers Journal Series is a multi-tier and interdisciplinary set of open-access, online journals, promising a paradigm shift from the current review, selection and dissemination processes in academic publishing. All Frontiers journals are driven by researchers for researchers; therefore, they constitute a service to the scholarly community. At the same time, the Frontiers Journal Series operates on a revolutionary invention, the tiered publishing system, initially addressing specific communities of scholars, and gradually climbing up to broader public understanding, thus serving the interests of the lay society, too.

Dedication to Quality

Each Frontiers article is a landmark of the highest quality, thanks to genuinely collaborative interactions between authors and review editors, who include some of the world's best academicians. Research must be certified by peers before entering a stream of knowledge that may eventually reach the public - and shape society; therefore, Frontiers only applies the most rigorous and unbiased reviews.
Frontiers revolutionizes research publishing by freely delivering the most outstanding research, evaluated with no bias from both the academic and social point of view. By applying the most advanced information technologies, Frontiers is catapulting scholarly publishing into a new generation.

What are Frontiers Research Topics?

Frontiers Research Topics are very popular trademarks of the Frontiers Journals Series: they are collections of at least ten articles, all centered on a particular subject. With their unique mix of varied contributions from Original Research to Review Articles, Frontiers Research Topics unify the most influential researchers, the latest key findings and historical advances in a hot research area! Find out more on how to host your own Frontiers Research Topic or contribute to one as an author by contacting the Frontiers Editorial Office: frontiersin.org/about/contact

GENETIC AND EPIGENETIC INSIGHTS INTO THE DEVELOPMENTAL ORIGINS OF HEALTH AND DISEASE

Topic Editors:
Tesfaye B. Mersha, Cincinnati Children's Hospital Medical Center, United States
Fasil Tekola-Ayele, National Institutes of Health (NIH), United States
Daniel Enquobahrie, University of Washington, United States

Citation: Mersha, T. B., Tekola-Ayele, F., Enquobahrie, D., eds. (2022). Genetic and Epigenetic Insights Into the Developmental Origins of Health and Disease. Lausanne: Frontiers Media SA. doi: 10.3389/978-2-88974-747-4

Table of Contents

frontiers in Genetics

EDITORIAL
published: 04 February 2022
doi: 10.3389/fgene.2021.814126

Editorial: Genetic and Epigenetic Insights Into the Developmental Origins of Health and Disease

Daniel A. Enquobahrie[1], *Fasil Tekola-Ayele*[2] *and Tesfaye B. Mersha*[3]*

[1]Department of Epidemiology, School of Public Health, University of Washington, Seattle, WA, United States, [2]Epidemiology Branch, Division of Population Health Research, Division of Intramural Research, Eunice Kennedy Shriver National Institute of Child Health and Human Development, National Institutes of Health, Bethesda, MD, United States, [3]Cincinnati Children's Hospital Medical Center, Department of Pediatrics, University of Cincinnati College of Medicine, Cincinnati, OH, United States

Keywords: genetics, epigenetics, environmental determinants, pre-natal, adulthood, childhood

Editorial on the Research Topic

Genetic and Epigenetic Insights Into the Developmental Origins of Health and Disease

The developmental origins of health and disease hypothesis posits that perturbations in the *in-utero* environment contribute to functional and metabolic programming as well as structural adaptations of fetal tissues predisposing the individual to chronic diseases during childhood and adulthood (Hales et al., 1991). Genetic and epigenetic studies document risk factors and molecular mechanisms that contribute to shared pathogenetic pathways between early life outcomes such as fetal growth and later-life chronic diseases. These studies have shown that shared genetic effects, non-genetic factors (such as social and environmental factors), as well as developmental programming can explain the relationships between early life and later life outcomes (Warrington et al., 2019; Tekola-Ayele et al., 2020a; Tekola-Ayele et al., 2020b; Juliusdottir et al., 2021).

Integrated genetic and epigenetic studies involving pregnant women, the placenta, and the offspring can lead to novel discoveries of molecular signals of early origins of childhood and adulthood diseases. The prevalence and disparity of complex diseases (across racial/ethnic groups) with early life origins has been increasing in the United States and around the world in recent decades. However, few studies integrate genetic, epigenetic, social, and environmental determinants of early life phenotypes to understand their links with diseases in later life. In this *Research Topic*, we gathered articles on genetic and epigenetic factors and their influences on pregnancy outcomes, and childhood and adult diseases.

Mancilla et al. reviewed the literature to examine health inequality within the context of social epigenomics. Sasaki et al. investigated the effect of sample handling on DNA methylation profiles. Candelo et al. investigated a possible association between Zika virus infection and cyclin-dependent kinase 5 regulatory subunit-associated protein 2 (CDK5RAP2) mutation. Le et al. investigated the mechanisms linking assisted reproductive technology (ART) to cholesterol metabolic and respiratory disorders later in life. Xu et al. investigated the use of maternal serum human leukocyte antigen-G (sHLA-G) to detect prenatal chromosomal abnormalities. Ferreira and Dantas Junior reported a case study of a neonate with Beare-Stevenson Syndrome whose father had Congenital Bilateral Absence of the Vas Deferens (CBAVD). Luo et al. presented a whole exome sequencing study of Joubert Syndrome (JBTS), a type of ciliopathies.

This topical collection presents original research, review articles, and case studies on a scope of exposures and health outcomes spanning the pre-natal period through adulthood. Future studies integrating a spectrum of genetic and epigenetic studies along with relevant exposures (including environmental exposures and lifestyle) have a potential to inform mechanisms that

OPEN ACCESS

Edited and reviewed by:
Michael E. Symonds, University of Nottingham, United Kingdom

***Correspondence:**
Tesfaye B. Mersha
tesfaye.Mersha@cchmc.org

Received: *12 November 2021*
Accepted: *29 November 2021*
Published: *04 February 2022*

Citation:
Enquobahrie DA, Tekola-Ayele F and Mersha TB (2022) Editorial: Genetic and Epigenetic Insights Into the Developmental Origins of Health and Disease. Front. Genet. 12:814126. doi: 10.3389/fgene.2021.814126

underlie the associations between maternal phenotypes, birth outcomes, and offspring adult diseases.

AUTHOR CONTRIBUTIONS

TM, DE, and FT-A contributed equally to this editorial.

FUNDING

This work was supported by the National Institutes of Health (NHLBI (R01 HL132344) and NHGRI (R01 HG011411)) grants support. It was also supported by the Intramural Research Program of the *Eunice Kennedy Shriver* National Institute of Child Health and Human Development, National Institutes of Health.

REFERENCES

Hales, C. N., Barker, D. J., Clark, P. M., Cox, L. J., Fall, C., Osmond, C., et al. (1991). Fetal and Infant Growth and Impaired Glucose Tolerance at Age 64. *BMJ* 303 (6809), 1019–1022. doi:10.1136/bmj.303.6809.1019

Juliusdottir, T., Steinthorsdottir, V., Stefansdottir, L., Sveinbjornsson, G., Ivarsdottir, E. V., Thorolfsdottir, R. B., et al. (2021). Distinction between the Effects of Parental and Fetal Genomes on Fetal Growth. *Nat. Genet.* 53 (8), 1135–1142. doi:10.1038/s41588-021-00896-x

Tekola-Ayele, F., Zeng, X., Ouidir, M., Workalemahu, T., Zhang, C., Delahaye, F., et al. (2020). DNA Methylation Loci in Placenta Associated with Birthweight and Expression of Genes Relevant for Early Development and Adult Diseases. *Clin. Epigenet* 12 (1), 78. doi:10.1186/s13148-020-00873-x

Tekola-Ayele, F., Zhang, C., Wu, J., Grantz, K. L., Rahman, M. L., Shrestha, D., et al. (2020). Trans-ethnic Meta-Analysis of Genome-wide Association Studies Identifies Maternal ITPR1 as a Novel Locus Influencing Fetal Growth during Sensitive Periods in Pregnancy. *Plos Genet.* 16 (5), e1008747. doi:10.1371/journal.pgen.1008747

Warrington, N. M., Beaumont, R. N., Horikoshi, M., Day, F. R., Helgeland, Ø., Laurin, C., et al. (2019). Maternal and Fetal Genetic Effects on Birth Weight and Their Relevance to Cardio-Metabolic Risk Factors. *Nat. Genet.* 51 (5), 804–814. doi:10.1038/s41588-019-0403-1

Conflict of Interest: The authors declare that the research was conducted in the absence of any commercial or financial relationships that could be construed as a potential conflict of interest.

Publisher's Note: All claims expressed in this article are solely those of the authors and do not necessarily represent those of their affiliated organizations, or those of the publisher, the editors and the reviewers. Any product that may be evaluated in this article, or claim that may be made by its manufacturer, is not guaranteed or endorsed by the publisher.

frontiers in Genetics

CASE REPORT
published: 25 February 2020
doi: 10.3389/fgene.2020.00104

Report of a Father With Congenital Bilateral Absence of the Vas Deferens Fathering a Child With Beare–Stevenson Syndrome

Leonardo C. Ferreira[1,2*] *and José H. Dantas Junior*[3]

[1] *Department of Biochemistry, Federal University of Rio Grande do Norte, Natal, Brazil,* [2] *Institute of Tropical Medicine of Rio Grande do Norte, Federal University of Rio Grande do Norte, Natal, Brazil,* [3] *University Hospital Onofre Lopes, Urologic Unit, Federal University of Rio Grande do Norte, Natal, Brazil*

Background: Apert, Pfeiffer, and Crouzon syndromes are autosomal dominant diseases characterized by craniosynostosis. They are paternal age effect disorders. The association between paternal age and Beare–Stevenson syndrome (BSS), a very rare and severe craniosynostosis, is uncertain. Gain-of-function mutations in *FGFR2* become progressively enriched in testes as men age and were shown to cause these syndromes.

Case report: Here, we describe a child affected with BSS, whose father was 36 years old and had congenital bilateral absence of the vas deferens (CBAVD). The child was heterozygous for the pathogenic *FGFR2* variant c.1124A > G p.Tyr375Cys. By reviewing the literature, we found that BSS fathers are older than BSS mothers (mean age in years: 39 ± 10 vs 30 ± 6, p = 0.006). Male age greater than 34 years and CBAVD are both factors associated with poor spermogram parameters, which may represent an additional selective pressure to sperm carrying *FGFR2* gain-of-function mutations.

Conclusion: These findings are consistent with the hypothesis that BSS is a paternal-origin genetic disorder. Further experimental studies would be needed to confirm this hypothesis.

Keywords: Beare–Stevenson, craniosynostosis, paternal age, CBAVD, FGFR2

OPEN ACCESS

Edited by:
Fasil Tekola Ayele, National Institutes of Health (NIH), United States

Reviewed by:
Andrew O. M. Wilkie, University of Oxford, United Kingdom
Muhammad Jawad Hassan, National University of Medical Sciences (NUMS), Pakistan

****Correspondence:***
Leonardo C. Ferreira
ferreiralc@cb.ufrn.br

Specialty section:
This article was submitted to Genetic Disorders, a section of the journal Frontiers in Genetics

Received: *18 October 2019*
Accepted: *29 January 2020*
Published: *25 February 2020*

Citation:
Ferreira LC and Dantas Junior JH (2020) Report of a Father With Congenital Bilateral Absence of the Vas Deferens Fathering a Child With Beare–Stevenson Syndrome. Front. Genet. 11:104. doi: 10.3389/fgene.2020.00104

BACKGROUND

Beare–Stevenson Syndrome (OMIM 123790) is a type of craniosynostosis characterized by premature fusion of the cranial sutures associated with *cutis gyrata* (corrugation of skin) as pathognomonic signs. In addition to skin and bone abnormalities, ocular proptosis, choanal atresia, and prominent umbilical stump are frequently found in children affected by this syndrome (Beare et al., 1969; Stevenson et al., 1978). Among the 21 BSS cases reviewed by Wenger et al., 11 died within the first year of life, and at least half of the deaths were due to cardiorespiratory arrest or unexpected sudden death (Wenger et al., 2015).

Mutations in genes encoding fibroblast growth factor receptors (*FGFR*) were shown to cause several craniosynostosis syndromes: Crouzon (*FGFR2*) and Pfeiffer (*FGFR1* and *FGFR2*), Apert

(*FGFR2*), Muenke (*FGFR3*), and Jackson–Weiss (*FGFR2*). So far, the genetic causes of BSS are known to be *FGFR2* p.Ser372Tyr and p.Tyr375Cys mutations (Ron et al., 2016), except for a unique BSS case associated with a 63 bp deletion in *FGFR2* exon 8 (Slavotinek et al., 2009). These are autosomal dominant syndromes caused by *de novo* mutations in germ cells in an unaffected parent. It has been estimated that about 80% of *de novo* germline point mutations arise in the male gametes, and a positive correlation exists between mutation rate and paternal age (Acuna-Hidalgo et al., 2016). There are apparently two mechanisms contributing to the paternal age effect (PAE): 1) Increase in DNA copy-error rate as paternal age increases, and 2) Positive selection during spermatogenesis conferred by gain-of-function mutations (Veltman and Brunner, 2012). Nine autosomal-dominant disorders, including Crouzon, Pfeiffer, Apert, and Muenke, have been experimentally shown to be caused by PAE mutations in *FGFR2, FGFR3, HRAS*, *PTPN11*, and *RET*. All five genes act in the RTK-RAS signaling pathway, which is involved with the clonal expansion of spermatogonial stem cells (Goriely et al., 2003; Goriely and Wilkie, 2012).

Paternal age greater than 50 years is associated with 6-, 8-, and 9.5-fold increases in relative risk for Pfeiffer, Crouzon, and Apert syndromes, respectively (Herati et al., 2017). In 1992, Hall et al. described a sixth BSS case and noted a mean paternal age of 36 years (compared to 28 years for the mothers) (Hall et al., 1992). McGaughran et al. reported a BSS case from a 62 year old father, which raised the hypothesis of advanced paternal age as a causal factor of the syndrome (McGaughran et al., 2006). Despite strong biological plausibility, BSS has not been systematically described in the literature as a genetic disease of paternal origin.

Structural abnormalities in the male reproductive tract are a common cause of reduced fertility (Singh et al., 2012). Congenital absence of the vas deferens, which can be unilateral (CUAVD) or bilateral (CBAVD), accounts for 1 to 2% of all male infertility (de Kretser, 1997). Almost 80% of CBAVD cases are associated with a detectable *CFTR* mutation. Among *CFTR* positive individuals, 46% have two mutations, and only 28% have a single mutation (Yu et al., 2012). Besides the CBAVD obstructive azoospermia effect, there is evidence for impaired spermatogenesis in individuals with CBAVD (Meng et al., 2001; Llabador et al., 2015).

This is the first report of a person with Beare–Stevenson Syndrome whose father had CBAVD. Here, we argue that sperm carrying gain-of-function variants in *FGFR2* may be under stronger positive selection during spermatogenesis due to the combined effect of CBAVD and advanced paternal age.

CASE PRESENTATION

Parents' Characteristics

The non-consanguineous parents were both 37 years old at the time of the child's birth (July, 2017). Their family histories showed no genetic diseases, and they were Brazilians. After 12 months of unsuccessfully attempting to conceive, the couple underwent medical evaluation for infertility in 2015. The mother was diagnosed with thrombophilia at that time. Serology tests for HIV, HBV, HCV, syphilis, toxoplasma, rubella IgM, and cytomegalovirus IgM were negative. Rubella and cytomegalovirus IgG were positive.

The father had colorblindness of unknown cause and a history of gastroplasty at age 31 followed by weight loss of approximately 40 kg. Physical examination revealed bilateral absence of vas deferens and absence of the left epididymis. The laboratory analysis detected azoospermia with ejaculated volumes between 1.5 and 2.0 ml; the results confirmed by spermograms performed in different laboratories. Sperm were not identified in any exam even after centrifugation. Scrotal ultrasonography detected absence of the right epididymis and absence of the left epididymis head and body. However, the testes were normal, and there was no evidence of varicocele. Cytogenetics and molecular investigation were performed to identify the cause for the male anatomical defect. G-band karyotyping showed a normal 46, XY chromosomal pattern. Since genetic variants in *CFTR* are the main cause of CBAVD, both mother and father were screened for *CFTR* pathogenic variants to estimate the risk of cystic fibrosis in offspring. Sanger sequencing of the coding region (including exon-intron boundaries) was performed, and deletions/duplications were assessed using multiplex ligation-dependent probe amplification (MRC-Holland SALSA MLPA probemix P091-D1). The parents were negative for pathogenic variants, although intronic variants, including the 5T allele in intron 8, were not investigated. Therefore, *CFTR* could not be ruled out as the cause of CBAVD.

Assisted Reproductive Technology

The couple underwent two cycles of *in vitro* fertilization (IVF) *via* the intra-cytoplasmic sperm injection (ICSI) method. In the first cycle (December, 2015), sperm were obtained *via* percutaneous epididymal sperm aspiration (PESA) under general anesthesia. The right epididymis was palpable during the procedure, which was inconsistent with the ultrasound result. The PESA was successful on the first puncture, yielding a high number of mobile sperm that were sufficient to proceed to fertilization. The mother had 14 mature eggs that were fertilized, producing four embryos that were frozen on d3 stage to avoid the risk of ovarian hyperstimulation syndrome. The embryos were transferred five months after IVF-ICSI in May (two embryos) and June (the other two embryos), but pregnancy did not occur. The second cycle was started in July 2016. Likewise, sperm were collected from the right epididymis under general anesthesia *via* PESA using two punctures, yielding a large amount of mobile sperm that were used for fertilization. At that time, eight ova were obtained from both ovaries. Six mature ova were fertilized, and three fresh embryos were transferred after three days at the d3 stage. The pregnancy test was positive after 15 days.

Clinical Findings

Here, we describe a male newborn child with molecular confirmed diagnosis of Beare–Stevenson Syndrome. Several anomalies were detected during prenatal care screening even before birth. Ultrasound examination detected absence of nasal

bone at 12 weeks of gestation and brachycephaly at 24 weeks. Both findings were further confirmed by fetal magnetic resonance images. Ultrasound at 27 weeks detected exophthalmia, flat forehead, small femurs, and discrete dilation of the kidneys and cerebral ventricles. A non-invasive prenatal maternal blood test was performed, which was negative for aneuploidies in chromosomes 13,18, 21, X, and Y.

The mother delivered a male newborn weighing 2,775 g and measuring 47 cm of height at 34.7 weeks gestation *via* Cesarean section. The child presented classical BSS clinical findings: clover-leaf cranial shape, midface hypoplasia, ocular hypertelorism and proptosis, choanal atresia, prominent umbilical stump, hypospadias, short toes, cutis gyrata, and natal tooth. Some of the craniofacial alterations were visualized using computed tomography (CT) at 5 days of life (**Figure 1**).

The newborn was intubated shortly after birth for apnea, and a tracheostomy was performed. He underwent a ventriculo-peritoneal shunt and blepharorraphy to relieve the hydrocephalus and ocular proptosis, respectively. In the 49th day he had a cardiorespiratory arrest due to obstruction of the tracheostomy. He survived, but he had several subsequent seizures. At 60 days of age he had another cardiorespiratory arrest and died.

At 21 days of life, a buccal swab DNA sample was tested for a panel of craniosynostosis-related genes, including *FGFR3*, *FGFR2*, *FGFR1*, and *TWIST1*. Molecular analysis by next generation sequencing (Nextera Exome Capture, Illumina HiSeq) confirmed that the infant was heterozygous for the pathogenic *FGFR2* variant NM_000141.4: c.1124A > G p.Tyr375Cys (rs121913478).

DISCUSSION

We present the first report of a BSS child whose father has CBAVD. This unique and unlikely finding, in addition to what is known about craniosynostosis genetics and *FGFR2*'s role in spermatogenesis, could be consistent with BSS as a paternal-origin genetic disorder. The main limitations of this report are that the parental origin of the *FGFR2* mutation could not be molecularly determined, and its level in the obtained semen samples was not quantified. To the best of our knowledge, this is the 30th BSS case reported worldwide, and the fourth from Brazil.

We concluded that BSS fathers are significantly older than BSS mothers (mean age 39.1 vs 30.4, $p = 0.006$) by analyzing the parental ages of BSS cases available in the literature (**Table 1**). However, it is important to acknowledge that differences between paternal vs maternal ages are common across populations and may be biased by the parent's year of birth. Interestingly, the

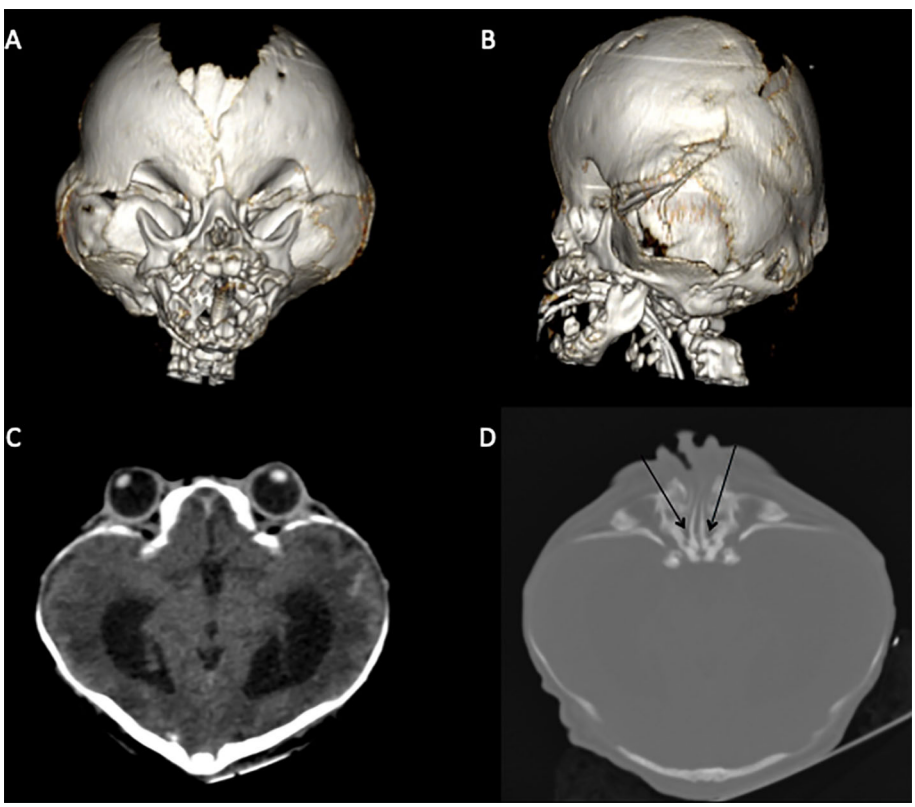

FIGURE 1 | CT scan highlighting classical BSS morphological characteristics. **(A**, **B)** brachycephaly due to premature fusion of coronal and lambdoid sutures, orbital deformity, and midface hypoplasia. **(C)** Hyperteleorbitism and clover-leaf cranial shape. **(D)** Choanal atresia (black arrows).

TABLE 1 | Parental ages in years (y) from published BSS cases.

Case	Reference	Country	Paternal age (y)	Maternal age (y)
1	(Beare et al., 1969)	North Ireland	40	38
2	(Stevenson et al., 1978)	US	NA	28
3	(Hall et al., 1992)	US	43	33
4	(Hall et al., 1992)	US[1]	30	28
5	(Hall et al., 1992)	US[1]	NA	21
6	(Hall et al., 1992)	US[1]	32	22
7	(Andrews et al., 1993)	Brazil	NA	23
8	(Bratanic et al., 1994)	Slovenia	43	39
9	(Ito et al., 1996)	Japan	NA	25
10	(Przylepa et al., 1996)	US[1]	NA	NA
11	(Krepelová et al., 1998)	Czech	24	24
12	(Wang et al., 2002)	Taiwan	34	31
13	(Akai et al., 2002)	Japan	NA	NA
14	(Izakovic et al., 2003)	US	NA	34
15	(Vargas et al., 2003)	Chile	36	28
16	(Vargas et al., 2003)	Brazil	30	32
17	(Upmeyer et al., 2005)	US	NA	NA
18	(Erol and Eser, 2006)	Turkey	NA	NA
19	(McGaughran et al., 2006)	Australia	62	28
20	(Eun et al., 2007)	Korea	50	32
21	(Fonseca et al., 2008)	Brazil	30	23
22	(Slavotinek et al., 2009)	US	48	40
23	(Tao et al., 2010)	US	48	39
24	(Barge-Schaapveld et al., 2011)	Netherlands	NA	NA
25	(Barge-Schaapveld et al., 2011)	Netherlands	NA	NA
26	(Stater et al., 2015)	US	NA	NA
27	(Wenger et al., 2015)	US	NA	36
28	(Wenger et al., 2015)	US	NA	22
29	(Ron et al., 2016)	US[1]	NA	36
30	(Ferreira et al., 2020)	Brazil	37	37
	Missing age information (%)		**14/30 (46.7)**	**6/30 (20.0)**
	Mean age (standard deviation)		**39.1 (10)**	**30.4 (6.3)**

P-value = 0.05 for comparison of missing age information rate Paternal vs Maternal (chi-squared test). P-value = 0.006 for comparison of means Paternal vs Maternal (t-test). NA, parental age not available at the original publication.

[1]It refers to corresponding author's location. It was not mentioned the location where the case was born.

magnitude of difference between paternal and maternal mean ages is about 5 years for Apert syndrome, with almost 50% of fathers being older than 35 years (Tolarova et al., 1997). It is also noteworthy from **Table 1** that paternal age is more frequently omitted (46.7%) than maternal age (20%), which is consistent with the historical bias of placing greater importance on maternal age when considering rare genetic diseases. We hypothesize a paternal age effect for BSS since Pfeiffer, Crouzon, Apert, and Beare–Stevenson syndromes are all craniosynostoses caused by mutations in *FGFR* genes.

Unlike oogenesis, spermatogenesis is a continuous process occurring from male puberty throughout life. There is an evident negative impact of advanced paternal age on sperm parameters. Based on semen analysis of 4,822 men, Stone et al. verified that daily sperm production significantly declines after 34 years of age (Stone et al., 2013). Hypospermatogenesis was histopathologically detected in 33/54 (61.1%) males with CBAVD that had been subjected to testicular sperm extraction (Llabador et al., 2015). By analyzing 85 CBAVD patients who had undergone PESA-ICSL, Elhanbly et al. demonstrated that paternal age was negatively correlated with sperm count, motility, vitality, and normal sperm morphology. They estimated a reduction in the number of retrieved-sperm of 0.53 million per 10 years (Elhanbly et al., 2015). In addition to age and CBAVD, a variety of metabolic (*e.g.* obesity and diabetes) and environmental (*e.g.* cadmium and dioxins) factors affect spermatogenesis (Neto et al., 2016).

The transcriptional dynamics of spermatogenesis are consistent with a five-stage process (Stage 0–Stage 4) involving cell types from five niches (Leydig, myoid, Sertoli, endothelial, and macrophage) (Guo et al., 2018). In this context, *FGFR3* and *FGFR2* were described as early spermatogonial markers (Guo et al., 2017; Guo et al., 2018). Gain-of-function mutations in *FGFR2* offer a selective advantage for spermatogonial cells by favoring clonal expansion in the testes, yielding enrichment in mutated sperm by at least 100-fold (Goriely et al., 2009). Thus, Goriely et al. coined the term "selfish spermatogonial selection" to describe the increase in the number of mutant sperm over time (*i.e.* male aging) caused by the mutation-driven clonal expansion process (Maher et al., 2018). Of note, Maher et al. (2018) identified a mutational clone in human testes for the *FGFR2* Ser372Cys, one of the mutations known to cause BSS. In situations like advanced paternal age and CBAVD, which are both characterized by poor spermogram parameters, the before-mentioned clonal expansion process would lead to a relative increase in the number of mutated sperm, compared to situations consistent with normal spermatogenesis. Therefore, we hypothesize that spermatogenesis in a 36 years old man with CBAVD is under additional selective pressure, making the *FGFR2* p.Tyr375Cys mutation even more advantageous to sperm.

FGFR2 is a pleiotropic gene widely expressed throughout the human body. The highest expression is found in the spinal cord, colon, uterus, and skin (data from GTExPortal, https://gtexportal.org/home/gene/FGFR2). Despite its ubiquitous presence in human tissues, *FGFR2* expression is crucial for proper lung-branching morphogenesis (Arman et al., 1999). Normal tracheal homeostasis depends on a suitable FGFR2 signaling pathway to promote asymmetric self-renewing division generating one basal cell and one luminal cell per basal cell division (Balasooriya et al., 2017). Tracheal cartilaginous sleeve (TCS), a rare life-threatening condition, has been found in some individuals affected by mutations in *FGFR* genes (Pickrell et al., 2017; Wenger et al., 2017). Notably, Wenger et al. identified TCS in 100% of *FGFR2* p.Try290Cys mutated children (Wenger et al., 2017), in addition to a previous report of TCS in a BSS case (Wenger et al., 2015). Seventy-five percent of TCS cases require tracheostomy, a procedure that is imperative to minimize the risk of sudden death in BSS-affected individuals. Therefore, medical staff should investigate TCS in BSS patients, and they must be prepared to surgically manage TCS (Stater et al., 2015).

Very recently, Zhang et al. developed a non-invasive prenatal sequencing test based on the unique molecular indexing method to diagnose dominant monogenic disorders. This test

successfully identified cases of *FGFR2*-related craniosynostosis, including Apert (*FGFR2*: c.758C > G), Pfeiffer (*FGFR2*: c.870G > T), and Crouzon (*FGFR2*: c.1032G > A) syndromes, and it accurately distinguished those cases from other *FGFR3*-related skeletal disorders (*e.g.* thanatophoric dysplasia and achondroplasia) (Zhang et al., 2019). This diagnostic approach would be useful in situations like the one presented in this case report. The molecular confirmation of BSS at the prenatal stage would allow both medical staff and family to cope with this life-threatening syndrome. Finally, two pharmacological approaches targeting different points of the FGF signaling pathway have been successfully used in *ex vivo* organ culture (Balek et al., 2017) and in BSS mice harboring the human-analog *FGFR2* p.Tyr375Cys mutation (Wang et al., 2012). We envision that prenatal molecular diagnosis may be an essential step toward the early application of therapeutic tools, aiming to ameliorate BSS symptoms and to extend life expectancy in these cases.

DATA AVAILABILITY STATEMENT

The DNA sequencing service was ordered by the study participants and performed by Mendelics, a private company. Therefore, we had no access to raw data.

ETHICS STATEMENT

This study involves three participants (i.e. father, mother and child). The parents provided written informed consent allowing their child to be included in this case report publication. In addition, as the parents are participants themselves, both the father and mother gave written informed consent to be included as study participants. The protocol was reviewed and approved by the Ethical Committee from Federal University of Rio Grande do Norte (ethical approval: 3.613.457).

AUTHOR CONTRIBUTIONS

LF conceptualized the case report into a scientific question, reviewed the literature, and drafted the manuscript. JD conducted clinical and surgical procedures in the male patient (i.e. father), critically reviewed the manuscript, and added important intellectual contributions.

FUNDING

This study was financed in part by the Coordenação de Aperfeiçoamento de Pessoal de Nível Superior - Brasil (CAPES) - Finance Code 001.

ACKNOWLEDGMENTS

The authors would like to thank the parents for sharing their family's medical record as a genuine wish to provide useful information for others with Beare–Stevenson Syndrome. We also acknowledge Mychelle M.G. Torres for her help with the description of maternal clinical characteristics and Manuel Moreira Neto for analyzing CT scan images and describing structural alterations. Finally, we would like to thank Selma M.B. Jeronimo, MD (Federal University of Rio Grande do Norte) and Richard D. Pearson, MD (University of Virginia) for kindly reviewing the manuscript.

REFERENCES

Acuna-Hidalgo, R., Veltman, J. A., and Hoischen, A. (2016). New insights into the generation and role of *de novo* mutations in health and disease. *Genome Biol.* 17, 241. doi: 10.1186/s13059-016-1110-1

Akai, T., Iizuka, H., Kishibe, M., Kawakami, S., Kobayashi, A., and Ozawa, T. (2002). A case of Beare-Stevenson cutis gyrata syndrome confirmed by mutation analysis of the fibroblast growth factor receptor 2 gene. *Pediatr. Neurosurg.* 37, 97–99. doi: 10.1159/000065112

Andrews, J. M., Martins, D. M. F. S., Ramos, R. R., and Ferreira, L. M. (1993). A severe case of Beare-Stevenson syndrome and associated congenital deformities. *Br. J. Plast. Surg.* 46, 443–446. doi: 10.1016/0007-1226(93)90053-E

Arman, E., Haffner-Krausz, R., Gorivodsky, M., and Lonai, P. (1999). Fgfr2 is required for limb outgrowth and lung-branching morphogenesis. *PNAS* 96, 11895–11899. doi: 10.1073/pnas.96.21.11895

Balasooriya, G. I., Goschorska, M., Piddini, E., and Rawlins, E. L. (2017). FGFR2 is required for airway basal cell self-renewal and terminal differentiation. *Development* 144, 1600–1606. doi: 10.1242/dev.135681

Balek, L., Gudernova, I., Vesela, I., Hampl, M., Oralova, V., Kunova Bosakova, M., et al. (2017). ARQ 087 inhibits FGFR signaling and rescues aberrant cell proliferation and differentiation in experimental models of craniosynostoses and chondrodysplasias caused by activating mutations in FGFR1, FGFR2 and FGFR3. *Bone* 105, 57–66. doi: 10.1016/j.bone.2017.08.016

Barge-Schaapveld, D. Q. C. M., Brooks, A. S., Lequin, M. H., van Spaendonk, R., Vermeulen, R. J., and Cobben, J. M. (2011). Beare-Stevenson syndrome: two Dutch patients with cerebral abnormalities. *Pediatr. Neurol.* 44, 303–307. doi: 10.1016/j.pediatrneurol.2010.11.015

Beare, J. M., Dodge, J. A., and Nevin, N. C. (1969). Cutis gyratum, acanthosis nigricans and other congenital anomalies. A new syndrome. *Br. J. Dermatol.* 81, 241–247. doi: 10.1111/j.1365-2133.1969.tb13975.x

Bratanic, B., Praprotnik, M., and Novosel-Sever, M. (1994). Congenital craniofacial dysostosis and cutis gyratum: the Beare-Stevenson syndrome. *Eur. J. Pediatr.* 153, 184–186. doi: 10.1007/s004310050118

de Kretser, D. M. (1997). Male infertility. *Lancet* 349, 787–790. doi: 10.1016/S0140-6736(96)08341-9

Elhanbly, S., El-Saied, M. A., Fawzy, M., El-Refaeey, A., and Mostafa, T. (2015). Relationship of paternal age with outcome of percutaneous epididymal sperm aspiration–intracytoplasmic sperm injection, in cases of congenital bilateral absence of the vas deferens. *Fertil Steril* 104, 602–606. doi: 10.1016/j.fertnstert.2015.06.020

Erol, D. D., and Eser, O. (2006). The expected difficult intubation of a patient with Beare-Stevenson syndrome. *Paediatr. Anaesth* 16, 801. doi: 10.1111/j.1460-9592.2006.01880.x

Eun, S.-H., Ha, K. S., Je, B.-K., Lee, E. S., Choi, B. M., Lee, J. H., et al. (2007). The first Korean case of Beare-Stevenson syndrome with a Tyr375Cys mutation in the fibroblast growth factor receptor 2 gene. *J. Korean Med. Sci.* 22, 352–356. doi: 10.3346/jkms.2007.22.2.352

Fonseca, R. F., Costa-Lima, M. A., Pereira, E. T., Castilla, E. E., and Orioli, I. M. (2008). Beare-Stevenson cutis gyrata syndrome: a new case of a c.1124C↷G

(Y375C) mutation in the FGFR2 gene. *Mol. Med. Rep.* 1, 753–755. doi: 10.3892/mmr_00000024

Goriely, A., and Wilkie, A. O. M. (2012). Paternal age effect mutations and selfish spermatogonial selection: causes and consequences for human disease. *Am. J. Hum. Genet.* 90, 175–200. doi: 10.1016/j.ajhg.2011.12.017

Goriely, A., McVean, G. A. T., Röjmyr, M., Ingemarsson, B., and Wilkie, A. O. M. (2003). Evidence for selective advantage of pathogenic FGFR2 mutations in the male germ line. *Science* 301, 643–646. doi: 10.1126/science.1085710

Goriely, A., Hansen, R. M. S., Taylor, I. B., Olesen, I. A., Jacobsen, G. K., McGowan, S. J., et al. (2009). Activating mutations in FGFR3 and HRAS reveal a shared genetic origin for congenital disorders and testicular tumors. *Nat. Genet.* 41, 1247–1252. doi: 10.1038/ng.470

Guo, J., Grow, E. J., Yi, C., Mlcochova, H., Maher, G. J., Lindskog, C., et al. (2017). Chromatin and single-cell RNA-seq profiling Reveal Dynamic Signaling and Metabolic Transitions during Human Spermatogonial Stem Cell Development. *Cell Stem Cell* 21, 533–546.e6. doi: 10.1016/j.stem.2017.09.003

Guo, J., Grow, E. J., Mlcochova, H., Maher, G. J., Lindskog, C., Nie, X., et al. (2018). The adult human testis transcriptional cell atlas. *Cell Res.* 28, 1141–1157. doi: 10.1038/s41422-018-0099-2

Hall, B. D., Cadle, R. G., Golabi, M., Morris, C. A., and Cohen, M. M. (1992). Beare-Stevenson cutis gyrata syndrome. *Am. J. Med. Genet.* 44, 82–89. doi: 10.1002/ajmg.1320440120

Herati, A. S., Zhelyazkova, B. H., Butler, P. R., and Lamb, D. J. (2017). Age-related alterations in the genetics and genomics of the male germ line. *Fertil Steril* 107, 319–323. doi: 10.1016/j.fertnstert.2016.12.021

Ito, S., Matsui, K., Ohsaki, E., Goto, A., Takagi, K., Koresawa, M., et al. (1996). A cloverleaf skull syndrome probably of Beare-Stevenson type associated with Chiari malformation. *Brain Dev.* 18, 307–311. doi: 10.1016/0387-7604(96)00020-4

Izakovic, J., Leitner, S., and Schachner, L. A. (2003). What syndrome is this? Beare-Stevenson cutis gyrata syndrome. *Pediatr. Dermatol.* 20, 358–360. doi: 10.1046/j.1525-1470.2003.20419.x

Krepelová, A., Baxová, A., Calda, P., Plavka, R., and Kapras, J. (1998). FGFR2 gene mutation (Tyr375Cys) in a new case of Beare-Stevenson syndrome. *Am. J. Med. Genet.* 76, 362–364. doi: 10.1002/(SICI)1096-8628(19980401)76:4<362::AID-AJMG15>3.0.CO;2-M

Llabador, M. A., Pagin, A., Lefebvre-Maunoury, C., Marcelli, F., Leroy-Martin, B., Rigot, J. M., et al. (2015). Congenital bilateral absence of the vas deferens: the impact of spermatogenesis quality on intracytoplasmic sperm injection outcomes in 108 men. *Andrology* 3, 473–480. doi: 10.1111/andr.12019

Maher, G. J., Ralph, H. K., Ding, Z., Koelling, N., Mlcochova, H., Giannoulatou, E., et al. (2018). Selfish mutations dysregulating RAS-MAPK signaling are pervasive in aged human testes. *Genome Res.* 28, 1779–1790. doi: 10.1101/gr.239186.118

McGaughran, J., Sinnott, S., Susman, R., Buckley, M. F., Elakis, G., Cox, T., et al. (2006). A case of Beare???Stevenson syndrome with a broad spectrum of features and a review of the FGFR2 Y375C mutation phenotype. *Clin. Dysmorphol* 15, 89–93. doi: 10.1097/01.mcd.0000194407.92676.9d

Meng, M. V., Black, L. D., Cha, I., Ljung, B.-M., Pera, R. A. R., and Turek, P. J. (2001). Impaired spermatogenesis in men with congenital absence of the vas deferens. *Hum. Reprod.* 16, 529–533. doi: 10.1093/humrep/16.3.529

Neto, F. T. L., Bach, P. V., Najari, B. B., Li, P. S., and Goldstein, M. (2016). Spermatogenesis in humans and its affecting factors. *Semin. In Cell Dev. Biol.* 59, 10–26. doi: 10.1016/j.semcdb.2016.04.009

Pickrell, B. B., Meaike, J. D., Cañadas, K. T., Chandy, B. M., and Buchanan, E. P. (2017). Tracheal cartilaginous sleeve in syndromic craniosynostosis: an underrecognized source of significant morbidity and mortality. *J. Craniofac Surg.* 28, 696–699. doi: 10.1097/SCS.0000000000003489

Przylepa, K. A., Paznekas, W., Zhang, M., Golabi, M., Bias, W., Bamshad, M. J., et al. (1996). Fibroblast growth factor receptor 2 mutations in Beare-Stevenson cutis gyrata syndrome. *Nat. Genet.* 13, 492–494. doi: 10.1038/ng0896-492

Ron, N., Leung, S., Carney, E., Gerber, A., and David, K. L. (2016). A case of Beare-Stevenson syndrome with unusual manifestations. *Am. J. Case Rep.* 17, 254–258. doi: 10.12659/AJCR.897177

Singh, R., Hamada, A. J., Bukavina, L., and Agarwal, A. (2012). Physical deformities relevant to male infertility. *Nat. Rev. Urol* 9, 156–174. doi: 10.1038/nrurol.2012.11

Slavotinek, A., Crawford, H., Golabi, M., Tao, C., Perry, H., Oberoi, S., et al. (2009). Novel *FGFR2* deletion in a patient with Beare-Stevenson-like syndrome. *Am. J. Med. Genet.* 149A, 1814–1817. doi: 10.1002/ajmg.a.32947

Stater, B. J., Oomen, K. P. Q., and Modi, V. K. (2015). Tracheal cartilaginous sleeve association with syndromic midface hypoplasia. *JAMA Otolaryngol Head Neck Surg.* 141, 73–77. doi: 10.1001/jamaoto.2014.2790

Stevenson, R. E., Ferlauto, G. J., and Taylor, H. A. (1978). Cutis gyratum and acanthosis nigricans associated with other anomalies: a distinctive syndrome. *J. Pediatr.* 92, 950–952. doi: 10.1016/S0022-3476(78)80371-0

Stone, B. A., Alex, A., Werlin, L. B., and Marrs, R. P. (2013). Age thresholds for changes in semen parameters in men. *Fertil. Steril.* 100, 952–958. doi: 10.1016/j.fertnstert.2013.05.046

Tao, Y.-C., Slavotinek, A. M., Vargervik, K., and Oberoi, S. (2010). Hypodontia in Beare-Stevenson syndrome: an example of dental anomalies in FGFR-related craniosynostosis syndromes. *Cleft Palate Craniofac. J.* 47, 253–258. doi: 10.1597/08-282.1

Tolarova, M. M., Harris, J. A., Ordway, D. E., and Vargervik, K. (1997). Birth prevalence, mutation rate, sex ratio, parents' age, and ethnicity in Apert syndrome. *Am. J. Med. Genet.* 72, 394–398. doi: 10.1002/(SICI)1096-8628(19971112)72:4<394::AID-AJMG4>3.0.CO;2-R

Upmeyer, S., Bothwell, M., and Tobias, J. D. (2005). Perioperative care of a patient with Beare-Stevenson syndrome. *Paediatr. Anaesth* 15, 1131–1136. doi: 10.1111/j.1460-9592.2005.01585.x

Vargas, R. A. P., Maegawa, G. H. B., Taucher, S. C., Leite, J. C. L., Sanz, P., Cifuentes, J., et al. (2003). Beare-Stevenson syndrome: two South American patients with FGFR2 analysis. *Am. J. Med. Genet. A* 121A, 41–46. doi: 10.1002/ajmg.a.20101

Veltman, J. A., and Brunner, H. G. (2012). De novo mutations in human genetic disease. *Nat. Rev. Genet.* 13, 565–575. doi: 10.1038/nrg3241

Wang, T.-J., Huang, C.-B., Tsai, F.-J., Wu, J.-Y., Lai, R.-B., and Hsiao, M. (2002). Mutation in the FGFR2 gene in a Taiwanese patient with Beare-Stevenson cutis gyrata syndrome. *Clin. Genet.* 61, 218–221. doi: 10.1034/j.1399-0004.2002.610309.x

Wang, Y., Zhou, X., Oberoi, K., Phelps, R., Couwenhoven, R., Sun, M., et al. (2012). p38 Inhibition ameliorates skin and skull abnormalities in Fgfr2 Beare-Stevenson mice. *J. Clin. Invest.* 122, 2153–2164. doi: 10.1172/JCI62644

Wenger, T. L., Bhoj, E. J., Wetmore, R. F., Mennuti, M. T., Bartlett, S. P., Mollen, T. J., et al. (2015). Beare-Stevenson syndrome: two new patients, including a novel finding of tracheal cartilaginous sleeve. *Am. J. Med. Genet.* 167, 852–857. doi: 10.1002/ajmg.a.36985

Wenger, T. L., Dahl, J., Bhoj, E. J., Rosen, A., McDonald-McGinn, D., Zackai, E., et al. (2017). Tracheal cartilaginous sleeves in children with syndromic craniosynostosis. *Genet. Med.* 19, 62–68. doi: 10.1038/gim.2016.60

Yu, J., Chen, Z., Ni, Y., and Li, Z. (2012). CFTR mutations in men with congenital bilateral absence of the vas deferens (CBAVD): a systemic review and meta-analysis. *Hum. Reprod.* 27, 25–35. doi: 10.1093/humrep/der377

Zhang, J., Li, J., Saucier, J. B., Feng, Y., Jiang, Y., Sinson, J., et al. (2019). Non-invasive prenatal sequencing for multiple Mendelian monogenic disorders using circulating cell-free fetal DNA. *Nat. Med.* 25, 439–447. doi: 10.1038/s41591-018-0334-x

Conflict of Interest: The authors declare that the research was conducted in the absence of any commercial or financial relationships that could be construed as a potential conflict of interest.

frontiers in Genetics

BRIEF RESEARCH REPORT
published: 24 March 2020
doi: 10.3389/fgene.2020.00224

Impact of *ex vivo* Sample Handling on DNA Methylation Profiles in Human Cord Blood and Neonatal Dried Blood Spots

*Aya Sasaki[1,2], Bona Kim[1,2], Kellie E. Murphy[2,3] and Stephen G. Matthews[1,2,3,4]**

[1] Department of Physiology, University of Toronto, Toronto, ON, Canada, [2] Lunenfeld-Tanenbaum Research Institute, Sinai Health System, Toronto, ON, Canada, [3] Department of Obstetrics and Gynaecology, University of Toronto, Toronto, ON, Canada, [4] Department of Medicine, University of Toronto, Toronto, ON, Canada

The profiling of DNA methylation modifications in peripheral blood has significant potential to determine risk factors for human disease. Little is known concerning the sensitivity of DNA methylation profiles to *ex vivo* sample handling. Here, we studied typical conditions prior to sample storage associated with cord blood samples obtained from clinical investigations using reduced representation bisulfite sequencing. We examined both whole blood collected shortly after birth and dried blood spots, a potentially important source of neonatal blood for investigation of the DNA methylome and the Developmental Origins of Health and Disease in human cohorts because they are routinely collected during clinical care. Samples were matched across different time conditions, as they were from the same cord blood samples obtained from the same individuals. Maintaining whole blood *ex vivo* up to 24 h (4°C) or dried blood spots up to 7 days (room temp.) had little effect on DNA methylation profiles. Minimal differences were detected between cord blood immediately frozen and dried blood spots. Our results indicate that DNA methylation profiles are resilient to *ex vivo* sample handling conditions prior to storage. These data will help guide future human studies focused toward determination of DNA methylation modifications in whole blood.

Keywords: DNA methylation, cord blood, blood cards, *ex vivo* storage, reduced representation bisulfite sequencing

OPEN ACCESS

Edited by:
Daniel Enquobahrie, University of Washington, United States

Reviewed by:
Shicheng Guo, University of Wisconsin–Madison, United States
Maurizio D'Esposito, Italian National Research Council, Italy

***Correspondence:**
Stephen G. Matthews
stephen.matthews@utoronto.ca

Specialty section:
This article was submitted to Epigenomics and Epigenetics, a section of the journal Frontiers in Genetics

Received: *04 November 2019*
Accepted: *26 February 2020*
Published: *24 March 2020*

Citation:
Sasaki A, Kim B, Murphy KE and Matthews SG (2020) Impact of ex vivo Sample Handling on DNA Methylation Profiles in Human Cord Blood and Neonatal Dried Blood Spots. Front. Genet. 11:224. doi: 10.3389/fgene.2020.00224

INTRODUCTION

Studies of gene expression have demonstrated that *ex vivo* incubation time alters the transcript abundance of many genes (Hartel et al., 2001; Rainen et al., 2002; Baechler et al., 2004; Debey et al., 2004). These genes are involved in the activation of stress and inflammation-induced pathways, cell cycle progression and apoptosis. Thus, the timing and procedures associated with blood collection are critical for accurate and sensitive measurements of the state of gene activity.

Assessment of DNA methylation in peripheral blood has significant potential for determining risk factors for human disease. As genomic-scale arrays and sequencing technologies are increasingly applied to the study of peripheral blood, it is important to consider the variables that may affect the interpretation of data. Storage times and temperatures often vary significantly from one laboratory to another because of differences in collection, transport, and processing of human

whole blood. However, little is known concerning the sensitivity of DNA methylation profiles to *ex vivo* sample handling conditions.

Neonatal dried blood spots are a potentially important source of neonatal blood for investigation of the DNA methylome and the Developmental Origins of Health and Disease in human cohorts because they are routinely collected during clinical care. There has also been increasing interest in the use of dried blood spots for epigenome-wide analysis, as DNA methylation profiles extracted from dried blood spots are strongly correlated with those of freshly collected blood (Hardin et al., 2009; Aberg et al., 2013; Hollegaard et al., 2013; Joo et al., 2013; Ghantous et al., 2014).

In the present study, we aimed to determine the effects of *ex vivo* sample handling prior to DNA extraction on DNA methylation profiles in cord blood. Our goal was to simulate common variations in the conditions under which cord blood is maintained prior to storage for research and clinical assessments using the same cord blood samples obtained from the same individuals. We examined whole cord blood collected within 30 min of birth and either immediately frozen or kept at 4°C. We also examined blood dried on Guthrie cards at room temperature to simulate procedures for neonatal blood collection for clinical assessments.

MATERIALS AND METHODS

Subjects and Blood Samples

A study overview is presented in **Figure 1**. Healthy subjects ($n = 7$) were recruited by Mount Sinai Hospital and the Research Centre for Women's and Infants' Health BioBank (Toronto, ON, Canada). This study was approved by the Mount Sinai Hospital Research Ethics Board (MSH REB# 17-0210-E) and the University of Toronto Research Ethics Boards. Umbilical cord blood from each subject was collected within 30 min of birth. For 4 subjects (**Figures 1A,B**), blood was deposited into four EDTA purple top vacutainers (Becton Dickinson). The first EDTA tube was frozen immediately and stored at −80°C. The second and third EDTA tubes were kept at 4°C for 4 and 24 h, respectively, and then stored at −80°C. The fourth EDTA purple top vacutainer was sent to Mount Sinai Services (Mount Sinai Hospital, Toronto, ON, Canada) for complete blood count (CBC) measurement using Sysmex XN-9000 (Sysmex). The purpose of CBC measurement was to reveal the distribution of different types of nucleated cells across subjects and examine if they were within the expected range for neonates. Part of the EDTA-treated cord blood was placed on a Guthrie card (75–80 μL of blood per spot; Whatman 903), left to air-dry for 4 h at room temperature and then stored at −80°C. One subject yielded insufficient blood for CBC or time course analysis. For three subjects (**Figure 1C**), blood was placed directly onto a Guthrie card without EDTA treatment (75–80 μL of blood per spot; Whatman 903). Cards were left to air-dry for 4 h, 24 h or 7 days at room temperature and then stored at −80°C. All samples were derived from singleton pregnancies delivered at term (≥37 weeks). Patients with gestational diabetes, diabetes, or hypertension were excluded.

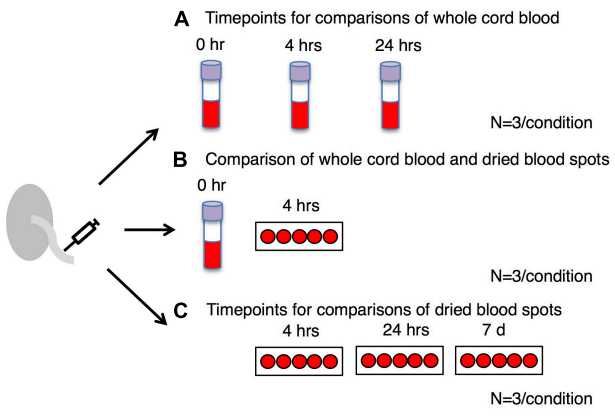

FIGURE 1 | Study overview. We examined DNA methylation profiles in whole blood: **(A)** treated with EDTA and frozen immediately after collection (0 h) compared to whole blood frozen after 4 h or 24 h at 4°C, **(B)** EDTA-treated dried blood spots frozen after 4 h at room temperature compared to whole blood frozen immediately, and **(C)** non-EDTA-treated dried blood spots frozen after 4 h, 24 h or 7 days at room temperature. The same samples obtained from the same individuals ($n = 3$) were used for each time point.

DNA Extraction and Quantification

DNA was extracted from whole blood and the blood spot cards using methods described previously (Ghantous et al., 2014), with minor modifications. Briefly, one half of a single blood spot was cut into small pieces and incubated with lysis buffer (1218 μL) and Proteinase K (33 μL) using Gensolve reagents (GenTegra: GVR-113) in an Incubator/vortex shaker set at 1400 rpm for 90 min, at 56°C (ThermoMixer® C, Eppendorf). The rest of the procedure followed the manufacturer's protocol. The lysate was processed using a QIAamp DNA Blood Mini Kit (Qiagen: Cat. #51104). The extracted DNA was quantified with a Quant-iT PicoGreen dsDNA assay (ThermoFisher: Cat.# P11496) and DNA quality was assessed by TapeStation (Centre for Applied Genomics in the Hospital for Sick Children, Toronto, ON, Canada). Samples with DNA Integrity Numbers (DINs) over 7 were used for further analysis.

Reduced Representation Bisulfite Sequencing (RRBS)

Reduced representation bisulfite sequencing (RRBS) libraries were generated from 100 ng of high-quality dsDNA for each sample using the RRBS Methyl-Seq System 1–16 (Ovation: Part # 0353) and EpiTect Fast DNA Bisulfite kit (Qiagen: Cat. #59824) following the manufacturer's protocols. *Msp*I restriction enzyme digestion and size selection were used to enrich libraries for gene regulatory elements containing CCGG motifs. The resulting libraries showed three peaks on the Bioanalyzer High Sensitivity DNA Chip (i.e., 200, 265, and 330 bp) due to expected *Msp*I-containing micro-satellite repeats in the human genome as well as the absence of peaks indicating unligated adapters. Representative output of the Bioanalyzer High Sensitivity DNA

Chip showing three peaks are available in the manufacturer's protocol (Ovation: Part # 0353). All libraries generated in this study met these criteria prior to sequencing. RRBS libraries meeting this criterion were sequenced in multiplexes of up to 10 samples, balanced by condition (Donnelly Sequencing Centre, University of Toronto, Toronto, ON, Canada) on a NextSeq500 (Illumina) following the manufacturer's protocols for single end reads at 75 bp read length.

Differentially Methylated CpG Sites (DMCs)

Adaptor sequences were trimmed using Trim Galore[1] followed by additional filtering and trimming using a python script provided by NuGEN to remove reads that did not contain an *Msp*I site signature at the 5′ end. The python script is available on GitHub[2]. The reads were then aligned using Bismark (Krueger and Andrews, 2011) and sorted by Samtools (Li et al., 2009). We then used MethPipe/Radmeth (Song et al., 2013; Dolzhenko and Smith, 2014) to identify significant differentially methylated CpG sites (DMCs) with at least 30X reads, an FDR $\leq$ 0.05 and with at least a 5% methylation difference. We followed the US National Institutes of Health Roadmap Epigenomics Project Guidelines using 30x sequencing depth in order to achieve a conservative estimate of methylation (Nih Roadmap Epigenomics Mapping Consortium, 2011; Hansen et al., 2012). CompEpitool (Kishore et al., 2015) was used to annotate the differentially methylated CpG sites to the human genome. The bisulfite conversion rate was calculated using methylKit (Akalin et al., 2012). The correlational analysis and clustering analysis were performed using default setting in methylKit for CpG sites in all samples.

Gene Pathway Enrichment

A list of differentially methylated genes identified by the DMC analysis was further explored using the Kyoto Encyclopedia of Genes and Genomes (KEGG) (Kanehisa and Goto, 2000) to examine functionally annotated gene pathways. The enrichment analysis was performed using the Molecular Signatures Database (msigDB) (Subramanian et al., 2005; Liberzon et al., 2011) with significant enrichment defined by an FDR $\leq$ 0.05.

RESULTS

Quality of the Samples and Reproducibility of the Data

The bisulfite conversion rate was greater than 99.4% for all of the samples. DNA methylation profiles were compared between whole cord blood collected at 0, 4, and 24 h (**Figure 1A**), whole cord blood collected and dried blood spots (**Figure 1B**) and dried blood spots collected at 4 h, 24 h, and 7 days (**Figure 1C**) collected from matched individuals. **Figure 2** provides a matrix of correlation coefficients for each experiment showing pair-wise comparisons between all samples. We found that the correlation coefficients were greater than 0.8 for all pair-wise comparisons, indicating high levels of reproducibility in our dataset (Bock, 2012; **Figure 2**). In addition, unsupervised clustering analysis revealed strong similarities across the sample types within each individual. DNA methylation differences between individuals were sufficient to discriminate matched pairs from unrelated samples (**Figure 3**). These effects were also reflected in higher correlations for sample types from the same individual compared to sample types across different individuals (**Figure 2**).

Examination of *ex vivo* Sample Handling on DNA Methylation in Whole Cord Blood

We examined whole cord blood samples left at 4°C for either 4 h or 24 h *ex vivo* (**Figure 1A**) compared to blood frozen immediately after collection. These comparisons yielded no significant differentially methylated CpG sites meeting our criteria (i.e., FDR $\leq$ 0.05, $\geq$5% difference in methylation). **Supplementary Table S1** shows the full list of DMCs at FDR $<$ 0.05 for whole cord blood. Complete Blood Count (CBC) analysis revealed that the distribution of different types of nucleated cells were similar across three subjects and within the expected range for neonates, including nucleated red blood cells (nRBCs) that are known to have a unique hypomethylated DNA methylation profile (**Supplementary Figure S1**; de Goede et al., 2016). Of note, the absolute numbers of nRBCs were 0.2, 0.15, and 0.1 10E9/L, constituting 1.3, 1.3, and 1% of the total blood cell count, respectively, for each subject.

Comparison of DNA Methylation in Whole Cord Blood and Dried Blood Spots

Next, we examined whole blood frozen immediately compared to blood spots dried for 4 h prior to freezing (**Figure 1B**). We identified 134 differentially methylated CpG sites that had greater than 5% methylation differences with FDRs $<$ 0.05 (n = 3 per condition). **Supplementary Table S2** shows the full list of DMCs at FDR $<$ 0.05 for the comparison of whole cord blood with dried blood spots. When annotated, these differentially methylated CpG sites corresponded to 23 genes (**Table 1**). We performed gene set functional analysis using the Kyoto Encyclopedia of Genes and Genomes (KEGG) pathways to identify common gene pathways associated with this gene set and found no significant gene pathway enrichment, either with the total gene list or gene lists separated by genomic regions (i.e., gene list with differential methylation in promoter regions or gene list with differential methylation in gene-body regions). We identified two genes with multiple CpG sites differentially methylated between whole blood and dried blood spots. TMEM183A (*transmembrane protein 183A*) showed 7 CpG sites, all hypermethylated, with methylation differences of 21.49 to 27.59% in the promoter region. PROZ (*protein Z, vitamin K-dependent plasma glycoprotein*), showed 6 CpG sites, all hypomethylated with methylation differences of −6.16 to −34.16% in the gene body. **Supplementary Table S2** provides the full list of differentially methylated CpG sites with associated genic regions and CpG locations.

[1]https://www.bioinformatics.babraham.ac.uk/projects/trim_galore/

[2]https://github.com/nugentechnologies/NuMetRRBS/blob/master/trimRRBSdiversityAdaptCustomers.py

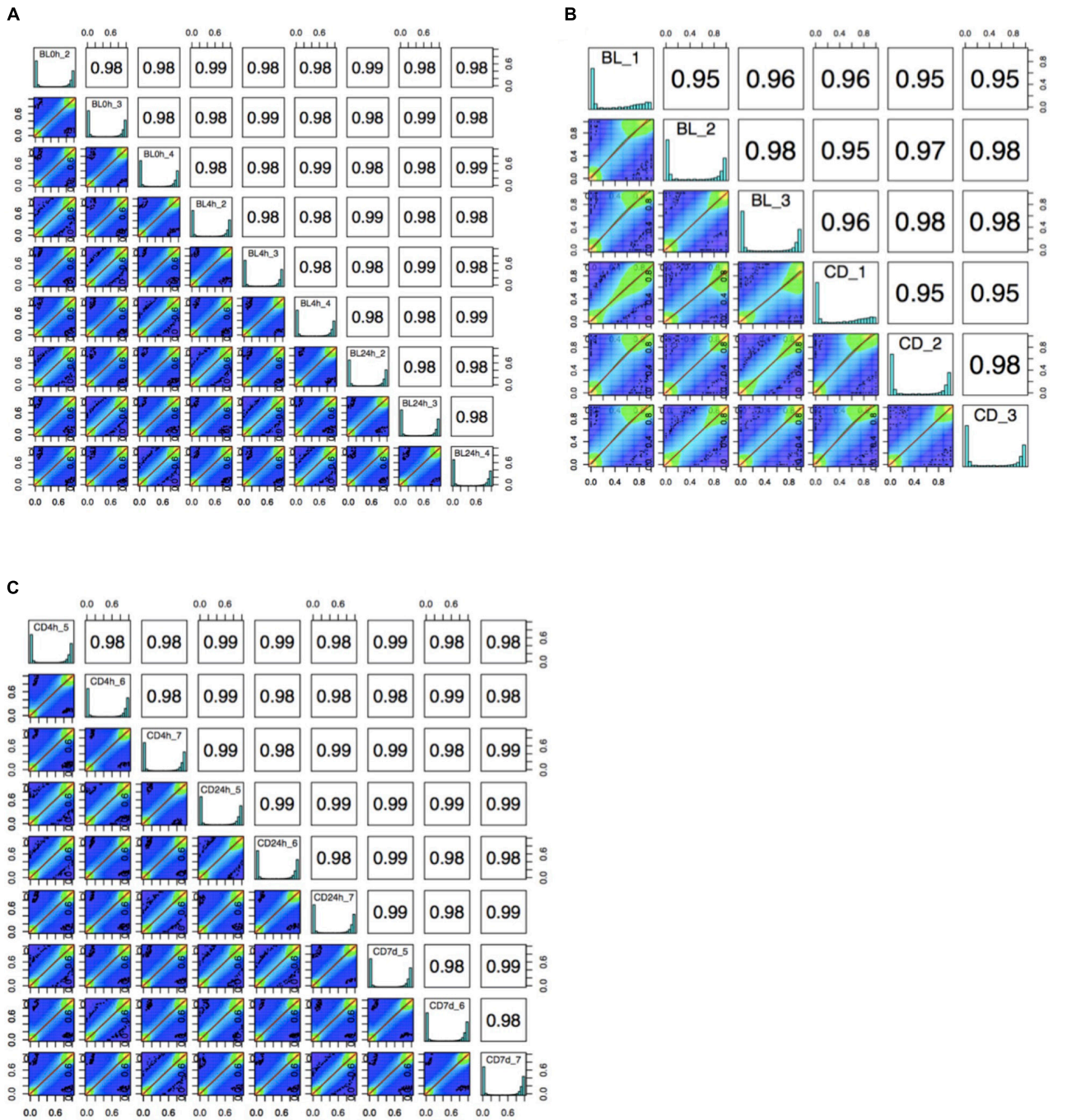

FIGURE 2 | A matrix of correlation coefficients and a set of scatterplots showing the relationship between samples for **(A)** comparisons of whole cord blood for matched samples at 0 h, 4 h, and 24 h (BL, whole cord blood, $n = 3$), **(B)** comparison of whole cord blood and dried blood spots for matched samples (BL, whole cord blood; CD, dried blood spots in cards, $n = 3$) and **(C)** comparisons of dried blood spots for matched samples at 4 h, 24 h, and 7 days (CD, dried blood spots in cards, $n = 3$).

Examination of *ex vivo* Sample Handling on DNA Methylation in Dried Blood Spots

Finally, we examined CpG methylation in blood cards left to dry for 24 h or 7 days at room temperature prior to freezing compared to dried blood spots that were immediately frozen after the 4 h drying phase (**Figure 1C**). There were no differences in CpG methylation after 24 h of blood card storage at room temperature. We identified 2 differentially methylated CpG sites meeting our criteria after 7 days of storage at room temperature compared to the 4 h sample. **Supplementary Table S3** shows the

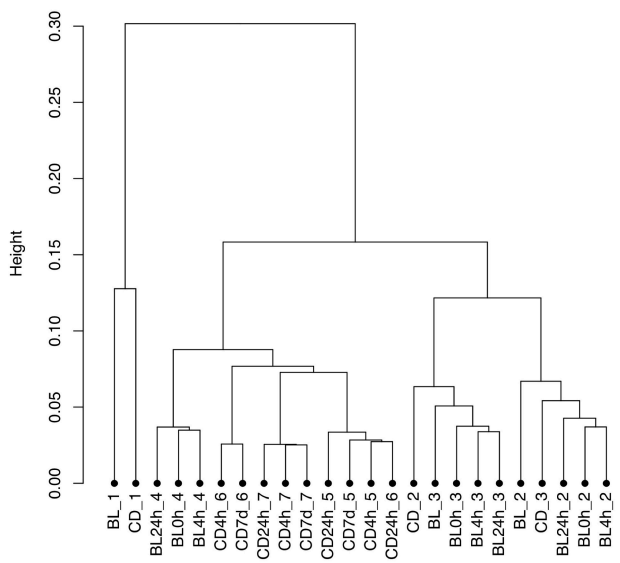

FIGURE 3 | Unsupervised clustering plot based on the methylation values. Samples from the same individual (BL, whole cord blood; CD, dried blood spots in cards) are labeled with the same number. The storage times are indicated 0, 4, and 24 h for timepoints for comparisons of whole cord blood and 4 h, 24 h, and 7 days for timepoints for comparisons of dried blood spots.

TABLE 1 | Differentially methylated CpG sites associated with genes between whole cord blood compared to dried blood spots from the same subjects.

Gene	# of CpGs	Avg. Meth Diff% (Range)	Genic Location
TMEM183A	7	25.2 (21.5 – 27.6)	Promoter
PROZ	6	−24.1 (−6.2 – −34.2)	Genebody
ABL1	2	8.6 (6.5 – 10.7)	Genebody
C11orf53	2	−16.1 (−9.7 – −22.4)	Genebody
CAMK1D	2	−14.8 (−10.1 – −19.5)	Genebody
COX16;SYNJ2BP-COX16	2	−8.3 (−6.2 – −10.3)	Genebody
DMRTA2	2	−4.2 (−14.7 – 6.3)	Genebody
MSLN	2	4.7 (−19.0 – 28.5)	Genebody;promoter
RALBP1	2	−9.7 (−9.6 – −9.8)	Genebody
ZNF101	2	7.5	Promoter
FAM20C	1	−9.4	Genebody
FAM228B;FAM228A	1	−24.0	Genebody;promoter
FASN	1	−6.8	Genebody;promoter
FILIP1	1	16.6	Promoter
GFI1	1	−19.9	Genebody;promoter
GSX1	1	12.5	Promoter
LINC00441	1	5.0	Promoter
MBP	1	5.3	Genebody
PIGQ	1	6.0	Genebody;promoter
RAB6B	1	9.4	Promoter
SAMD11	1	−38.5	Genebody
SIRPA	1	5.3	Genebody
SLC38A10	1	−9.0	Genebody;promoter

A list of differentially methylated genes is shown sorted by the number of differentially methylated CpG sites.

full list of DMCs at FDR < 0.05 for the comparisons of dried blood spots. When these CpG sites were annotated, one of the CpG sites corresponded to a gene: S100Z (*S100 calcium binding protein Z*) with a methylation difference of 6.48% (88.70% at 4 h vs. 82.22% at 7 days). **Supplementary Table S4** shows each of the differentially methylated CpG sites along with their associated genic regions and locations.

DISCUSSION

In this study, we used time-course sampling combined with genome-wide sequencing of gene regulatory elements to examine the influence of handling procedures prior to sample storage on DNA methylation profiles in neonatal blood. We found that different periods of incubation of either whole cord blood or dried blood spots at room temperature had very little effect on DNA methylation profiles. In addition, minimal differences in DNA methylation were detected between whole cord blood immediately frozen compared to blood spots dried for 4 h prior to freezing. DNA methylation profiles in dried blood spots were also similar to those of whole cord blood, except for a small subset of genes. Our findings suggest that DNA methylation profiles are resilient to conditions typical of sample handling procedures for blood collected for research and clinical assessments. These data should provide important information for future prospective and retrospective human studies investigating DNA methylation modifications in whole blood. Importantly, in the present study samples were matched across different time conditions, as they were from the same cord blood samples obtained from the same individuals. The counts for nRBCs were similar across subjects, and these values were similar to mean values previously reported for term babies without complications (Christensen et al., 2011). The results obtained using RRBS are known to correlate strongly with those from commonly used microarray approaches (i.e., illumina450K arrays). Notably, however, the use of RRBS in this study increased by 10-fold the range of genome coverage compared to genome-wide microarray approaches. In addition, we used a threshold of methylation differences >5% in our comparisons (although, we also provide data for the full range of differential methylation meeting an FDR < 0.05). This threshold approximates the detection limits of other platforms such as DNA pyrosequencing (Mikeska et al., 2011). Therefore, we expect that our results will be generalizable across commonly used DNA methylation analysis approaches targeting gene regulatory elements.

Among 23 genes that showed differential methylation between whole cord blood and dried blood spots, we identified only 2 genes with multiple differentially methylated CpG sites; TMEM183A (*transmembrane protein 183A*) and PROZ (*protein Z, vitamin K-dependent plasma glycoprotein*), which showed 7 and 6 significant differentially

methylated CpG sites, respectively. TMEM183A is a gene of currently unknown function. The PROZ gene encodes a liver vitamin K-dependent glycoprotein and is synthesized in the liver that is then secreted into the plasma. The protein encoded by PROZ plays a role in regulating blood coagulation by inhibiting activity of coagulation protease. Deficiencies in PROZ protein are associated with an increased risk of ischemic arterial diseases (Lichy et al., 2004, 2006). Our results indicate that the genes that were most affected by air-drying blood were not related to biological processes that are of interest in most studies examining biomarkers of maternal exposures in cord blood.

Our findings contrast with the reported effects of sample handling on gene expression. It has been well documented that sample handling conditions influence the transcription of hundreds of genes (Hartel et al., 2001; Rainen et al., 2002; Baechler et al., 2004; Debey et al., 2004). These genes are involved in the activation of stress and inflammation-induced pathways, cell-cycle progression and apoptosis, which may confound the interpretation of gene expression results obtained from blood. Although DNA methylation is considered a relatively stable epigenetic modification (Bird, 2002), recent studies suggest that DNA methylation modifications at some loci are more dynamic than previously thought. For example, longitudinal analysis has shown that DNA methylation at some sites oscillates across the circadian cycle (Oh et al., 2018). However, we found that DNA methylation profiles are stable and resilient to *ex vivo* handling conditions in whole cord blood as well as in dried blood spots, at least in gene regulatory elements assessed with our approach. Four genes that were previously shown in an analysis of gene expression to be sensitive to *ex vivo* storage (Baechler et al., 2004) also showed differential methylation in dried blood spots compared to whole blood in the present study (**Table 1**). These genes included FASN (*fatty acid synthase*), GFI1 (*growth factor independent 1 transcription repressor),* MBP (*myelin basic protein*) and RALBP1 (*ralA binding protein 1*), suggesting that these genes may be sensitive to handling conditions at the level of gene expression and DNA methylation.

Notable strengths of this study are the use of a within-subjects design and a conservative read number (30X), although this study is not without limitations, including small sample size, which may have impacted our ability to detect very small changes in DNA methylation. Also, as sequencing reads obtained using RRBS are enriched at gene regulatory elements with a high CpG content relative to other loci, it may be that larger differences related to sample handling conditions occur outside of these regions. Finally, although the focus of this study was on typical handling conditions associated with the collection of clinical samples, we recognize that future work is needed to study the full range of conceivable handling conditions that may affect DNA methylome profiles. The current study focused on procedures for sample handling in clinical settings, which typically range from immediate to overnight sample storage time (up to 7 days in the case of blood cards) followed by freezing. A limited number of other studies have examined archival samples of dried blood. For example, Hollegaard et al. (2013) showed in matched samples of adult whole blood from two individuals, that methylation signatures were highly correlated between the whole blood and dried blood spots stored at room temperature for 3 years. Also, Joo et al. (2013) showed that matched samples of 5 adult buffy coat and dried blood spots stored at room temperature were highly correlated after 3 years of storage at room temperature. Although methylation analysis is feasible in older archival samples [e.g., samples collected >20 years ago (Hollegaard et al., 2013)], the ability to match these archival samples with immediately collected samples is a limitation in our current understanding of the potential impact of a wider range of storage conditions on DNA methylation. Nevertheless, with the recent advent of high-throughput epigenomic technologies that require high quality DNA, our findings on the relative stability of DNA methylation with varying sample handling and preparation conditions – including those pertaining to blood cards – can help guide current and future studies. There is emerging appreciation of the utility of cord blood and dried blood spots collected at birth as a resource for mechanistic, prognostic and diagnostic epigenetic studies of the Developmental Origins of Health and Disease, and our findings support such a strategy.

In summary, we have demonstrated that DNA methylation profiles are quite stable in whole cord blood, as well as, in dried blood spots following various *ex vivo* manipulations. Our findings stand to increase the scope of biological resources suitable for epigenome-wide association studies. This further adds to the potential use of neonatal dried blood spot samples in screening beyond genetic assessments and paves the way for population-based studies of epigenetic modifications after birth.

DATA AVAILABILITY STATEMENT

The data discussed in this article have been deposited in NCBI's Gene Expression Omnibus (Edgar et al., 2002) and are accessible through GEO Series accession number GSE146468 (https://www.ncbi.nlm.nih.gov/geo/query/acc.cgi?acc=GSE146468).

ETHICS STATEMENT

The studies involving human participants were reviewed and approved by the Mount Sinai Hospital Research Ethics Board. The patients/participants provided their written informed consent to participate in this study.

AUTHOR CONTRIBUTIONS

AS and SM designed the research and wrote the manuscript. AS and BK performed the research. AS analyzed the data. KM provided the materials and supervised the patient enrolment and

acquisition of biological samples. SM supervised the research. All authors approved the final version of the manuscript.

FUNDING

AS was supported by the postdoctoral fellowships from Brain Canada and Kids Brain Health Network, and the Canadian Institutes of Health Research (CIHR). This work was funded by a Foundation grant from CIHR (FDN-148368) to SM.

ACKNOWLEDGMENTS

The authors acknowledge the contribution and support of the Ontario Birth Study Team members. In addition, the authors thank and are extremely grateful to all the women who took part in this study. Funding for the Ontario Birth Study has been provided by the Mount Sinai Hospital, Mount Sinai Hospital Foundation, and the Lunenfeld-Tanenbaum Research Institute. The authors also thank the RCWIH BioBank, the Lunenfeld-Tanenbaum Research Institute, and the Mount Sinai Hospital/UHN Department of Obstetrics and Gynaecology for assistance in this study (http://biobank.lunenfeld.ca).

SUPPLEMENTARY MATERIAL

The Supplementary Material for this article can be found online at: https://www.frontiersin.org/articles/10.3389/fgene.2020.00224/full#supplementary-material

REFERENCES

Aberg, K. A., Xie, L. Y., Nerella, S., Copeland, W. E., Costello, E. J., and Van Den Oord, E. J. (2013). High quality methylome-wide investigations through next-generation sequencing of DNA from a single archived dry blood spot. *Epigenetics* 8, 542–547. doi: 10.4161/epi.24508

Akalin, A., Kormaksson, M., Li, S., Garrett-Bakelman, F. E., Figueroa, M. E., Melnick, A., et al. (2012). methylKit: a comprehensive R package for the analysis of genome-wide DNA methylation profiles. *Genome Biol.* 13:R87. doi: 10.1186/gb-2012-13-10-r87

Baechler, E. C., Batliwalla, F. M., Karypis, G., Gaffney, P. M., Moser, K., Ortmann, W. A., et al. (2004). Expression levels for many genes in human peripheral blood cells are highly sensitive to ex vivo incubation. *Genes Immun.* 5, 347–353. doi: 10.1038/sj.gene.6364098

Bird, A. (2002). DNA methylation patterns and epigenetic memory. *Genes Dev.* 16, 6–21. doi: 10.1101/gad.947102

Bock, C. (2012). Analysing and interpreting DNA methylation data. *Nat. Rev. Genet.* 13, 705–719. doi: 10.1038/nrg3273

Christensen, R. D., Henry, E., Andres, R. L., and Bennett, S. T. (2011). Reference ranges for blood concentrations of nucleated red blood cells in neonates. *Neonatology* 99, 289–294. doi: 10.1159/000320148

de Goede, O. M., Lavoie, P. M., and Robinson, W. P. (2016). Characterizing the hypomethylated DNA methylation profile of nucleated red blood cells from cord blood. *Epigenomics* 8, 1481–1494. doi: 10.2217/epi-2016-0069

Debey, S., Schoenbeck, U., Hellmich, M., Gathof, B. S., Pillai, R., Zander, T., et al. (2004). Comparison of different isolation techniques prior gene expression profiling of blood derived cells: impact on physiological responses, on overall expression and the role of different cell types. *Pharmacogenom. J.* 4, 193–207. doi: 10.1038/sj.tpj.6500240

Dolzhenko, E., and Smith, A. D. (2014). Using beta-binomial regression for high-precision differential methylation analysis in multifactor whole-genome bisulfite sequencing experiments. *BMC Bioinform.* 15:215. doi: 10.1186/1471-2105-15-215

Edgar, R., Domrachev, M., and Lash, A. E. (2002). Gene Expression Omnibus: NCBI gene expression and hybridization array data repository. *Nucleic Acids Res.* 30, 207–210. doi: 10.1093/nar/30.1.207

Ghantous, A., Saffery, R., Cros, M. P., Ponsonby, A. L., Hirschfeld, S., Kasten, C., et al. (2014). Optimized DNA extraction from neonatal dried blood spots: application in methylome profiling. *BMC Biotechnol.* 14:60. doi: 10.1186/1472-6750-14-60

Hansen, K. D., Langmead, B., and Irizarry, R. A. (2012). BSmooth: from whole genome bisulfite sequencing reads to differentially methylated regions. *Genome Biol.* 13:R83. doi: 10.1186/gb-2012-13-10-r83

Hardin, J., Finnell, R. H., Wong, D., Hogan, M. E., Horovitz, J., Shu, J., et al. (2009). Whole genome microarray analysis, from neonatal blood cards. *BMC Genet.* 10:38. doi: 10.1186/1471-2156-10-38

Hartel, C., Bein, G., Muller-Steinhardt, M., and Kluter, H. (2001). Ex vivo induction of cytokine mRNA expression in human blood samples. *J. Immunol. Methods* 249, 63–71. doi: 10.1016/s0022-1759(00)00334-3

Hollegaard, M. V., Grauholm, J., Norgaard-Pedersen, B., and Hougaard, D. M. (2013). DNA methylome profiling using neonatal dried blood spot samples: a proof-of-principle study. *Mol. Genet. Metab.* 108, 225–231. doi: 10.1016/j.ymgme.2013.01.016

Joo, J. E., Wong, E. M., Baglietto, L., Jung, C. H., Tsimiklis, H., Park, D. J., et al. (2013). The use of DNA from archival dried blood spots with the infinium human Methylation 450 array. *BMC Biotechnol.* 13:23. doi: 10.1186/1472-6750-13-23

Kanehisa, M., and Goto, S. (2000). KEGG: kyoto encyclopedia of genes and genomes. *Nucleic Acids Res.* 28, 27–30.

Kishore, K., De Pretis, S., Lister, R., Morelli, M. J., Bianchi, V., Amati, B., et al. (2015). methylPipe and compEpiTools: a suite of R packages for the integrative analysis of epigenomics data. *BMC Bioinform.* 16:313. doi: 10.1186/s12859-015-0742-6

Krueger, F., and Andrews, S. R. (2011). Bismark: a flexible aligner and methylation caller for Bisulfite-Seq applications. *Bioinformatics* 27, 1571–1572. doi: 10.1093/bioinformatics/btr167

Li, H., Handsaker, B., Wysoker, A., Fennell, T., Ruan, J., Homer, N., et al. (2009). The sequence alignment/map format and SAMtools. *Bioinformatics* 25, 2078–2079. doi: 10.1093/bioinformatics/btp352

Liberzon, A., Subramanian, A., Pinchback, R., Thorvaldsdottir, H., Tamayo, P., and Mesirov, J. P. (2011). Molecular signatures database (MSigDB) 3.0. *Bioinformatics* 27, 1739–1740. doi: 10.1093/bioinformatics/btr260

Lichy, C., Dong-Si, T., Reuner, K., Genius, J., Rickmann, H., Hampe, T., et al. (2006). Risk of cerebral venous thrombosis and novel gene polymorphisms of the coagulation and fibrinolytic systems. *J. Neurol.* 253, 316–320. doi: 10.1007/s00415-005-0988-4

Lichy, C., Kropp, S., Dong-Si, T., Genius, J., Dolan, T., Hampe, T., et al. (2004). A common polymorphism of the protein Z gene is associated with protein Z plasma levels and with risk of cerebral ischemia in the young. *Stroke* 35, 40–45. doi: 10.1161/01.str.0000106909.75418.e4

Mikeska, T., Felsberg, J., Hewitt, C. A., and Dobrovic, A. (2011). Analysing DNA methylation using bisulphite pyrosequencing. *Epigenet. Protoc.* 761, 33–53. doi: 10.1007/978-1-61779-316-5_4

Nih Roadmap Epigenomics Mapping Consortium (2011). *Standards and Guidelines for Whole Genome Shotgun Bisulfite Sequencing*. Available at: http://www.roadmapepigenomics.org/protocol (accessed February 3, 2020).

Oh, G., Ebrahimi, S., Carlucci, M., Zhang, A., Nair, A., Groot, D. E., et al. (2018). Cytosine modifications exhibit circadian oscillations that are involved in epigenetic diversity and aging. *Nat. Commun.* 9:644. doi: 10.1038/s41467-018-03073-7

Rainen, L., Oelmueller, U., Jurgensen, S., Wyrich, R., Ballas, C., Schram, J., et al. (2002). Stabilization of mRNA expression in whole blood samples. *Clin. Chem.* 48, 1883–1890. doi: 10.1093/clinchem/48.11.1883

Song, Q., Decato, B., Hong, E. E., Zhou, M., Fang, F., Qu, J., et al. (2013). A reference methylome database and analysis pipeline to facilitate integrative and comparative epigenomics. *PLoS One* 8:e81148. doi: 10.1371/journal.pone.0081148

Subramanian, A., Tamayo, P., Mootha, V. K., Mukherjee, S., Ebert, B. L., Gillette, M. A., et al. (2005). Gene set enrichment analysis: a knowledge-based approach for interpreting genome-wide expression profiles. *Proc. Natl. Acad. Sci. U.S.A.* 102, 15545–15550. doi: 10.1073/pnas.0506580102

Conflict of Interest: The authors declare that the research was conducted in the absence of any commercial or financial relationships that could be construed as a potential conflict of interest.

frontiers in Genetics

CASE REPORT
published: 17 June 2020
doi: 10.3389/fgene.2020.00561

Candidate Genes Associated With Neurological Findings in a Patient With Trisomy 4p16.3 and Monosomy 5p15.2

*Thiago Corrêa[1], Fabiano Poswar[2], Bruno César Feltes[3] and Mariluce Riegel[1,2]**

[1]Post-Graduate Program in Genetics and Molecular Biology, Genetics Department, Universidade Federal do Rio Grande do Sul, Porto Alegre, Brazil, [2]Medical Genetics Service, Hospital de Clínicas de Porto Alegre, Porto Alegre, Brazil, [3]Department of Theoritical Informatics, Institute of Informatics, Universidade Federal do Rio Grande do Sul, Porto Alegre, Brazil

In this report, we present a patient with brain alterations and dysmorphic features associated with chromosome duplication seen in 4p16.3 region and chromosomal deletion in a critical region responsible for Cri-du-chat syndrome (CdCS). Chromosomal microarray analysis (CMA) revealed a 41.1 Mb duplication encompassing the band region 4p16.3–p13, and a 14.7 Mb deletion located between the bands 5p15.33 and p15.1. The patient's clinical findings overlap with previously reported cases of chromosome 4p duplication syndrome and CdCS. The patient's symptoms are notably similar to those of CdCS patients as she presented with a weak, high-pitched voice and showed a similar pathogenicity observed in the brain MRI. These contiguous gene syndromes present with distinct clinical manifestations. However, the phenotypic and cytogenetic variability in affected individuals, such as the low frequency and the large genomic regions that can be altered, make it challenging to identify candidate genes that contribute to the pathogenesis of these syndromes. Therefore, systems biology and CMA techniques were used to investigate the extent of chromosome rearrangement on critical regions in our patient's phenotype. We identified the candidate genes *PPARGC1A*, *CTBP1*, *TRIO*, *TERT*, and *CCT5* that are associated with the neuropsychomotor delay, microcephaly, and neurological alterations found in our patient. Through investigating pathways that associate with essential nodes in the protein interaction network, we discovered proteins involved in cellular differentiation and proliferation, as well as proteins involved in the formation and disposition of the cytoskeleton. The combination of our cytogenomic and bioinformatic analysis provided these possible explanations for the unique clinical phenotype, which has not yet been described in scientific literature.

Keywords: Cri-du-chat, 4p16.3, *PPARGC1A*, *CTBP1*, *TRIO*, *TERT*, *CCT5*

OPEN ACCESS

Edited by:
Nagwa Elsayed Afify Gaboon, Ain Shams University, Egypt

Reviewed by:
Maria Isabel Melaragno, Federal University of São Paulo, Brazil
Rita Genesio, University of Naples Federico II, Italy

****Correspondence:***
Mariluce Riegel
mriegel@hcpa.edu.br

Specialty section:
This article was submitted to Genetic Disorders, a section of the journal Frontiers in Genetics

Received: *06 December 2019*
Accepted: *11 May 2020*
Published: *17 June 2020*

Citation:
Corrêa T, Poswar F, Feltes BC and Riegel M (2020) Candidate Genes Associated With Neurological Findings in a Patient With Trisomy 4p16.3 and Monosomy 5p15.2. Front. Genet. 11:561. doi: 10.3389/fgene.2020.00561

BACKGROUND

Cri-du-chat syndrome (CdCS; OMIM #123450) is a genetic condition caused by a deletion in the short arm of chromosome 5. The phenotype is characterized by a cat-like cry, microcephaly, facial dysmorphism, psychomotor delays, and intellectual disability (Nguyen et al., 2015). Deletions, which occur at the end of the chromosome, as well as interstitial which result

after two breaks, compose 80–90% of CdCS cases (Cerruti Mainardi, 2006). Unbalanced parental translocation occurs in approximately 10–15% of patients (Perfumo et al., 2000; Cerruti Mainardi, 2006). In addition, complex rearrangements, such as mosaicism, *de novo* translocation, or ring chromosomes, account for less than 10% of the cases (Perfumo et al., 2000). Wolf-Hirschhorn syndrome (WHS; OMIM #194190) is a contiguous gene deletion syndrome on the short arm of chromosome 4. It is characterized by facial dysmorphia, growth retardation, intellectual incapacity, and seizures (Zollino et al., 2008). However, duplication of the WHS critical region is a rare chromosomal condition causing mild clinical phenotypes, such as speech delay, facial dysmorphia, seizures, and delayed neuro and psychomotor development (Patel et al., 1995; Hannes et al., 2010; Carmany and Bawle, 2011; Cyr et al., 2011). However, the phenotypic and cytogenetic variability in affected individuals, such as the low frequency and the large genomic regions that can be altered, make it challenging to identify the candidate genes that contribute to the pathogenesis of these syndromes.

Here, we present an individual with duplication in the 4p16.3 region and deletion in the 5p15.2 region. The altered chromosomal segments are located in the critical regions of WHS and CdCS, respectively. This study reports a case never highlighted before in the literature. Systems biology and CMA were used to investigate the impact of chromosome rearrangement on critical regions in our patient's phenotype.

CASE PRESENTATION

A 5-day-old female was referred for investigation of congenital abnormalities such as imperforate anus and rectovaginal fistula, as well as atrial septal defect. Family history is noteworthy as it highlights consanguineous parents, and a brother who died with similar clinical presentation of imperforate anus, congenital heart defect, and clubfeet (**Figure 1A**). The pregnancy of the patient was uneventful, and the girl was born at home at the gestational age of 36 weeks, weighing 2,160 g, and a total length of 39 cm. On her first physical examination in our center, she had a low weight (2,045 g), down slanting palpebral fissures, short palpebral fissures, ptosis, widely spaced eyes, thin upper lip, clubfeet, overlapping fingers, micrognathia, and a high-pitched cry. Neurological examination was extraordinary as there was hypertonia of extremities and an absence of the Moro reflex. At the age of 1 month, the patient suffered seizure episodes with eye deviation that were controlled with phenobarbital drugs. In the electroencephalogram, acute wave discharges with multifocal distribution were observed in both hemispheres with predominance over the left temporal region. The brainstem illustrated that there was auditory potential; however, the scan showed abnormalities within the visual region. A brain MRI performed at the age of 5 months showed a thin corpus callosum, white matter volume loss, pontine hypoplasia, and dysgenesis of the cerebellar vermis (**Figures 1B,C**). Despite this, myelination was in accordance with her age. After being subjected to surgical procedures which had no complications, she was discharged at the age of 5 months and 25 days. Although the patient had a tracheostomy and a nasoenteral tube, she was, clinically, in a stable condition.

Karyotyping identified typical patterns of GTG bands in the mother (46,XX), and paternal reciprocal translocation with breakpoints in 4p16.3 and 5p15.2 regions [46,XY,t(4;5)(p16.3;p15.2)]. The proband was identified with 4p16.3–p13 trisomy and 5p15.33–p15.2 monosomy [46,XX,der(5) t(4,5)(p16.3;p15.2)pat]. Fluorescence *in-situ* hybridization (FISH) analysis confirmed three fluorescence signals for the 4p16.3 band, and only one fluorescence signal in the 5p15.2 proband. CMA revealed duplication in chromosome 4 (41.1 Mb) encompassing the bands 4p16.3–p13. The approximate genomic position was defined in chr4:71552–41263831 (GRCh38/hg38), comprising 198 genes (**Figure 2A**). Chromosome 5 was outlined with a deletion of 14.7 Mb located between the bands 5p15.33 and p15.1. The genomic position was estimated in chr5:269963–15032936 (GRCh38/hg38), comprising 50 genes (**Figure 2B**).

LABORATORY INVESTIGATIONS

Cytogenetic Studies

Karyotyping was performed on metaphase spreads prepared from peripheral blood samples. The chromosomal analysis was conducted through GTG banding at a 550-band resolution, and at least 100 cells were analyzed. FISH experiments were performed following standard techniques with commercially available locus-specific probes such as a dual-color commercial probe for the CdCS and WHSCR (Cytocell, UK). The *CTNND2* probe for 5p15.2 (red spectrum) contains a sequence homologous to the D5S2883 locus and covers approximately 159 kb of this locus. The probe for the 4p16.3 (red spectrum) contained a sequence that was homologous to the D4S166 locus and covered approximately 223 kb of this locus. At least 30 cells were analyzed per hybridization. The sample was mapped using CMA, using a 60-mer oligonucleotide-based microarray with a theoretical resolution of 40 kb (8 × 60 K, Agilent Technologies Inc., Santa Clara, CA, USA). The arrays were analyzed using a microarray scanner (G2600D) and feature extraction software (version 9.5.1, Agilent Technologies). The images were analyzed using Cytogenomics v2.0 and v2.7 with the statistical algorithm ADM-2 and a sensitivity threshold of 6.0.

Network Design

The protein-protein interaction (PPI) metasearch engine STRING 11.0 (http://string-db.org/) was used to create PPI networks based on deleted or duplicated genes located in the altered chromosomal regions. CMA, with a subsequent search in the UCSC genome browser of the human genome assembly (December 2013), retrieved 591 genes and predicted genes

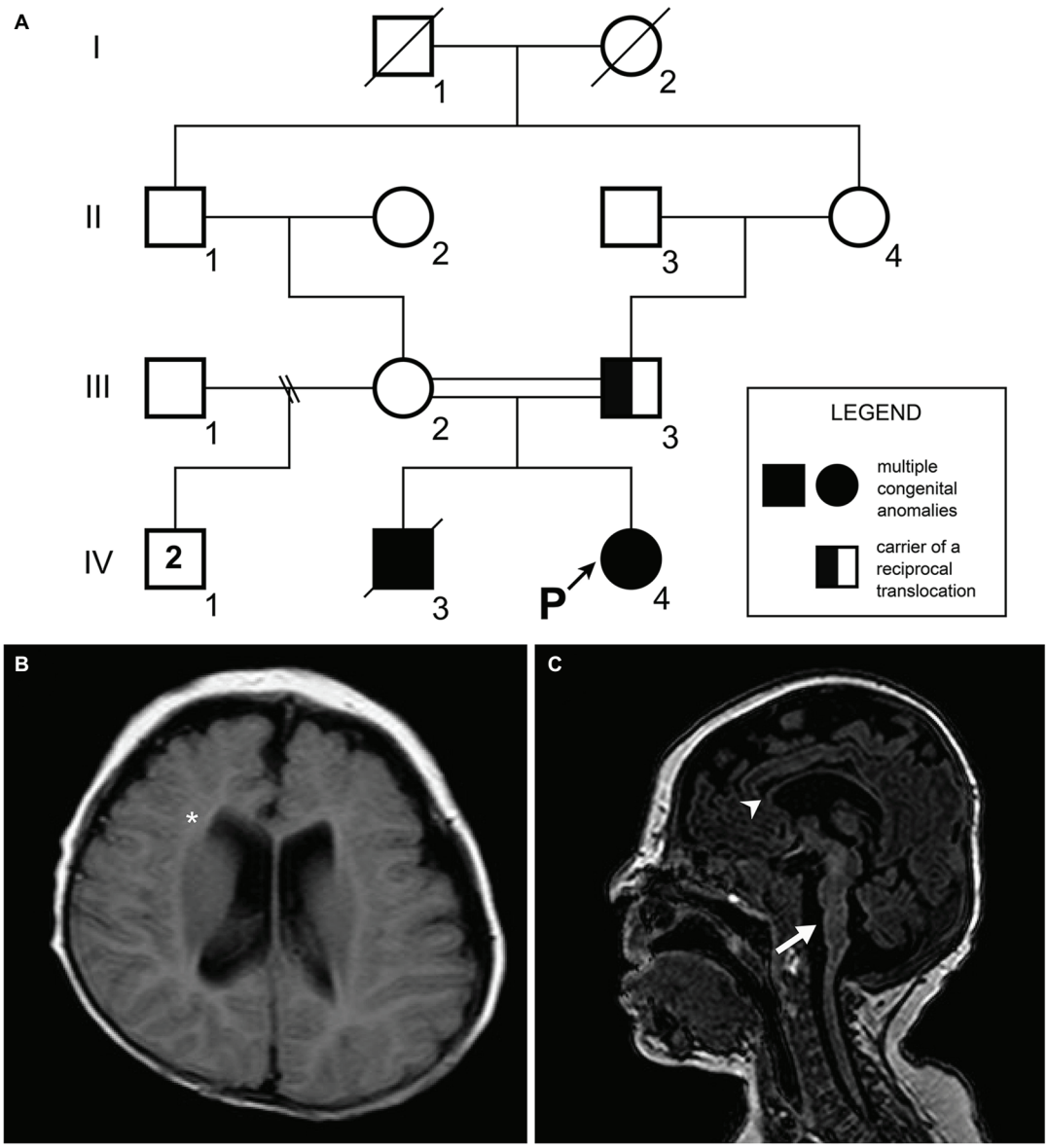

FIGURE 1 | (A) Patient's pedigree. A recessive trait was initially suspected on the basis of the parental consanguinity with recurrence in the offspring. The proband's father (individual III.3) was a carrier of a balanced chromosomal translocation. **(B)** Transverse FLAIR image. Notice the white matter volume loss (asterisk). **(C)** Sagittal T1 weighted image showing thin corpus callosum (arrowhead) and pontine hypoplasia with dysgenesis of the cerebellar vermis (arrow).

belonging to the duplicate area, as well as 246 from the deleted region (Kent et al., 1976; von Mering et al., 2005). The parameters used in STRING were: (i) degree of confidence, 0.400; (ii) 500 proteins in the first and second shell; and (iii) methods used were neighborhood, experiments, databases, and co-occurrence. The final PPI network was obtained through STRING and analyzed using Cytoscape 3.7.0 (Shannon et al., 2003).

GO and Centralities Analysis

The Gene Ontology (GO), Kyoto Encyclopedia of Genes and Genomes (KEGG), and Reactome libraries were searched using the ClueGO Cytoscape plugin (Bindea et al., 2009). Significant GO predictions were selected based on a $p \leq 0.05$, with the Bonferroni family-wise false discovery rate (FDR) test. Node degree and betweenness centralities were measured to identify hub-bottleneck (H-B) nodes from the PPI network using the Cytoscape plugin and CentiScaPe 3.2.1 (Scardoni et al., 2009).

Molecular Pathway Reconstruction

The PathLinker Cytoscape plugin was used to identify and reconstruct possible signaling pathways of interest from our PPI network (Murali et al., 2017). PathLinker computes the

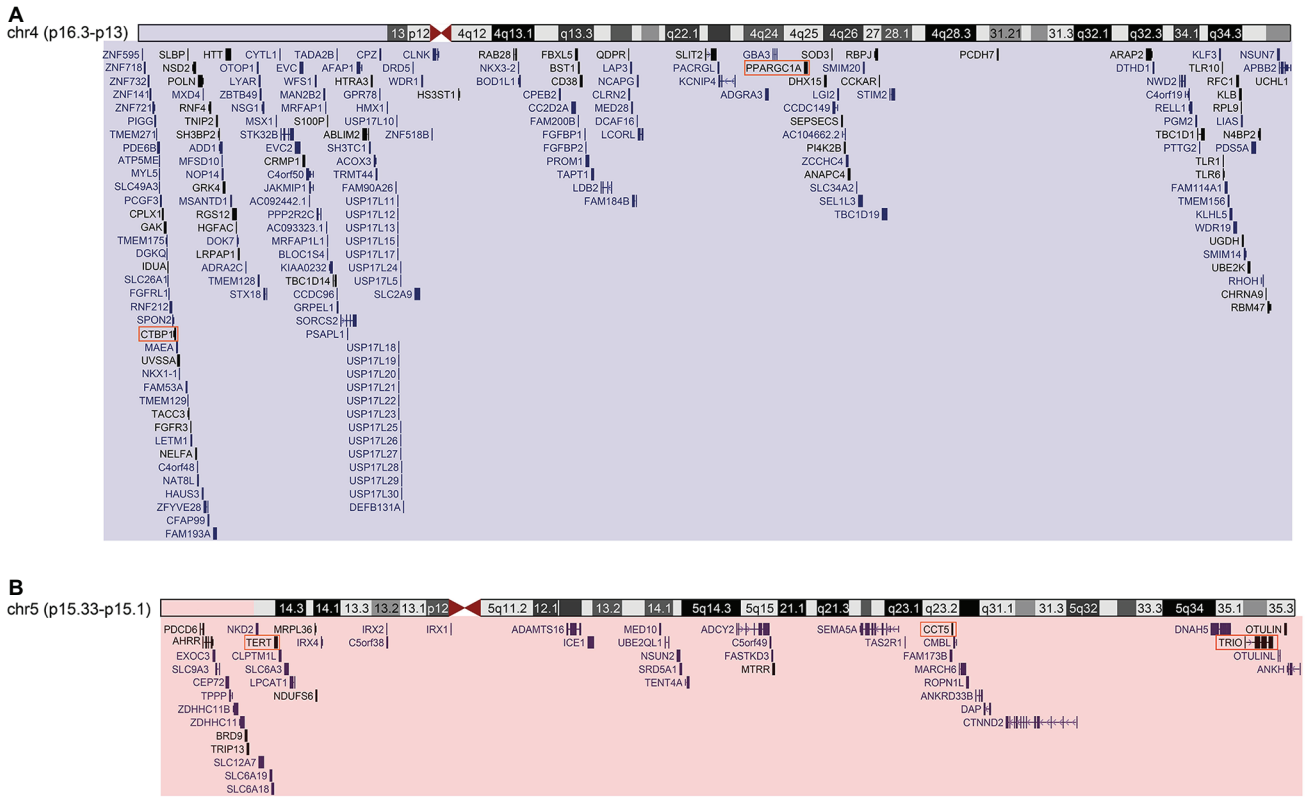

FIGURE 2 | (A) Cytogenomic profile of the region of chromosome 4 duplication. Segment duplicated highlighted in blue rectangle. UCSC-Genome Browser-Dec.2013 (GRCh38/hg38) – genomic position/search term: chr4:71552-41263831 – track: GENCODE V29. **(B)** Cytogenomic profile of the deleted region of chromosome 5. Segment deleted highlighted in red rectangle. UCSC-Genome Browser-Dec.2013 (GRCh38/hg38) – genomic position/search term: chr5:269963-15032936 – track: GENCODE V29. Orange squares are genes considered H-B.

k shortest paths that connect any source to any target in the network, and subsequently generates a subnetwork. It also creates a table with a rank of the shortest paths (Murali et al., 2018). The deleted gene network in the Cri-du-chat region (CdCR-Net) was used as a background, and the H-B CCT5, TERT, and TRIO were used as a source and targets for paths calculations. The parameters used in PathLinker were: (i) k: 50 (number of paths the user seeks); (ii) edge penalty: 1; and (iii) edge weight: weight probabilities, whereby it considers the edge weights as multiplicative, which result in the *k* highest cost paths (Murali et al., 2017).

DISCUSSION

Here, we have presented a patient with brain alterations and dysmorphic features resulting from chromosomal deletion in the critical region related to CdCS and duplication in the critical region related to WHS. The patient's clinical findings overlap with previously reported cases of both 4p duplication syndrome and CdCS (**Table 1**). Overall, the patients presentation is notably similar to CdCS patients as she presented with a weak, high-pitched voice and also showed similar pathogenicity observed in the brain MRI. Furthermore, the patient's anorectal malformations are also similar to what can be observed in certain cases of CdCS (Marcelis et al., 2011). Nevertheless, she presents with some features that are common to both conditions discussed, or those more frequently described in patients with abnormalities of the critical region of WHS.

To identify possible candidates that could help explain this scenario, a centrality analysis was carried out to identify H-B. These proteins represent nodes with high degree and betweenness scores, which are frequently related to the control of information flow between groups of proteins with central functions in a biological network (Hahn and Kern, 2005; Scardoni et al., 2009).

Two H-B were identified in the WHR-Net (**Supplementary Figure S1A**). The H-B PPARGC1A is a transcriptional coactivator of a subset of genes related to oxidative phosphorylation, which regulate glucose and lipid metabolism, mitochondrial biogenesis, and muscle fiber development (Terada et al., 2002; Tunstall et al., 2002; Puigserver and Spiegelman, 2003; Finck et al., 2006). As expected, and through the enrichment analysis, PPARGC1A was found to be associated with the regulation of progesterone synthesized in the biosynthetic pathway (**Supplementary Figure S1B**).

TABLE 1 | Comparison of the clinical manifestations of this patient, and previously reported patients with Cri-du-chat syndrome and Trisomy 4p syndrome.

Clinical manifestations	This patient	Cri-du-chat patients (Honjo, 2018; Mainardi, 2001)*	Trisomy 4p patients (Patel et al., 1995; Dallapiccola, 1977)*,**
Imperforate anus	Present	–	–
Preterm birth	Present	+	+
Micrognathia	Present	++	+
Low birth weight	Present	+	+
Psychomotor retardation	Present	++	++
Downslanting palpebral fissures	Present	++	++
Widely spaced eyes	Present	++	+
Abnormalities of the fingers	Present	++	++
Prominent heels	Present	–	++
Weak, high-pitched voice	Present	++	–
Growth deficiency	Present	++	++
Seizures	Present	+	+
Microcephaly	Present	++	++
Pontine hypoplasia	Present	++	–

*++, presence of the manifestation in 50% or more of the patients; +, presence of the manifestation in more than 10%, but less than 50% of the patients; –, not frequently reported. *Based on overall reported frequencies in patients with variable chromosomal breakpoints. **Most previously reported trisomy 4p patients also have other chromosomal imbalances and variable breakpoints.*

The deregulation of transcription and mitochondrial function caused by PPARGC1A is associated with conditions such as amyotrophic lateral sclerosis, Parkinson's disease, Alzheimer's disease, and Huntington's disease (Weydt et al., 2006; Eschbach et al., 2013; Jesse et al., 2017). Additionally, the second H-B, CTBP1 plays a role in the regulation of gene expression during embryonic development, as well as participation in axial patterning and cellular proliferation and differentiation (Hildebrand and Soriano, 2002; Van Hateren et al., 2006). A *de novo* heterozygous missense mutation in the *CTBP1* (R331W) causes hypotonia, developmental delay, ataxia, and intellectual disability (Beck et al., 2016, 2019). As heterozygous null variants of *CTBP1* are commonly found in unaffected individuals, gain of function rather than loss of function mechanisms are more likely to be associated with these clinical findings (Beck et al., 2019). Moreover, *PPARGC1A* and *CTBP1* are duplicated in the 4p region in the patients with neuropsychomotor delay, intellectual disability, and speech delay (**Figure 2A**; Cotter et al., 2001; Paskulin et al., 2009; Carmany and Bawle, 2011). Consequently, topological analysis indicates that the increased dosage of the *PPARGC1A* and *CTBP1* genes may have contributed to the neuropsychomotor delay and neurological alterations found in our patient (**Table 1**).

TRIO, TERT, and CCT5 were identified as H-B in the CdCR-Net (**Supplementary Figure S2A**). TRIO has functions in cell migration and morphogenesis during cerebellum development, including neurite and axon outgrowth (Briancon-Marjollet et al., 2008; Peng et al., 2010; Tao et al., 2019). *Trio* knockout causes reduction in the extension of granule neurons from the cerebellum and severe ataxia in mice (Peng et al., 2010). Furthermore, the *TRIO* haploinsufficiency in mice increases anxiety; impairs sociability and motor coordination, disrupts learning capacity and spatial memory, and decreases brain and neuron size (Zong et al., 2015; Katrancha et al., 2019). In this sense, the hemizygosity of *TRIO* may have contributed to the clinical findings in our patient at the age of 5 months, such as the thin corpus callosum, white matter volume loss, pontine hypoplasia, and dysgenesis of the cerebellar vermis (**Figures 1B,C**).

Moreover, damages in spatial memory are associated with TERT as its knockout in the hippocampus of adult mice impairs spatial memory processes during neural development (Zhou et al., 2017). The deficiency of *TERT* may also result in microvascular dysfunction in mice (Ait-Aissa et al., 2018). Furthermore, we found that TERT was associated with the negative regulation of apoptotic processes of endothelial cells in GO analysis (**Supplementary Figure S2B**). In addition, TERT shows interaction with CCT5 in the Y2H library screen (Wang et al., 2013). The H-B CCT5 is involved in cilia morphogenesis and survival of sensory neurons (Posokhova et al., 2011). Mutations in this gene may cause neurodegenerative diseases, such as spastic paraplegia and sensory neuropathy (Bouhouche et al., 2006; Pavel et al., 2016; Pereira et al., 2017). Additionally, *TERT* and *CCT5*, located in the critical region of CdCS, are associated with microcephaly and intellectual disability, reported in patients from several other studies (**Figure 2B**; Cerruti Mainardi, 2006). In this sense, deletion of *TERT* and *CCT5* genes could be involved with psychomotor retardation and microcephaly as presented in the present case (**Table 1**).

To investigate the importance of the H-B from CdCR-Net and their associated pathways (**Figure 3A**), we identified TRIO, GNG2, PRKACA, TUBA1A, and CCT5 as having the highest path score (**Figure 3B**). These proteins are involved in signaling mechanisms, including differentiation and proliferation, as well as roles in the formation and disposition of the cytoskeleton (Yajima et al., 2012; Tseng et al., 2017). In the latter case, TRIO, TUBA1A, and CCT5 play roles in the folding of actin and tubulin; reorganization; and assembly of the cytoskeleton during migration, growth, and differentiation of neurons (Seipel et al., 1999; Tian et al., 2010; Tracy et al., 2014). Genes that contribute to a common disorder tend to share core bioprocesses (**Figure 3C**; Goh et al., 2007). For instance, the chaperonin complex, CCT, which is also formed by the subunit CCT5, facilitates the formation of the heterodimeric form of the G-protein gamma subunits, similar to the GNG2 protein (Lukov et al., 2005). The formation of tubulin folding intermediates is also produced by CCT, in which unfolded actins and tubulins, such as TUBA1A are transferred to cytosolic chaperonin CCT (Frydman et al., 1992; McCormack et al., 2001). Interestingly, mutations or loss function of *TRIO*, *TUBA1A*, and *CCT5* is associated with intellectual

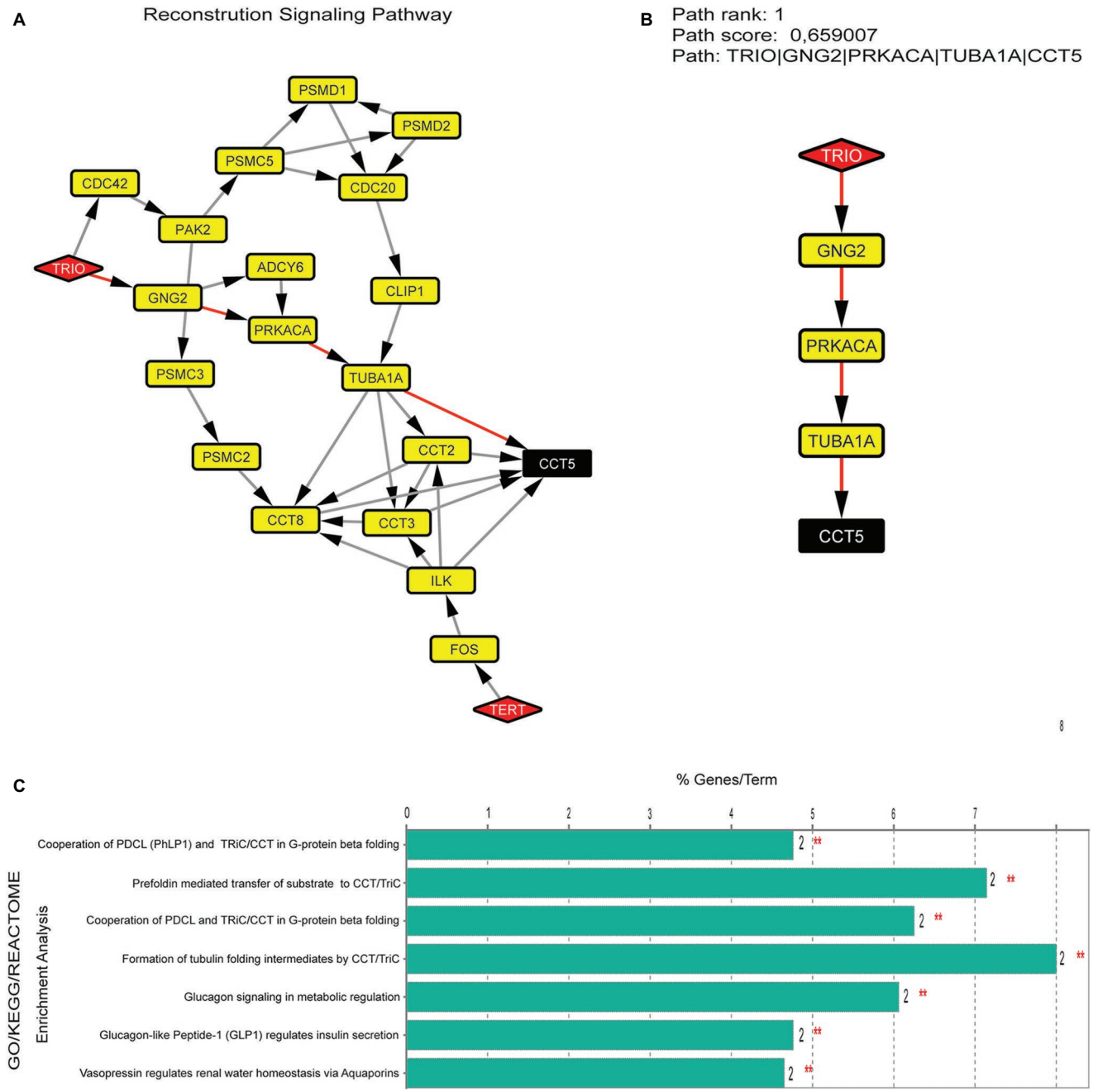

FIGURE 3 | (A) Signaling pathway identified between H-B (TRIO, CCT5, and TERT), using the Pathlinker plugin. **(B)** Pathway better ranked by path score between 50 possible pathways. **(C)** Enrichment analysis in proteins present in the pathway (TRIO, GNG2, PRKACA, TUBA1A, and CCT5).

disability, defects in dendritic branching, synapse function, sensory neuropathy, and microcephaly in humans (Bouhouche et al., 2006; Morris-Rosendahl et al., 2008; Kumar et al., 2010; Ba et al., 2016; Pavel et al., 2016; Pengelly et al., 2016; Belvindrah et al., 2017).

Essential human genes are expected to encode central proteins, such as the H-B genes, and be expressed in different tissues (Goh et al., 2007; Loscalzo and Barabasi, 2011). The haploinsufficiency of the H-B genes observed in our PPI-network could affect pathways related to the cilia morphogenesis, dendritic branching, and synapse function, including neurite and axon outgrowth, which consequently could have led to the neurodevelopment delay and microcephaly observed in our patient. In addition, the identification of CTBP1, PPARGC1A, CCT5, TERT, and TRIO with different approaches brought new insights on

the pathogenesis involved in these rare chromosomal rearrangements, such as those presented here, in a case never reported before.

DATA AVAILABILITY STATEMENT

All datasets generated for this study are included in the article/**Supplementary Material**.

ETHICS STATEMENT

The study includes a statement on ethics approval and consent. The study was approved by the Ethics in Research Committee of Hospital de Clínicas de Porto Alegre (HCPA), under the reference number 10-560. Written informed consent form was obtained from the guardians of the participant for the publication of this paper.

AUTHOR CONTRIBUTIONS

TC, BF and MR conceived, designed the study and analyzed all the data. FP analyzed the clinical data. All authors contributed to the writing manuscript. MR revised the manuscript.

FUNDING

TC was supported by Conselho Nacional de Desenvolvimento Científico e Tecnológico (CNPq). BF was also supported by CNPq (151680/2019-1).

SUPPLEMENTARY MATERIAL

The Supplementary Material for this article can be found online at: https://www.frontiersin.org/articles/10.3389/fgene.2020.00561/full#supplementary-material.

REFERENCES

Ait-Aissa, K., Kadlec, A. O., Hockenberry, J., Gutterman, D. D., and Beyer, A. M. (2018). Telomerase reverse transcriptase protects against angiotensin ii-induced microvascular endothelial dysfunction. *Am. J. Physiol. Heart Circ. Physiol.* 314, H1053–H1060. doi: 10.1152/ajpheart.00472.2017

Ba, W., Yan, Y., Reijnders, M. R. F., Schuurs-Hoeijmakers, J. H. M., Feenstra, I., Bongers, E. M. H. F., et al. (2016). TRIO loss of function is associated with mild intellectual disability and affects dendritic branching and synapse function. *Hum. Mol. Genet.* 25, 892–902. doi: 10.1093/hmg/ddv618

Beck, D. B., Cho, M. T., Millan, F., Yates, C., Hannibal, M., O'Connor, B., et al. (2016). A recurrent de novo CTBP1 mutation is associated with developmental delay, hypotonia, ataxia, and tooth enamel defects. *Neurogenetics* 17, 173–178. doi: 10.1007/s10048-016-0482-4

Beck, D. B., Subramanian, T., Vijayalingam, S., Ezekiel, U. R., Donkervoort, S., Yang, M. L., et al. (2019). A pathogenic CtBP1 missense mutation causes altered cofactor binding and transcriptional activity. *Neurogenetics* 20, 129–143. doi: 10.1007/s10048-019-00578-1

Belvindrah, R., Natarajan, K., Shabajee, P., Bruel-Jungerman, E., Bernard, J., Goutierre, M., et al. (2017). Mutation of the α-tubulin Tuba1a leads to straighter microtubules and perturbs neuronal migration. *J. Cell Biol.* 216, 2443–2461. doi: 10.1083/jcb.201607074

Bindea, G., Mlecnik, B., Hackl, H., Charoentong, P., Tosolini, M., Kirilovsky, A., et al. (2009). ClueGO: a Cytoscape plug-in to decipher functionally grouped gene ontology and pathway annotation networks. *Bioinformatics* 25, 1091–1093. doi: 10.1093/bioinformatics/btp101

Bouhouche, A., Benomar, A., Bouslam, N., Chkili, T., and Yahyaoui, M. (2006). Mutation in the epsilon subunit of the cytosolic chaperonin-containing t-complex peptide-1 (Cct5) gene causes autosomal recessive mutilating sensory neuropathy with spastic paraplegia. *J. Med. Genet.* 43, 441–443. doi: 10.1136/jmg.2005.039230

Briancon-Marjollet, A., Ghogha, A., Nawabi, H., Triki, I., Auziol, C., Fromont, S., et al. (2008). Trio mediates Netrin-1-induced Rac1 activation in axon outgrowth and guidance. *Mol. Cell. Biol.* 28, 2314–2323. doi: 10.1128/MCB.00998-07

Carmany, E. P., and Bawle, E. V. (2011). Microduplication of 4p16.3 due to an unbalanced translocation resulting in a mild phenotype. *Am. J. Med. Genet. Part A* 155, 819–824. doi: 10.1002/ajmg.a.33916

Cerruti Mainardi, P. (2006). Cri du Chat syndrome. *Orphanet J. Rare Dis.* 1, 1–9. doi: 10.1186/1750-1172-1-33

Cotter, P. D., Kaffe, S., Li, L., Gershin, I. F., and Hirschhorn, K. (2001). Loss of subtelomeric sequence associated with a terminal inversion duplication of the short arm of chromosome 4. *Am. J. Med. Genet.* 102, 76–80. doi: 10.1002/1096-8628(20010722)102:1<76::AID-AJMG1389>3.0.CO;2-4

Cyr, A. B., Nimmakayalu, M., Longmuir, S. Q., Patil, S. R., Keppler-Noreuil, K. M., and Shchelochkov, O. A. (2011). A novel 4p16.3 microduplication distal to WHSC1 and WHSC2 characterized by oligonucleotide array with new phenotypic features. *Am. J. Med. Genet. Part A* 155, 2224–2228. doi: 10.1002/ajmg.a.34120

Dallapiccola, B., Mastroiacovo, P. P., Montali, E., and Sommer, A. (1977). Trisomy 4p: five new observations and overview. *Clin. Genet.* 12, 344–356. doi: 10.1111/j.1399-0004.1977.tb00953.x

Eschbach, J., Schwalenstöcker, B., Soyal, S. M., Bayer, H., Wiesner, D., Akimoto, C., et al. (2013). PGC-1α is a male-specific disease modifier of human and experimental amyotrophic lateral sclerosis. *Hum. Mol. Genet.* 22, 3477–3484. doi: 10.1093/hmg/ddt202

Finck, B. N., Kelly, D. P., Finck, B. N., and Kelly, D. P. (2006). PGC-1 coactivators: inducible regulators of energy metabolism in health and disease. *J. Clin. Invest.* 116, 615–622. doi: 10.1172/JCI27794.PGC-1

Frydman, J., Nimmesgern, E., Erdjument-Bromage, H., Wall, J. S., Tempst, P., and Hartl, F. U. (1992). Function in protein folding of TRiC, a cytosolic ring complex containing TCP-1 and structurally related subunits. *EMBO J.* 11, 4767–4778. doi: 10.1002/j.1460-2075.1992.tb05582.x

Goh, K. I., Cusick, M. E., Valle, D., Childs, B., Vidal, M., and Barabási, A. L. (2007). The human disease network. *Proc. Natl. Acad. Sci. U. S. A.* 104, 8685–8690. doi: 10.1073/pnas.0701361104

Hahn, M. W., and Kern, A. D. (2005). Comparative genomics of centrality and essentiality in three eukaryotic protein-interaction networks. *Mol. Biol. Evol.* 22, 803–806. doi: 10.1093/molbev/msi072

Hannes, F., Drozniewska, M., Vermeesch, J. R., and Haus, O. (2010). Duplication of the Wolf-Hirschhorn syndrome critical region causes neurodevelopmental delay. *Eur. J. Med. Genet.* 53, 136–140. doi: 10.1016/j.ejmg.2010.02.004

Hildebrand, J. D., and Soriano, P. (2002). Overlapping and unique roles for C-terminal binding protein 1 (CtBP1) and CtBP2 during mouse development. *Mol. Cell. Biol.* 22, 5296–5307. doi: 10.1128/MCB.22.15.5296-5307.2002

Honjo, R. S., Mello, C. B., Pimenta, L. S. E., Nuñes-Vaca, E. C., Benedetto, L. M., Khoury, R. B. F., et al. (2018). Cri du Chat syndrome: Characteristics of 73 Brazilian patients. *J. Intellect. Disabil. Res.* 62, 467–473. doi: 10.1111/jir.12476

Jesse, S., Bayer, H., Alupei, M. C., Zügel, M., Mulaw, M., Tuorto, F., et al. (2017). Ribosomal transcription is regulated by PGC-1alpha and disturbed in Huntington's disease. *Sci. Rep.* 7, 1–10. doi: 10.1038/s41598-017-09148-7

Katrancha, S. M., Shaw, J. E., Zhao, A. Y., Myers, S. A., Cocco, A. R., Jeng, A. T., et al. (2019). Trio haploinsufficiency causes neurodevelopmental disease-associated deficits. *Cell Rep.* 26, 2805–2817.e9. doi: 10.1016/j.celrep.2019.02.022

Kent, W. J., Sugnet, C. W., Furey, T. S., and Roskin, K. M. (1976). The human genome browser at UCSC W. *J. Med. Chem.* 19, 1228–1231. doi: 10.1101/gr.229102

Kumar, R. A., Pilz, D. T., Babatz, T. D., Cushion, T. D., Harvey, K., Topf, M., et al. (2010). TUBA1A mutations cause wide spectrum lissencephaly (smooth brain) and suggest that multiple neuronal migration pathways converge on alpha tubulins. *Hum. Mol. Genet.* 19, 2817–2827. doi: 10.1093/hmg/ddq182

Loscalzo, J., and Barabasi, A. L. (2011). Systems biology and the future of medicine. *Wiley Interdiscip. Rev. Syst. Biol. Med.* 3, 619–627. doi: 10.1002/wsbm.144

Lukov, G. L., Hu, T., McLaughlin, J. N., Hamm, H. E., and Willardson, B. M. (2005). Phosducin-like protein acts as a molecular chaperone for G protein βγ dimer assembly. *EMBO J.* 24, 1965–1975. doi: 10.1038/sj.emboj.7600673

Mainardi, P. C., Perfumo, C., Calì, A., Coucourde, G., Pastore, G., Cavani, S., et al. (2001). Clinical and molecular characterisation of 80 patients with 5p deletion: genotype-phenotype correlation. *J. Med. Genet.* 38, 151–158. doi: 10.1136/jmg.38.3.151

Marcelis, C., de Blaauw, I., and Brunner, H. (2011). Chromosomal anomalies in the etiology of anorectal malformations: a review. *Am. J. Med. Genet. Part A* 155, 2692–2704. doi: 10.1002/ajmg.a.34253

McCormack, E. A., Llorca, O., Carrascosa, J. L., Valpuesta, J. M., and Willison, K. R. (2001). Point mutations in a hinge linking the small and large domains of β-actin result in trapped folding intermediates bound to cytosolic chaperonin CCT. *J. Struct. Biol.* 135, 198–204. doi: 10.1006/jsbi.2001.4385

Morris-Rosendahl, D. J., Najm, J., Lachmeijer, A. M. A., Sztriha, L., Martins, M., Kuechler, A., et al. (2008). Refining the phenotype of α-1a tubulin (TUBA1A) mutation in patients with classical lissencephaly. *Clin. Genet.* 74, 425–433. doi: 10.1111/j.1399-0004.2008.01093.x

Murali, T. M., Gil, D. P., and Law, J. N. (2017). The PathLinker app: connect the dots in protein interaction networks. *F1000Res.* 6, 1–12. doi: 10.12688/f1000research.9909.1

Murali, T. M., Huang, L. J., and Law, J. N. (2018). Automating the PathLinker app for Cytoscape. *F1000Res.* 7, 1–9. doi: 10.12688/f1000research.14616.1

Nguyen, J. M., Qualmann, K. J., Okashah, R., Reilly, A., Alexeyev, M. F., and Campbell, D. J. (2015). 5p deletions: current knowledge and future directions. *Am. J. Med. Genet. Part C Semin. Med. Genet.* 169, 224–238. doi: 10.1002/ajmg.c.31444

Paskulin, G. A., Riegel, M., Cotter, P. D., Kiss, A., Rosa, R. F. M., Zen, P. R. G., et al. (2009). Inv dup del(4)(:p13→p16.3::p16.3→qter) in a girl without typical manifestations of wolf-Hirschhorn syndrome. *Am. J. Med. Genet. Part A* 149, 1302–1307. doi: 10.1002/ajmg.a.32888

Patel, S. V., Dagnew, H., Parekh, A. J., Koenig, E., Conte, R. A., Macera, M. J., et al. (1995). Clinical manifestations of trisomy 4p syndrome. *Eur. J. Pediatr.* 154, 425–431. doi: 10.1007/BF02029349

Pavel, M., Imarisio, S., Menzies, F. M., Jimenez-Sanchez, M., Siddiqi, F. H., Wu, X., et al. (2016). CCT complex restricts neuropathogenic protein aggregation via autophagy. *Nat. Commun.* 7:13821. doi: 10.1038/ncomms13821

Peng, Y. J., He, W. Q., Tang, J., Tao, T., Chen, C., Gao, Y. Q., et al. (2010). Trio is a key guanine nucleotide exchange factor coordinating regulation of the migration and morphogenesis of granule cells in the developing cerebellum. *J. Biol. Chem.* 285, 24834–24844. doi: 10.1074/jbc.M109.096537

Pengelly, R. J., Greville-Heygate, S., Schmidt, S., Seaby, E. G., Jabalameli, M. R., Mehta, S. G., et al. (2016). Mutations specific to the Rac-GEF domain of TRIO cause intellectual disability and microcephaly. *J. Med. Genet.* 53, 735–742. doi: 10.1136/jmedgenet-2016-103942

Pereira, J. H., McAndrew, R. P., Sergeeva, O. A., Ralston, C. Y., King, J. A., and Adams, P. D. (2017). Structure of the human TRiC/CCT subunit 5 associated with hereditary sensory neuropathy. *Sci. Rep.* 7, 1–9. doi: 10.1038/s41598-017-03825-3

Perfumo, C., Mainardi, P., Cali, A., Coucourde, G., Zara, F., Cavani, S., et al. (2000). The first three mosaic Cri du chat syndrome patients with two rearranged cell lines. *J. Med. Genet.* 37, 967–972. doi: 10.1136/jmg.37.12.967

Posokhova, E., Song, H., Belcastro, M., Higgins, L., Bigley, L. R., Michaud, N. A., et al. (2011). Disruption of the chaperonin containing TCP-1 function affects protein networks essential for rod outer segment morphogenesis and survival. *Mol. Cell. Proteomics* 10:M110.000570. doi: 10.1074/mcp.M110.000570

Puigserver, P., and Spiegelman, B. M. (2003). Peroxisome proliferator-activated receptor-γ coactivator 1α (PGC-1α): transcriptional coactivator and metabolic regulator. *Endocr. Rev.* 24, 78–90. doi: 10.1210/er.2002-0012

Scardoni, G., Petterlini, M., and Laudanna, C. (2009). Analyzing biological network parameters with CentiScaPe. *Bioinformatics* 25, 2857–2859. doi: 10.1093/bioinformatics/btp517

Seipel, K., Medley, Q. G., Kedersha, N. L., Zhang, X. A., O'Brien, S. P., Serra-Pages, C., et al. (1999). Trio amino-terminal guanine nucleotide exchange factor domain expression promotes actin cytoskeleton reorganization, cell migration and anchorage-independent cell growth. *J. Cell Sci.* 112, 1825–1834.

Shannon, P., Markiel, A., Ozier, O., Baliga, N. S., Wang, J. T., Ramage, D., et al. (2003). Cytoscape: a software environment for integrated models of biomolecular interaction networks. *Genome Res.* 13, 2498–2504. doi: 10.1101/gr.1239303

Tao, T., Sun, J., Peng, Y., Wang, P., Chen, X., Zhao, W., et al. (2019). Distinct functions of Trio GEF domains in axon outgrowth of cerebellar granule neurons. *J. Genet. Genomics* 46, 87–96. doi: 10.1016/j.jgg.2019.02.003

Terada, S., Goto, M., Kato, M., Kawanaka, K., Shimokawa, T., and Tabata, I. (2002). Effects of low-intensity prolonged exercise on PGC-1 mRNA expression in rat epitrochlearis muscle. *Biochem. Biophys. Res. Commun.* 296, 350–354. doi: 10.1016/S0006-291X(02)00881-1

Tian, G., Jaglin, X. H., Keays, D. A., Francis, F., Chelly, J., and Cowan, N. J. (2010). Disease-associated mutations in TUBA1A result in a spectrum of defects in the tubulin folding and heterodimer assembly pathway. *Hum. Mol. Genet.* 19, 3599–3613. doi: 10.1093/hmg/ddq276

Tracy, C. M., Gray, A. J., Cuellar, J., Shaw, T. S., Howlett, A. C., Taylor, R. M., et al. (2014). Programmed cell death protein 5 interacts with the cytosolic chaperonin containing tailless complex polypeptide 1 (CCT) to regulate β-tubulin folding. *J. Biol. Chem.* 289, 4490–4502. doi: 10.1074/jbc.M113.542159

Tseng, I. C., Huang, W. J., Jhuang, Y. L., Chang, Y. Y., Hsu, H. P., and Jeng, Y. M. (2017). Microinsertions in PRKACA cause activation of the protein kinase a pathway in cardiac myxoma. *J. Pathol.* 242, 134–139. doi: 10.1002/path.4899

Tunstall, R. J., Mehan, K. A., Wadley, G. D., Collier, G. R., Bonen, A., Hargreaves, M., et al. (2002). Exercise training increases lipid metabolism gene expression in human skeletal muscle. *Am. J. Physiol. Endocrinol. Metab.* 283, 66–72. doi: 10.1152/ajpendo.00475.2001

Van Hateren, N., Shenton, T., and Borycki, A. G. (2006). Expression of avian C-terminal binding proteins (Ctbp1 and Ctbp2) during embryonic development. *Dev. Dyn.* 235, 490–495. doi: 10.1002/dvdy.20612

von Mering, C., Jensen, L. J., Snel, B., Hooper, S. D., Krupp, M., Foglierini, M., et al. (2005). STRING: known and predicted protein-protein associations, integrated and transferred across organisms. *Nucleic Acids Res.* 33, 433–437. doi: 10.1093/nar/gki005

Wang, W., Yang, L., Hu, L., Li, F., Ren, L., Yu, H., et al. (2013). Inhibition of UBE2D3 expression attenuates radiosensitivity of MCF-7 human breast cancer cells by increasing hTERT expression and activity. *PLoS One* 8:e64660. doi: 10.1371/journal.pone.0064660

Weydt, P., Pineda, V. V., Torrence, A. E., Libby, R. T., Satterfield, T. F., Lazarowski, E. R. R., et al. (2006). Thermoregulatory and metabolic defects in Huntington's disease transgenic mice implicate PGC-1α in Huntington's disease neurodegeneration. *Cell Metab.* 4, 349–362. doi: 10.1016/j.cmet.2006.10.004

Yajima, I., Kumasaka, M. Y., Tamura, H., Ohgami, N., and Kato, M. (2012). Functional analysis of GNG2 in human malignant melanoma cells. *J. Dermatol. Sci.* 68, 172–178. doi: 10.1016/j.jdermsci.2012.09.009

Zhou, Q. G., Liu, M. Y., Lee, H. W., Ishikawa, F., Devkota, S., Shen, X. R., et al. (2017). Hippocampal TERT regulates spatial memory formation through modulation of neural development. *Stem Cell Reports* 9, 543–556. doi: 10.1016/j.stemcr.2017.06.014

Zollino, M., Murdolo, M., Marangi, G., Pecile, V., Galasso, C., Mazzanti, L., et al. (2008). On the nosology and pathogenesis of wolf-Hirschhorn syndrome: genotype-phenotype correlation analysis of 80 patients and literature review. *Am. J. Med. Genet. Part C Semin. Med. Genet.* 148, 257–269. doi: 10.1002/ajmg.c.30190

Zong, W., Liu, S., Wang, X., Zhang, J., Zhang, T., Liu, Z., et al. (2015). Trio gene is required for mouse learning ability. *Brain Res.* 1608, 82–90. doi: 10.1016/j.brainres.2015.02.040

Conflict of Interest: The authors declare that the research was conducted in the absence of any commercial or financial relationships that could be construed as a potential conflict of interest.

frontiers in Genetics

REVIEW
published: 20 August 2020
doi: 10.3389/fgene.2020.00903

Understanding the Interplay Between Health Disparities and Epigenomics

*Viviana J. Mancilla[1†], Noah C. Peeri[2†], Talisa Silzer[1†], Riyaz Basha[3,4], Martha Felini[3,4], Harlan P. Jones[1,4], Nicole Phillips[1,4], Meng-Hua Tao[2,4], Srikantha Thyagarajan[1,4] and Jamboor K. Vishwanatha[1,4]**

[1] Department of Microbiology, Immunology and Genetics, Graduate School of Biomedical Sciences, University of North Texas Health Science Center, Fort Worth, TX, United States, [2] Department of Biostatistics and Epidemiology, School of Public Health, University of North Texas Health Science Center, Fort Worth, TX, United States, [3] Department of Pediatrics, Texas College of Osteopathic Medicine, University of North Texas Health Science Center, Fort Worth, TX, United States, [4] Texas Center for Health Disparities, University of North Texas Health Science Center, Fort Worth, TX, United States

OPEN ACCESS

Edited by:
Tesfaye B. Mersha,
Cincinnati Children's Hospital Medical Center, United States

Reviewed by:
Janine M. LaSalle,
University of California, Davis, United States
Mark Nicholas Cruickshank,
The University of Western Australia, Australia
Sarah Martin Merrill,
The University of British Columbia, Canada

***Correspondence:**
Jamboor K. Vishwanatha
Jamboor.Vishwanatha@unthsc.edu

[†] These authors have contributed equally to this work

Specialty section:
This article was submitted to Epigenomics and Epigenetics, a section of the journal Frontiers in Genetics

Received: 27 November 2019
Accepted: 21 July 2020
Published: 20 August 2020

Citation:
Mancilla VJ, Peeri NC, Silzer T, Basha R, Felini M, Jones HP, Phillips N, Tao M-H, Thyagarajan S and Vishwanatha JK (2020) Understanding the Interplay Between Health Disparities and Epigenomics. Front. Genet. 11:903. doi: 10.3389/fgene.2020.00903

Social epigenomics has emerged as an integrative field of research focused on identification of socio-environmental factors, their influence on human biology through epigenomic modifications, and how they contribute to current health disparities. Several health disparities studies have been published using genetic-based approaches; however, increasing accessibility and affordability of molecular technologies have allowed for an in-depth investigation of the influence of external factors on epigenetic modifications (e.g., DNA methylation, micro-RNA expression). Currently, research is focused on epigenetic changes in response to environment, as well as targeted epigenetic therapies and environmental/social strategies for potentially minimizing certain health disparities. Here, we will review recent findings in this field pertaining to conditions and diseases over life span encompassing prenatal to adult stages.

Keywords: epigenetics, cancer, health disparities, chronic disease, social determinants of health

INTRODUCTION

Social epigenomics is defined as the study of how social experiences affect our genes and biology. Though social epigenomics is a relatively new area of research, studies exploring the individual and combinatorial influence of social, environmental, and genetic factors on health have become increasingly abundant. Social epigenomics is uniquely positioned at the intersection of population health and precision medicine, allowing us to understand how exposure to social and environmental stressors modifies the way in which genes are expressed and ultimately alter our risk for disease. This area of research is important when it comes to understanding the biological effects of environmental (e.g., food availability, pollution, green space, etc.) or social stressors (e.g., abuse, socioeconomic stress, etc.) and how they contribute to the rising health disparities commonly affecting minority communities; however, health disparities within minority populations have not been well addressed using epigenetic approaches. This space has gained increasing interest over recent years, as reflected by the $26.2 million-dollar National Institutes of Health (NIH) initiative entitled Social Epigenomics Research Focused on Minority Health and Health Disparities that was introduced in 2017.

Several recent and exciting discoveries have been made in the area of social epigenomics, which have allowed researchers to slowly disentangle the roles that social, environmental, and genetic factors may play on health and disease risk. The areas reviewed here are: (1) key social

determinants of health, (2) common epigenetic mechanisms that affect human biology, (3) intersection of social determinants and epigenetics over the human life span, and (4) challenges and current limitations of social epigenomic studies.

KEY SOCIAL DETERMINANTS OF HEALTH

Social determinants of health can be viewed as "conditions in the environments in which people are born, live, learn, work, play, worship, and age"; these conditions influence health outcomes throughout the life course and in a multitude of ways (Institute of Medicine et al., 2006; Office of Disease Prevention and Health Promotion, 2020). Many of these determinants are intertwined, revealing a complex web of interconnected relationships, with both a direct and indirect impact on population health. Several key factors encompass the broad definition of social determinants including family and neighborhood effects, exposure to chronic stress, socioeconomic status (SES), educational attainment, access to health care, job availability, and exposure to crime and violence (Braveman and Gottlieb, 2014). Neighborhood effects can refer to the physical environment where an individual or family lives, or the social environment, which can be defined by a vast state of relationships between individuals within a neighborhood (Chaix, 2009). With respect to the physical environment, in urban and disadvantaged neighborhoods, epidemiologic studies consistently report that exposure to pollutants and allergens leads to worsening lung health (discussed in further detail in the early-life section) (Braveman and Gottlieb, 2014). Furthermore, in disadvantaged neighborhoods, there tends to be higher availability of alcohol, tobacco, fast-food restaurants, combined with lower availability of healthy food options (i.e., food deserts) and areas for recreation which lead to worse health outcomes (Braveman and Gottlieb, 2014). This leads to increased intake of unhealthy foods, less opportunity for physical activity, and as a result of alcohol consumption, an increased risk for alcohol-related traumatic injury (Braveman and Gottlieb, 2014). Furthermore, increased exposure to chronic stress in these populations has been associated with epigenetic changes and has been theorized, in part, due to a lack of social and familial support networks for coping (Cunliffe, 2016). Individual-level and neighborhood-level effects are closely intertwined and likely reciprocally influence one another. Disease is naturally an individual-level event, and as such, neighborhood-level influences exert their effects through behaviors and biologic processes (Diez Roux, 2001). For example, the availability (or lack thereof) of healthy food options in a neighborhood may drive individual-level choices for nutrition, leading to increased intake of polyunsaturated fats which may generate mutagenic free radical and oxidative stress (Bartsch and Nair, 2004; Alegría-Torres et al., 2011). This, in turn, may lead to epigenetic alterations that affect downstream biological processes, ultimately manifesting in disease (e.g., oxidative stress-induced lung cancer) (Lawless et al., 2009), though the underlying biology is often much more complex. In the context of neighborhood effects, home-level effects present another domain within which disparities can occur. The impact of poor housing conditions on health has been extensively studied (Krieger and Higgins, 2002); for example, the impact of indoor air quality on the risk or exacerbation of asthma. Studies have found that the onset and severity of asthma may be affected by interactions between the physical environment and epigenetic factors (e.g., *ADRB2 5'-UTR* methylation) (Fu et al., 2012). As a result of differences in the social determinants of health between populations, health disparities are commonplace. One proposed mechanism connecting these determinants with health outcomes is epigenetics. However, research focusing on the interplay between epigenetic (or epigenomic) changes and these determinants is limited. Epigenetics by no means fully explains these disparities, though it provides insight into the interplay between the environment and genetics in the context of disease risk, pathology, and severity.

Differences in the distribution of these social determinants are evident in the United States. Health disparities exist in many forms, including higher rates of chronic disease and premature death among minority racial and ethnic groups when compared to Caucasians, although the trends are not universal (National Academies of Sciences et al., 2017). Interestingly, in some minority groups, for example, Hispanic immigrants, better health outcomes are seen when compared to non-Hispanic whites (known as the "immigrant paradox"); however, this association diminishes as time spent in the United States increases (National Academies of Sciences et al., 2017). A stepwise socioeconomic gradient has recently been observed in the United States, overall and within racial and ethnic groups, with improvements in health increasing as social advantage increases (measured by SES); those among the most affluent and educated have the best health outcomes, while those with moderate and low income have worse health outcomes (Braveman et al., 2011). These social determinants may play a significant role in influencing overall health and disease risk potentially *via* epigenetic modifications affecting downstream molecular processes.

COMMON EPIGENETIC MECHANISMS THAT AFFECT HUMAN BIOLOGY

Since the mid-20th century when Waddington first introduced the concept of epigenetics, its definition has transformed, reflecting our increase in understanding of the molecular mechanisms underlying human biology from conception to death; for a recent review on the history of epigenetics terminology and findings, refer to Felsenfeld (2014). Epigenetics is presently defined as mitotically inheritable modifications to DNA that do not directly alter the sequence. These modifications can be *de novo* or inherited *via* genetic imprinting. Though epigenetic signatures are well known for their role in determining cell fate, epigenetic marks can also change in response to genetic and environmental factors over time, resulting in subsequent biological changes that may be tissue or cell type specific. The mechanisms responsible for regulating these modifications are capable of altering gene expression at multiple levels (e.g.,

transcriptional, post-transcriptional, translational, and post-translational).

DNA Methylation

DNA methylation is one of the most extensively studied epigenetic modifications. Several different types of DNA methylation exist [e.g., 5-methylcytosine (5-mC), 5-hydroxymethylcytosine (5-hmC)]; however, here, we will only review the most common form, 5-mC. This modification is characterized by the addition of methyl groups to the fifth position carbon of cytosine nucleotides; often, these cytosines are located adjacent to guanine (this position is termed a "CpG site"). Of the different regions within the human genome, gene promoters are typically enriched for C-G dinucleotides, yielding regions called "CpG islands." DNA methyltransferases (DNMTs) transfer donated methyl groups from S-Adenosyl Methionine (SAM) complexes to target sites; DNMT1 enzymes serve to maintain pre-existing sites, while DNMT3A and DNMT3B transferases serve to establish *de novo* methylation marks. Though methylation within promoter regions is often negatively correlated, methylation within the gene body has been found to be positively correlated with gene expression, suggesting site-specific effects (Jones et al., 2015). Further, DNA methylation patterns are known to be tissue specific and highly conserved; interestingly, this conservation is thought to be controlled, in part, by DNA sequence at transcription factor binding sites (Zhou et al., 2017). For a recent review on the effects of DNA methylation on transcription factor binding, refer to Héberlé and Bardet (2019).

Histone Modifications

Eukaryotic chromatin structure consists of highly condensed, repeating "bead-like" structures called nucleosomes, which are units composed of approximately 147 base pairs of DNA wound around an octomeric histone core (consisting of two copies each of H2A, H2B, H3, and H4 histones) with linker histones (H1) connecting octamers of neighboring nucleosomes. Regulation of gene expression at the chromatin level can occur through chromatin remodeling (e.g., Swi/Snf complexes) and/or addition of covalent modifications such as acetyl, methyl, ubiquitin, phosphate, and biotin groups to basic (e.g., lysine, arginine) residues embedded in exposed histone N-terminal tails. As histone proteins play a significant role in DNA packaging, alterations to side chains can impact transcriptional activation/repression and efficiency of DNA repair mechanisms (Shen et al., 2006). Addition and removal of these modifications are regulated by enzymes termed "writers" and "erasers," respectively, while the downstream effects of these modifications on gene expression are interpreted and dictated by protein factors termed "readers" (Gillette and Hill, 2015).

The most extensively studied histone modifications are acetylation and methylation, which have both direct and indirect effects on transcription (Bannister and Kouzarides, 2011). The action of each modification is regulated by enzymes termed "readers," "writers," and "erasers." Acetylation status is primarily regulated by histone acetyltransferases (HATs) and histone deacetylases (HDACs). Acetyl groups added to lysine residues by HATs are typically read by small bromodomain proteins and allow for neutralization of the positive charge, leading to subsequent weakening of histone–DNA interactions and relaxation of chromatin structure (Marmorstein and Zhou, 2014). This provides regulatory and transcription factors with propensity for DNA to bind and enhance transcription. Though acetylation occurs throughout multiple regions of the genome, promoter and enhancer regions are often enriched with histone acetylation marks (Bannister and Kouzarides, 2011). Conversely, histone methylation status is primarily regulated by histone methyltransferases (HMTs) and histone demethylases (HDMs). Methyl groups are donated by SAM and transferred by HMTs to H3 and H4 arginine and lysine side chains, which are then read by a variety of different protein readers (depending on location and number of methyl groups) (Musselman et al., 2012). These methyl marks promote both transcriptional repression and activation, depending on the genomic context, by regulating DNA supercoiling (Barski et al., 2007).

The biological consequences of these modifications are further complicated, as there is evidence to suggest that chromatin structure varies based on type, location, and number of modifications, including cross-talk effects among different modification types (Molina-Serrano et al., 2013). For example, trimethylation of H3 lysine residues (H3K4me3) has been shown to occur only in the absence of H3 arginine dimethylation (H3R2me2a) (Molina-Serrano et al., 2013). Though histone modifications are important for various developmental processes, dysregulation or changes in the patterns of these epigenomic marks have also been implicated in aging and several diseases.

Micro-RNAs and Long Non-coding RNAs

Both micro-RNAs (miRNAs) and long non-coding RNAs (LncRNAs) play important roles in regulating gene expression. MiRNAs range in size from approximately 22 to 26 nucleotides in length. They contain 2–7 base pairs of complementary sequence (termed "seed sequence") that bind to a stretch of nucleotides, often in the 3'-untranslated region (3'-UTR) of the target mRNA [though ubiquitous binding to other gene regions has been observed (O'Brien et al., 2018)], leading to either degradation of the transcript or inhibition of translation. Often, members of the same miRNA families, or rather those with similar seed sequences, target the same gene families or biological pathways (Backes et al., 2018). LncRNAs are >200 nucleotides in length and can influence gene expression through chromatin remodeling as well as interaction with transcriptional and post-transcriptional processing machineries (Cao, 2014).

INTERSECTION OF SOCIAL DETERMINANTS AND EPIGENETICS OVER THE HUMAN LIFE SPAN

Epigenetic modifications are dynamic in nature, and their patterns have been observed to change in response to environmental and psychosocial factors and have also been implicated in several disease states. These changes can occur at the level of chromatin, DNA, and RNA as highlighted in the

previous section. These modifications also exhibit high levels of plasticity throughout the course of the human life span, though this plastic nature inevitably slows over time. Here, we briefly review recent findings implicating the intersection of social determinants and epigenetics, though this review is not exhaustive.

Figure 1 highlights the complex nature of health disparities over the human life span. Race/ethnicity or underlying ancestral genetic variation may be associated with risk for particular conditions but may also drive epigenetic alterations (not shown) that later contribute to disease risk and/or pathology. Regardless of genetic factors, social determinants of health, in combination with a variety of environmental exposures over time, may also contribute to disease risk.

Early Life

Prenatal Alcohol Exposure

Prenatal exposure to toxic agents, such as alcohol, radiation, environmental pollution, and maternal infections, can lead to a range of adverse developmental outcomes. *In utero*-derived disorders can be difficult to discuss and diagnose as mothers can become focal points of blame, sometimes leading to dishonest or reserved discussions between the mother and health care provider. For example, exposure to alcohol early in pregnancy can have the most detrimental effects. However, most mothers who drink early in pregnancy often do not know that they are pregnant at the time or may not report drinking while being pregnant due to social consequences. This prevents proper and timely diagnosis of a child who may be showing early signs of fetal alcohol spectrum disorder (FASD), classically characterized by neurocognitive deficiencies, impaired self-regulation, and adaptive function; these characteristics can also persist into adulthood (Lussier et al., 2017).

Fetal alcohol spectrum disorder was first described by Jones and Smith (1973) in 1973 and broadly includes several neurodevelopmental disorders described by physical, cognitive, memory, behavioral, and learning difficulties. Hallmarks of FASD include congenital malformations, deformities, chromosomal abnormalities, and mental/behavioral conditions. These issues persist throughout the afflicted child's lifetime which is often shortened and includes premature onset of chronic disease. Although FASD may not affect all who are prenatally exposed to alcohol, worldwide prevalence is estimated to be approximately 1–5% (May et al., 2009; Lange et al., 2017). Further breakdown of FASD demographics within developed countries highlights a major health disparity, whereby groups most affected tend to be of lower income and/or belong to a minority. Notably, Inuit

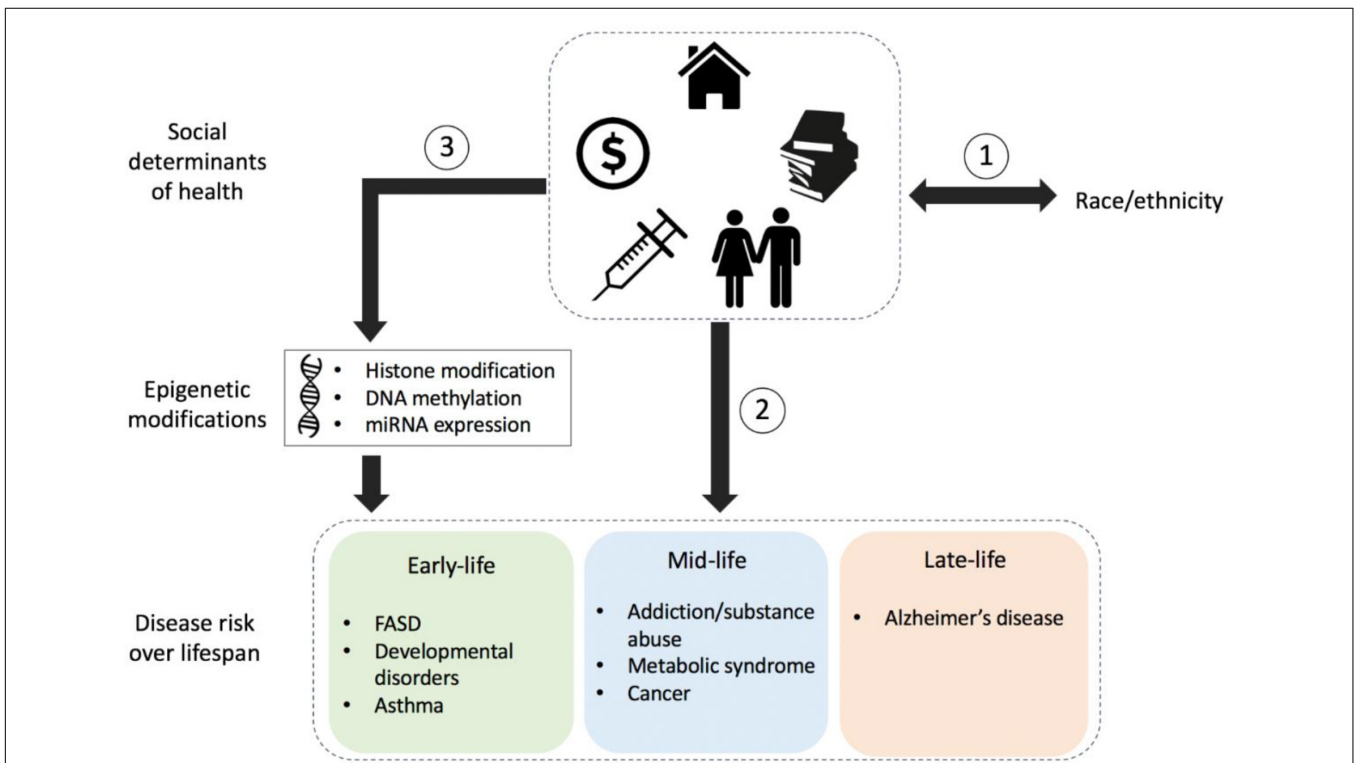

FIGURE 1 | Schematic detailing the influence of socio-environmental factors on health and risk for disease. (1) Race/ethnicity is often associated with an individual's social determinants of health including local neighborhood, social environment, education levels, socioeconomic status, and access to health care. (2) The social determinants of health can influence the risk for disease throughout the lifetime, regardless of genetics; however, (3) they can also influence epigenetic modifications such as those to histones, DNA, or micro-RNA (miRNA), thereby influencing biological functions that have downstream effects on health and disease susceptibility throughout the life span. Conditions and/or diseases within the colored boxes indicate socio-epigenomic links at different stages throughout the human life span: early-life, mid-life, and late-life; conditions detailed here are not exhaustive. FASD, fetal alcohol spectrum disorder.

and Native Americans hold the highest rate of FASD followed by African Americans (Tenkku et al., 2009). Interestingly, Hispanic females vary in risk depending on origin of birth. According to a review by Bakhireva et al. (2009), Latinas born in the United States were shown to be more likely to drink when compared to Latinas born outside of the country due to differences in cultural norms. Several explanations for this observation have been proposed including higher education and income and loss of traditional community leading to an increased rate of unhealthy behaviors. On the other hand, immigrants may also experience increased alcohol consumption due to the stress of assimilation. Current estimates of FASD occurrence are believed to be an underestimation due to several reasons including the fact that assessment relies on mothers to report drinking, which again is shrouded in stigma, thus delaying the diagnostic process. A recent review describes that although individuals with higher SES may drink about as much if not more than individuals with lower SES, they do not experience as many of the negative outcomes of alcohol consumption (Collins, 2016). It is suggested that although further studies are required to determine the mechanisms, the outcomes may be moderated by race, ethnicity, and gender.

Recent rodent models have identified altered DNA methylation patterns in protocadherin genes and deregulation of genes possibly due to prenatal alcohol exposure with follow-up buccal swabs from children showing similar patterns (Laufer et al., 2017). For example, upon alcohol exposure, embryo growth was restricted due to hypomethylation of the regulatory region of the *H19* gene present in the human placenta, suggesting the incidence of genomic imprinting (Haycock and Ramsay, 2009).

In response to the lack of investigation into the social impact of FASD diagnosis, efforts have been made to promote studies in this field of research. Translating to the Community (T2C) is an initiative established by researchers at the University of Manitoba and is the first Canadian social epigenetic biobank for Aboriginal communities that are known to have a disproportionate prevalence of FASD (Elias et al., 2018). The biobank is focused on the collection of biological samples (e.g., saliva, blood), social-contextual health-survey data, and clinical data in order to identify risk factors, social and biological pathways implicated in FASD. Efforts such as T2C may allow for a better understanding of the biological basis of FASD and identification of environmental and/or societal factors that increase the risk for FASD and have led to current disparities. Biobanks have historically lacked diversity; however, T2C, All of Us, and the United Kingdom Biobank are some of the organizations working toward inclusion (Collins and Varmus, 2015; Bycroft et al., 2018).

Micro-RNAs, Stress, and Pregnancy

MiRNAs are small non-coding segments of RNA which modulate gene expression by inhibiting translation. Expression of miRNAs is regulated by RNA polymerase II (similar to mRNA), and they are transported from cell to cell *via* exosomes (Hayashi and Hoffman, 2017). Circulating miRNAs in biofluid are believed to be a potential biomarker for a number of conditions (Gilad et al., 2008). Differential miRNA expression has been observed between tumors and normal tissue in multiple cancer types (Lu et al., 2005). Interestingly, certain maternally derived miRNAs (e.g., MIR517A) have been shown to be of placental origin, circulate within the mother's plasma, and are cleared shortly following delivery (Luo et al., 2009). The expression levels of miRNA cluster C14MC and other pregnancy-specific miRNAs fluctuate over a normal pregnancy and throughout fetal development (Morales-Prieto et al., 2013). However, changes in miRNA expression have also been described throughout several pregnancy complications including preeclampsia, preterm birth, and gestational diabetes (Ospina-Prieto et al., 2016; Cao et al., 2017; Fallen et al., 2018). During pregnancy, miRNAs regulate multiple targets involved in immune suppression, tumor regulation, and protein trafficking.

The expression of pregnancy-related miRNAs is susceptible to environmental changes including psychological and physical stress, which may affect the development of the child or lead to disease onset. Diseases triggered by stress are typically multifactorial in nature and can vary in severity due to a combinatorial effect of gestational stage, maternal age, and race. As studies have shown, miRNA expression fluctuates over the lifetime in response to environmental stimuli. MiRNA profiling has the potential to serve as a less invasive method of fetal monitoring compared to other commonly used methods such as amniocentesis.

The Maternal and Developmental Risks from Environmental and Social Stressors (MADRES) cohort was created to help understand health disparities in low-income females in Los Angeles by collecting biosamples and information over the course of pregnancy and early life (Bastain et al., 2019). This center focuses on individual and cumulative factors (e.g., stress, environmental toxin exposure) involved in childhood obesity and excess pregnancy-related weight gain and postpartum retention. Information and biological samples from mothers and infants are collected during pregnancy, at birth, and throughout the first year of the child's life. The collected information/samples include: questionnaires regarding household size, education, income, access to health care, proximity to freeways, and exposure to industry-derived toxins to assist in determining extrinsic stress; biospecimens including blood, urine, hair, nail clippings, feces, and saliva from pregnant mothers prior to and during birth; additional specimens collected at birth include umbilical cord blood, newborn blood, and placental tissue. The center assesses the health of both the mother and child using several different biological assays, including DNA methylation and metal exposure levels. The questionnaires provide measures of several levels of stress (Perceived Stress Scale, Prenatal Distress Questionnaire, and Center for Epidemiologic Studies). Studies utilizing information collected from this cohort highlighted the importance of collecting longitudinal data to assess the health of both mother and baby through the course of pregnancy, particularly in minority communities, to identify the factors that may be contributing to health disparities (Bastain et al., 2019).

Asthma Disparities

Asthma is one of the most common chronic diseases in children. It is often diagnosed in children who live in inner-city areas, neighborhoods near areas of high automotive traffic and

emissions, or who attend day-care centers in early childhood (Ochoa Sangrador and Vázquez Blanco, 2018). Asthma is characterized by difficulty in breathing due to respiratory airway swelling and inflammation. Several factors such as environmental proximity to pollutants, genetic predisposition, and race/ethnicity have been shown to affect the onset of asthma. A recent review shows that the average prevalence of asthma among children in the United States is approximately 8%, while the prevalence within inner-city environments is 28% (Coleman et al., 2019). This is a health disparity, as most inner-city populations are primarily comprised of minorities with lower SES.

The United States Department of Health and Human Services reported that between the years of 2008 and 2010, the prevalence of asthma varied based on age, sex, and race (Akinbami et al., 2012). Recent findings reveal a sex bias in the prevalence and severity of asthma, which also varies by age group (Fu et al., 2014). In addition, racial differences have been noted, with a higher prevalence of asthma within African American populations when compared to Caucasians. Interestingly, there are ethnic differences in the prevalence of asthma within Hispanic population subgroups, with Puerto Ricans showing a 16.1% compared to 5.4% among Mexicans (Akinbami et al., 2012). Understanding racial and ethnic disparities within this population, for example, is further complicated by the "Hispanic paradox," referring to the finding that Hispanic Americans tend to have better health outcomes compared to non-Hispanic White Americans despite being of lower SES (Franzini et al., 2001). It is important to note that the term "Hispanic" describes an admixed population with Spanish influence, typically including Native and African descendance; the degree and origins of admixture contribute to diversity within this population.

Several research groups have explored the role of ancestry on lung function in humans and using animal models (Brehm et al., 2012). Genome-wide association studies have identified genes associated with the development of asthma, with several genes reported to be involved in inflammation and immune function along respiratory airways. For example, *ORMDL3* overexpression in children was associated with asthma onset (Moffatt et al., 2010) and was later shown to increase airway remodeling in mice (Miller et al., 2014). In a Puerto Rican cohort, differential methylation was observed at sites located within genes involved in regulating respiratory airway integrity and function (*CDHR3* and *CDH26*) and immune response (*FBXL7, NTRK1,* and *SLC9A3*) (Forno et al., 2019).

A study by Miller and Chen (2006) showed a lowered bronchodilator response (BDR) and increased exposure to stress in Puerto Rican children. The study found that children with asthma who were exposed to chronic stress that was comparable to children without asthma displayed increased glucocorticoid receptor and β_2-adrenergic receptor gene expression (Miller and Chen, 2006). CpG methylation patterns within *ADCYAP1R1* (receptor for adenylate cyclase), leading to polypeptide overexpression, are implicated in people suffering from posttraumatic stress disorder (PTSD) and anxiety (Chen et al., 2013). These combined findings were supported by a recent study in which a variant of *ADCYAP1R1* in combination with extrinsic stress led to reduced BDR in children with asthma and reduced levels of ADRB2 in CD4 + T cells (Brehm et al., 2015); the CD4+ cell type has been shown to have a significant role in an asthmatic response (Ling and Luster, 2016). Longitudinal epigenomic studies in different racial and ethnic groups investigating the development of asthma are needed. Studies of this nature may allow researchers to tease out associations between asthma prevalence and African ancestry, particularly in admixed populations such as Puerto Ricans.

Midlife

Chronic Stress

Stress can exist in many forms ranging from biological stressors such as injury or illness to social stressors including low SES, fewer years of education, challenging relationship among family members, and neighborhood environments. Though acute stressors often do not pose a burden on health, situations in which an individual is chronically subjected to stress may have adverse effects on health and longevity (Schneiderman et al., 2005). Risk for several diseases has been associated with exposure to and duration of stress. Based on the 2006 Health and Retirement study, minority populations, such as African Americans and Hispanics, were reported to experience a greater stress burden when compared to Caucasians; these stressors are generally related to financial or housing situations (Brown et al., 2018). However, differences also exist in how certain subpopulations perceive and react to stress, with African American and Hispanics reported to be less likely to emotionally react to stressful situations in comparison to Caucasians (Brown et al., 2018).

Some of the disparities in stress response among different racial/ethnic subgroups may be due, in part, to biological vulnerability like genetic background and ancestry (Schneiderman et al., 2005). A comprehensive review by Argentieri et al. (2017) discusses how social and environmental stressors impact the risk for diseases such as hypertension, cardiovascular disease, cancer, and Alzheimer's disease (AD) through epigenomic mechanisms. These studies demonstrated the role of differential DNA methylation in hypothalamic–pituitary–adrenal (HPA) axis genes, *CRH*, *CRH-R1/2*, *CRH-BP*, *AVP*, *POMC*, *ACTH*, *ACTH-R*, *NR3C1*, *FKBP5*, and *HSD11β1/2*, in different human diseases that exhibit health disparity. For example, differential methylation of HPA axis genes such as dehydrogenase *HSD11B1*, glucocorticoid receptor *NR3C1*, and chaperone *FKBP5* has been shown to be associated with environmental and social stressors such as childhood trauma, SES, and discrimination, as well as diseases such as hypertension, cancer, AD, and depression (Argentieri et al., 2017).

Addiction and Substance Abuse

Racial and ethnic disparities related to addiction and substance abuse are known to exist, though these disparities often show an abnormal trend due to combinatorial effects host genetics, health care, and SES. Based on data collected from the 12-year Northwestern Juvenile Project, non-Hispanic Whites, specifically males, were found to be at higher risk for drug abuse compared to African Americans and Hispanics (Welty et al., 2016). However, availability and/or affordability of addiction treatment may also

contribute to this disparity. Failure to complete or enroll in addiction treatment for either drug or alcohol is frequently attributed to lack of health care, low SES, and unemployment. These conditions are commonly linked to African American, Hispanic, and Native American racial/ethnic groups (Saloner and Le Cook, 2014). In addition, emotional stressors and social adversities may also contribute to changes in epigenetic patterning, which in turn play a role in determining the type of response (positive or negative) an individual may have to a substance (Irner et al., 2012).

Epigenetic alterations have been linked to addiction and substance abuse. Studies by Kogan et al. (2018) have shown increased DNA methylation of oxytocin receptor *OXTR* in relation to stress, substance abuse, and high-risk sexual behavior in African American juveniles (∼19–23 years of age at baseline). *OXTR* is known to play a key role in buffering of stress responses and has been shown to be associated with increased stress and substance abuse symptomatology in young African American males (as demonstrated in the African American Men's Project) (Kogan et al., 2018). Change in methylation status at *OXTR* was shown to be attributed in part to early-life adversity such as lack of prosocial ties. This gives support to the idea that social environments earlier in life are capable of shaping DNA methylation profiles leading to susceptibility to substance abuse in adolescence and mid-life stages.

Another layer of disparity in the context of addiction and substance abuse has been shown at the level of sex. An isolated study showed significant differences in gray matter volume within the brain between sexes in response to cigarette smoking (Wetherill et al., 2015). Sex differences in response to nicotine have also been observed, with females being less sensitive to nicotine, while males show greater reward responses to nicotine (Perkins et al., 2018). Females also appeared to be more responsive to varenicline, a pharmaceutical drug often used to treat smoking addictions (McKee et al., 2016). This emphasizes the importance of studying sex differences within ethnic subgroups in order to fully understand how individuals respond to a substance and to identify effective therapeutic strategies for treating substance abuse/addictions.

Metabolic Syndrome

Another common age-related condition that impairs health particularly in developed countries such as the United States is metabolic syndrome (MetS). This condition is characterized by insulin resistance, high fasting triglycerides, low high-density lipoprotein (HDL) cholesterol, incidence of hypertension, and obesity. Major disparities exist in MetS, with the highest prevalence observed among African Americans and Hispanic Americans (Ervin, 2009; Karlamangla et al., 2010; Heiss et al., 2014). In addition to disparity at the level of race/ethnicity, disparities also exist between sexes; for example, Mexican American females have a higher prevalence of MetS compared to males (Heiss et al., 2014). This sex-based disparity may be attributed in part to the significant differences in biological measures commonly used to diagnose the condition (Pradhan, 2014). The heritable risk of MetS is approximately 30%; however, it is considered to be largely a disease of lifestyle, with diet and exercise serving as important risk factors (Povel et al., 2011). Due to the significant involvement of environmental factors in determining MetS risk, many studies have explored the epigenetic mechanisms involved in MetS etiology/pathology.

Epigenetic mechanisms such as DNA methylation have been implicated in risk for MetS and related conditions. Racial/ethnic disparities in metabolic phenotypes do exist, as shown by the disproportionate prevalence of MetS in Mexican Americans. Groups have identified differentially methylated CpG sites in peripheral blood mononuclear cells (PBMCs) significantly associated with MetS, obesity, and hypertriglyceridemic waist (HTGW) (i.e., high waist circumference and elevated serum triglyceride concentration) in individuals of European and Hispanic ancestry (Ali et al., 2014; Mamtani et al., 2016). In Caucasian populations, methylation of *SOCS3,* which plays key roles in leptin and insulin signaling, has been shown to be significantly associated with MetS and other metabolic-related measures (as shown in participants enrolled in the Take Off Pounds Sensibly Family Study of Epigenetics) (Ali et al., 2014). Interestingly, in the same study, the degree of *SOCS3* methylation was inversely correlated with *SOCS3* expression, whereby hypermethylation led to declines in gene expression (Ali et al., 2014), suggesting a molecular explanation for the physiologic dysregulation observed in individuals with MetS. In Mexican Americans, differential methylation of *CPT1A* and *ABCG1*, involved in long-chain fatty acid and triglyceride metabolism, respectively, was found to be significantly associated with HTGW (as shown in participants of the San Antonio Family Heart Study) (Mamtani et al., 2016).

This emphasizes the importance of future studies to explore the epigenetic mechanisms underlying pre-MetS conditions such as obesity and bioenergetics dysregulation. Carless and colleagues have proposed to study to identify DNA methylation associated with several physiological measures of energy homeostasis and obesity utilizing the Viva la Familia (VIVA). This study was addressed to underpin the biological relevance of the onset and progression of metabolic disorders to tissues involved in the bioenergetics processes.

This avenue of research is not just important for developing future treatment and prevention strategies for combating MetS in individuals of different ancestral backgrounds. Metabolic dysregulation is also a well-known comorbidity factor for several age-related conditions that also display racial/ethnic health disparity (Brown et al., 2018). These conditions include cardiovascular disease, cancer, and neurodegenerative disease such as AD (Alzheimer's Association, 2019).

Late Life

Aging is a complex process whereby overall physiological functions decline over time, progressively influencing an individual's susceptibility to disease. How an individual ages can provide information on driving factors that maintain a healthy state. Though genetic factors may partially determine human longevity (∼20–30%) and health, epigenetics serves as a meaningful bridge between genotype and phenotype, allowing us to identify how experiences and lifestyle affect aging and risk for disease (Pal and Tyler, 2016). A number of epigenetic

modifications have been studied in humans and experimental animal models ranging in biological complexity (Pal and Tyler, 2016). These modifications are known to be dynamic throughout the life span (both in dividing and non-dividing cells), and changes to different epigenetic marks occur throughout the aging process, though the directionality of these modifications is dependent upon the genomic context. Further, advanced age is an important risk factor for a number of complex diseases; however, chronological age is not always informative of the true biological condition or disease risk of an individual. In recent years, epigenetic signatures such as DNA methylation have been investigated as biomarkers for predicting morbidity and mortality risk (Hannum et al., 2013; Horvath, 2013; Levine et al., 2018; Lu et al., 2019).

Cancer

Several types of cancers exhibit health disparities in the context of sex, race/ethnicity, SES, and geographic location. Throughout the literature, it is apparent that both histone and DNA modifications are associated with tumorigenic processes and may serve a therapeutic potential (Wee et al., 2014). Several clinical trials have revealed that therapies targeting histone and DNA modification can be effective in treating cancers. However, how these epigenetic modifications control metastasis and recurrence of cancers still remains an open area of study. Here, we broadly discuss the role that epigenetics may play in driving cancer disparities and the potential utility of epigenetic-based therapies targeting "readers," "writers," and "erasers." For the purposes of brevity, we focus on colorectal cancer (CRC), colon cancer, and cervical cancer.

Though several types of cancer exist, cervical and CRC models have been used to demonstrate how social factors affect epigenetic patterning and impact racial cancer disparities. Racial/ethnic disparities in cervical cancer incidence and mortality rates are well documented. Cervical cancer mortality rates are twice as high in African American populations compared to non-Hispanic whites in the United States (Rates, 2007; Downs et al., 2008). Furthermore, non-Hispanic white women are more likely to be diagnosed at an earlier stage of cervical cancer than African Americans, Native Americans, or Hispanics (Gilliland et al., 1998; Del Carmen et al., 1999; Rates, 2007; Downs et al., 2008). Both incidence and mortality of CRC are higher among African Americans when compared to all other racial and ethnic groups (Gillette and Hill, 2015). Rates of CRC were reported to decline following the introduction of new prevention and screening methods such as at-home fecal occult blood test (FOBT) and increases in the recommended frequency of colonoscopies. Despite these efforts, the disparity failed to disappear, highlighting the multifactorial nature of the disease (Siegel et al., 2013). Differential epigenetic modifications may underlie these cancer disparities; research within the field has been advancing in recent years (Nebbioso et al., 2018).

Age-related cancers are often highly heterogeneous and arise due to combined interaction of genetic, environmental, and lifestyle factors. Several research groups have sought to understand how epigenetic changes are implicated in cancer etiology (Jones and Laird, 1999; Feinberg, 2004). One such example is cervical cancer, which has been linked extensively with human papillomavirus (HPV) 16 infection. Following HPV infection, two oncogenic proteins, early proteins 6 and 7 (E6, E7), activate the cell cycle growth and prevent cellular apoptosis, thereby allowing for accumulation of DNA damage (Graham, 2017). The mechanism involved in the etiology of cervical cancer involves the binding of E6-associated protein with ubiquitin ligase and deregulation of apoptosis *via* p53 leading to cellular proliferation and cancer (Graham, 2017).

The combined effects of HPV infection, smoking, and alcohol consumption have been shown to play a role in cervical cancer risk and disparity. American Indian (AI) women are known to smoke at rates four times greater than Caucasian women and most HPV-positive AI women are smokers (Karuri et al., 2017). Schmidt-Grimminger et al. (2011) have found that the carcinogen benzo[a]pyrene (BaP), commonly found in cigarette smoke, increases the expression of HPV oncogenes (E6/E7), suggesting that HPV infection and smoking may increase the incidence and severity of cervical cancers in AI women; this may account for some of the disparities in cervical cancer incidence and diagnosis between AI women and Caucasian women (Bell et al., 2011).

Targeting of epigenetic "readers," "writers," and "erasers" has been proposed as a therapeutic strategy for cancer treatment. However, target specificity toward tumorigenic vs. normal tissue and pharmacokinetic efficacy are important considerations due to the potential pleiotropic effects on cellular functions (Rajendran et al., 2019). Many therapeutic strategies for cancer treatment have largely been focused on targeting "writers" and "erasers." Thus far, two classes of epigenetic drugs have been approved by the United States Food and Drug Administration, DNMT and HDAC inhibitors, with other targets in late-stage clinical trials [e.g., bromodomain and extra-terminal (BET) inhibitors (BETis)] (Roberti et al., 2019). Interest in the use of natural substances as epigenetic therapies for certain cancer subtypes has increased in recent years as a result of their potential to be more effective chemopreventive and chemotherapeutic strategies (Meeran et al., 2010). One example is the compound sulforaphane (SFN), an isothiocyanate found in cruciferous vegetables. SFN may serve as an efficient, more accessible, and affordable anticancer agent. SFN and its associated metabolites have been found to act as natural HDAC inhibitors, through their propensity for acetylation activity on *CCAR2-encoded protein* (cell cycle and apoptosis regulator 2) (Parnaud et al., 2004). Overexpression of *CCAR2* has previously been correlated with poor survival outcomes in colon cancer (Clarke et al., 2008; Best et al., 2017). Human clinical trials provide strong evidence for the chemopreventive effects of SFN on carcinogenesis by preventing tumor growth and increasing sensitivity of cancer cells to chemotherapy (Jiang et al., 2018). SFN has been found to induce apoptosis of tumors in a mouse model through inhibition of HDACs (Jiang et al., 2018). SFN has also been shown to significantly decrease the expression of DNMTs through allowing for modulation of cyclin D2 expression ultimately promoting pancreatic cancer cell death (Jiang et al., 2018). New and effective treatments, nutritional adaptations such as Nano-Curcumin (Nano-CUR) and food items enriched with SFN that target

epigenetic regulatory mechanisms, may help diminish gaps in cancer-related health disparities.

Another natural substance proposed as an epigenetic therapy for cancer is curcumin. Curcumin has been shown to downregulate HPV18 transcription and exhibit enhanced cytotoxic activity in HPV-infected cells (Zaman et al., 2016). Furthermore, Nano-CUR, a nanoparticle formulation designed for increased absorption, was shown to abrogate the expression of BaP-induced E6/E7 (Zaman et al., 2016). In the context of CRC, oncogenic LncRNA *MALAT1* can be used as an indicator of poor prognosis (Xu et al., 2018). Analysis using The Cancer Genome Atlas (TCGA) demonstrated a higher expression of *MALAT1* in African American CRC tissue compared to Caucasians. Thus, *MALAT1* represents a marker for the disparate CRC incidence and severity in African Americans and Caucasians. Nano-CUR has been proposed as an effective epigenetic treatment modality for HPV-based CRC and, more selectively, cervical cancers in populations with greater rates of smoking without the same toxicity as current anticancer therapies including chemo and radiation therapy regimens.

Most research to date has focused on targeting "writers" and "erasers" as therapeutic strategies for epigenetic cancer treatment. The discovery of BETis has resulted in an increased focus on targeting chromatin modification "readers." Recent studies have shown that two BETis are effective in the downregulation of the *MYC* oncogene in several cancer subtypes, suggesting the importance of these inhibitors in oncogenic regulation and for cancer therapies (Filippakopoulos et al., 2010; Dawson Mark and Kouzarides, 2012). The role of BETis in cancer stems from their interference with the cancer cell cycle progression and DNA repair (Mio et al., 2019). Multiple BETis have shown promise for their therapeutic effects across several subtypes of cancers (Sahai et al., 2016). As such, BETis use has begun in clinical trials, providing another target for epigenetic cancer treatment. Preliminary clinical trials have revealed the effectiveness of BETis in cancer therapy. One benefit of their use is that they are unable to singularly bind a bromodomain-containing family member, which could reduce their therapeutic side effects (Simó-Riudalbas and Esteller, 2015; Ronnekleiv-Kelly et al., 2017). However, further research is needed to investigate "readers" dysfunction in cancer and identify the chemical compounds and probes capable of inhibiting "readers" (Mio et al., 2019).

Alzheimer's Disease

Alzheimer's disease is a multifactorial disease with both genetic and lifestyle factors impacting risk. Though early-onset forms of the disease display an inheritance pattern that is more Mendelian in nature, understanding the etiology of late-onset AD (LOAD) proves rather difficult due, in part, to the issue of "missing heritability." This concept refers to the limited contribution that genetic variants have in explaining the heritable risk of LOAD. Because of this, several groups have begun to explore the role of epigenetics and the different environmental and lifestyle factors that may contribute to AD risk.

It is known that major disparities exist in AD prevalence and pathology across race/ethnicity, with Hispanics and African Americans having 1.5 and 2 times increased risk, respectively (Gaugler et al., 2019). Within the United States, the incidence of AD is known to be especially elevated in Hispanic and African American females (Matthews et al., 2019). Though genetic factors may explain some of this disparity, a great deal is thought to be due to external factors such as diet, lifestyle, and physical environment. Risk for AD is already known to be higher in individuals of advanced age, lower SES, and/or who suffer from a comorbid condition such as obesity, MetS, and hypertension (Gaugler et al., 2019).

Some research groups have taken an innovative approach toward understanding AD risk by determining how early life exposures (as early as neonatal stages) to extrinsic (e.g., metal toxicity), intrinsic (e.g., cytokines, hormones), and dietary factors (e.g., nutrient imbalance) impact gene expression and ultimately physiological development and function. Lahiri et al. (2007) have proposed the Latent Early-life Associated Regulation (LEARn) model of AD that early life exposures, which are determined in part by social disparities, can disrupt gene regulation, though this perturbation does not become pathogenic until later stages in life. This model is similar to the "two-hit hypothesis" for cancer, whereby an initial insult alters gene expression, followed by a latent period; if a second insult arises later in life, the alteration then becomes aberrant. It further proposes that overproduction of amyloid precursor protein (APP) and amyloid beta in late life may be triggered by early-life changes to the methylation status of promoters for *APP* and other related genes (Lahiri et al., 2007). Their group has also proposed epigenetic therapies such as mithramycin and tolfenamic acid to target amyloid pathways; these have been shown to exhibit downstream impact on neuronal structures including cell body, neurite length, and branch points (Bayon et al., 2017). Though AD is an age-related disease, emphasis must be placed on further understanding how early-life and mid-life environments and exposures influence AD risk in later-life stages.

CHALLENGES AND CURRENT LIMITATIONS OF SOCIAL EPIGENOMIC STUDIES

It is important to acknowledge that studies within the field of social epigenomics are often met with several challenges and limitations; this includes adequate study design, sample availability, experimental techniques, statistical analysis, and biologic interpretation of results (Bakulski and Fallin, 2014). Though social epigenomics may be useful in addressing racial/ethnic disparities in the context of health and disease, there is a lack of epigenetics literature investigating minority populations, with a great majority of studies focusing on homogeneous populations (i.e., Caucasians). This absence is primarily due to limited availability of samples from minority groups, which can be attributed to biased sampling and difficulty in recruiting/retaining research subjects. Much of the past literature has been focused on clinically recruited populations, which introduce bias and are problematic, specifically for studies investigating the effects of different social/environmental factors. One such example is Berkson's bias, whereby clinic

attendance is impacted by exposure and/or accessibility to clinical settings and presence of pre-existing diseases and/or conditions, resulting in distortion of experimental findings (Westreich, 2012). For example, evidence suggests that individuals belonging to minority populations hold mistrust toward researchers and health care personnel in fear of being exploited or mistreated (Yancey et al., 2006). Efforts to mitigate this mistrust have been made by some groups, primarily through improving communication and becoming more involved in the community (Yancey et al., 2006). Additionally, in most population-based studies, race is often self-reported, which does not capture the biological ancestry of an individual. Ancestry-informative markers (AIM) in the form of single-nucleotide polymorphisms (SNPs) provide utility in further defining population structure to allow for a more comprehensive understanding of the molecular factors associated with certain health disparities.

With epigenetic changes occurring throughout the course of an individual's lifetime, it is difficult to capture the full effect of epigenetic changes on risk of disease. It is important to consider that any measurement is only a snapshot in time of a reversible modification, which further complicates biological interpretation. Samples collected at the time of disease diagnosis do not allow researchers the luxury of assuming a role for epigenetic changes in disease onset. Access to longitudinal data or sampling can be useful in teasing out some of the biological changes occurring downstream of epigenetic modifications; however, generation of this type of data is time-consuming and quite costly. Furthermore, depending on the epigenetic modification in question, sample storage can also greatly impact experimental results. Stability of different epigenetic modifications varies across sample conditions. For example, DNA methylation remains relatively stable in frozen tissue, while chromatin analysis necessitates fresh tissue (Bakulski and Fallin, 2014). Additionally, tissue samples are highly heterogeneous in nature and contain several cell types; adjustment for the proportions of each cell type whether by experimental methods (i.e., flow cytometry; limited to fresh tissue) or statistical methods (i.e., cell type correction) is essential for deconvoluting the effects of cell type on epigenetic modifications (Bakulski and Fallin, 2014). High-throughput methods also demand multiple batches to be analyzed, which need to be corrected for in the analysis stage of these studies (Bakulski and Fallin, 2014). The biologic interpretation of results from epigenomic studies remains a challenge, specifically, understanding the direct mechanisms for how various exposures cause epigenetic changes and lead to disease.

Difficulties often arise in teasing out gene–environment interactions. Genetic variants (i.e., SNPs) have been associated with racial/ethnic health disparities. For a recent review on the utility of investigating genetic data in the context of health disparities, refer to Mersha and Abebe (2015). Importantly, SNPs have also been associated with altered epigenetic modifications. For example, genotypes at certain loci have been shown to result in differential patterns of methylation (Smith et al., 2014); these positions are otherwise referred to as methylation quantitative trait loci. Since SNPs can affect both intermediate (i.e., epigenetic modifications) and downstream (i.e., conditions/diseases) phenotypes, complex analysis strategies must be used to tease apart these relationships. The use of statistical and epidemiological principles in testing causal associations presents some promise for epigenomic research. Directed acyclic graphs (DAGs) can be used to visually explain the potential direct and indirect causal mechanisms between exposure and outcome, as well as identify potential factors for mediation analysis (Mueller et al., 2020). For example, environmental exposures can lead to epigenetic changes, affecting disease risk downstream. Testing mediation effects between exposures and corresponding epigenetic changes can help identify mechanisms that mediate the exposure–outcome relationship (VanderWeele, 2016; Gao et al., 2019). Unfortunately, mediation analysis does have its limitations, the use of mediation requires a large sample size, oftentimes unavailable in epigenetic studies. An alternative strategy is Mendelian randomization (MR) which utilizes genetic variants as proxies for a valid instrumental variable for estimation of the causal effect between an exposure and outcome, overcoming confounding and reverse causation (an issue common to epigenetic research) (Smith and Ebrahim, 2003; Relton and Davey Smith, 2015). Another statistical method for elucidating causal inference is inverse probability of treatment weighting (IPTW), a form of propensity weighting for inclusion in statistical analysis. IPTW is useful in controlling for selection bias in epigenetic studies. Within the context of epigenomic research, this statistical method relies on creating a propensity score and inverts the score to weigh individual covariates in order to estimate the level to which epigenetic changes would exist if different racial or ethnic groups experienced similar built and social environments (Beck et al., 2016). IPTW has proven useful in teasing out causation of racial disparities for some conditions. For example, in a study adjacent to the Greater Cincinnati Asthma Risks Study, 695 African American and White children from an urban pediatric hospital were studied to identify potential asthma onset predictors (Beck et al., 2016). Preliminary results showed racial disparities in exposure to risk factors including allergen sensitization and socioeconomic hardships. However, upon further examination using IPTW-adjusted survival analysis controlling for a number of exposures, the risk for readmission for asthma was comparable between groups. This suggests that methods such as those mentioned above may be useful for socio-epigenomic researchers in determining disease causality.

CONCLUSION

This review article has focused on the social epigenetic mechanisms that may lead to chronic diseases and resulting health disparities in specific populations. The review draws from transdisciplinary sciences encompassing basic research, public health, and medicine, as well as community organizations, to highlight the current state of knowledge, future directions, and the challenges and limitations of socio-epigenetics research. Understanding the impacts that environment and lifestyle factors have on biological processes and how these factors can be modified to improve the state of health on a global scale is the

primary goal of social-epigenetic research. We have discussed the ways in which social and environmental factors impact biological processes through epigenetic changes leading to susceptibility to certain conditions and/or diseases throughout different life stages (**Figure 1**) and how these changes contribute to health disparities. Approaches which may help in mitigating the complex health disparities impacted by epigenetic-related mechanisms were highlighted including pharmaceutical targeting of epigenetic imprinting, adaptations to specific nutrition/diet-based therapy like consumption of cruciferous vegetables, improvements to our local environments like creation of increased green space and related community infrastructure, and psychosocial practices. We also addressed current challenges and limitations in social epigenomics research and highlighted the need for more minority population-based cohorts in social epigenomic studies.

AUTHOR CONTRIBUTIONS

VM, NP, and TS: review and manuscript writing. RB, MF, HJ, NP, M-HT, and ST: supervision, administration, and manuscript review. JV: conceptualization, funding, administration, and manuscript review. All authors contributed to the article and approved the submitted version.

FUNDING

This research reported in this publication was supported by the National Institute on Minority Health and Health Disparities of the National Institutes of Health under Award Numbers U54MD006882 and S21MD012472.

ACKNOWLEDGMENTS

The funding for the conference on which this review is based was made possible by the National Institute on Minority Health and Health Disparities of the National Institutes of Health under Award Numbers U54MD006882 and S21MD012472. The views presented in the written review were presented by speakers and moderators and do not reflect the official policies of the Department of Health and Human Services, nor does mention of trade names, commercial practices, or organizations imply endorsement by the United States Government. The authors would like to thank the speakers of the 14th Annual Texas Conference on Health Disparities for presenting the information on their research. The authors also thank all the community organization members who took part in the conference.

REFERENCES

Alzheimer's Association (2019). 2019 Alzheimer's disease facts and figures. *Alzheimer's Dement.* 15, 321–387. doi: 10.1016/j.jalz.2019.01.010

Akinbami, L. J., Moorman, J. E., Bailey, C., Zahran, H. S., King, M., Johnson, C. A., et al. (2012). Trends in asthma prevalence, health care use, and mortality in the United States, 2001-2010. *NCHS Data Brief.* 94, 1–8.

Alegría-Torres, J. A., Baccarelli, A., and Bollati, V. (2011). Epigenetics and lifestyle. *Epigenomics* 3, 267–277.

Ali, O., Cerjak, D., Kent, J. W., James, R., Blangero, J., and Zhang, Y. (2014). Obesity, central adiposity and cardiometabolic risk factors in children and adolescents: a family-based study. *Pediatr. Obes.* 9, e58–e62. doi: 10.1111/j.2047-6310.2014.218.x

Argentieri, M. A., Nagarajan, S., Seddighzadeh, B., Baccarelli, A. A., and Shields, A. E. (2017). Epigenetic pathways in human disease: the impact of DNA methylation on stress-related pathogenesis and current challenges in biomarker development. *EBioMedicine* 18, 327–350. doi: 10.1016/j.ebiom.2017.03.044

National Academies of Sciences, Engineering, and Medicine, Health and Medicine Division, Board on Population Health and Public Health Practice, Committee on Community-Based Solutions to Promote Health Equity in the United States (2017). *Communities in Action: Pathways to Health Equity*. eds A. Baciu, Y. Negussie, A. Geller, and J. N. Weinstein (Washington, DC: National Academies Press).

Backes, C., Fehlmann, T., Kern, F., Kehl, T., Lenhof, H. P., Meese, E., et al. (2018). miRCarta: a central repository for collecting miRNA candidates. *Nucleic Acids Res.* 46, D160–D167.

Bakhireva, L. N., Young, B. N., Dalen, J., Phelan, S. T., and Rayburn, W. F. (2009). Periconceptional binge drinking and acculturation among pregnant Latinas in New Mexico. *Alcohol* 43, 475–481. doi: 10.1016/j.alcohol.2009.08.002

Bakulski, K. M., and Fallin, M. D. (2014). Epigenetic epidemiology: promises for public health research. *Environ. Mol. Mutagen.* 55, 171–183. doi: 10.1002/em.21850

Bannister, A. J., and Kouzarides, T. (2011). Regulation of chromatin by histone modifications. *Cell Res.* 21, 381–395. doi: 10.1038/cr.2011.22

Barski, A., Cuddapah, S., Cui, K., Roh, T. Y., Schones, D. E., Wang, Z., et al. (2007). High-resolution profiling of histone methylations in the human genome. *Cell* 129, 823–837. doi: 10.1016/j.cell.2007.05.009

Bartsch, H., and Nair, J. (2004). Oxidative stress and lipid peroxidation-derived DNA-lesions in inflammation driven carcinogenesis. *Cancer Detect. Prevent.* 28, 385–391. doi: 10.1016/j.cdp.2004.07.004

Bastain, T. M., Chavez, T., Habre, R., Girguis, M. S., Grubbs, B., Toledo-Corral, C., et al. (2019). Study Design, Protocol and Profile of the Maternal And Developmental Risks from Environmental and Social Stressors (MADRES) Pregnancy Cohort: a Prospective Cohort Study in Predominantly Low-Income Hispanic Women in Urban Los Angeles. *BMC Pregnancy Childbirth* 19:189. doi: 10.1186/s12884-019-2330-7

Bayon, B. L., Maloney, B., Chopra, N., White, F. A., Xu, X.-M., Ratan, R. R., et al. (2017). SP1-MODULATING COMPOUNDS AS A NOVEL DRUG TARGET FOR ALZHEIMER'S DISEASE (AD). *Alzheimer's Dement.* 13:1241.

Beck, A. F., Huang, B., Auger, K. A., Ryan, P. H., Chen, C., and Kahn, R. S. (2016). Explaining racial disparities in child asthma readmission using a causal inference approach. *JAMA Pediatr.* 170, 695–703.

Bell, M. C., Schmidt-Grimminger, D., Jacobsen, C., Chauhan, S. C., Maher, D. M., and Buchwald, D. S. (2011). Risk factors for HPV infection among American Indian and white women in the Northern Plains. *Gynecol. Oncol.* 121, 532–536. doi: 10.1016/j.ygyno.2011.02.032

Best, S. A., Nwaobasi, A. N., Schmults, C. D., and Ramsey, M. R. (2017). CCAR2 is required for proliferation and tumor maintenance in human squamous cell carcinoma. *J. Invest. Dermatol.* 137, 506–512. doi: 10.1016/j.jid.2016.09.027

Braveman, P., Egerter, S., and Williams, D. R. (2011). The social determinants of health: coming of age. *Annu. Rev. Public Health.* 32, 381–398. doi: 10.1146/annurev-publhealth-031210-101218

Braveman, P., and Gottlieb, L. (2014). The social determinants of health: it's time to consider the causes of the causes. *Public Health Rep.* 129(Suppl. 2), 19–31.

Brehm, J. M., Acosta-Perez, E., Klei, L., Roeder, K., Barmada, M. M., Boutaoui, N., et al. (2012). African ancestry and lung function in Puerto Rican children. *J. Allergy Clin. Immunol.* 129, 1484–90e6.

Brehm, J. M., Ramratnam, S. K., Tse, S. M., Croteau-Chonka, D. C., Pino-Yanes, M., Rosas-Salazar, C., et al. (2015). Stress and Bronchodilator Response in Children with Asthma. *Am. J. Respir. Crit. Care Med.* 192, 47–56.

Brown, L. L., Mitchell, U. A., and Ailshire, J. A. (2018). Disentangling the stress process: race/ethnic differences in the exposure and appraisal of chronic stressors among older adults. *J. Gerontol. Ser. B* 75, 650–660. doi: 10.1093/geronb/gby072

Bycroft, C., Freeman, C., Petkova, D., Band, G., Elliott, L. T., Sharp, K., et al. (2018). The UK Biobank resource with deep phenotyping and genomic data. *Nature* 562, 203–209. doi: 10.1038/s41586-018-0579-z

Cao, J. (2014). The functional role of long non-coding RNAs and epigenetics. *Biol. Proc. Online* 16:11.

Cao, Y. L., Jia, Y. J., Xing, B. H., Shi, D. D., and Dong, X. J. (2017). Plasma microRNA-16-5p, -17-5p and -20a-5p: novel diagnostic biomarkers for gestational diabetes mellitus. *J. Obstet. Gynaecol. Res.* 43, 974–981. doi: 10.1111/jog.13317

Chaix, B. (2009). Geographic life environments and coronary heart disease: a literature review, theoretical contributions, methodological updates, and a research agenda. *Annu. Rev. Public Health* 30, 81–105. doi: 10.1146/annurev.publhealth.031308.100158

Chen, W., Boutaoui, N., Brehm, J. M., Han, Y.-Y., Schmitz, C., Cressley, A., et al. (2013). ADCYAP1R1 and Asthma in Puerto Rican Children. *Am. J. Respir. Crit. Care Med.* 187, 584–588.

Clarke, J. D., Dashwood, R. H., and Ho, E. (2008). Multi-targeted prevention of cancer by sulforaphane. *Cancer Lett.* 269, 291–304. doi: 10.1016/j.canlet.2008.04.018

Coleman, A. T., Teach, S. J., and Sheehan, W. J. (2019). Inner-city asthma in childhood. *Immunol. Allergy Clin. North Am.* 39, 259–270.

Collins, F. S., and Varmus, H. (2015). A new initiative on precision medicine. *N. Engl. J. Med.* 372, 793–795. doi: 10.1056/nejmp1500523

Collins, S. E. (2016). Associations between socioeconomic factors and alcohol outcomes. *Alcohol Res.* 38, 83–94.

Cunliffe, V. T. (2016). The epigenetic impacts of social stress: how does social adversity become biologically embedded? *Epigenomics* 8, 1653–1669. doi: 10.2217/epi-2016-0075

Dawson Mark, A., and Kouzarides, T. (2012). Cancer epigenetics: from mechanism to therapy. *Cell* 150, 12–27. doi: 10.1016/j.cell.2012.06.013

Del Carmen, M. G., Montz, F., Bristow, R. E., Bovicelli, A., Cornelison, T., and Trimble, E. (1999). Ethnic differences in patterns of care of stage 1A1 and stage 1A2 cervical cancer: a SEER database study. *Gynecol. Oncol.* 75, 113–117. doi: 10.1006/gyno.1999.5543

Diez Roux, A. V. (2001). Investigating neighborhood and area effects on health. *Am. J. Public Health* 91, 1783–1789. doi: 10.2105/ajph.91.11.1783

Downs, L. S., Smith, J. S., Scarinci, I., Flowers, L., and Parham, G. (2008). The disparity of cervical cancer in diverse populations. *Gynecol. Oncol.* 109(2 Suppl), S22–S30.

Elias, B., Hanlon-Dearman, A., Head, B., and Hicks, G. G. (2018). Translating to the Community (T2C): a protocol paper describing the development of Canada's first social epigenetic FASD biobank. *Biochem. Cell Biol.* 96, 275–287. doi: 10.1139/bcb-2017-0278

Ervin, R. B. (2009). Prevalence of Metabolic Syndrome Among Adults 20 years of age and over, by sex, age, race and ethnicity, and body mass index; United States, 2003-2006. *Natl. Health Stat. Rep.* 5, 1–7.

Fallen, S., Baxter, D., Wu, X., Kim, T. K., Shynlova, O., Lee, M. Y., et al. (2018). Extracellular vesicle RNAs reflect placenta dysfunction and are a biomarker source for preterm labour. *J. Cell Mol. Med.* 22, 2760–2773. doi: 10.1111/jcmm.13570

Feinberg, A. P. (2004). The epigenetics of cancer etiology. *Semin. Cancer Biol.* 14, 427–432. doi: 10.1016/j.semcancer.2004.06.005

Felsenfeld, G. (2014). A brief history of epigenetics. *Cold. Spring Harb. Perspect. Biol.* 6:a018200. doi: 10.1101/cshperspect.a018200

Filippakopoulos, P., Qi, J., Picaud, S., Shen, Y., Smith, W. B., Fedorov, O., et al. (2010). Selective inhibition of BET bromodomains. *Nature* 468, 1067–1073.

Forno, E., Wang, T., Qi, C., Yan, Q., Xu, C. J., Boutaoui, N., et al. (2019). DNA methylation in nasal epithelium, atopy, and atopic asthma in children: a genome-wide study. *Lancet Respir. Med.* 7, 336–346. doi: 10.1016/s2213-2600(18)30466-1

Franzini, L., Ribble, J. C., and Keddie, A. M. (2001). Understanding the Hispanic paradox. *Ethn. Dis.* 11, 496–518.

Fu, A., Leaderer, B. P., Gent, J. F., Leaderer, D., and Zhu, Y. (2012). An environmental epigenetic study of ADRB2 5'-UTR methylation and childhood asthma severity. *Clin. Exp. Allergy* 42, 1575–1581. doi: 10.1111/j.1365-2222.2012.04055.x

Fu, L., Freishtat, R. J., Gordish-Dressman, H., Teach, S. J., Resca, L., Hoffman, E. P., et al. (2014). Natural progression of childhood asthma symptoms and strong influence of sex and puberty. *Ann. Am. Thoracic Soc.* 11, 939–944. doi: 10.1513/annalsats.201402-084oc

Gao, Y., Yang, H., Fang, R., Zhang, Y., Goode, E. L., and Cui, Y. (2019). Testing mediation effects in high-dimensional epigenetic studies. *Front. Genet.* 10:1195. doi: 10.3389/fgene.2019.01195

Gaugler, J., James, B., Johnson, T., Marin, A., and Weuve, J. (2019). 2019 Alzheimer's disease facts and figures. *Alzheimers Dement.* 15, 321–387.

Gilad, S., Meiri, E., Yogev, Y., Benjamin, S., Lebanony, D., Yerushalmi, N., et al. (2008). Serum MicroRNAs Are Promising Novel Biomarkers. *PLoS One* 3:e3148. doi: 10.1371/journal.pone.0003148

Gillette, T. G., and Hill, J. A. (2015). Readers, writers, and erasers: chromatin as the whiteboard of heart disease. *Circ. Res.* 116, 1245–1253. doi: 10.1161/circresaha.116.303630

Gilliland, F. D., Hunt, W. C., and Key, C. R. (1998). Trends in the survival of american indian, hispanic, and non-hispanic white cancer patients in new mexico and arizona, 1969-1994. *Cancer* 82, 1769–1783. doi: 10.1002/(sici)1097-0142(19980501)82:9<1784::aid-cncr26>3.0.co;2-#

Graham, S. V. (2017). The human papillomavirus replication cycle, and its links to cancer progression: a comprehensive review. *Clin. Sci.* 131, 2201–2221. doi: 10.1042/cs20160786

Hannum, G., Guinney, J., Zhao, L., Zhang, L., Hughes, G., Sadda, S., et al. (2013). Genome-wide methylation profiles reveal quantitative views of human aging rates. *Mol. Cell* 49, 359–367. doi: 10.1016/j.molcel.2012.10.016

Hayashi, T., and Hoffman, M. P. (2017). Exosomal microRNA communication between tissues during organogenesis. *RNA Biol.* 14, 1683–1689. doi: 10.1080/15476286.2017.1361098

Haycock, P. C., and Ramsay, M. (2009). Exposure of mouse embryos to ethanol during preimplantation development: effect on DNA methylation in the h19 imprinting control region. *Biol. Reprod.* 81, 618–627. doi: 10.1095/biolreprod.108.074682

Héberlé, É, and Bardet, A. F. (2019). Sensitivity of transcription factors to DNA methylation. *Essays Biochem.* 63, 727–741. doi: 10.1042/ebc20190033

Heiss, G., Snyder, M. L., Teng, Y., Schneiderman, N., Llabre, M. M., Cowie, C., et al. (2014). Prevalence of metabolic syndrome among Hispanics/Latinos of diverse background: the Hispanic Community Health Study/Study of Latinos. *Diabetes Care* 37, 2391–2399. doi: 10.2337/dc13-2505

Institute of Medicine, Board on Health Sciences Policy, Committee on Assessing Interactions Among Social, Behavioral, and Genetic Factors in Health (2006). *Genes, Behavior, and the Social Environment: Moving Beyond the Nature/Nurture Debate*. eds L. M. Hernandez, and D. G. Blazer (Washington DC: The National Academies Collection: Reports funded by National Institutes of Health).

Horvath, S. (2013). DNA methylation age of human tissues and cell types. *Genome Biol.* 14:R115.

Irner, T. B., Teasdale, T. W., Nielsen, T., Vedal, S., and Olofsson, M. (2012). Substance use during pregnancy and postnatal outcomes. *J. Addict. Dis.* 31, 19–28. doi: 10.1080/10550887.2011.642765

Jiang, X., Liu, Y., Ma, L., Ji, R., Qu, Y., Xin, Y., et al. (2018). Chemopreventive activity of sulforaphane. *Drug Des. Devel. Ther.* 12, 2905–2913. doi: 10.2147/dddt.s100534

Jones, K., and Smith, D. (1973). Recognition of the fetal alcohol syndrome in early infancy. *Lancet* 302, 999–1001. doi: 10.1016/s0140-6736(73)91092-1

Jones, M. J., Goodman, S. J., and Kobor, M. S. (2015). DNA methylation and healthy human aging. *Aging Cell* 14, 924–932. doi: 10.1111/acel.12349

Jones, P. A., and Laird, P. W. (1999). Cancer-epigenetics comes of age. *Nat. Genet.* 21, 163–167. doi: 10.1038/5947

Karlamangla, A. S., Merkin, S. S., Crimmins, E. M., and Seeman, T. E. (2010). Socioeconomic and ethnic disparities in cardiovascular risk in the United States, 2001-2006. *Ann. Epidemiol.* 20, 617–628. doi: 10.1016/j.annepidem.2010.05.003

Karuri, A. R., Kashyap, V. K., Yallapu, M. M., Zafar, N., Kedia, S. K., Jaggi, M., et al. (2017). Disparity in rates of HPV infection and cervical cancer in underserved US populations. *Front. Biosci.* 9:254–269. doi: 10.2741/s486

Kogan, S. M., Cho, J., Beach, S. R. H., Smith, A. K., and Nishitani, S. (2018). Oxytocin receptor gene methylation and substance use problems among young African American men. *Drug Alcohol. Depend.* 192, 309–315. doi: 10.1016/j.drugalcdep.2018.08.022

Krieger, J., and Higgins, D. L. (2002). Housing and health: time again for public health action. *Am. J. Public Health* 92, 758–768. doi: 10.2105/ajph.92.5.758

Lahiri, D. K., Maloney, B., Basha, M. R., Ge, Y. W., and Zawia, N. H. (2007). How and when environmental agents and dietary factors affect the course of Alzheimer's disease: the "LEARn" model (latent early-life associated regulation) may explain the triggering of AD. *Curr. Alzheimer Res.* 4, 219–228. doi: 10.2174/156720507780362164

Lange, S., Probst, C., Gmel, G., Rehm, J., Burd, L., and Popova, S. (2017). Global prevalence of fetal alcohol spectrum disorder among children and youth: a systematic review and meta-analysis. *JAMA Pediatr.* 171, 948–956.

Laufer, B. I., Chater-Diehl, E. J., Kapalanga, J., and Singh, S. M. (2017). Long-term alterations to DNA methylation as a biomarker of prenatal alcohol exposure: from mouse models to human children with fetal alcohol spectrum disorders. *Alcohol* 60, 67–75. doi: 10.1016/j.alcohol.2016.11.009

Lawless, M. W., O'Byrne, K. J., and Gray, S. G. (2009). Oxidative stress induced lung cancer and COPD: opportunities for epigenetic therapy. *J. Cell Mol. Med.* 13, 2800–2821. doi: 10.1111/j.1582-4934.2009.00845.x

Levine, M. E., Lu, A. T., Quach, A., Chen, B. H., Assimes, T. L., Bandinelli, S., et al. (2018). An epigenetic biomarker of aging for lifespan and healthspan. *Aging* 10, 573–591. doi: 10.18632/aging.101414

Ling, M. F., and Luster, A. D. (2016). Allergen-Specific CD4(+) T Cells in Human Asthma. *Ann. Am. Thorac. Soc.* 13(Suppl. 1), S25–S30.

Lu, A. T., Quach, A., Wilson, J. G., Reiner, A. P., Aviv, A., Raj, K., et al. (2019). DNA methylation GrimAge strongly predicts lifespan and healthspan. *Aging* 11, 303–327. doi: 10.18632/aging.101684

Lu, J., Getz, G., Miska, E. A., Alvarez-Saavedra, E., Lamb, J., Peck, D., et al. (2005). MicroRNA expression profiles classify human cancers. *Nature* 435, 834–838. doi: 10.1038/nature03702

Luo, S. S., Ishibashi, O., Ishikawa, G., Ishikawa, T., Katayama, A., Mishima, T., et al. (2009). Human villous trophoblasts express and secrete placenta-specific microRNAs into maternal circulation via exosomes. *Biol. Reprod.* 81, 717–729. doi: 10.1095/biolreprod.108.075481

Lussier, A. A., Weinberg, J., and Kobor, M. S. (2017). Epigenetics studies of fetal alcohol spectrum disorder: where are we now? *Epigenomics* 9, 291–311. doi: 10.2217/epi-2016-0163

Mamtani, M., Kulkarni, H., Dyer, T. D., Göring, H. H. H., Neary, J. L., Cole, S. A., et al. (2016). Genome- and epigenome-wide association study of hypertriglyceridemic waist in Mexican American families. *Clin. Epigenet.* 8:6.

Marmorstein, R., and Zhou, M.-M. (2014). Writers and readers of histone acetylation: structure, mechanism, and inhibition. *Cold Spring Harb. Perspect. Biol.* 6:a018762. doi: 10.1101/cshperspect.a018762

Matthews, K. A., Xu, W., Gaglioti, A. H., Holt, J. B., Croft, J. B., Mack, D., et al. (2019). Racial and ethnic estimates of Alzheimer's disease and related dementias in the United States (2015-2060) in adults aged >/=65 years. *Alzheimer's Dement.* 15, 17–24. doi: 10.1016/j.jalz.2018.06.3063

May, P. A., Gossage, J. P., Kalberg, W. O., Robinson, L. K., Buckley, D., Manning, M., et al. (2009). Prevalence and epidemiologic characteristics of FASD from various research methods with an emphasis on recent in-school studies. *Dev. Disabil. Res. Rev.* 15, 176–192. doi: 10.1002/ddrr.68

McKee, S. A., Smith, P. H., Kaufman, M., Mazure, C. M., and Weinberger, A. H. (2016). Sex Differences in varenicline efficacy for smoking cessation: a meta-analysis. *Nicotine Tob. Res.* 18, 1002–1011. doi: 10.1093/ntr/ntv207

Meeran, S. M., Ahmed, A., and Tollefsbol, T. O. (2010). Epigenetic targets of bioactive dietary components for cancer prevention and therapy. *Clin. Epigenet.* 1, 101–116. doi: 10.1007/s13148-010-0011-5

Mersha, T. B., and Abebe, T. (2015). Self-reported race/ethnicity in the age of genomic research: its potential impact on understanding health disparities. *Hum. Genom.* 9:1.

Miller, G. E., and Chen, E. (2006). Life stress and diminished expression of genes encoding glucocorticoid receptor and beta2-adrenergic receptor in children with asthma. *Proc. Natl. Acad. Sci. U.S.A.* 103, 5496–5501. doi: 10.1073/pnas.0506312103

Miller, M., Rosenthal, P., Beppu, A., Mueller, J. L., Hoffman, H. M., Tam, A. B., et al. (2014). ORMDL3 transgenic mice have increased airway remodeling and airway responsiveness characteristic of asthma. *J. Immunol.* 192, 3475–3487. doi: 10.4049/jimmunol.1303047

Mio, C., Bulotta, S., Russo, D., and Damante, G. (2019). Reading cancer: chromatin readers as druggable targets for cancer treatment. *Cancers* 11:61. doi: 10.3390/cancers11010061

Moffatt, M. F., Gut, I. G., Demenais, F., Strachan, D. P., Bouzigon, E., Heath, S., et al. (2010). A large-scale, consortium-based genomewide association study of asthma. *N. Engl. J. Med.* 363, 1211–1221. doi: 10.1056/nejmoa0906312

Molina-Serrano, D., Schiza, V., and Kirmizis, A. (2013). Cross-talk among epigenetic modifications: lessons from histone arginine methylation. *Biochem. Soc. Trans.* 41, 751–759. doi: 10.1042/bst20130003

Morales-Prieto, D. M., Ospina-Prieto, S., Chaiwangyen, W., Schoenleben, M., and Markert, U. R. (2013). Pregnancy-associated miRNA-clusters. *J. Reprod. Immunol.* 97, 51–61. doi: 10.1016/j.jri.2012.11.001

Mueller, W., Steinle, S., Parkka, J., Parmes, E., Liedes, H., Kuijpers, E., et al. (2020). Urban greenspace and the indoor environment: pathways to health via indoor particulate matter, noise, and road noise annoyance. *Environ. Res.* 180:108850. doi: 10.1016/j.envres.2019.108850

Musselman, C. A., Lalonde, M.-E., Côté, J., and Kutateladze, T. G. (2012). Perceiving the epigenetic landscape through histone readers. *Nat. Struct. Mol. Biol.* 19, 1218–1227. doi: 10.1038/nsmb.2436

Nebbioso, A., Tambaro, F. P., Dell'Aversana, C., and Altucci, L. (2018). Cancer epigenetics: moving forward. *PLoS Genet.* 14:e1007362. doi: 10.1371/journal.pgen.1007362

O'Brien, J., Hayder, H., Zayed, Y., and Peng, C. (2018). Overview of MicroRNA biogenesis, mechanisms of actions, and circulation. *Front. Endocrinol.* 9:402. doi: 10.3389/fendo.2018.00402

Ochoa Sangrador, C., and Vázquez Blanco, A. (2018). Day-care center attendance and risk of Asthma-A systematic review. *Allergol. Immunopathol.* 46, 578–584. doi: 10.1016/j.aller.2018.03.006

Office of Disease Prevention and Health Promotion (2020). *Social Determinants of Health HealthyPeople.gov2020*. Rockville, MD: Office of Disease Prevention and Health Promotion.

Ospina-Prieto, S., Chaiwangyen, W., Herrmann, J., Groten, T., Schleussner, E., Markert, U. R., et al. (2016). MicroRNA-141 is upregulated in preeclamptic placentae and regulates trophoblast invasion and intercellular communication. *Transl. Res.* 172, 61–72. doi: 10.1016/j.trsl.2016.02.012

Pal, S., and Tyler, J. K. (2016). Epigenetics and aging. *Sci. Adv.* 2:e1600584.

Parnaud, G., Li, P., Cassar, G., Rouimi, P., Tulliez, J., Combaret, L., et al. (2004). Mechanism of sulforaphane-induced cell cycle arrest and apoptosis in human colon cancer cells. *Nutr. Cancer* 48, 198–206. doi: 10.1207/s15327914nc4802_10

Perkins, K. A., Karelitz, J. L., and Kunkle, N. (2018). Evaluation of menthol per se on acute perceptions and behavioral choice of cigarettes differing in nicotine content. *J. Psychopharmacol.* 32, 324–331. doi: 10.1177/0269881117742660

Povel, C. M., Boer, J. M., and Feskens, E. J. (2011). Shared genetic variance between the features of the metabolic syndrome: heritability studies. *Mol. Genet. Metab.* 104, 666–669. doi: 10.1016/j.ymgme.2011.08.035

Pradhan, A. D. (2014). Sex differences in the metabolic syndrome: implications for cardiovascular health in women. *Clin. Chem.* 60, 44–52. doi: 10.1373/clinchem.2013.202549

Rajendran, P., Johnson, G., Li, L., Chen, Y. S., Dashwood, M., Nguyen, N., et al. (2019). Acetylation of CCAR2 Establishes a BET/BRD9 Acetyl Switch in Response to Combined Deacetylase and Bromodomain Inhibition. *Cancer Res.* 79, 918–927. doi: 10.1158/0008-5472.can-18-2003

Rates, R. S. (2007). *SEER Cancer Statistics Review 1975-2004*. Bethesda, MD: NIH.

Relton, C. L., and Davey Smith, G. (2015). Mendelian randomization: applications and limitations in epigenetic studies. *Epigenomics* 7, 1239–1243. doi: 10.2217/epi.15.88

Roberti, A., Valdes, A. F., Torrecillas, R., Fraga, M. F., and Fernandez, A. F. (2019). Epigenetics in cancer therapy and nanomedicine. *Clin. Epigenet.* 11:81.

Ronnekleiv-Kelly, S. M., Sharma, A., and Ahuja, N. (2017). Epigenetic therapy and chemosensitization in solid malignancy. *Cancer Treat. Rev.* 55, 200–208. doi: 10.1016/j.ctrv.2017.03.008

Sahai, V., Redig, A. J., Collier, K. A., Eckerdt, F. D., and Munshi, H. G. (2016). Targeting BET bromodomain proteins in solid tumors. *Oncotarget* 7, 53997–54009. doi: 10.18632/oncotarget.9804

Saloner, B., and Le Cook, B. (2014). An ACA provision increased treatment for young adults with possible mental illnesses relative to comparison group. *Health Aff.* 33, 1425–1434. doi: 10.1377/hlthaff.2014.0214

Schmidt-Grimminger, D. C., Bell, M. C., Muller, C. J., Maher, D. M., Chauhan, S. C., and Buchwald, D. S. (2011). HPV infection among rural American Indian women and urban white women in South Dakota: an HPV prevalence study. *BMC Infect. Dis.* 11:252. doi: 10.1186/1471-2334-11-252

Schneiderman, N., Ironson, G., and Siegel, S. D. (2005). Stress and health: psychological, behavioral, and biological determinants. *Annu. Rev. Clin. Psychol.* 1, 607–628. doi: 10.1146/annurev.clinpsy.1.102803.144141

Shen, J., Reis, J., Morrison, D. C., Papasian, C., Raghavakaimal, S., Kolbert, C., et al. (2006). Key inflammatory signaling pathways are regulated by the proteasome. *Shock* 25, 472–484. doi: 10.1097/01.shk.0000209554.46704.64

Siegel, R., Naishadham, D., and Jemal, A. (2013). Cancer statistics, 2013. *CA* 63, 11–30. doi: 10.3322/caac.21166

Simó-Riudalbas, L., and Esteller, M. (2015). Targeting the histone orthography of cancer: drugs for writers, erasers and readers. *Br. J. Pharmacol.* 172, 2716–2732. doi: 10.1111/bph.12844

Smith, A. K., Kilaru, V., Kocak, M., Almli, L. M., Mercer, K. B., Ressler, K. J., et al. (2014). Methylation quantitative trait loci (meQTLs) are consistently detected across ancestry, developmental stage, and tissue type. *BMC Genom.* 15:145. doi: 10.1186/1471-2164-15-145

Smith, G. D., and Ebrahim, S. (2003). 'Mendelian randomization': can genetic epidemiology contribute to understanding environmental determinants of disease? *Int. J. Epidemiol.* 32, 1–22. doi: 10.1093/ije/dyg070

Tenkku, L. E., Morris, D. S., Salas, J., and Xaverius, P. K. (2009). Racial disparities in pregnancy-related drinking reduction. *Matern. Child Health J.* 13, 604–613. doi: 10.1007/s10995-008-0409-2

VanderWeele, T. J. (2016). Mediation Analysis: a Practitioner's Guide. *Ann. Rev. Public Health* 37, 17–32.

Wee, S., Dhanak, D., Li, H., Armstrong, S. A., Copeland, R. A., Sims, R., et al. (2014). Targeting epigenetic regulators for cancer therapy. *Ann. N. Y. Acad. Sci.* 1309, 30–36. doi: 10.1111/nyas.12356

Welty, L. J., Harrison, A. J., Abram, K. M., Olson, N. D., Aaby, D. A., McCoy, K. P., et al. (2016). Health disparities in drug- and alcohol-use disorders: a 12-Year Longitudinal Study of Youths After Detention. *Am. J. Public Health* 106, 872–880. doi: 10.2105/ajph.2015.303032

Westreich, D. (2012). Berkson's bias, selection bias, and missing data. *Epidemiology* 23, 159–164. doi: 10.1097/ede.0b013e31823b6296

Wetherill, L., Agrawal, A., Kapoor, M., Bertelsen, S., Bierut, L. J., Brooks, A., et al. (2015). Association of substance dependence phenotypes in the COGA sample. *Addict. Biol.* 20, 617–627. doi: 10.1111/adb.12153

Xu, Y., Zhang, X., Hu, X., Zhou, W., Zhang, P., Zhang, J., et al. (2018). The effects of lncRNA MALAT1 on proliferation, invasion and migration in colorectal cancer through regulating SOX9. *Mol. Med.* 24:52.

Yancey, A. K., Ortega, A. N., and Kumanyika, S. K. (2006). Effective recruitment and retention of minority research participants. *Annu. Rev. Public Health* 27, 1–28. doi: 10.1146/annurev.publhealth.27.021405.102113

Zaman, M. S., Chauhan, N., Yallapu, M. M., Gara, R. K., Maher, D. M., Kumari, S., et al. (2016). Curcumin nanoformulation for cervical cancer treatment. *Sci. Rep.* 6:20051.

Zhou, J., Sears, R. L., Xing, X., Zhang, B., Li, D., Rockweiler, N. B., et al. (2017). Tissue-specific DNA methylation is conserved across human, mouse, and rat, and driven by primary sequence conservation. *BMC Genom.* 18:724. doi: 10.1186/s12864-017-4115-6

Conflict of Interest: The authors declare that the research was conducted in the absence of any commercial or financial relationships that could be construed as a potential conflict of interest.

frontiers in Genetics

CASE REPORT
published: 14 October 2020
doi: 10.3389/fgene.2020.576235

Novel Compound Heterozygous Variants in *MKS1* Leading to Joubert Syndrome

Minna Luo[1,2†], Ruida He[3†], Zaisheng Lin[3†], Yue Shen[1,2], Guangyu Zhang[4], Zongfu Cao[1,2], Chao Lu[1,2], Dan Meng[5], Jing Zhang[3], Xu Ma[1,2*] and Muqing Cao[3*]*

[1] National Research Institute for Family Planning, Beijing, China, [2] National Human Genetic Resources Center, Beijing, China, [3] Key Laboratory of Cell Differentiation and Apoptosis of Chinese Ministry of Education, Department of Pathophysiology, Shanghai Jiao Tong University School of Medicine, Shanghai, China, [4] Department of Children Rehabilitation, The Third Affiliated Hospital of Zhengzhou University, Zhengzhou, China, [5] Tianjin Key Laboratory of Food and Biotechnology, School of Biotechnology and Food Science, Tianjin University of Commerce, Tianjin, China

OPEN ACCESS

Edited by:
Fasil Tekola-Ayele,
National Institutes of Health (NIH),
United States

Reviewed by:
Sheng Wang,
University of California,
San Francisco, United States
Jeffrey Dennis Calhoun,
Northwestern University,
United States
Ruxandra Bachmann-Gagescu,
University of Zurich, Switzerland

***Correspondence:**
Jing Zhang
Jingzhang@shsmu.edu.cn
Xu Ma
maxu_nhgrc@163.com
Muqing Cao
muqingcao@sjtu.edu.cn

[†] These authors have contributed equally to this work

Specialty section:
This article was submitted to Genetics of Common and Rare Diseases, a section of the journal Frontiers in Genetics

Received: 25 June 2020
Accepted: 14 September 2020
Published: 14 October 2020

Citation:
Luo M, He R, Lin Z, Shen Y, Zhang G, Cao Z, Lu C, Meng D, Zhang J, Ma X and Cao M (2020) Novel Compound Heterozygous Variants in MKS1 Leading to Joubert Syndrome. Front. Genet. 11:576235. doi: 10.3389/fgene.2020.576235

Joubert syndrome (JBTS) and Meckel–Gruber syndrome (MKS) are rare recessive disorders caused by defects of cilia, and they share overlapping clinical features and allelic loci. Mutations of *MKS1* contribute approximately 7% to all MKS cases and are found in some JBTS patients. Here, we describe a JBTS patient with two novel mutations of *MKS1*. Whole exome sequencing (WES) revealed c.191-1G > A and c.1058delG compound heterozygous variants. The patient presented with typical cerebellar vermis hypoplasia, hypotonia, and developmental delay, but without other renal/hepatic involvement or polydactyly. Functional studies showed that the c.1058delG mutation disrupts the B9 domain of MKS1, attenuates the interactions with B9D2, and impairs its ciliary localization at the transition zone (TZ), indicating that the B9 domain of MKS1 is essential for the integrity of the B9 protein complex and localization of MKS1 at the TZ. This work expands the mutation spectrum of *MKS1* and elucidates the clinical heterogeneity of *MKS1*-related ciliopathies.

Keywords: cilia, ciliopathy, Joubert syndrome, B9 proteins, *MKS1*

INTRODUCTION

Caused by defects of cilia, a variety of disorders are named ciliopathies (Hildebrandt et al., 2011; Novarino et al., 2011; Reiter and Leroux, 2017). Joubert syndrome (JBTS) and Meckel–Gruber syndrome (MKS) are two kinds of typical ciliopathies sharing overlapping clinical phenotypes, such as central nervous system malformation, renal/liver disease, and polydactyly (Brancati et al., 2010; Sattar and Gleeson, 2011; Hartill et al., 2017). JBTS is characterized by cerebellar vermis hypoplasia, which shows a typical molar tooth sign (MTS) on magnetic resonance imaging (MRI) (Joubert et al., 1969; Bachmann-Gagescu et al., 2020). Additional clinical symptoms may also be associated with brain malformations, including cystic kidney disease, liver fibrosis, polydactyly, or retinal dystrophy (Bachmann-Gagescu et al., 2020). Most JBTS patients are expected to have normal life spans (Dempsey et al., 2017). MKS is a rare lethal ciliopathy characterized by occipital encephalocele, cystic renal dysplasia, and postaxial polydactyly (Hartill et al., 2017). Ciliary defects in MKS result in perinatal lethality.

Genetic analysis has revealed that JBTS and MKS share more than 10 allelic loci (Kyttala et al., 2006; Baala et al., 2007; Valente et al., 2010; Dowdle et al., 2011; Garcia-Gonzalo et al., 2011), most of which encode proteins concentrated to the ciliary transition zone (TZ), a specialized region at the ciliary base controlling the composition of cilia (Chih et al., 2011; Garcia-Gonzalo et al., 2011; Sang et al., 2011). MKS1 is a TZ protein found in MKS, JBTS, and Bardet–Biedl syndrome (BBS), which is a ciliopathy characterized by obesity, retinitis pigmentosa, polydactyly, intellectual disability, and renal abnormalities (Kyttala et al., 2006; Dawe et al., 2007; Slaats et al., 2016). Mutations of the *MKS1* gene contribute to approximately 7% of all reported MKS cases (Hartill et al., 2017), but only a few mutations in *MKS1* have been reported to cause JBTS (Romani et al., 2014; Bachmann-Gagescu et al., 2015; Bader et al., 2016; Irfanullah et al., 2016; Vilboux et al., 2017). In the present study, we identified a patient with two novel *MKS1* mutations in a JBTS cohort. In contrast to most reported JBTS cases with $\geq$ 1 non-truncating mutation of *MKS1*, this patient carried two mutations leading to truncated forms of MKS1. Further studies showed that the truncated protein failed to interact with B9D2 and attenuated the TZ localization. These findings extend the spectrum of *MKS1* mutations in ciliopathies.

MATERIALS AND METHODS

Whole Exome Sequencing and Variants Analysis

The exomes were captured by using the Agilent SureSelect Human All Exon V6 Kit (Agilent Technologies Inc.) and sequencing on an Illumina NovaSeq 6000 platform (Illumina Inc., CA, United States). Burrows−Wheeler Aligner and SAMtools were used to align the NGS reads to the hg19 reference genome (GRCh37). PCR duplicates were removed by Picard tools. Variants and small InDels were called by Genome Analysis Toolkit (GATK), annotated with Ensembl Variant Effect Predictor (McLaren et al., 2016) and filtered as described previously (Luo et al., 2019). Finally, all the variants were annotated according to American College of Medical Genetics and Genomics (ACMG) guidelines (Richards et al., 2015), and the variants from known causative genes of JBTS were analyzed with priority. Sanger sequencing was performed for variant validation.

RNA Extraction and PCR

Tempus^{TM} Blood RNA Tube (Thermo Fisher Scientific, MA, United States) and Tempus^{TM} Spin RNA Isolation Kit (Thermo Fisher Scientific, MA, United States) were used for blood collection and RNA extraction, respectively. SuperScript IV First-Strand Synthesis System Kit (Thermo Fisher Scientific, MA, United States) was used for reverse transcription. The forward primer (5′-CCGAGTCCACCTGCAAAGAA-3′) used for cDNA amplification crossed the junction of exon 1 and exon 2, while the reverse primer (5′-TTCTCCCCCTCCGTCTCAAT-3′) was located at the beginning of exon 8. For qPCR, the primers of *MKS1* 5′-AAGGTGGCTCACTTCTCCTACC-3′ and 5′-AGAGGACCTCACAGTAGAGCAC-3′ and the primers of *GAPDH* 5′-GTCTCCTCTGACTTCAACAGCG-3′ and 5′-ACCACCCTGTTGCTGTAGCCAA-3′ were used.

Plasmid Constructs

The cDNAs of *MKS1* and *B9D2* were amplified by PCR from a cDNA library prepared from HEK293 cells. *MKS1* variants were cloned into the pLV-FLAG lentiviral vector. *B9D2* was inserted into pCMV-HA. All plasmid sequences were validated by Sanger sequencing.

Cell Culture, Plasmid Transfection, Lentivirus Package, and Infection

HEK293T cells were grown in Dulbecco's modified Eagle medium (DMEM, Sigma, MO, United States) supplemented with 10% FBS (Sigma, MO, United States), 100 U/ml penicillin, and 0.1 mg/ml streptomycin. RPE1 cells were grown in DMEM/F12 (1:1 mixture) (Sigma, MO, United States) supplemented with 10% FBS, 100 U/ml penicillin, and 0.1 mg/ml streptomycin. Transfections of HEK293T cells were performed using linearized polyethyleneimine (PEI) (Polysciences Inc., PA, United States). pLV-FLAG plasmids harboring *MKS1* variants were transfected into HEK293 cells with psPAX2 and pMD2.g by the PEI method. Media containing virus were filtered through a 0.45 μm membrane filter and added into plates with RPE1 cells in the presence of 6 μg/ml polybrene (Santa Cruz, TX, United States). After 48 h of infection, RPE1 cells were selected with 10 μg/ml puromycin for 2 weeks.

Co-immunoprecipitation and Western Blot Analysis

For co-immunoprecipitation (co-IP), transfected HEK293T cells were rinsed with ice-cold PBS and scraped into IP lysis buffer (20 mM Tris–HCl, pH = 7.5; 150 mM NaCl; 0.5 mM EDTA; and 0.5% Triton X-100) supplemented with protease inhibitor cocktail. After 20 min, cell lysates were cleared by 10,000 × *g* centrifugation at 4°C for 10 min. The supernatant was used for the co-IP assay by shaking with FLAG M2 beads (Sigma-Aldrich, MO, United States) for 2 h at 4°C. After three washes, proteins binding to FLAG beads were eluted with IP buffer containing 200 μg/ml 3 × FLAG peptides (Sigma-Aldrich, MO, United States).

For Western blot analysis, whole cell lysates or the elution products from the co-IP were denatured with 2 × SDS sample buffer, resolved on SDS-polyacrylamide gel electrophoresis, and subjected to Western blotting. The following antibodies were used for Western blot analysis: anti-FLAG (1:5,000, Sigma-Aldrich, MO, United States), anti-HA (1:3,000, Sigma-Aldrich, MO, United States), goat anti-mouse IRDye 680RD (1:15,000; LI-COR, NE, United States), and goat anti-rabbit IRDye 800CW (1:20,000; LI-COR, NE, United States).

Immunostaining and Confocal Imaging

For immunostaining, RPE1 cells were seeded on coverslips in six-well plates. After serum starvation for 48 h, cells were washed with PBS and fixed with 4% paraformaldehyde for 10 min, and the fixed cells were permeabilized by −20°C cold methanol or

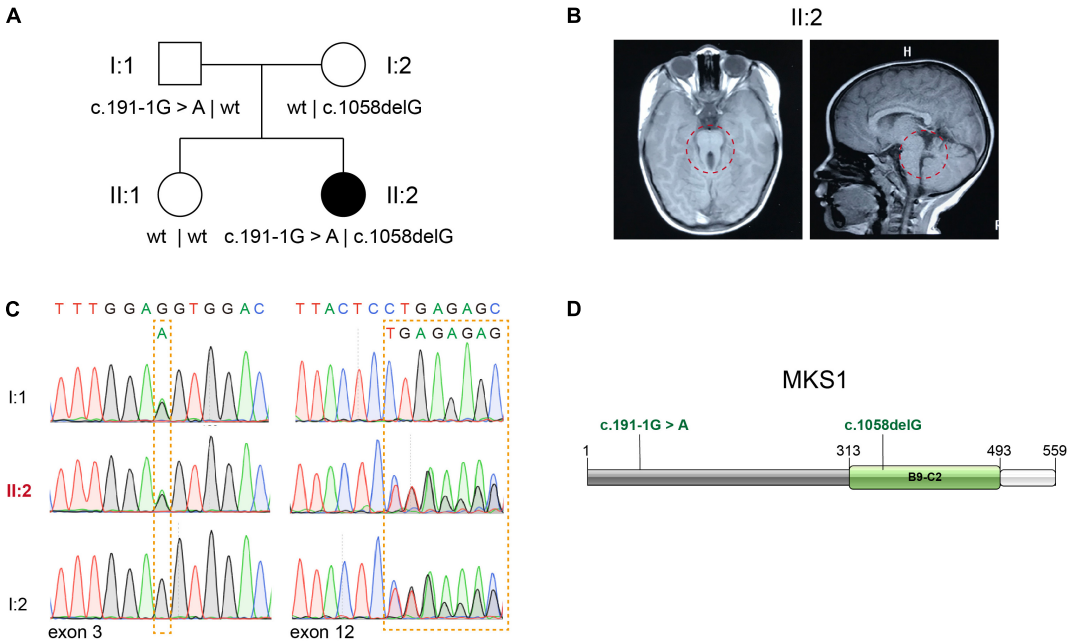

FIGURE 1 | Identification of novel *MKS1* mutations in a patient with Joubert syndrome. **(A)** Pedigree of family referred for a clinical diagnosis of Joubert syndrome (JBTS). **(B)** Brain MRI of the proband showing the typical molar tooth sign and cerebellar vermis hypoplasia. **(C)** Electropherograms of Sanger sequences showing *MKS1* sequences of the proband and her parents. **(D)** Schematic diagram of MKS1 domain structure and the mutations of the affected individual. The B9 domain is labeled as B9-C2.

0.3% Triton X-100 for 10 min. After washing twice with PBS, cells were stained using primary antibodies in blocking buffer (PBS containing 1% bovine serum albumin and 0.1% Triton X-100) for 1 h at room temperature. After washing with PBS twice, cells were incubated with secondary antibodies in blocking buffer for 1 h at room temperature. DNA was visualized by DAPI (Sigma-Aldrich, MO, United States). Samples were visualized using a FV3000 confocal microscope (Olympus, Tokyo, Japan) with a 40 × /NA1.4 objective (Olympus, Tokyo, Japan). Data from three independent experiments was used for intensity quantification.

RESULTS

Novel Mutations of *MKS1* Are Associated With Joubert Syndrome

Whole exome sequencing (WES) of 151 patients in a JBTS cohort resulted in the identification of two likely pathogenic *MKS1* variants. The proband, II:2, is the second child of non-consanguineous parents without related medical history (**Figure 1A**). She was born full-term by normal delivery, weighing 4,050 g and measuring 55 cm in height. The proband was hospitalized at the age of 5 months, and she was diagnosed with hypotonia and developmental delay. Brain MRI showed typical molar tooth sign, indicating severe cerebellar vermis hypoplasia (**Figure 1B**). No renal/hepatic involvement, polydactyly, or agenesis of the corpus callosum was observed (**Table 1**). Several rare deleterious variants in the known JBTS genes were found by WES (**Supplementary Table 1**). WES found the compound heterozygous variants in the *MKS1* gene (GenBank: NM_017777.3), but other variants are heterozygous (**Supplementary Table 1**). The paternally inherited variant of *MKS1* is mutated at the canonical splice acceptor site, and it is also known as rs201362733 with a rare frequency (0.00001202) in gnomAD (**Figures 1C,D**). The maternally inherited variant, c.1058delG, is a deletion of one nucleotide causing a frameshift

TABLE 1 | Clinical features and genotype.

Sample name	129C
Gender	Female
Age	5 months
Ethnic	Chinese
Mutation 1	c.191-1G > A
	p.S64Mfs*12
Mutation 2	c.1058delG
	p.G353Efs*2
Molar tooth sign	+
Developmental delay	+
Respiratory abnormality	–
Hypotonia	+
Oculomotor apraxia	–
Retinal involvement	NA
Renal involvement	–
Liver involvement	–
Limb anomalies	–
Agenesis of the corpus callosum	–

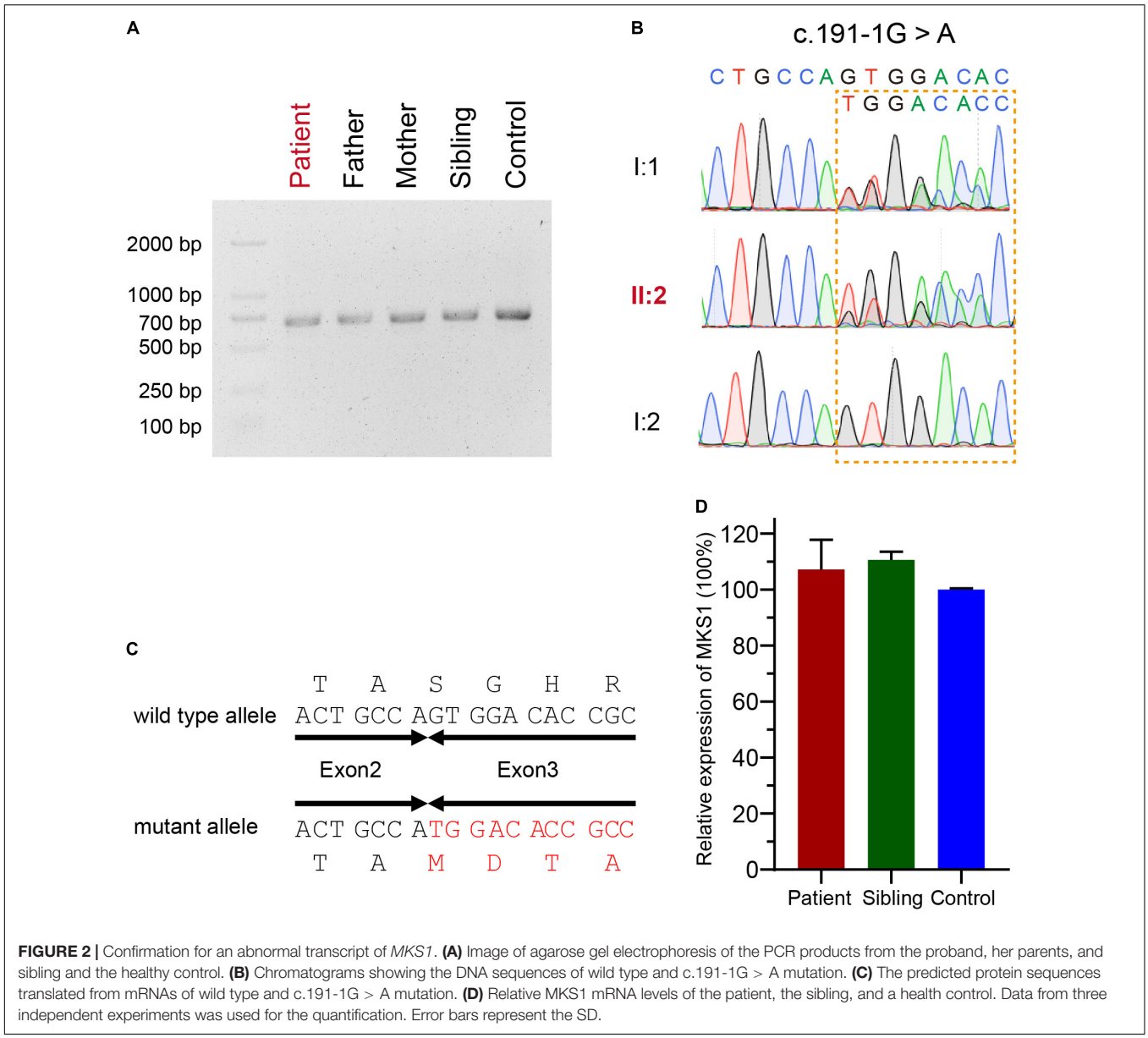

FIGURE 2 | Confirmation for an abnormal transcript of *MKS1*. **(A)** Image of agarose gel electrophoresis of the PCR products from the proband, her parents, and sibling and the healthy control. **(B)** Chromatograms showing the DNA sequences of wild type and c.191-1G > A mutation. **(C)** The predicted protein sequences translated from mRNAs of wild type and c.191-1G > A mutation. **(D)** Relative MKS1 mRNA levels of the patient, the sibling, and a health control. Data from three independent experiments was used for the quantification. Error bars represent the SD.

and premature stop, p.G353Efs*2 (**Figures 1C,D**). Thus, both of the two variants of *MKS1* were classified as "pathogenic," according to the ACMG guidelines (Richards et al., 2015). The absence of these two variants in her sister revealed that she is not a carrier.

Confirmation for an Abnormal Transcript of *MKS1*

The mutational effect of c.191-1G > A was validated by reverse transcription PCR. Surprisingly, only one band was observed in the proband, her father, her mother, her sister, and a healthy control (**Figure 2A**). Sanger sequencing showed one nucleotide deletion at the beginning of exon 3 rather than skipping exon 3, which was caused by the failure of correct splicing in c.191-1G > A mutated samples (the proband and father) (**Figures 2B,C**). This deletion resulted in a frameshift and a premature stop, which is annotated as p.S64Mfs*12. The mRNA level was comparable to the sibling and healthy control (**Figure 2D**).

The B9 Domain of MKS1 Is Required for the Transition Zone Localization and Interaction With B9D2

B9-containing proteins are highly conserved proteins present only in organisms assembling cilia (Barker et al., 2014). *MKS1* encodes a protein with 559 amino acids and the B9 domain localizes at the C-terminus. The c.191-1G > A variant was predicted to generate a short peptide containing 64 correct amino acids, suggesting complete loss of function. The c.1058delG variant caused early termination of the translation of MKS1,

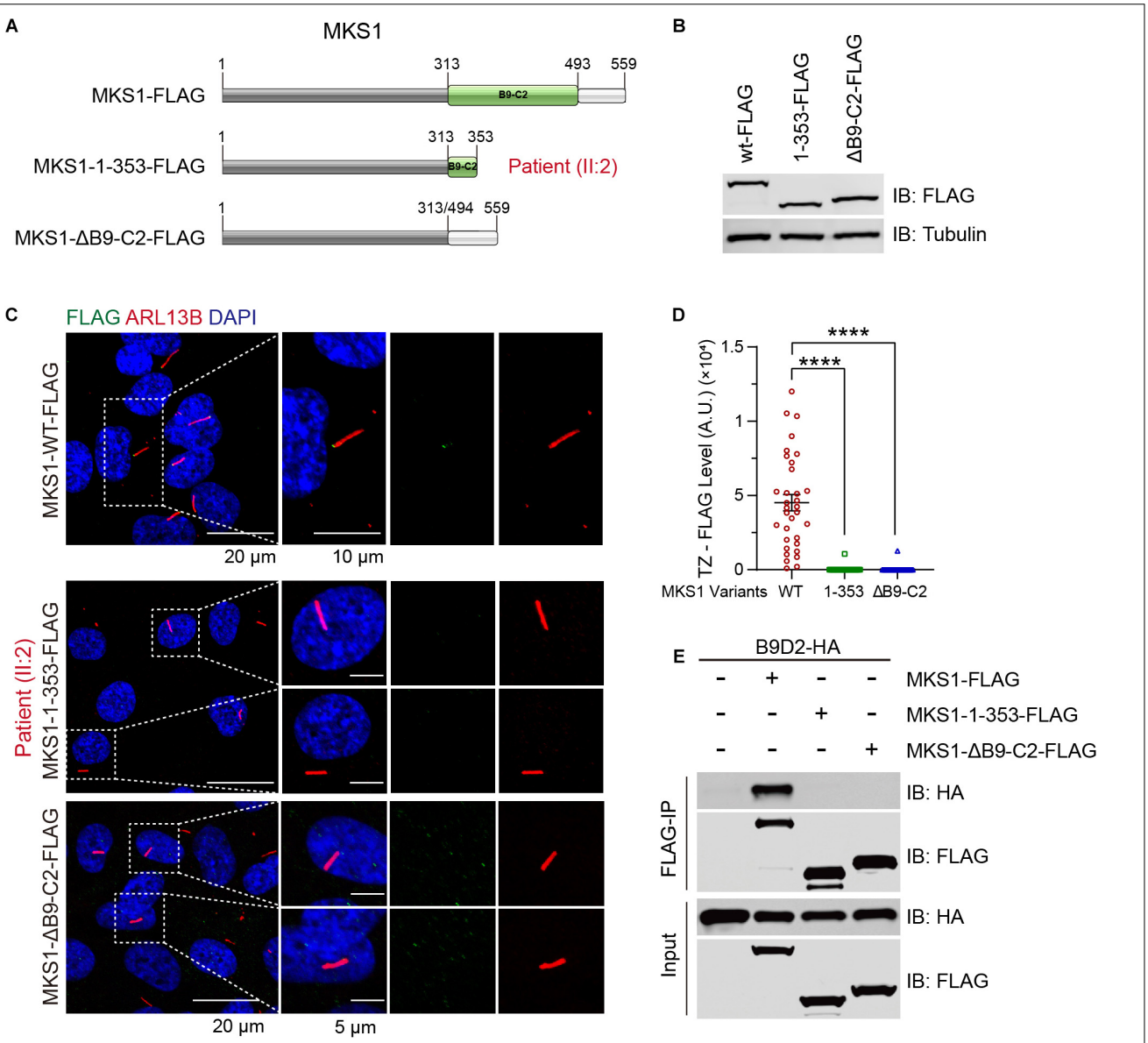

FIGURE 3 | MKS1 mutant fails to localize at the transition zone and lose the interaction with B9D2. **(A)** Schematic diagram of the domain structure of MKS1 variants (wild type, MKS1 1-353, and MKS1 lacking B9 domain). **(B)** Immunoblot analysis of RPE1 cell lines stably expressed FLAG-tagged MKS1 variants shown in **(A)**. **(C)** Immunostaining of RPE1 cells expressing FLAG-tagged MKS1 variants. MKS1 variants (FLAG, green), cilia (ARL13B, red), and nuclei (DAPI, blue). **(D)** Quantification of MKS1 variant levels at the transition zone. Each dot represents the signal of one cell. Data from three independent experiments was used for the quantification. Error bars represent mean ± SD. Statistical significance was determined by an unpaired Student's *t*-test (****$p < 0.0001$). **(E)** Immunoprecipitation of FLAG-tagged MKS1 variants with B9D2.

which caused the partial loss of the B9 domain (314–493) and loss of the C-terminal tail (494–559). To confirm the pathogenicity, we established RPE1 cell lines stably expressing FLAG-tagged wild-type, MKS1 1-353 (to mimic p.G353Efs*2), or B9 domain lacking MKS1 (**Figure 3A**). Immunoblots confirmed the expression of the variants (**Figure 3B**). Previous studies have shown that MKS1 mainly localizes at the ciliary transition zone (Dowdle et al., 2011; Garcia-Gonzalo et al., 2011; Sang et al., 2011; Slaats et al., 2016). Therefore, we determined whether the MKS1 1-353 disrupted the localization of MKS1 by immunostaining. Almost all cells expressing wild-type *MKS1* had FLAG signal at the transition zone, but the localization of MKS1 1-353 or the B9 domain-lacking mutant was largely attenuated (**Figures 3C,D**). It has been shown that the three B9 proteins, MKS1, B9D1, and B9D2, form a protein complex, the integrity of which is essential for their function (Chih et al., 2011; Dowdle et al., 2011; Garcia-Gonzalo et al., 2011; Sang et al., 2011). In this complex, MKS1 predominantly interacts with B9D2 (Dowdle et al., 2011). To test whether the mutation affects B9 protein complex formation, we performed co-immunoprecipitation assays. Immunoblots

showed that wild-type MKS1 but not the MKS1 1-353 or B9 domain-lacking MKS1 interacted with B9D2 (**Figure 3E**). These results demonstrate that the B9 domain is essential for the localization and activity of MKS1 protein.

DISCUSSION

In this study, we report a JBTS patient with two novel *MKS1* mutations displaying global developmental delay, MTS, and hypotonia. Additional brain anomalies such as agenesis of the corpus callosum, which is more frequent in MKS than JBTS (Bader et al., 2016), were not observed. This patient belongs to JBTS, because no renal or liver involvement and no limb anomalies were displayed.

A hypothesis has been proposed for the genotype–phenotype correlation as follows: two null alleles of *MKS1* result in MKS; one null allele and one hypomorphic allele result in JBTS; and two hypomorphic alleles result in BBS (Bader et al., 2016). In this study, the proband has two truncating mutations but has JBTS. This situation has also occurred in three other cases as follows: homozygous splice acceptor site mutation of c.1461-2A > G in COR340 (Romani et al., 2014), homozygous frameshift mutation of c.1528dupC (p.R510Pfs*81) in UW31-3, and homozygous splice acceptor site mutation of c.1589-2A > T in UW150-3 (Bachmann-Gagescu et al., 2015; Slaats et al., 2016). Taken together, these findings suggested that the genotype–phenotype correlation is more complicated in *MKS1*-mutated ciliopathies.

Previous landmark studies have shown that the integrity of the B9 complex may be essential for the control of the entry and exit of ciliary components (Dowdle et al., 2011; Sang et al., 2011). We found that loss of the B9 domain of MKS1 largely attenuates its transition zone localization and disrupts the interaction with B9D2. These findings are consistent with previous studies. Three major protein modules locate at the TZ region, namely the NPHP complex, the B9 complex, and the TMEM–TCTN complex. The disruption of the B9 complex possibly changes the structure of the three key modules and results in ciliopathies.

In summary, we identified two novel null mutants of *MKS1* resulting in JBTS, expanding the genetic basis of JBTS. Our findings further implicate that clinical features of *MKS1* mutations are more complicated than the previously proposed genotype–phenotype correlation model of the *MKS1* gene. Finally, these findings will be helpful for the genetic testing of JBTS patients and their families.

DATA AVAILABILITY STATEMENT

The data in this study are available from MC, upon reasonable request.

ETHICS STATEMENT

The studies involving human participants were reviewed and approved by the Ethics Committee of the National Research Institute for Family Planning of China. Written informed consent to participate in this study was provided by the participants' legal guardian/next of kin. Written informed consent was obtained from the individual(s), and minor(s)' legal guardian/next of kin, for the publication of any potentially identifiable images or data included in this article.

AUTHOR CONTRIBUTIONS

MC, XM, JZ, and ML conceived and directed the project. GZ collected the blood sample and medical information of the patients. YS analyzed and interpreted the medical data. ML, YS, and CL prepared the samples and performed the WES. ZC and ML analyzed and interpreted the WES data. RH, ZL, and DM performed the biochemical analysis and imaging. MC, XM, JZ, and ML wrote the manuscript with the help of all the other authors. All authors contributed to the article and approved the submitted version.

FUNDING

The work was supported by the National Key Research and Development Program of China (2016YFC1000307) to XM, the National Natural Science Foundation of China (91954123, 31972887) to MC, Clinical Research Projects of Shanghai Municipal Health Commission (20194Y0133) to MC, the Non-Profit Central Research Institute Fund of the National Research Institute for Family Planning (2020GJZ05) to ML, the National Natural Science Foundation of China (31701172) to DM, and the Natural Science Foundation of Tianjin (18JCQNJC09900) to DM.

ACKNOWLEDGMENTS

We are very grateful to the patients and their parents for their participation in this study and their permission regarding this publication.

SUPPLEMENTARY MATERIAL

The Supplementary Material for this article can be found online at: https://www.frontiersin.org/articles/10.3389/fgene.2020.576235/full#supplementary-material

REFERENCES

Baala, L., Romano, S., Khaddour, R., Saunier, S., Smith, U. M., Audollent, S., et al. (2007). The meckel-gruber syndrome gene, MKS3, is mutated in Joubert syndrome. *Am. J. Hum. Genet.* 80, 186–194. doi: 10.1086/510499

Bachmann-Gagescu, R., Dempsey, J. C., Bulgheroni, S., Chen, M. L., D'Arrigo, S., Glass, I. A., et al. (2020). Healthcare recommendations for Joubert syndrome. *Am. J. Med. Genet. A* 182, 229–249. doi: 10.1002/ajmg.a.61399

Bachmann-Gagescu, R., Dempsey, J. C., Phelps, I. G., O'Roak, B. J., Knutzen, D. M., Rue, T. C., et al. (2015). Joubert syndrome: a model for untangling recessive

disorders with extreme genetic heterogeneity. *J. Med. Genet.* 52, 514–522. doi: 10.1136/jmedgenet-2015-103087

Bader, I., Decker, E., Mayr, J. A., Lunzer, V., Koch, J., Boltshauser, E., et al. (2016). MKS1 mutations cause Joubert syndrome with agenesis of the corpus callosum. *Eur. J. Med. Genet.* 59, 386–391. doi: 10.1016/j.ejmg.2016.06.007

Barker, A. R., Renzaglia, K. S., Fry, K., and Dawe, H. R. (2014). Bioinformatic analysis of ciliary transition zone proteins reveals insights into the evolution of ciliopathy networks. *BMC Genomics* 15:531. doi: 10.1186/1471-2164-15-531

Brancati, F., Dallapiccola, B., and Valente, E. M. (2010). Joubert Syndrome and related disorders. *Orphanet. J. Rare Dis.* 5:20. doi: 10.1186/1750-1172-5-20

Chih, B., Liu, P., Chinn, Y., Chalouni, C., Komuves, L. G., Hass, P. E., et al. (2011). A ciliopathy complex at the transition zone protects the cilia as a privileged membrane domain. *Nat. Cell Biol.* 14, 61–72. doi: 10.1038/ncb2410

Dawe, H. R., Smith, U. M., Cullinane, A. R., Gerrelli, D., Cox, P., Badano, J. L., et al. (2007). The meckel-gruber syndrome proteins MKS1 and meckelin interact and are required for primary cilium formation. *Hum. Mol. Genet.* 16, 173–186. doi: 10.1093/hmg/ddl459

Dempsey, J. C., Phelps, I. G., Bachmann-Gagescu, R., Glass, I. A., Tully, H. M., and Doherty, D. (2017). Mortality in Joubert syndrome. *Am. J. Med. Genet. A.* 173, 1237–1242. doi: 10.1002/ajmg.a.38158

Dowdle, W. E., Robinson, J. F., Kneist, A., Sirerol-Piquer, M. S., Frints, S. G., Corbit, K. C., et al. (2011). Disruption of a ciliary B9 protein complex causes Meckel syndrome. *Am. J. Hum. Genet.* 89, 94–110. doi: 10.1016/j.ajhg.2011.06.003

Garcia-Gonzalo, F. R., Corbit, K. C., Sirerol-Piquer, M. S., Ramaswami, G., Otto, E. A., Noriega, T. R., et al. (2011). A transition zone complex regulates mammalian ciliogenesis and ciliary membrane composition. *Nat. Genet.* 43, 776–784. doi: 10.1038/ng.891

Hartill, V., Szymanska, K., Sharif, S. M., Wheway, G., and Johnson, C. A. (2017). Meckel-gruber syndrome: an update on diagnosis, clinical management, and research advances. *Front. Pediatr.* 5:244. doi: 10.3389/fped.2017.00244

Hildebrandt, F., Benzing, T., and Katsanis, N. (2011). Ciliopathies. *N. Engl. J. Med.* 364, 1533–1543. doi: 10.1056/NEJMra1010172

Irfanullah, K. S., Ullah, I., Nasir, A., Meijer, C. A., Laurense-Bik, M., Dunnen, J. T. D., et al. (2016). Hypomorphic MKS1 mutation in a Pakistani family with mild Joubert syndrome and atypical features: expanding the phenotypic spectrum of MKS1-related ciliopathies. *Am. J. Med. Genet. A* 170, 3289–3293. doi: 10.1002/ajmg.a.37934

Joubert, M., Eisenring, J. J., Robb, J. P., and Andermann, F. (1969).). Familial agenesis of the cerebellar vermis. A syndrome of episodic hyperpnea, abnormal eye movements, ataxia, and retardation. *Neurology* 19, 813–825. doi: 10.1212/wnl.19.9.813

Kyttala, M., Tallila, J., Salonen, R., Kopra, O., Kohlschmidt, N., Paavola-Sakki, P., et al. (2006). MKS1, encoding a component of the flagellar apparatus basal body proteome, is mutated in Meckel syndrome. *Nat. Genet.* 38, 155–157. doi: 10.1038/ng1714

Luo, M., Cao, L., Cao, Z., Ma, S., Shen, Y., Yang, D., et al. (2019). Whole exome sequencing reveals novel CEP104 mutations in a Chinese patient with Joubert syndrome. *Mol. Genet. Genomic Med.* 7:e1004. doi: 10.1002/mgg3.1004

McLaren, W., Gil, L., Hunt, S. E., Riat, H. S., Ritchie, G. R., Thormann, A., et al. (2016). The ensembl variant effect predictor. *Genome Biol.* 17:122. doi: 10.1186/s13059-016-0974-4

Novarino, G., Akizu, N., and Gleeson, J. G. (2011). Modeling human disease in humans: the ciliopathies. *Cell* 147, 70–79. doi: 10.1016/j.cell.2011.09.014

Reiter, J. F., and Leroux, M. R. (2017). Genes and molecular pathways underpinning ciliopathies. *Nat. Rev. Mol. Cell Biol.* 18, 533–547. doi: 10.1038/nrm.2017.60

Richards, S., Aziz, N., Bale, S., Bick, D., Das, S., Gastier-Foster, J., et al. (2015). Standards and guidelines for the interpretation of sequence variants: a joint consensus recommendation of the American college of medical genetics and genomics and the association for molecular pathology. *Genet. Med.* 17, 405–424. doi: 10.1038/gim.2015.30

Romani, M., Micalizzi, A., Kraoua, I., Dotti, M. T., Cavallin, M., Sztriha, L., et al. (2014). Mutations in B9D1 and MKS1 cause mild Joubert syndrome: expanding the genetic overlap with the lethal ciliopathy Meckel syndrome. *Orphanet. J. Rare Dis.* 9:72. doi: 10.1186/1750-1172-9-72

Sang, L., Miller, J. J., Corbit, K. C., Giles, R. H., Brauer, M. J., Otto, E. A., et al. (2011). Mapping the NPHP-JBTS-MKS protein network reveals ciliopathy disease genes and pathways. *Cell* 145, 513–528. doi: 10.1016/j.cell.2011.04.019

Sattar, S., and Gleeson, J. G. (2011). The ciliopathies in neuronal development: a clinical approach to investigation of Joubert syndrome and Joubert syndrome-related disorders. *Dev. Med. Child Neurol.* 53, 793–798. doi: 10.1111/j.1469-8749.2011.04021.x

Slaats, G. G., Isabella, C. R., Kroes, H. Y., Dempsey, J. C., Gremmels, H., Monroe, G. R., et al. (2016). MKS1 regulates ciliary INPP5E levels in Joubert syndrome. *J. Med. Genet.* 53, 62–72. doi: 10.1136/jmedgenet-2015-103250

Valente, E. M., Logan, C. V., Mougou-Zerelli, S., Lee, J. H., Silhavy, J. L., Brancati, F., et al. (2010). Mutations in TMEM216 perturb ciliogenesis and cause Joubert. Meckel and related syndromes. *Nat. Genet.* 42, 619–625. doi: 10.1038/ng.594

Vilboux, T., Doherty, D. A., Glass, I. A., Parisi, M. A., Phelps, I. G., Cullinane, A. R., et al. (2017). Molecular genetic findings and clinical correlations in 100 patients with Joubert syndrome and related disorders prospectively evaluated at a single center. *Genet. Med.* 19, 875–882. doi: 10.1038/gim.2016.204

Conflict of Interest: The authors declare that the research was conducted in the absence of any commercial or financial relationships that could be construed as a potential conflict of interest.

frontiers in Genetics

ORIGINAL RESEARCH
published: 26 January 2021
doi: 10.3389/fgene.2020.497264

Evaluation of Maternal Serum sHLA-G Levels for Trisomy 18 Fetuses Screening at Second Trimester

Danping Xu[1], Yiyang Zhu[1], Lanfang Li[1], Yingping Xu[1], Weihua Yan[2], Meizhen Dai[2] and Linghong Gan[2]*

[1] *Reproductive Center, Taizhou Hospital of Zhejiang Province, Wezhou Medical University, Wenzhou, China,* [2] *Medical Research Center, Taizhou Hospital of Zhejiang Province, Wezhou Medical University, Wenzhou, China*

Human leukocyte antigen-G (HLA-G) has been widely acknowledged to play critical roles in fetal-maternal maintenance. However, the significance of using maternal serum sHLA-G to detect prenatal chromosomal abnormality has not been investigated. In China, prenatal screening using maternal α-fetoprotein (AFP), unconjugated estriol (uE3), and free β subunit human chorionic gonadotropin (β-hCG) in the second trimester has been widely applied. In this study, we evaluated the use of sHLA-G as a screening marker, compared with traditional second trimester prenatal screening. Serum samples from 1,019 singleton women in their second trimester were assessed. Among them, 139 infants were confirmed with trisomy 21 (T21) by karyotyping, 83 were confirmed with trisomy 18 (T18), and the remaining 797 infants had no abnormalities. The sHLA-G levels in maternal sera were significantly lower in pregnant women with T18 fetuses (median: 47.8 U/ml, range: 9.8–234.2 U/ml) and significantly higher in those with T21 fetuses (median: 125.7 U/ml, range: 28.7–831.7 U/ml), compared with the normal controls (median: 106.3 U/ml, range: 50.5–1136.4 U/ml) ($p < 0.001$). The risk values of the screening of T21 or T18 fetuses were assessed using mean and standard deviation $\log_{10}$ analyte multiples of median (MoM) which showed that the predictive values of sHLA-G were the same as free β-hCG, and superior to AFP and uE3 for T18 screening. Logistic regression analysis revealed that sHLA-G MoM was the highest risk factor associated with pregnant women carrying T18 fetuses [Exp(B): 171.26, 95% CI: 36.30–807.97, $p < 0.001$]. Receiver operating characteristic (ROC) analysis revealed that the area under ROC curve for sHLA-G MoM was 0.915 (95% CI, 0.871–0.959, $p < 0.001$), for AFP MoM was 0.796 (95% CI, 0.730–0.861, $p < 0.001$), for free β-hCG MoM was 0.881 (95% CI, 0.829–0.934, $p < 0.001$), and for uE3 MoM was 0.876 (95% CI, 0.828–0.923, $p < 0.001$) in the T18 group. sHLA-G MoM demonstrated the best sensitivity and negative predictive value. For the first time, our findings reveal that sHLA-G is a better second trimester screening marker for the detection of T18 fetuses and the combined application of sHLA-G with AFP, free β-hCG, and uE3 could improve clinical screening for T18 fetuses.

Keywords: human leukocyte antigen-G, soluble HLA-G, pregnancy, fetus, chromsome, trisomy

OPEN ACCESS

Edited by:
Daniel Enquobahrie, University of Washington, United States

Reviewed by:
Rubi Nieves Rodríguez Díaz, University of La Laguna, Spain
Jin Han, Guangzhou Women and Children's Medical Center, China

****Correspondence:***
Danping Xu
411087356@qq.com

Specialty section:
This article was submitted to Applied Genetic Epidemiology, a section of the journal Frontiers in Genetics

Received: *11 September 2019*
Accepted: *23 December 2020*
Published: *26 January 2021*

Citation:
Xu D, Zhu Y, Li L, Xu Y, Yan W, Dai M and Gan L (2021) Evaluation of Maternal Serum sHLA-G Levels for Trisomy 18 Fetuses Screening at Second Trimester. Front. Genet. 11:497264. doi: 10.3389/fgene.2020.497264

INTRODUCTION

China is a large country, with a population size of more than 1.3 billion people. With an aging population in mind, the Chinese government canceled the birth control policy on October 29, 2015. The number of pregnant women increased sharply. Trisomy 18 syndrome (T18), also known as Edwards syndrome, is one of the most common aneuploidies diagnosed in the prenatal period. Most T18 fetuses are miscarried, so the overall prevalence in China is difficult to estimate, but the prevalence of newborn babies with T18 is 1 in 5,000 live births. Although non-invasive prenatal testing (NIPT) could be used to screen for T18 in the early stages of pregnancy, its cost meant it could not be made widely available. In China, combined serological screening in the first and second trimesters had been widely introduced in recent years and there were also some regions or individuals who simply chose the second trimester screening. Therefore, it is important to improve the detection rate and to reduce the false-positive rate for diagnosing this condition.

Human leukocyte antigen-G (HLA-G) was cloned and identified by Geraghty in 1987 and its expression was first observed in human trophoblasts by Kovats et al. (1990). Since then, a large number of studies have explored the biological roles and clinical significance of HLA-G in the arena of reproductive immunology (Ferreira et al., 2017). At least seven isoforms of HLA-G have now been well-defined, including four membrane-bound (mHLA-G; HLA-G1 to -G4) and three soluble (sHLA-G; HLA-G5 to -G7) isoforms; and additional novel isoforms have been proposed as a result of alternative splicing of the primary transcripts (Tronik-Le Roux et al., 2017; Lin and Yan, 2018). Both mHLA-G and sHLA-G have comprehensive immune suppression functions including inhibition of T cells, natural killer (NK) cell cytotoxicity (Huang et al., 2009; Chen et al., 2013), and stimulating proliferation of regulatory cells such as regulatory T cells (Tregs) and myeloid-derived suppressor cells (MDSCs) (Tilburgs et al., 2015; Kostlin et al., 2017). The underlying mechanisms involve interactions between the HLA-Gs and their receptors, such as the immune inhibitory receptor immunoglobulin-like transcripts (ILT)2 and ILT4, which are expressed on various immune cells (Nowak et al., 2017; Lin and Yan, 2018). The concept that HLA-G plays critical roles in semi-allograft maternal-fetal immune tolerance has been well-established (Ferreira et al., 2017; Persson et al., 2017). It is worth noting that a recent study reported that crosstalk between HLA-G and ILT2 is able to stimulate the $CD49a^{+}Eomesodermin^{+}$uterine NK (uNK) secretion of growth-promoting factors (Fu et al., 2017), which contribute to fetal growth. The authors also found that decreased growth-promoting factors (GPFs) secretion was able to impair fetal development and resulted in fetal growth restriction.

In the context of pregnancy complications, decreased maternal peripheral sHLA-G levels have been observed in cases of recurrent miscarriage, pre-eclampsia, and intrauterine growth restriction (Laskowska et al., 2012; He et al., 2016; Zidi et al., 2016). The interaction of HLA-G with the receptors expressed on uNK cells (the dominant leukocyte population at the maternal-fetal interface) can play essential roles in a successful pregnancy, including spiral artery remodeling, trophoblast invasion and control of viral infection (Yan et al., 2007; van Beekhuizen et al., 2010; Tilburgs et al., 2015).

However, whether maternal peripheral blood sHLA-G levels can be used to diagnose prenatal chromosomal abnormality remains unknown. In this study, the levels of sHLA-G in maternal sera were determined using ELISAs on serum samples from pregnant women whose fetuses or babies presented with normal (797 women) or abnormal karyotypes (222 women). The relationship between maternal sHLA-G levels and the status of fetal karyotypes was evaluated to determine the potential for sHLA-G in the second trimester as a tool for prenatal screening.

SUBJECTS AND METHODS

Study Population

We retrospectively reviewed pregnant women who received second trimester prenatal screening from May 2007 to May 2017 in our Taizhou prenatal screening and diagnostics center, Taizhou Hospital of Zhejiang Province, China. During this period, 508,715 pregnant women received prenatal screening and all of them were between the ages of 18 and 35, with gestational weeks ranging from 15 to 19 weeks. Because of the low incidence of T18 and T21 fetuses, a case-control study was selected. A sample of cases and controls were selected from a cohort of 508,715 pregnant women. The participant selection method is shown in **Figure 1**. Risk estimation was based on the levels of the prenatal serum markers α-fetoprotein (AFP), free β subunit human chorionic gonadotropin (β-HCG), and unconjugated estriol (uE3). Within this cohort, 25,417 high-risk cases and 634 low-risk cases underwent invasive prenatal diagnosis with amniocentesis and amniotic fluid karyotype analysis. In addition, chromosome karyotypes for peripheral blood or umbilical cord blood were analyzed from 594 babies and dead fetuses. In large hospitals in Zhejiang province, karyotype analysis and the genetic testing for deafness have become necessary tests for newborns in recent years. Therefore, all newborns will participate in peripheral blood karyotype analysis in the future.

In China, children under 1 year old had many important physical examinations. The examinations included measurement of height, weight, and head circumference, the fontanelle size, the number of baby teeth, vision development, and genital development. All pregnant women who received prenatal screening in our center were followed up with 1 year after their babies' birth. In total, second trimester screening for T18 and T21 had a detection rate of 66 of 83 T18 cases (79.5%) and 105 of 139 T21 cases (75.5%) for a 5% false-positive rate, respectively. We found 222 fetuses or babies with abnormal karyotypes, including 139 with trisomy 21 (T21) and 83 with trisomy 18 (T18). These mothers were treated as experimental groups. In contrast, the mothers of fetuses or babies with normal karyotypes were treated as controls. Various problems might occur during pregnancy, such as a high risk of abnormality, polyhydramnios, oligohydramnios, bright light in the fetal ventricle, single umbilical artery. These problems do not affect the health of children after the exclusion of abnormal karyotypes.

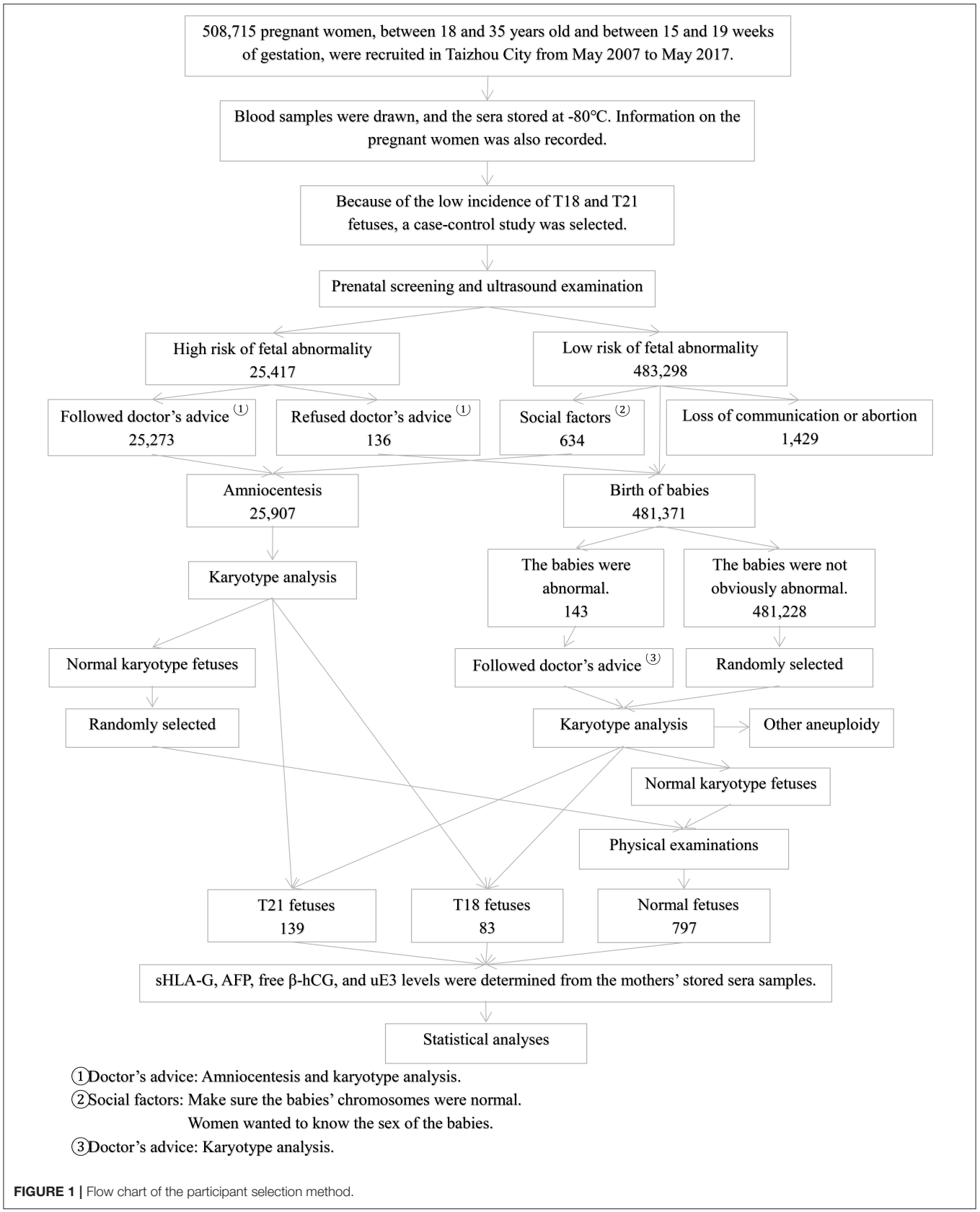

FIGURE 1 | Flow chart of the participant selection method.

Therefore, these factors were included in the control group. All fetuses or babies were singletons who were naturally conceived. We excluded all pregnant women whose babies presented with problems at the follow up examinations, who had multiple babies, or who conceived by *in vitro* fertilization.

The remaining subjects were divided into two groups: amniocentesis and non-puncture groups. Karyotype analysis was performed on the amniotic fluid from pregnant women in the amniocentesis group, which was further divided into two groups based on the reason for puncture: high risk of abnormality due to prenatal screening and other reasons. The total control group was randomly selected from among these participants. In the control group selected from the non-puncture group, peripheral blood was collected from the children (within 2 years old) for karyotype analysis. Subjects with karyotype abnormalities were excluded and 797 cases were finally selected to comprise the normal control group. All of the children who were examined by ultrasound were normal in the normal control group.

In the control group selected from the amniocentesis group, 297 pregnant women were at high risk of abnormality by prenatal screening, 115 pregnant women were diagnosed with abnormality by ultrasound (48 cases with polyhydramnios, 11 cases with oligohydramnios, 34 cases with bright light in the fetal ventricle, and 22 cases with single umbilical artery) and 49 women had normal pregnancies. The 49 pregnant women were urged to take amniotic fluid for chromosome examination due to social factors.

This study was approved by the Ethics Committee of Taizhou Hospital of Zhejiang Province, and all patients provided informed consent after prenatal screening, in accordance with the Declaration of Helsinki. Both karyotype analysis and physical examination were the screening gold standards in this study and were performed on all fetuses or babies. We applied the double-blind method to sample selection and detection. All of the sera were stored in a refrigerator at −80°C. **Table 1** summarizes the subject information of the pregnant women.

sHLA-G Enzyme-Linked Immunosorbent Assay (ELISA)

Serum sHLA-G levels were determined using a sHLA-G ELISA kit (sHLA-G ELISA kit, RD194070100R; Exbio, Prague, Czech Republic), according to the manufacturer's protocol.

Second Trimester Screening

Blood drawn from pregnant women for prenatal screening was used to detect the biochemical markers AFP, uE3, and free β-hCG using time-resolved immunofluorimetry (AutoDELFIA® AFP/Free hCGβ Dual and Unconjugated Estriol, PerkinElmer Life and Analytical Sciences, Turku, Finland). Invasive prenatal diagnostic techniques were performed to confirm the abnormalities when the pregnant woman was at a high risk for abnormalities. All of the babies were followed up until the first year after birth.

Statistical Analyses

Statistical analysis was performed using the Statistical Package for the Social Sciences (SPSS) software program, version 13.0 (SPSS, Inc., Chicago, IL). The sHLA-G results were expressed as multiples of the median (MoM) of the control group after logarithmic transformation. AFP, uE3, and free β-hCG levels were expressed as MoM of the appropriate gestational control group after logarithmic transformation. Differences in sHLA-G MoM, AFP MoM, uE3 MoM, and free β-hCG MoM were evaluated by Mann-Whitney *U*-test. A Bivariate correlation analysis was used to analyze the relationship of all analytes. A calculation of the risk value using combinations of four analytes, the maternal age risk, and the maternal weight risk was performed according to Gaussian distribution (Reynolds and Penney, 1990; Spencer et al., 1994, 1999). A Logistic regression analysis was used to assess the risk factors for pregnant women with fetuses possessing abnormal chromosomes. A Receiver operating characteristic (ROC) curve analysis was performed to evaluate the power of maternal sHLA-G levels to discriminate fetuses with normal karyotypes from

TABLE 1 | Maternal age, weight, and sHLA-G level of the study population.

Grouping	*N*	Median weight (range)	Median age (range)	Median sHLA-G (range)
Pregnant women with T21 fetuses	139	54.5 (36.8–93.0)	28.65 (18.0–34.9)	125.7 (28.7–831.7)
Pregnant women with T18 fetuses	83	55.0 (35.0–75.0)	28.45 (21.2–34.3)	47.8 (9.8–234.2)
Controls with normal fetuses	797	54.5 (36.8–93.0)	28.13 (18.0–34.99)	106.3 (50.5–1136.4)
Amniocentesis group				
High risk of prenatal screening	297	55.0 (39.0–88.0)	29.2 (18.8–35.0)	121.5 (56.0–1136.4)
Ultrasonic abnormality	115	56.0 (40.0–89.0)	28.3 (18.2–35.0)	105.3 (50.5–937.6)
Polyhydramnios	48	56.5 (40.0–89.0)	29.1 (18.2–35.0)	113.4 (50.8–631.2)
Oligohydramnios	11	50.0 (43.0–57.0)	27.3 (18.7–32.4)	82.0 (61.0–215.0)
Bright light in the fetal ventricle	34	59.0 (45.0–76.0)	27.5 (18.7–34.9)	104.2 (50.5–207.0)
Single umbilical artery	22	55.0 (40.0–73.0)	27.4 (20.1–33.5)	103.9 (54.8–937.6)
Karyotype analysis is strongly required due to social factors	49	54.0 (40.0–82.0)	28.4 (18.2–34.3)	98.3 (56.1–801.8)
Non-puncture group				
Peripheral blood karyotype analysis was performed within 2 years old	336	54.0 (36.8–93.0)	27.1 (18.0–35.0)	100.9 (50.5–705.6)

those with chromosomal abnormalities. The cut-off value for the ROC curve analysis was determined by Youden's index (Fluss et al., 2005). Preliminary experimental results for the calculation of sample size showed that the sensitivity and specificity of sHLA-G MoM was 85% and 88%, respectively. The sample size was calculated by software according to the above rates. The minimum number of subjects required was 784, with an allowable error of 0.1 in a two-tailed test with $p < 0.05$. A $p < 0.05$ was considered to be statistically significant.

RESULTS

Maternal sHLA-G Levels in Fetuses With Normal and Abnormal Chromosomes

Maternal sHLA-G levels in pregnant women carrying fetuses with normal chromosomes were at a median level of 106.3 U/ml (range: 50.5–1136.4), whereas women carrying T18 fetuses had a median level of 47.8 U/ml (range: 9.8–234.2), and those with T21 fetuses had a median level of 125.7 U/ml (range: 28.7–831.7). Statistical analyses showed that maternal sHLA-G levels in

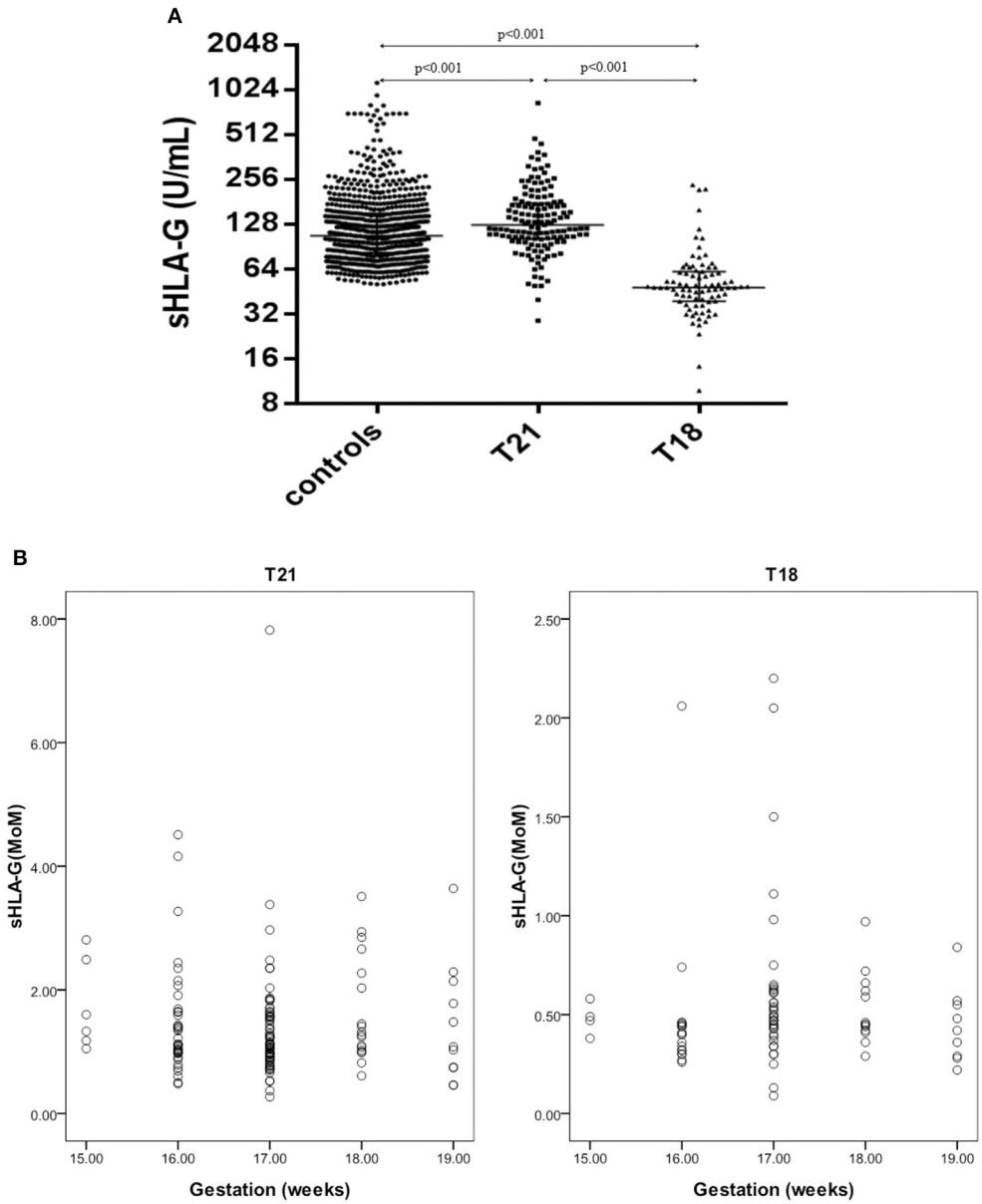

FIGURE 2 | sHLA-G levels and MoM values in pregnant women with T21 fetuses ($n = 139$), T18 fetuses ($n = 83$), and normal control fetuses ($n = 797$). **(A)** Comparison of sHLA-G levels in pregnant women with T21 fetuses, T18 fetuses, and normal control fetuses. **(B)** Scatter diagram of the sHLA-G MoM values of the T21 and T18 groups.

women carrying T21 fetuses were dramatically higher compared to women with normal fetuses (125.7 U/ml vs. 106.3 U/ml; $p < 0.001$), while maternal sHLA-G levels significantly decreased in pregnant women with T18 fetuses (47.8 U/ml vs. 106.3 U/ml; $p < 0.001$) compared to pregnant women with normal chromosome fetuses (**Figure 2**).

Overall, sHLA-G levels were not associated with the gestational age of the fetus. When the 297 high-risk cases were removed, the median sHLA-G levels first decreased and then increased with the gestational weeks, but there was no statistical difference (data not shown).

Evaluation of sHLA-G Levels as a Second Trimester Screening Marker in Comparison to Levels of AFP, uE3, and Free β-hCG

To consider variation of marker levels with gestational age, the maternal serum AFP, uE3, and free β-hCG MoM values were used (Spencer et al., 1994, 1999). The AFP, uE3, free β-hCG, and sHLA-G MoM values of the T18 group were remarkably lower than those of the control group (**Table 2**, all $p < 0.001$). The AFP and uE3 MoM values of the T21 group were statistically lower than the control group, but the free β-hCG and sHLA-G MoM values were noticeably higher than the control group (**Table 2**, all $p < 0.001$).

The risk values were calculated by mean and standard deviation (SD) $\log_{10}$ analyte MoM (**Table 2**), then adding the maternal age and weight risk. According to the Gaussian distribution formula, the smaller the numerical values of SD and the greater the distances of the mean between experimental and control groups, the better the analyte for the calculation of the risk values. From the data in **Table 2**, sHLA-G (T18 group: −0.3269 and 0.21661, control: 0.0455 and 0.22564) had the same predictive value as free β-hCG (T18 group: −0.6133 and 0.52362, control: 0.0622 and 0.39822) for T18 screening. A Bivariate correlation analysis was used to analyze the relationship

TABLE 2 | Distribution of data in controls and pregnant women with T21 or T18 fetuses.

	Controls with normal fetuses ($n = 797$)	Pregnant women with T21 fetuses ($n = 139$)	Pregnant women with T18 fetuses ($n = 83$)
Median AFP MoM	1	0.7149	0.5401
Median free β-hCG MoM	1	2.5804	0.2219
Median UE3 MoM	1	0.7891	0.8330
Median sHLA-G MoM	1	1.1800	0.4500
Mean Log_{10} AFP MoM	−0.0067	−0.1457	−0.1978
Mean Log_{10} free β-hCG MoM	0.0622	0.3651	−0.6133
Mean Log_{10} UE3 MoM	−0.0163	−0.1390	−0.3538
Mean Log_{10} sHLA-G MoM	0.0455	0.1014	−0.3269
SD Log_{10} AFP MoM	0.16057	0.20747	0.25615
SD Log_{10} free β-hCG MoM	0.39822	0.45804	0.52362
SD Log_{10} UE3 MoM	0.16962	0.23251	0.28058
SD Log_{10} sHLA-G MoM	0.22564	0.22433	0.21661
Correlation			
AFP vs. free β-hCG	−0.134 ($P < 0.01$)	0.167 ($P = 0.05$)	0.191 ($P > 0.05$)
AFP vs. UE3	0.525 ($P < 0.01$)	0.228 ($P < 0.05$)	−0.054 ($P > 0.05$)
AFP vs. sHLA-G	−0.075 ($P < 0.05$)	0.003 ($P > 0.05$)	−0.033 ($P > 0.05$)
free β-hCG vs. UE3	−0.293 ($P < 0.01$)	−0.075 ($P > 0.05$)	0.233 ($P = 0.034$)
free β-hCG vs. sHLA-G	0.095 ($P < 0.01$)	0.291 ($P < 0.01$)	−0.030 ($P > 0.05$)
UE3 vs. sHLA-G	−0.052 ($P > 0.05$)	0.164 ($P > 0.05$)	0.212 ($P > 0.05$)

TABLE 3 | The multivariate logistic regression analyses of the various parameters for pregnant women with abnormal chromosome fetuses.

Variate	Pregnant women with T21 fetuses		Pregnant women with T18 fetuses	
	Exp(B) (95% C-I)	*p*	Exp(B) (95% CI)	*p*
Age	1.02 (0.99–1.04)	0.215	1.01 (0.97–1.06)	0.548
Weight	0.99 (0.94–1.04)	0.574	0.98 (0.90–1.07)	0.701
AFP MoM	6.50 (3.28–12.88)	< 0.001	1.60 (0.99–2.59)	0.055
Free β-hCG MoM	0.76 (0.70–0.83)	< 0.001	1.30 (0.98–1.72)	0.74
UE3 MoM	3.73 (1.83–7.60)	< 0.001	51.11 (16.84–155.11)	< 0.001
sHLA-G MoM	0.98 (0.82–1.18)	0.839	171.26 (36.30–807.97)	< 0.001

of all analytes. The results showed that the sHLA-G level was not dependent on AFP, uE3, and free β-hCG in pregnant women with T18 fetuses (**Table 2**).

Assessment of the Efficacy of sHLA-G, AFP, uE3, and Free β-hCG as a Marker for Second Trimester Screening Using Logistic Regression

The multivariate logistic regression analyses of age, weight, sHLA-G MoM, AFP MoM, uE3 MoM, and free β-hCG MoM are presented in **Table 3**. It was found that the sHLA-G MoM [Exp(B): 171.26, 95% CI: 36.30–807.97, $p < 0.001$] and uE3 MoM [Exp(B): 51.11, 95% CI: 16.84–155.11, $p < 0.001$] were risk factors for pregnant women with T18 fetuses.

ROC Analysis for sHLA-G, AFP, uE3, and Free β-hCG as a Screening Marker

ROC curves were used to evaluate the performance of four analytes to discriminate pregnant women with normal chromosome fetuses from those with abnormal chromosome fetuses. For the screening of T21 abnormalities, the area under ROC curve for sHLA-G MoM was 0.601 (95% CI, 0.551–0.650, $p < 0.001$), for AFP MoM was 0.719 (95% CI, 0.670–0.769, $p < 0.001$), free β-hCG MoM was 0.732 (95% CI, 0.689–0.776, $p < 0.001$), and uE3 MoM was 0.698 (95% CI, 0.653–0.743, $p < 0.001$) (**Figure 3**). For the screening of T18 abnormalities, the area under ROC curve for sHLA-G MoM was 0.915 (95% CI, 0.871–0.959, $p < 0.001$), AFP MoM was 0.796 (95% CI, 0.730–0.861, $p < 0.001$), free β-hCG MoM was 0.881 (95% CI, 0.829–0.934, $p < 0.001$), and uE3 MoM was 0.876 (95% CI, 0.828–0.923, $p < 0.001$) (**Figure 3**).

The cut-off value was determined by Youden's index based on the ROC curve. ROC curve analysis revealed that the MoM value of sHLA-G could powerfully discriminate T18 fetuses with the cut-off < 0.646 (sensitivity: 85.5%, specificity: 87.7%; AUC: 0.915; $p < 0.001$) from the normal control group fetuses (**Table 4**).

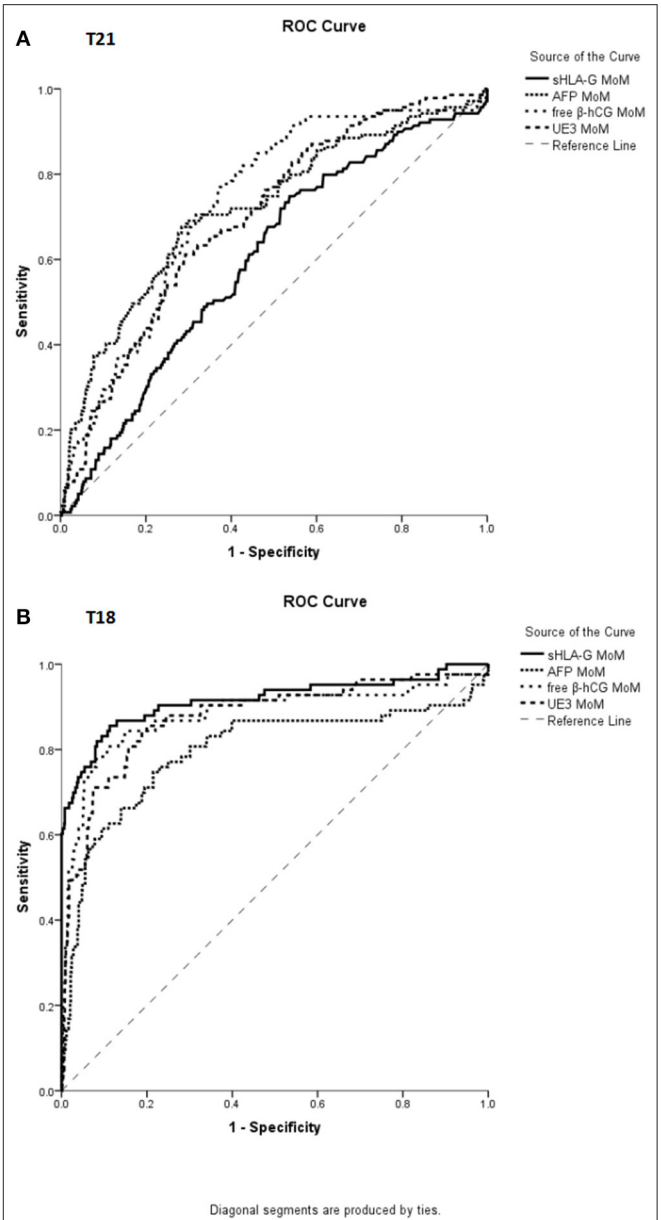

FIGURE 3 | ROC curve analysis for the MoM value of sHLA-G, AFP, free β-hCG, and uE3 in distinguishing pregnant women with normal fetuses from abnormal karyotype fetuses. **(A)** For screening T21, the area under ROC curve for sHLA-G MoM was 0.601 (95% CI, 0.551–0.650, $p < 0.001$), AFP MoM was 0.719 (95% CI, 0.670–0.769, $p < 0.001$), free β-hCG MoM was 0.732 (95% CI, 0.689–0.776, $p < 0.001$), and uE3 MoM was 0.698 (95% CI, 0.653–0.743, $p < 0.001$). **(B)** For screening T18, the area under ROC curve for sHLA-G MoM was 0.915 (95% CI, 0.871–0.959, $p < 0.001$), AFP MoM was 0.796 (95% CI, 0.730–0.861, $p < 0.001$), free β-hCG MoM was 0.881 (95% CI, 0.829–0.934, $p < 0.001$), and uE3 MoM was 0.876 (95% CI, 0.828–0.923, $p < 0.001$).

DISCUSSION

HLA-G was first shown to be expressed on the trophoblast and many studies have since been performed to investigate the role of HLA-G expression in fetal-maternal and reproductive immunology (Kovats et al., 1990; Rajagopalan, 2014). The interactions of HLA-G with its receptors (such as ILT2, ILT4, and KIR2DL4, expressed on uNK cells) have been shown to promote the maintenance of fetal-maternal immunotolerance during pregnancy and have a positive impact on fetal development and growth (Moffett and Colucci, 2015; Ferreira et al., 2017). However, the relationship between maternal peripheral sHLA-G levels and the status of fetal chromosome abnormality was previously unknown. In this study, maternal sera were obtained from women who underwent second trimester prenatal screening, and the chromosomes of fetuses and babies were analyzed by karyotyping. We assessed whether the maternal sHLA-G levels have predictive value for the status of fetal chromosome abnormality. Our data showed that maternal sHLA-G levels in pregnant women with T21 fetuses were significantly higher than in those with normal chromosome fetuses, while maternal sHLA-G levels significantly decreased in pregnant women with T18 fetuses.

Previous studies have revealed that higher levels of sHLA-G in an embryo culture is related to better embryo development, cleavage stages, and to a higher pregnancy rate (Kotze et al.,

TABLE 4 | Sensitivity and specificity for the MoM value of sHLA-G, AFP, free β-hCG, and UE3 at specified cutoffs.

Variables	sHLA-G MoM	AFP MoM	free β-hCG MoM	UE3 MoM
Cutoff	0.646	0.746	0.353	0.76
AUC ± SE	0.915 ± 0.023	0.796 ± 0.034	0.881 ± 0.027	0.876 ± 0.024
(95% CI)	(0.871–0.959)	(0.730–0.861)	(0.829–0.934)	(0.828–0.923)
Sensitivity (%)	85.5%	75.9%	78.3%	84.3%
Specificity (%)	88.7%	78.5%	91.8%	80.1%
PPV (%)	44.1%	26.9%	50.0%	30.6%
NPV (%)	98.3%	96.9%	97.6%	98.0%
PLR	7.58	3.54	9.60	4.23
NLR	0.16	0.31	0.24	0.20
P	< 0.001	< 0.001	< 0.001	< 0.001

2013; Diaz et al., 2019). sHLA-G detection has been presented as a non-invasive method for embryo selection and a predictor of pregnancy outcome (Kotze et al., 2010; Rebmann et al., 2010). Based on the sHLA-G levels in the culture supernatant from a 46-h embryo, specific embryos were selected as beneficial to pregnancy and implantation rates, regardless of age (Sher et al., 2004, 2005). In pregnancy disorders, decreased HLA-G expression in extravillous trophoblasts is linked to the incidence of pre-eclampsia. In a cohort of women with placenta-mediated complications of pregnancy (such as pre-eclampsia, fetal growth restriction, stillbirth, and placental abruption), plasma sHLA-G levels were significantly lower at the beginning of pregnancy in these subjects compared with the control group (Marozio et al., 2017). Plasma sHLA-G was also found to be dramatically decreased in women with recurrent abortion compared to normal pregnancies or women with only one abortion (Zidi et al., 2016). A recent study showed that HLA-G expressed on fetal villus tissues was noticeably reduced in trisomy 16-induced early embryonic death (EED) and patients with EED, but normal fetal chromosomes (EEDNC) compared to villous tissues from patients undergoing elective abortion with normal fetal chromosomes (EANC) (Yao et al., 2019).

In our study, maternal sHLA-G levels in pregnant women with T21 fetuses were significantly higher than in those with normal chromosome fetuses, while maternal sHLA-G levels significantly decreased in pregnant women with T18 fetuses. Because it was the first study on pregnancy with chromosomal abnormal fetus and sHLA-G, there was no correlational research to explain the results. Several possible reasons for these results can be speculated. (1) HLA-G was expressed on the trophoblast cell. Arizawa and Nakayama (1992) showed that there was a tendency for heavy placentas in T21, and a tendency for light placentas in T18 and T13. The quantity of trophoblast cell and the placenta size with T18, T21, and normal fetuses might be different (Kennerknecht and Terinde, 1990). These differences might affect the expression and secretion of sHLA-G level. (2) A high sHLA-G level in pregnant women with T21 fetuses might be the reason for their high survival rate.

Prenatal risk screening using maternal serological markers and fetal karyotype diagnosis is an important measure to prevent birth defects and genetic diseases such as the T18 and T21 syndromes. Maternal serological screening using AFP, uE3, and free β-hCG in the second trimester has been widely applied in China and the performance of these markers in prenatal screening has been well-documented (Tu et al., 2016; Zhou et al., 2018). However, other serological markers (such as inhibin) and protocols (such as non-invasive prenatal screening tests (NIPT) and first trimester screening) are also carried out to improve the capacity and quality of prenatal screening (Nshimyumukiza et al., 2018; Breveglieri et al., 2019).

Multiple factors influencing pregnancy were considered in the selection of the control group, but we observed some factors, noted in **Table 1**, that might have an impact on the sHLA-G level. In order to better compare the screening efficacy of maternal sHLA-G levels, these factors should be considered. Indeed, the need to take these factors into account has inspired our future research directions.

The mean and SD $\log_{10}$ analyte MoM values indicated that maternal sHLA-G possessed the same predictive value as free β-hCG in distinguishing the T18 group from the control group, according to Gaussian distribution (Reynolds and Penney, 1990). A Logistic regression analysis showed that sHLA-G MoM, and uE3 MoM were risk factors for pregnant women with T18 fetuses, while ROC analysis revealed that maternal sHLA-G MoM could efficiently discriminate the T18 and T21 fetuses from the normal group. Indeed, the area under ROC curve, sensitivity, and NPV (negative predictive value) of sHLA-G MoM revealed that sHLA-G levels performed better than AFP MoM, free β-hCG MoM, and uE3 MoM in discriminating T18 fetuses from normal fetuses.

Our findings, for the first time, reveal that maternal sHLA-G could be a novel screening marker for T21 and T18 fetuses, particularly for T18. However, a larger cohort is needed to establish a new combined screening formula for clinical use. In addition, the application of sHLA-G in early pregnancy screening is a further research direction of our group.

DATA AVAILABILITY STATEMENT

The datasets generated for this study are available on request to the corresponding author.

ETHICS STATEMENT

This study was approved by the Ethics Committee of Taizhou Hospital of Zhejiang Province. The patients/participants provided their written informed consent to participate in this study.

AUTHOR CONTRIBUTIONS

DX, YZ, and WY contributed to the study design. MD and LG were in charge of specimen selection. LL and YX performed the laboratory work. DX contributed to the analysis of the data and wrote the manuscript. All authors read and approved the final manuscript.

FUNDING

This work was supported by Zhejiang Province Public Welfare Technology Application Research Project (2017C33217).

ACKNOWLEDGMENTS

Thanks to Editage and Reyna Deeya Ballim.

REFERENCES

Arizawa, M., and Nakayama, M. (1992). Pathological analysis of the placenta in trisomies 21, 18 and 13. *Nihon Sanka Fujinka Gakkai Zasshi* 44, 9–13.

Breveglieri, G., D'Aversa, E., Finotti, A., and Borgatti, M. (2019). Non-invasive Prenatal Testing Using Fetal DNA. *Mol. Diagn. Ther*. 23, 291–299. doi: 10.1007/s40291-019-00385-2

Chen, B. G., Xu, D. P., Lin, A., and Yan, W. H. (2013). NK cytolysis is dependent on the proportion of HLA-G expression. *Hum. Immunol*. 74, 286–289. doi: 10.1016/j.humimm.2012.12.005

Diaz, R. R., Zamora, R. B., Sanchez, R. V., Perez, J. G., and Bethencourt, J. C. A. (2019). Embryo sHLA-G secretion is related to pregnancy rate. *Zygote* 27, 78–81. doi: 10.1017/S0967199419000054

Ferreira, L. M. R., Meissner, T. B., Tilburgs, T., and Strominger, J. L. (2017). HLA-G: at the interface of maternal-fetal tolerance. *Trends Immunol*. 38, 272–286. doi: 10.1016/j.it.2017.01.009

Fluss, R., Faraggi, D., and Reiser, B. (2005). Estimation of the Youden Index and its associated cutoff point. *Biom J*. 47, 458–472. doi: 10.1002/bimj.200410135

Fu, B., Zhou, Y., Ni, X., Tong, X., Xu, X., Dong, Z., et al. (2017). Natural killer cells promote fetal development through the secretion of growth-promoting factors. *Immunity* 47, 1100–1113.e6. doi: 10.1016/j.immuni.2017.11.018

He, Y., Chen, S., Huang, H., and Chen, Q. (2016). Association between decreased plasma levels of soluble human leukocyte antigen-G and severe pre-eclampsia. *J. Perinat. Med*. 44, 283–290. doi: 10.1515/jpm-2015-0062

Huang, Y. H., Zozulya, A. L., Weidenfeller, C., Schwab, N., and Wiendl, H. (2009). T cell suppression by naturally occurring HLA-G-expressing regulatory $CD4^+$ T cells is IL-10-dependent and reversible. *J. Leukoc. Biol*. 86, 273–281. doi: 10.1189/jlb.1008649

Kennerknecht, I., and Terinde, R. (1990). Intrauterine growth retardation associated with chromosomal aneuploidy confined to the placenta. Three observations: triple trisomy 6,21,22; trisomy 16; and trisomy 18. *Prenat Diagn*. 10, 539–544. doi: 10.1002/pd.1970100810

Kostlin, N., Ostermeir, A. L., Spring, B., Schwarz, J., Marme, A., Walter, C. B., et al. (2017). HLA-G promotes myeloid-derived suppressor cell accumulation and suppressive activity during human pregnancy through engagement of the receptor ILT4. *Eur. J. Immunol*. 47, 374–384. doi: 10.1002/eji.201646564

Kotze, D., Kruger, T. F., Lombard, C., Padayachee, T., Keskintepe, L., and Sher, G. (2013). The effect of the biochemical marker soluble human leukocyte antigen G on pregnancy outcome in assisted reproductive technology–a multicenter study. *Fertil. Steril*. 100, 1303–1309. doi: 10.1016/j.fertnstert.2013.07.1977

Kotze, D. J., Hansen, P., Keskintepe, L., Snowden, E., Sher, G., and Kruger, T. (2010). Embryo selection criteria based on morphology VERSUS the expression of a biochemical marker (sHLA-G) and a graduated embryo score: prediction of pregnancy outcome. *J. Assist. Reprod. Genet*. 27, 309–316. doi: 10.1007/s10815-010-9403-x

Kovats, S., Main, E. K., Librach, C., Stubblebine, M., Fisher, S. J., and DeMars, R. (1990). A class I antigen, HLA-G, expressed in human trophoblasts. *Science* 248, 220–223. doi: 10.1126/science.2326636

Laskowska, M., Laskowska, K., and Oleszczuk, J. (2012). Maternal soluble human leukocyte antigen-G levels in pregnancies complicated by foetal intrauterine growth restriction with and without preeclampsia. *Pregnancy Hypertens* 2, 168–173. doi: 10.1016/j.preghy.2012.01.008

Lin, A., and Yan, W. H. (2018). Heterogeneity of HLA-G expression in cancers: facing the challenges. *Front. Immunol*. 9:2164. doi: 10.3389/fimmu.2018.02164

Marozio, L., Garofalo, A., Berchialla, P., Tavella, A. M., Salton, L., Cavallo, F., et al. (2017). Low expression of soluble human leukocyte antigen G in early gestation and subsequent placenta-mediated complications of pregnancy. *J. Obstet. Gynaecol. Res*. 83, 1391–1396. doi: 10.1111/jog.13377

Moffett, A., and Colucci, F. (2015). Co-evolution of NK receptors and HLA ligands in humans is driven by reproduction. *Immunol. Rev*. 267, 283–297. doi: 10.1111/imr.12323

Nowak, I., Wilczynska, K., Wilczynski, J. R., Malinowski, A., Radwan, P., Radwan, M., et al. (2017). KIR, LILRB and their Ligands' genes as potential biomarkers in recurrent implantation failure. *Arch. Immunol. Ther. Exp*. 65, 391–399. doi: 10.1007/s00005-017-0474-6

Nshimyumukiza, L., Menon, S., Hina, H., Rousseau, F., and Reinharz, D. (2018). Cell-free DNA noninvasive prenatal screening for aneuploidy versus conventional screening: A systematic review of economic evaluations. *Clin. Genet*. 94, 3–21. doi: 10.1111/cge.13155

Persson, G., Melsted, W. N., Nilsson, L. L., and Hviid, T. V. F. (2017). HLA class Ib in pregnancy and pregnancy-related disorders. *Immunogenetics* 69, 581–595. doi: 10.1007/s00251-017-0988-4

Rajagopalan, S. (2014). HLA-G-mediated NK cell senescence promotes vascular remodeling: implications for reproduction. *Cell. Mol. Immunol*. 11, 460–466. doi: 10.1038/cmi.2014.53

Rebmann, V., Switala, M., Eue, I., and Grosse-Wilde, H. (2010). Soluble HLA-G is an independent factor for the prediction of pregnancy outcome after ART: a German multi-centre study. *Hum. Reprod*. 25, 1691–1698. doi: 10.1093/humrep/deq120

Reynolds, T. M., and Penney, M. D. (1990). The mathematical basis of multivariate risk screening: with special reference to screening for Down's syndrome associated pregnancy. *Ann. Clin. Biochem*. 27(Pt 5), 452–458. doi: 10.1177/000456329002700506

Sher, G., Keskintepe, L., Batzofin, J., Fisch, J., Acacio, B., Ahlering, P., et al. (2005). Influence of early ICSI-derived embryo sHLA-G expression on pregnancy and implantation rates: a prospective study. *Hum. Reprod*. 20, 1359–1363. doi: 10.1093/humrep/deh758

Sher, G., Keskintepe, L., Nouriani, M., Roussev, R., and Batzofin, J. (2004). Expression of sHLA-G in supernatants of individually cultured 46-h embryos: a potentially valuable indicator of 'embryo competency' and IVF outcome. *Reprod. Biomed. Online* 9, 74–78. doi: 10.1016/S1472-6483(10)62113-X

Spencer, K., Aitken, D. A., Crossley, J. A., McCaw, G., Berry, E., Anderson, R., et al. (1994). First trimester biochemical screening for trisomy 21: the role of free beta hCG, alpha fetoprotein and pregnancy associated plasma protein A. *Ann. Clin. Biochem*. 31, 447–454. doi: 10.1177/000456329403100504

Spencer, K., Souter, V., Tul, N., Snijders, R., and Nicolaides, K. H. (1999). A screening program for trisomy 21 at 10-14 weeks using fetal nuchal translucency, maternal serum free beta-human chorionic gonadotropin and pregnancy-associated plasma protein-A. *Ultrasound Obstet Gynecol*. 13, 231–237. doi: 10.1046/j.1469-0705.1999.13040231.x

Tilburgs, T., Evans, J. H., Crespo, A. C., and Strominger, J. L. (2015). The HLA-G cycle provides for both NK tolerance and immunity at the maternal-fetal interface. *Proc. Natl. Acad. Sci. U.S.A.* 112, 13312–13317. doi: 10.1073/pnas.1517724112

Tronik-Le Roux, D., Renard, J., Verine, J., Renault, V., Tubacher, E., et al. (2017). Novel landscape of HLA-G isoforms expressed in clear cell renal cell carcinoma patients. *Mol. Oncol.* 11, 1561–1578. doi: 10.1002/1878-0261.12119

Tu, S., Rosenthal, M., Wang, D., Huang, J., and Chen, Y. (2016). Performance of prenatal screening using maternal serum and ultrasound markers for Down syndrome in Chinese women: a systematic review and meta-analysis. *BJOG* 123, 12–22. doi: 10.1111/1471-0528.14009

van Beekhuizen, H. J., Joosten, I., Lotgering, F. K., Bulten, J., and van Kempen, L. C. (2010). Natural killer cells and HLA-G expression in the basal decidua of human placenta adhesiva. *Placenta* 31, 1078–1084. doi: 10.1016/j.placenta.2010.09.016

Yan, W. H., Lin, A., Chen, B. G., Zhou, M. Y., Dai, M. Z., Chen, X. J. et al. (2007). Possible roles of KIR2DL4 expression on uNK cells in human pregnancy. *Am. J. Reprod. Immunol.* 57, 233–242. doi: 10.1111/j.1600-0897.2007.00469.x

Yao, T., Hou, H., Liu, G., Wu, J., Qin, Z., Sun, Y., et al. (2019). Quantitative proteomics suggest a potential link between early embryonic death and trisomy 16. *Reprod. Fertil. Dev.* 31, 1116–1126. doi: 10.1071/RD17319

Zhou, Y., Du, Y., Zhang, B., and Wang, L. (2018). Integrating multiple of the median values of serological markers with the risk cut-off value in Down syndrome screening. *Biosci. Trends* 12, 613–619. doi: 10.5582/bst.2018.01232

Zidi, I., Rizzo, R., Bouaziz, A., Laaribi, A. B., Zidi, N., Di Luca, D., et al. (2016). sHLA-G1 and HLA-G5 levels are decreased in Tunisian women with multiple abortion. *Hum. Immunol.* 77, 342–345. doi: 10.1016/j.humimm.2016.01.019

Conflict of Interest: The authors declare that the research was conducted in the absence of any commercial or financial relationships that could be construed as a potential conflict of interest.

frontiers in Genetics

ORIGINAL RESEARCH
published: 19 March 2021
doi: 10.3389/fgene.2021.530028

A Possible Association Between Zika Virus Infection and CDK5RAP2 Mutation

Estephania Candelo[1,2], Ana Maria Sanz[3], Diana Ramirez-Montaño[2], Lorena Diaz-Ordoñez[2], Ana Maria Granados[4], Fernando Rosso[3], Julian Nevado[5], Pablo Lapunzina[5] and Harry Pachajoa[2,6]**

[1] Universidad Icesi, Ear Institute University College London and Fundación Valle del Lili, Cali, Colombia, [2] Center for Research on Congenital Anomalies and Rare Diseases (CIACER), Department of Basic Medical Sciences, Universidad Icesi, Cali, Colombia, [3] Fundacion Valle del Lili, Cali, Colombia, [4] Neuroradiology Department Fundación Valle del Lili, Cali, Colombia, [5] Instituto de Genética Médica y Molecular (INGEMM), IdiPAZ, HospitalUniversitario La Paz, Madrid, CIBER de Enfermedades Raras (CIBERER), ISCIII, Madrid, Spain, [6] Genetics Department, Fundación Valledel Lili, Cali, Colombia

OPEN ACCESS

Edited by:
Daniel Enquobahrie, University of Washington, United States

Reviewed by:
Carlos Brites, Federal University of Bahia, Brazil
Lavinia Schuler-Faccini, Federal University of Rio Grande do Sul, Brazil

***Correspondence:**
Estephania Candelo
ecandelo@icesi.edu.co; f6003926@fvl.org.co
Harry Pachajoa
hmpachajoa@icesi.edu.co; h.pachajoa@fvl.org.co

Specialty section:
This article was submitted to Genetics of Common and Rare Diseases, a section of the journal Frontiers in Genetics

Received: *27 January 2020*
Accepted: *27 January 2021*
Published: *19 March 2021*

Citation:
Candelo E, Sanz AM, Ramirez-Montaño D, Diaz-Ordoñez L, Granados AM, Rosso F, Nevado J, Lapunzina P and Pachajoa H (2021) A Possible Association Between Zika Virus Infection and CDK5RAP2 Mutation. Front. Genet. 12:530028. doi: 10.3389/fgene.2021.530028

Introduction: Flaviviridae family belongs to the Spondweni serocomplex, which is mainly transmitted by vectors from the *Aedes* genus. Zika virus (ZIKV) is part of this genus. It was initially reported in Brazil in December 2014 as an unknown acute generalized exanthematous disease and was subsequently identified as ZIKV infection. ZIKV became widespread all over Brazil and was linked with potential cases of microcephaly.

Case report: We report a case of a 28-year-old Colombian woman, who came to the Obstetric Department with an assumed conglomerate of fetal abnormalities detected *via* ultrasonography, which was performed at 29.5 weeks of gestation. The patient presented with multiple abnormalities, which range from a suggested Arnold–Chiari malformation, compromising the lateral and third ventricles, liver calcifications, bilateral pyelocalic dilatations, other brain anomalies, and microcephaly. At 12 weeks of gestation, the vertical transmission of ZIKV was suspected. At 38.6 weeks of gestation, the newborn was delivered, with the weight in the 10th percentile (3,180 g), height in the 10th percentile (48 cm), and cephalic circumference under the 2nd percentile (31 cm). Due to the physical findings, brain magnetic resonance imaging (MRI) was performed, revealing a small and deviated brain stem, narrowing of the posterior fossa, a giant posterior fossa cyst with ventricular dilatation, a severe cortical and white matter thinning, cerebellar vermis with hypoplasia, and superior and lateral displacement of the cerebellum. In addition, hydrocephalus was displayed by the axial sequence, and the cerebral cortex was also compromised with lissencephaly. Schizencephaly was found with left frontal open-lip, and no intracranial calcifications were found. Two novel heterozygous nonsense mutations were identified using whole-exome sequencing, and both are located in exon 8 under the affection of ZIKV congenital syndrome (CZS) that produced a premature stop codon resulting in the truncation of the cyclin-dependent kinase 5 regulatory subunit-associated protein 2 (CDK5RAP2) protein.

Conclusion: We used molecular and microbiological assessments to report the initial case of vertically transmitted ZIKV infection with congenital syndrome associated with a neurological syndrome, where a mutation in the *CDK5RAP2* gene was also identified. The *CDK5RAP2* gene encodes a pericentriolar protein that intervenes in microtubule nucleation and centriole attachment. Diallelic mutation has previously been associated with primary microcephaly.

Keywords: Colombia, microcephaly, whole-exome sequencing, Zika virus, vertical transmission, brain abnormalities, CDK5RAP2

INTRODUCTION

Flavivirus commonly spreads through vectors from the *Aedes* genus (Hayes, 2009). Zika virus (ZIKV) is a member of this family. It was first reported in Brazil in December 2014 as an unknown generalized exanthematous disease and was later described as ZIKV infection (Lowe et al., 2018). By May 2015, ZIKV had become widespread in Brazil and was linked with potential microcephaly cases in November 2015. Subsequently, ZIKV disseminated rapidly to other South American and Caribbean countries in the majority of the territory and across 22 territories around Brazil, where the vector was already present. By January 2016, almost 30,000 cases of ZIKV infection had been revealed (Candelo et al., 2019). After the Americas outbreak, the WHO declared a public health emergency of international interest in February 2016 (World Health Organization [WHO], 2016).

ZIKV infection was declared a public health emergency when strong evidence was associated with the hypothesis that it caused microcephaly and congenital abnormalities during pregnancy and increasing evidence supported this link with the detection of ZIKV in fetal brain tissue (Mlakar et al., 2016; Schuler-Faccini et al., 2016; Ventura et al., 2016; Wang and Ling, 2016; Passi et al., 2017), amniotic fluid (Calvet et al., 2016), and placenta, which also supported the vertical transmission of ZIKV (Besnard et al., 2014). Further research using *in vitro* and *in vivo* studies has established that the virus is highly neurotropic (Garcez et al., 2016; Sirohi et al., 2016; Tang et al., 2016; Ahmad et al., 2017). A recent study shows that ZIKV targets neuroprogenitor cells, which are derived from pluripotent stem cells, from which the ZIKV particles are released. When neuroprogenitor cells are infected by the ZIKV particles, the apoptotic process is activated, and it intensifies cell death and disrupts the cell cycle resulting in decreased neuroprogenitor cell growth, most likely due to transcriptional dysregulation in cell cycle-related pathways (Tang et al., 2016).

Before 2015, the yearly number of cases of microcephaly in Brazil was repeatedly less than 200 (Cosme et al., 2017). Furthermore, 4,783 suspected cases of microcephaly were reported between November 2015 and January 30, 2016, including newborn and fetal losses. From these cases, only 36.6% (404) were classified as confirmed cases of microcephaly from the 1,103 cases that had undergone clinical, laboratory, and imaging examinations. ZIKV was only detected in 15 newborn and 2 fetal losses (1.54%). The majority of the probable cases were under investigation, and a considerable proportion represented misdiagnosis and overreporting noise due to uncertainty, with both variables probably inflating the prevalence (Victora et al., 2016). In humans, classic Zika fever is a self-limiting sickness characterized by fever, maculopapular rash, headache, conjunctivitis, and myalgia (Ioos et al., 2014). Clinical manifestation only occurs in 20% of the population affected, and the majority of infections are asymptomatic. A serological survey conducted in Salvador in Northeast Brazil indicated a peak seroprevalence of 63% in 2016, with 205,578 and 13,353 cases of ZIKV infection reported in 2016 and 2017, respectively (Netto et al., 2017; Secretaria de Vigilância em Saúde-Ministério da Saúde, 2017).

The ZIKV epidemic in Colombia started in August 2015, but laboratory evidence of ZIKV infection was not reported until October 2015. By April 2016, 65,726 suspected cases of ZIKV had been reported, of which only 2,485 (4%) were confirmed by reverse-transcription (RT)-polymerase chain reaction (PCR) assay. Furthermore, 11,944 pregnant women were reported as potential cases of ZIKV infection, but only 1,484 (12%) of these were confirmed. From this population, 50 newborns were reported as possible ZIKV congenital syndrome (CZS), but ZIKV infection was confirmed in only 4 (8%) of them (Pacheco et al., 2016).

In this case report, we used molecular, microbiological, and genetic assessments to characterize the first known case of vertically transmitted ZIKV infection and congenital syndrome associated with a neurological syndrome, where a mutation in cyclin-dependent kinase 5 regulatory subunit-associated protein 2 (CDK5RAP2) was identified. The *CDK5RAP2* gene encodes a pericentriolar protein that mediates microtubule nucleation and centriole attachment (Fong et al., 2008), and diallelic variants of this gene have been priorly linked with isolated microcephaly syndrome.

CASE REPORT

In mid-2016, a 28-year-old previously healthy Colombian woman with later prenatal care attention came to the Perinatology and Obstetric Department at Fundación Valle del Lili-University Hospital due to numerous fetal abnormalities observed in ultrasonography done at 29.5 weeks of gestation, which demonstrated brain anomalies with a possible Arnold–Chiari malformation, compromised lateral and third ventricles, liver calcifications, bilateral pyelocaliceal dilatations, microcephaly, and an apparent clubfoot. All relevant antecedents during

pregnancy were considered (smoking, alcohol, drugs, or any other perinatal infection). The patient had experienced an episode of illness for 2–7 days that was characterized by fever, myalgias, and vomiting. She went to the hospital, where ZIKV was presumed, and RT-PCR of the amniotic fluid was done, with a positive result at 12 weeks of gestation. The findings confirmed ZIKV vertical transmission and congenital infection. Inadequate prenatal follow-ups were performed until the fetal examination at 29.5 weeks, which showed multiple malformations.

At the time of delivery, the mother was traveling from a remote area of the country. She went into labor on the way to the hospital and gave birth in the ambulance. According to the medical records and first ultrasonography date, delivery was at 38.6 weeks of gestation. The male newborn weighed 3,180 g (10th percentile), with a height of 48 cm (10th percentile) and a cephalic circumference of 31 cm (under the 2nd percentile) according to the WHO Growth Charts from the Centers for Disease Control and Prevention (CDC) (WHO Child Growth Standards, 2019; World Health Organization, 2019). Transfontanelle ultrasonography reported microcephaly, an increase of the width and number of the circumvolutions due to pachygyria, and ventriculomegaly in the infratemporal and supratemporal fossae. There was also a non-discharging cerebrospinal fluid-filled cleft lined with gray matter on the left lateral ventricle going to the cerebral cortex, closed-lip schizencephaly, subcortical echogenic and punctiform, cystic image on the posterior fossae communicated with the fourth ventricle, thin corpus callosum, and pathological calcification in the liver, brain (cortical and subcortical), and placenta. As part of the evaluation approach to a newborn with brain abnormalities, TORCH testing was performed to rule out the most frequent congenital infections (syphilis, toxoplasmosis, rubella, hepatitis B, HIV, cytomegalovirus, herpesvirus 1 and 2, and parvovirus B19) as causal etiology.

The mother reported that the newborn was irritable, with an abnormal pattern of crying and hyperexcitability. The physical examination showed distal tremors, hypertonia, trunk hyperextension, spasticity, increased deep tendon reflexes, persistent primitive responses, clenched fists, strabismus, and nystagmus. Microcephaly was present, which was characterized by craniofacial disproportion, decreased vertical size of the skull, a sloping forehead, and pronounced supraorbital ridges, giving the appearance of oversized facial features and proptosis. Epicanthal folds, retrognathia, excess skin over the entire scalp and forehead, and occipital and nuchal skin folds were also found, giving the appearance of a short neck. The forehead presented with bilateral depressions and prominent overlapping metopic and sagittal sutures with supratemporal depressions and a large visible occipital prominence. An examination of the extremities revealed hand contractures, camptodactyly, feet contractures, prominent calcanei, multiple dimples, and arthrogryposis (**Figure 1**). Because of the multiple abnormalities, a complete genetic assessment was performed on the newborn and his mother.

After 1 year of follow-up, a complete checkup was performed. The findings showed irritability, an abnormal pattern of crying, hyperexcitability, hypertonia, spasticity, clenched fists,

FIGURE 1 | Representation of the patient phenotype. **(a,b)** The patient showed distal tremors, hypertonia, trunk hyperextension, spasticity, microcephaly, craniofacial disproportion, and a decreased vertical skull size. **(c)** Multiple dimples and arthrogryposis. **(d)** Feet contractures and prominent calcaneus. **(e)** Clenched fists, hand contractures, and camptodactyly. **(f)** Strabismus. **(g)** Excess skin over the entire scalp and forehead and occipital and nuchal skin folds, generating the appearance of a short neck. **(h)** Sloping of the forehead and prominence of supraorbital ridges, which creates an appearance of proptosis and oversized facial features, epicanthal folds, and retrognathia. Bilateral depressions were present on the forehead.

strabismus, clinodactyly of the fifth finger, and an ogival palate. Microcephaly was still present, with a few of the previously observed characteristics, such as a small skull, retrognathia, and a prominent metopic suture. A physical examination of the extremities found hand contracture and camptodactyly, feet contracture, prominent calcanei, multiple dimples, arthrogryposis, and a severe delay in the developmental milestones. A brain magnetic resonance imaging (MRI) showed microcephaly, with a giant posterior fossa cyst, ventricular dilatation, hypoplasia of the cerebral vermis, and an anomalous cerebral cortex with lissencephaly (**Figure 2**).

METHODS

ZIKV Sample Collection

Following the National Institutes of Health recommendations, amniocentesis was performed at 12 weeks of gestation for ZIKV infection case suspicions. Ultrasound-guided transabdominal amniocentesis was done, and around 5 ml of amniotic liquid was aspirated and instantly stored at −80°C for testing. Further samples were taken from the cerebrospinal fluid when the infant was born, and the blood, amniotic fluid, and placenta were also taken, as is previously described in Candelo et al. (2019).

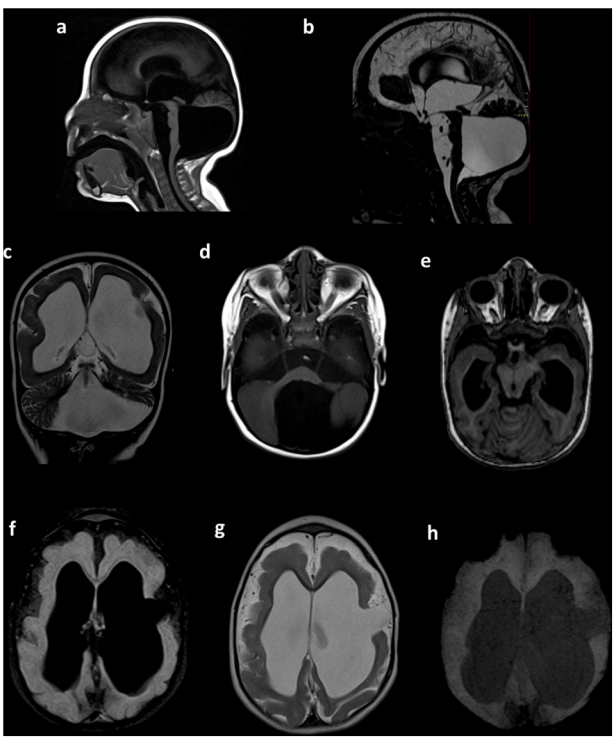

FIGURE 2 | Brain MRI. Sagittal T1-weighted **(a)** and sagittal constructive interference in steady state (CISS) **(b)** sequences showing microcephaly with a giant posterior fossa cyst, a small and displacement of the brain stem, and tightening of the posterior fossa. Coronal T2-weighted images **(c)** showing ventricular dilatation, cortical and white matter narrowing, and posterior fossa cyst. Axial T1-weighted images **(d)** showing a posterior fossa cyst. Axial T1-weighted multiplanar reconstruction **(e)** showing a narrow posterior fossa, cerebellar vermis with hypoplasia, and superior and lateral deviation of the cerebellum. Axial FLAIR **(f)** and axial T2-weighted sequences **(g)** showing hydrocephalus and anomalous cerebral cortex with lissencephaly and left frontal open-lip schizencephaly. Axial susceptibility-weighted image **(h)**, with the absence of intracranial calcifications. Preliminary data of this study were previously presented in the IBRO meeting 2019 (Candelo et al., 2019).

ZIKV Detection

The molecular identification of ZIKV in the amniotic fluid and cerebrospinal fluid was done by using a SuperScript III Platinum One-Step RT-PCR system (Invitrogen, Carlsbad, CA, United States) run by the Colombian Government National Institutes of Health using the primers ZIKV 1087, ZIKV 1163, and ZIKV 1108-FAM, followed by the Lanciotti protocol (Lanciotti et al., 2008). For hybridization and extension, an ABI 7500 Real-Time PCR System (Thermo Fisher Scientific, Waltham, MA, United States) was operated (Pacheco et al., 2016).

Samples were obtained from the mother and the newborn and those from viral isolation trials for ZIKV RNA, using a TaqMan RT-PCR assay and quantitative RT-PCR for ZIKV following the CDC protocol (Centers for Disease Control and Prevention, 2019). Standard methods were used to determine the levels of ZIKV IgM, IgG, and neutralizing antibody titers. Additionally, we tested for other flaviviruses and arthropod-borne viruses. In addition, the antibody levels of infectious diseases that might produce congenital abnormalities, such as toxoplasma, cytomegalovirus, syphilis, herpes, rubella, hepatitis, parvovirus B19, and HIV, were tested in the mother and the newborn (TORCH test), as is described previously in the literature (Candelo et al., 2019).

Karyotyping and Array Comparative Genomic Hybridization Analysis

The classical cytogenetics G-banding technique was performed after the patient had given birth to do a blood karyotype analysis. The karyotype analysis was performed on cells in metaphase using a microscope and the CytoVision (Leica) karyotype software system. After extracting DNA from the patient's peripheral blood cells, 1 μg was used for array comparative genomic hybridization (a-CGH) utilizing KaryoArray 3.0 (8 × 60K; Agilent Technologies, Santa Clara, CA, United States) and was marked by fluorescence to compare the patient's DNA with the control sample. DNA hybridization was done with a human genomic microarray of 860 K oligonucleotides using commercially available Agilent-based arrays, which were analyzed using an Agilent scanner with Feature Extraction 9.1 software. The aberration detection method 2 algorithm was used to determine any statistically significant aberrations. This was defined as the minimum number of oligonucleotides to consider an alteration. Subsequently, the medium resolution of the array was one oligonucleotide per 9 Kb in the regions of maximum interest, such as microdeletions and microduplications, centromeres, and telomeres. The algorithm in CGH Analytics version

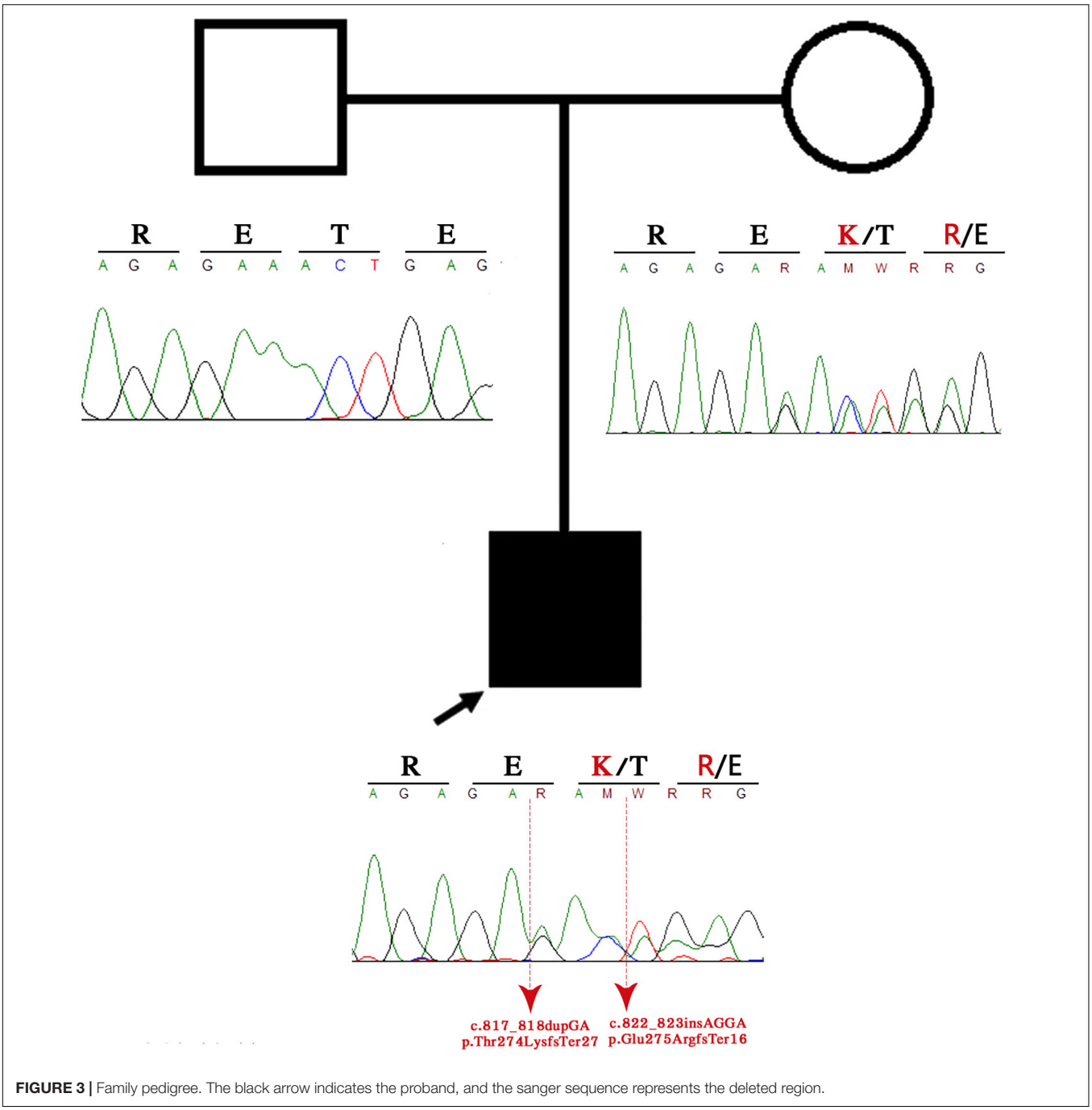

FIGURE 3 | Family pedigree. The black arrow indicates the proband, and the sanger sequence represents the deleted region.

3.5 software (Agilent Technologies) was used (Blanco-Kelly et al., 2017), as is described previously in the literature (Candelo et al., 2019).

Whole-Exome Sequencing Methods

The whole-exome sequencing (WES) was captured by using a SureSelect Human All Exon capture kit (Agilent) of 51 Mb, and sequencing was done by using an Illumina Hiseq 2000 sequencing system (Illumina, San Diego, CA, United States). During the sequencing, paired readings of 101 nucleotides in length were acquired. The different variants were analyzed by focusing on genes related to microcephaly. Only variants in the coding region and flanking intronic regions with minor allele frequency <1% were evaluated and compared using datasets acquired from the 1000 Genomes Project Consortium, dbSNP, Exome Variant Server, and Exome Aggregation Consortium databases. Variants in around 20 bp of flanking intron regions were examined and sequenced by Sanger sequencing (Candelo et al., 2019). Parental

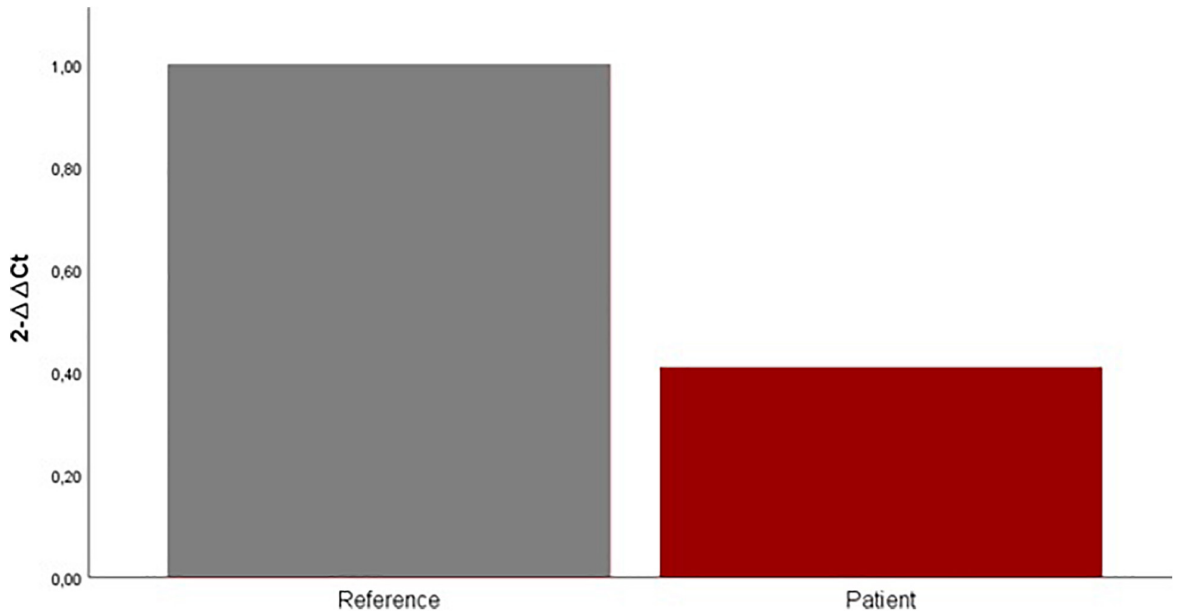

FIGURE 4 | Expression levels of CDK5RAP2 measured by qRT-PCR in the patient (red column) and set of reference samples (gray column). Each GAPDH-normalized mRNA level was further normalized against the corresponding mRNA level. Data are shown as fold change relative to the set of reference samples (defined as 1.0). Data are represented as mean ± SD.

carrier status of the clinical relevant variants was confirmed by Sanger Sequencing analysis, as is described previously in the literature (Candelo et al., 2019).

In silico Analysis

Two heterozygous nonsense mutations in CDK5RAP2 were analyzed with variant functional prediction software tools (DANN, MutationTaster, Condel, SIDT, and FATHMM) in order to predict the pathogenicity of the mutations. In addition, these variants were searched in Human Gene Mutation Database (HGMD), Leiden Open Variation Database (LOVD), and ClinVar database, as is described previously in the literature (Candelo et al., 2019).

Tissue Expression of CDK5RAP2

Isolation of total RNA from the patient's and parents' mouth swab was done with the TRIzol reagent (Life Technologies, CA, United States). RNA integrity and concentrations were both analyzed using a 1% agarose gel and Nanodrop®ND-1000 Spectrophotometer (Thermo Fisher Scientific, MA, United States). RNA reverse transcription was performed by a High-Capacity cDNA Reverse Transcription Kit (Applied Biosystems, CA, United States) using 100 ng of total RNA according to the manufacturer's instructions. For quantitative PCR (qPCR), cDNA was amplified using CDK5RAP2 primers 5′-GTTGGGGAAATGGTCTGCTCC-3′ and 3′-TATGTTCAGTGGGGCCATGA-5′. PCR amplification was performed in a 20-μl volume that contained: 10 μl of the EXPRESS SYBR®GreenER™ qPCR SuperMixes (0.25×) kit (Applied Biosystems, CA, United States), 0.4 μl of each of the primers (1×), 0.04 μl ROX (50 nM), 1 μl of cDNA, and 8.16 μl of water. Real-time PCR was performed in a 7500-Fast real time PCR instrument, and reaction was carried out with the following conditions: 95°C for 20 s, followed by 40 cycles of: 95°C for 1 s and 60°C for 20 s and for the melt curve: 95°C for 15 s, 60°C for 60 s, 95°C for 15 s, and 60°C for 15 s. GAPDH mRNA was used as an internal control (house-keeping gene), and the relative expression of each transcript was calculated using the $2^{-\Delta\ \Delta\ Ct}$ method. RT-PCR reactions were performed for each sample in triplicate. For the set of reference samples, we used mRNA extracted from the patient, parents, and two additional healthy individuals (Bond et al., 2005). Data are presented in **Figure 4** as mean ± SD (Bond et al., 2005).

Ethics and Consent

Written informed consent was obtained from the patient's parents for the publication of the case details and accompanying images. All research was conducted according to the Declaration of Helsinki, and the research protocol was registered with the following number #253. This study received approval from the Ethics Committee of Fundación Valle del Lili (Act 11/2016).

RESULTS

Molecular Diagnosis

Serum and urine samples were tested for chikungunya virus, dengue virus, and ZIKV. The RT-quantitative PCR assays for dengue and chikungunya viruses were negative for whole samples

and positive for ZIKV in the amniotic liquid of the patient but negative in the urine and serum samples from the fetus and mother. Serology tests of the serum and urine using anti-dengue virus IgM, anti-dengue-virus IgG, anti-chikungunya-virus IgM and IgG, and anti-ZIKV displayed negative results in the enzyme-linked immunosorbent assays (ELISAs). The samples also tested negative for TORCH (toxoplasmosis, HIV, rubella, syphilis, cytomegalovirus, hepatitis, parvovirus B19, and herpes simplex 1 and 2), as is described previously in the literature (Candelo et al., 2019).

Karyotype and a-CGH

Fetal karyotyping displayed regular 46, XY (male) profiles. No losses and/or gains of genomic material were detected in the fetal DNA sample, as is described previously in the literature (Candelo et al., 2019).

Whole-Exome Sequencing

WES detected two heterozygous variants in the *CDK5RAP2* gene at positions p.Thr274LysfsTer27 and p.Glu275ArgfsTer16, respectively, when compared with the human reference template (GRCh38) or mutation databases (LOVD and HGMD). These variants result in a stop codon causing the early termination of the protein. Bioinformatic analysis was performed using the University of California Santa Cruz Genome Browser, which showed that the region was highly conserved between species and was located near to a regulatory element, such as H3K27Ac, and between a promoter and enhancer region. According to the AmiGO gene ontology browser and Kyoto Encyclopedia of Genes and Genomes, this gene has multiple functions, such as G2/M transition of the mitotic cell cycle, establishment of mitotic spindle orientation, microtubule cytoskeleton organization, maintaining centrosome function, spindle pole assembly and orientation, microtubule bundle formation, and protein binding (Fong et al., 2008; **Figure 3**).

In silico Analysis

We identified two novel heterozygous nonsense mutations, both located in exon 8 under the affection of CZS, which produced a premature stop codon resulting in the truncation of CDK5RAP2 protein. There has been no pervious reporting of these variants in the literature. A functional prediction of the variants using gene prediction software classified them as harmful variants (disease-causing). At the moment, they are classified as "probably pathogenic" according to the American College of Medical Genetics and Genomics guidelines (see **Table 2**).

Tissue Expression of CDK5RAP2

Quantitative gene expression analysis using real-time PCR showed that mRNA levels of CDK5RAP2 were downregulated in the patient mouth swab sample. Our results suggest an approximately 0.6-fold decrease of CDK5RAP2 expression in the patient mouth swab sample compared with the control mouth swab sample (**Figure 4**).

DISCUSSION

The term CZS was created to characterize the range of congenital abnormalities associated with ZIKV infection, including microcephaly to ocular injury and hearing loss (Walker et al., 2019). At the beginning of the ZKV outbreak, two fetuses from pregnant women from the state of Paraiba, Brazil were diagnosed with microcephaly and were thought to belong to the microcephaly cluster because they both suffered from symptoms related to ZIKV infection. In previous cases with central nervous system (CNS) abnormalities, brain atrophy, with coarse calcifications involving the white matter of the frontal lobes, including the caudate, lentostriatal vessels, and cerebellum, was mainly observed (Walker et al., 2019). The cerebral hemispheres were severely asymmetric, with marked unilateral ventriculomegaly, displacement of the midline, thinning of the parenchyma on the dilated side, failed visualization of the corpus callosum, and almost complete disappearance or failure to develop the thalami (Walker et al., 2019). The pons and brainstem were thin and continuous with a heterogenous small mass at the basal ganglia (Walker et al., 2019). The anomalies were limited to the brain in most cases. These brain abnormalities included cerebral calcifications, microcephaly, Blake's pouch cyst, agenesis of the vermis, cerebral atrophy, mega cisterna magna, and ventriculomegaly (Walker et al., 2019). Maternal ZIKV infection is estimated to result in 5–13% of birth defects cases, with higher incidence when infection occurs earlier in pregnancy and microcephaly resulting in approximately 6.33% (interquartile range, 4–5.5%) of congenital ZIKV infections (Brasil et al., 2016; Honein et al., 2017; Shapiro-Mendoza et al., 2017; Hoen et al., 2018; Sanz Cortes et al., 2018; Shiu et al., 2018; Walker et al., 2018). The spectrum of anomalies associated with ZIKV is broad, and there are potential postnatal long-term neurocognitive deficits due to maternal–fetal exposure, which can lead to the loss of neural stem cells (neurogenic arrest) (Adams Waldorf et al., 2018).

Recent studies have suggested that placental injury and infarctions might affect fetal oxygenation (Hirsch et al., 2018). Furthermore, type I interferon triggered fetal death and altered placental development in mouse models of ZIKV infection (Yockey et al., 2018). Although the molecular mechanisms of ZIKV microcephaly remain unelucidated, it is understood that the flavivirus facilitates viral replication and spreading by dysregulating and bypassing the innate immune response to replicate in the unchecked host cells (Keller et al., 2006). Then, the virus kidnaps and modifies the genomic RNA in the colonized cells to mimic endogenous host cell processes, allowing the viral replication to remain undetected (Daffis et al., 2010). The synergic effect of ZIKV protein products interferes with the innate immune response by binding to the downstream interferon pathway (Donald et al., 2016) and disrupting Janus kinase signaling, which is fundamental for the expression of any antiviral factor (Grant et al., 2016). ZIKV directly infects and spreads in the neural stem cells in the fetus and produces neurogenic arrest by possible P53 activation and inhibition of the mTOR pathways, which promote a switch from glycolysis to oxidative phosphorylation and might consequently produce

TABLE 1 | Clinical manifestation overlap.

	Congenital ZIKV syndrome	CDK5RAP2 syndrome	Present case	Overlap
Cranial morphology	Severe microcephaly	Microcephaly		
	Overlapping cranial suture	Sparse eyebrows		
	Prominent occipital bone (75%)			
	Redudant Scal and Nucal Skin (47.9%)			
	Severe Neurological impairment			
	Craniofacial disproportion (95.8%)			
	Bilateral depression of the frontal and parietal bone (83.3%)			
Brain findings	Calcifications (Mainly subcortical)			
	Ventriculomegaly	Midly dilated ventricular system		
	Dysmorphic ventricles			
	Skull Collapse			
	Decreased cranial vault			
	Small Cerebellum			
	Irregular Cortex			
	Shallow Sulci	Prominent Sulci and shallow and wide sulci		
	Abnormal gyral pattern (mostly polymicrogyria)	Simplified gyriform pattern		
	Hypoplasia or absence of the corpus callosum	Agenesis of corpus callosum and Thinning		
	Wallerian degeneration	Megacisterna Magna		
	hypoplasia			
	Cerebral Atrophy			
	Decreased myelination			
Ocular anomalies	Microphtalmia	Microphalmia		
	Coloboma	Anophtalmia		
	Cataracts	Cataracts		
	Intraocular calcifications			
	Chorioretinal atrophy			
	Focal Pigmentary			
	Mottling of the retina			
	Optic Nerve atrophy/anomalies			
Facial findings		Sloping Forehead		
		Beaked Nose		
	Epicanthal folds	Micrognathia		
	Nistagmus	Midface hypoplasia		
	Strabismus	Strabismus		
		Upslanting or Downslating palpebral fissure		
		Low-set ears		
		High arched palated		
Contractures	Arthrogryposis	Ataxia		
	Unilateral or bilateral Clubfoot			
	Trunk hyperextension or hyperflexion			
	Multiple dimples			
	Bilateral congenital hip dislocation			
Neurological squeale	Cognitive disabilities	Cognitive disabilities		
	Seizures	Seizures		
	Swallowing difficulties			
	Global Developmental Delay	Global Developmental Delay		
	Failure to thrive	Failure to thrive		

(Continued)

TABLE 1 | Continued

	Congenital ZIKV syndrome	CDK5RAP2 syndrome	Present case	Overlap
	Hearing Impairment (Sensorineural)	Hearing Loss (Sensorineural)		
	Hypertonia	Hyperactive and aggressive		
	Spasticity	Spastic Extremities		
	Irritability	Dystonic Movements		
	Hypotonia	Hypotonia		
	Excessive crying	Jerking of the whole body		
	Distal Tremors			
	Dysphagia	Speech Delay or Loss		
Skeletal findings	Feet Contracture			
	Increased deep tendon reflex	Delayed bone age		
	Clenched Fists	Brachymesophalangy		
	Hand contracture-Camptodactyly	Simian Creases		
		Pes Planus		
		Fifth finger clinodactyly		

Each column represents each clinical condition according to the literature. The clinical manifestation of congenital ZIKV syndrome is represented in yellow, and the CDK5RAP2 syndrome is represented in green. The present case column exhibits the symptoms and signs in the respective color that represents each syndrome, and blue shows the combination of a clinical manifestation shared from both conditions. The last column represents the overlap of clinical manifestation between the two conditions.

TABLE 2 | In silico analysis of the CDK5RAP2 variants.

Variant	Protein effect	ClinVar	DANN	EIGEN	MutPred	MutationTaster	SIFT	PolyPhen-2
c.1156C > T	p.Thr274LysfsTer27	NR	0.9987	Pathogenic	Pathogenic	Disease causing	Damaging	Probably damaging
c.280C > T	p.Glu275ArgfsTer16	NR	0.9993	Pathogenic	Pathogenic	Disease causing	Damaging	Probably damaging

immature differentiation and apoptosis of neural precursor cells (NPCs) by targeting cell proliferation and generating cell cycle arrest, causing microcephaly and cortical thinning (Li et al., 2016).

Global gene analysis expression studies have demonstrated the upregulation and downregulation of multiple genes implicated in the immune response, apoptosis, and microcephaly (Li et al., 2016). There were few ZIKV-infected cells in the midbrain and the cortical plate, where post-mitotic neurons are based, ZIKV leads to cortex thinning without lamination disturbances, and in the mouse model, there were significantly fewer mitotic cells in the ventricular zone, accompanied by more centrosomes at the ventricular surface that were facing away from the nuclei (Li et al., 2016). Furthermore, the ZIKV-infected brain showed a lower number of NPCs in the M phase. In an experimental mouse model infected with ZIKV, global transcriptome analyses (RNA-sequencing) identified genes related to cytokine production and cytokine response; several genes related to cell proliferation, differentiation, and migration were downregulated; and most of the microcephaly-related genes were downregulated (*ASPM*, *CASC5*, *CENPF*, *MCPH1*, *RBBP8*, *STIL*, and *TBR2*). These genes were shown to share putative homologs that were co-expressed with CDK5RAP2, and molecular interaction occurred between *ASPM* and *CDK5RAP2* (Li et al., 2016). The gene disrupted in our present case indicates that *CDK5RAP2* might play a disruptive role in the arrest of ZIKV-infected NPCs. The products of many of these genes are enriched in NPCs and affect the mitotic cell behaviors centered around the centrosome and DNA repair. For example, a mutation in this compound heterozygous variant produces a stop codon mutation and decreased protein expression, which is translated as a decreased or loss of functional protein associated with a reduced number of NPCs due to asymmetric division (Merfeld et al., 2017). Another study proved that cerebral organoids created from human cells with disrupted CDK5RAP2 were smaller, contained fewer progenitors, and disrupted cell polarity (Lancaster et al., 2013). Research has also demonstrated that centrosome activity is more fundamental for the development of brain tissue than for any other tissue by associating *CDK5RAP2* gene disruption with microcephaly and ZIKV congenital infection (Merfeld et al., 2017).

The *MAPRE1* gene (also known as EB1) codes a protein that is located in the microtubules, especially at the growing ends, in interphase cells. The CDK5RAP2–MAPRE1 complex induces microtubule bundling and assembling, suggesting that this complex regulates microtubule dynamics. The mutations p.T274KTer27 and p.E275RTer16 produce a truncated protein with loss of the protein–protein interactions in the CDK5RAP2–MAPRE1 complex. This loss affects the self-assembling dynamics of the microtubules, resulting in the dysregulation of neuron production and brain size (Fong et al., 2009). CDK5RAP2 has a domain that is highly homologous to centrosomin motif 2, essential for pericentric interaction, which is fundamental for chromosomal and Golgi localization of the CDK5RAP2 protein. The resultant protein of the gene that contained the patient mutation lacks the centrosomin 2 domain, which suggests a loss in its localization to centrosomes and the Golgi complex as well

as dysregulation of the cellular cycle, related to disturbances in microtubule dynamics (Wang et al., 2010). Model pregnant mice with ZIKV infection have been reported to show apoptosis, cell cycle arrest, and inhibition of NPC differentiation, generating the phenotype observed in our case (**Figure 2**), cortical thinning, and microcephaly. The disruption of CDK5RAP2 and the genes previously mentioned and the putative homologous co-expression of these genes might lead to microcephaly, with a lower NPC content and a disruption in cell polarity creating the phenotype observed in our patient (Merfeld et al., 2017).

Patients with autosomal-recessive primary microcephaly are widely known as having an isolated brain disorder without other system involvement. The present piece of evidence demonstrates the overlapping of the two syndromes on clinical manifestations (**Tables 1**, **2**). The proband exhibits the majority of congenital ZIKV signs and symptoms with some of the CDK5RAP2 characteristics and overlapping of both conditions (**Table 1**), which suggest and confirm assumptions that have been postulated by previous authors (Tan et al., 2014; Li et al., 2016), where it is proposed that ZIKV might not just disrupt the neural stem pool, but it could also interfere with gene expression and metabolic pathways in the same cells, which are crucial for neural development (Tan et al., 2014; Li et al., 2016). For that reason, we hypothesized that CDK5RAP2 variants might interact as a second hit effect in the existence of congenital ZIKV infection as in the present case their father is a carrier of p.Thr274LysfsTer27 and p.Glu275ArgfsTer16 without any specific phenotype. However, the proband has an overlapping phenotype of congenital ZIKV syndrome and CDK5RAP2 microcephaly disorder (**Table 1** and **Figures 3**, **4**). Furthermore, in the following studies, around 11 genes related to microcephaly have been demonstrated to be downregulated in the tissue from ZIKV-associated microcephaly, including the gene (*CDK5RAP2*) found in this case, which is also related and required for the maintenance of the germ cell pool during embryonic development and is linked with molecular evolutionary pathways for regulating the brain size (Evans et al., 2006; Zaqout et al., 2017). This indicates that the variable expressivity of the phenotype in patients with congenital ZIKV syndrome might be directly associated with the type and mechanism of gene disruption and the time of the viral exposure, which could generate the downregulation of these genes and it will be seen in patients as an absence of nucleotide variants compare with the human reference template in WES as was seen in the previous study (Candelo et al., 2019). In addition, severe affection might generate the genetic profile seen in this patient (**Table 1** and **Figure 3**). Further investigation must focus on using genome-wide association data to confirm this association.

In summary, our study describes a case of vertical ZIKV transmission associated with a congenital ZIKV syndrome and linked with a neurological syndrome, with microbiological, molecular, and genetic assessments, where two cis-novel variants in CDK5RAP2 were found. The *CDK5RAP2* gene encodes a pericentriolar protein that mediates microtubule nucleation and centriole attachment. A diallelic mutation on this gene has been previously associated with primary microcephaly.

DATA AVAILABILITY STATEMENT

The original contributions presented in the study are included in the article/supplementary material, further inquiries can be directed to the corresponding author/s.

ETHICS STATEMENT

This study was approved by the Ethics Committee of Fundación Valle del Lili.

AUTHOR CONTRIBUTIONS

All authors made a substantial contribution to the work reported, whether that is in the conception, study design, execution, acquisition of data, analysis and interpretation, or in all these areas. They took part in drafting, revising, or critically reviewing the article and gave final approval of the version to be published. They have agreed on the journal to which the article has been submitted and agreed to be accountable for all aspects of the work.

ACKNOWLEDGMENTS

We acknowledge the patient and his parents and the people who have contributed in some to the development and execution of this project and Tobias Yates for his language editing.

REFERENCES

Adams Waldorf, K. M., Nelson, B. R., Stencel-Baerenwald, J. E., Studholme, C., Kapur, R. P., Armistead, B., et al. (2018). Congenital Zika virus infection as a silent pathology with loss of neurogenic output in the fetal brain. *Nat. Med.* 24, 368–374.

Ahmad, I., Baig, S. M., Abdulkareem, A. R., Hussain, M. S., Sur, I., Toliat, M. R., et al. (2017). Genetic heterogeneity in Pakistani microcephaly families revisited. *Clin. Genet.* 92, 62–68. doi: 10.1111/cge.12955

Besnard, M., Lastere, S., Teissier, A., Cao-Lormeau, V., and Musso, D. (2014). Evidence of perinatal transmission of Zika virus, French Polynesia, December 2013 and February 2014. *Euro Surveill.* 19:20751.

Blanco-Kelly, F., Palomare, M., Vallespin, E., Villaverde, C., Martin-Arenas, R., Velez-Monsalve, C., et al. (2017). Improving molecular diagnosis of aniridia and WAGR syndrome using customized targeted array-based CGH. *PLoS One* 12:e0172363. doi: 10.1371/journal.pone.0172363

Bond, J., Roberts, E., Springell, K., Lizarraga, S., Scott, S., Higgins, J., et al. (2005). A centrosomal mechanism involving CDK5RAP2 and CENPJ controls brain size. *Nat. Genet.* 37, 353–355. doi: 10.1038/ng1539

Brasil, P., Pereira, J. P., Moreira, E., Ribeiro Nogueira, R. M., Damarceno, L., Wakimoto, M., et al. (2016). Zika Virus infection in pregnant women in rio de Janeiro. *N. Engl. J. Med.* 375, 2321–2334.

Calvet, G., Aguiar, R. S., Melo, A. S. O., Sampaio, S. A., de Filipis, I., Fabian, A., et al. (2016). Detection and sequencing of Zika virus from amniotic fluid of

fetuses with microcephaly in Brazil: a case study. *Lancet Infect. Dis.* 16, 653–660. doi: 10.1016/s1473-3099(16)00095-5

Candelo, E., Caicedo, G., Rosso, F., Ballesteros, A., Orrego, J., Escobar, L., et al. (2019). First report case with negative genetic study (array CGH, exome sequencing) in patients with vertical transmission of Zika virus infection and associated brain abnormalities. *Appl. Clin. Genet.* 12, 141–150. doi: 10.2147/tacg.s190661

Centers for Disease Control and Prevention (2019). *Growth Charts - WHO Child Growth Standards*. Avilable at: https://www.cdc.gov/growthcharts/who_charts.htm (accessed December 18, 2020).

Cosme, H. W., Lima, L. S., and Barbosa, L. G. (2017). Prevalência de anomalias congênitas e fatores associados em recém-nascidos do município de são paulo no período de 2010 a 2014. *Rev. Paul. Pediatr.* 35, 33–38. doi: 10.1590/1984-0462/;2017;35;1;00002

Daffis, S., Szretter, K. J., Schriewer, J., Soonjeon Youn, J.-L., Erret, J., Lin, T.-Y., et al. (2010). 2'-O methylation of the viral mRNA cap evades host restriction by IFIT family members. *Nature* 468, 452–456. doi: 10.1038/nature09489

Donald, C. L., Brennam, B., Cumberworth, S. L., Rezelj, V. V., Clark, J. J., Cordeiro, M. T., et al. (2016). Full genome sequence and sfRNA interferon antagonist activity of zika virus from Recife. Brazil. *PLoS Negl. Trop. Dis.* 10:e0005048. doi: 10.1371/journal.pntd.0005048

Evans, P. D., Vallender, E. J., and Lahn, B. T. (2006). Molecular evolution of the brain size regulator genes CDK5RAP2 and CENPJ. *Gene* 375, 75–79. doi: 10.1016/j.gene.2006.02.019

Fong, K.-W., Choi, Y.-K., Rattner, J. B., and Qi, R. Z. (2008). CDK5RAP2 is a pericentriolar protein that functions in centrosomal attachment of the gamma-tubulin ring complex. *Mol. Biol. Cell* 19, 115–125. doi: 10.1091/mbc.e07-04-0371

Fong, K.-W., Hau, S.-Y., Kho, Y.-S., Jia, Y., He, L., Qi, R. Z., et al. (2009). Interaction of CDK5RAP2 with EB1 to track growing microtubule tips and to regulate microtubule dynamics. *Mol. Biol. Cell* 20, 3660–3670. doi: 10.1091/mbc.e09-01-0009

Garcez, P. P., Correia Loiola, E., Madeiro da Costa, R., Higa, L. M., Trindade, P., Delvecchio, R., et al. (2016). Zika virus impairs growth in human neurospheres and brain organoids. *Science* 352, 816–818. doi: 10.1126/science.aaf6116

Grant, A., Ponia, S. S., Tripathi, S., Balasubramaniam, V., Miorin, L., Sourisseau, M., et al. (2016). Zika Virus Targets Human STAT2 to Inhibit Type I Interferon Signaling. *Cell Host Microbe* 19, 882–890. doi: 10.1016/j.chom.2016.05.009

Hayes, E. B. (2009). Zika virus outside Africa. *Emerg. Infect. Dis.* 15, 1347–1350. doi: 10.3201/eid1509.090442

Hirsch, A. J., Roberts, V. H. J., Grigsby, P., Haese, N., Schabel, M. C., Wang, X., et al. (2018). Zika virus infection in pregnant rhesus macaques causes placental dysfunction and immunopathology. *Nat. Commun.* 9:263.

Hoen, B., Schaub, B., Funk, A. L., Ardillon, V., Boullard, M., Cabie, A., et al. (2018). Pregnancy outcomes after ZIKV infection in French territories in the americas. *N. Engl. J. Med.* 378, 985–994. doi: 10.1056/nejmoa1709481

Honein, M. A., Dawson, A. L., Peterson, E. E., Jones, A. M., Lee, E. H., Yazdy, M. M., et al. (2017). Birth defects among fetuses and infants of US women with evidence of possible Zika Virus infection during pregnancy. *JAMA* 317, 59–68. doi: 10.1001/jama.2016.19006

Ioos, S., Mallet, H.-P., Goffart, I.-L., Gauthier, V., Cardoso, T., Herida, M., et al. (2014). Current Zika virus epidemiology and recent epidemics. *Med. Mal. Infect.* 44, 302–307. doi: 10.1016/j.medmal.2014.04.008

Keller, B. C., Fredericksen, B. L., Samuel, M. A., Mock, R. E., Mason, P. W., Diamond, M. S., et al. (2006). Resistance to alpha/beta interferon is a determinant of West Nile virus replication fitness and virulence. *J. Virol.* 80, 9424–9434. doi: 10.1128/jvi.00768-06

Lancaster, M. A., Renner, M., Martin, C.-A., Wenzel, D., Bicknell, L. S., Hurles, M. E., et al. (2013). Cerebral organoids model human brain development and microcephaly. *Nature* 501, 373–379.

Lanciotti, R. S., Kosoy, O. L., Laven, J. J., Velez, J. O., Lambert, A. J., Johnson, A. J., et al. (2008). Genetic and serologic properties of Zika virus associated with an epidemic. Yap State, Micronesia, 2007. *Emerg. Infect. Dis.* 14, 1232–1239. doi: 10.3201/eid1408.080287

Li, C., Xu, D., Ye, Q., Hong, S., Jiang, Y., Liu, X., et al. (2016). Zika Virus disrupts neural progenitor development and leads to microcephaly in mice. *Cell Stem Cell* 19, 120–126. doi: 10.1016/j.stem.2016.04.017

Lowe, R., Barcellos, C., Brasil, P., Cruz, O. G., Honorio, N. A., Kuper, H., et al. (2018). The Zika Virus epidemic in Brazil: from discovery to future implications. *Int. J. Environ. Res. Public. Health* 15:96. doi: 10.3390/ijerph15010096

Merfeld, E., Ben-Avi, L., Kennon, M., and Cerveny, K. L. (2017). Potential mechanisms of Zika-linked microcephaly. *Wiley Interdiscip. Rev. Dev. Biol.* 6:e273.

Mlakar, J., Korva, M., Tul, N., Popovic, C. M., Mraz, J., Kolenc, M., et al. (2016). Zika Virus associated with microcephaly. *N. Engl. J. Med.* 374, 951–958.

Netto, E. M., Moreira-Soto, A., Pedroso, C., Hoser, C., Funk, S., Kucharski, A. J., et al. (2017). High Zika Virus seroprevalence in salvador, northeastern brazil limits the potential for further outbreaks. *mBio* 8:e1390-17.

Pacheco, O., Beltran, M., Nelson, C. A., Valencia, D., Tolosa, N., Farr, S. L., et al. (2016). Zika Virus Disease in Colombia - preliminary report. *N. Engl. J. Med.* 383:e44. doi: 10.1056/NEJMoa1604037

Passi, D., Sharma, S., Dutta, S. R., and Ahmed, M. (2017). Zika Virus diseases – the new face of an ancient enemy as global public health emergency (2016): brief review and recent updates. *Int. J. Prev. Med.* 8:6.

Sanz Cortes, M., Rivera, A. M., Yepez, M., Guimaraes, C., Diaz Yunes, I., Zarutskie, A., et al. (2018). Clinical assessment and brain findings in a cohort of mothers, fetuses and infants infected with ZIKA virus. *Am. J. Obstet. Gynecol.* 218, 440.e1–440.e36.

Schuler-Faccini, L., Ribeiro, E. M., Feitosa, I. M., Horovitz, D. D. G., Calvacanti, D. P., Pessoa, A., et al. (2016). Possible association between Zika Virus infection and microcephaly - Brazil, 2015. *MMWR Morb. Mortal. Wkly. Rep.* 65, 59–62.

Secretaria de Vigilância em Saúde-Ministério da Saúde (2017). *Monitoramento Dos Casos de Dengue Febre de Chikungunya e Febre Pelo Virus Zika ate a Semana Epidemiologica 35*. Available online at: http://portalarquivos.saude.gov.br/images/pdf/2017/setembro/15/2017-028-Monitoramento-dos-casos-de-dengue--febre-de-chikungunya-e-febre-pelo-virus-Zika-ate-a-Semana-Epidemiologica-35.pdf (Accessed May 1, 2018).

Shapiro-Mendoza, C. K., Rice, M. E., Galang, R. R., Fulton, A. C., VanMaldeghem, K., Valencia-Prado, M., et al. (2017). Pregnancy outcomes after maternal Zika Virus infection during pregnancy - U.S. Territories, January 1, 2016-April 25, 2017. *MMWR Morb. Mortal. Wkly. Rep.* 66, 615–621.

Shiu, C., Starker, R., Kwal, J., Bartlett, M., Crane, A., Greissman, S., et al. (2018). Zika Virus testing and outcomes during pregnancy, Florida, USA. *Emerg. Infect. Dis. J.* 24, 1–8. doi: 10.3201/eid2401.170979

Sirohi, D., Chen, Z., Sun, L., Klose, T., Pierson, T. C., Rossmann, M. G., et al. (2016). The 3.8 Å resolution cryo-EM structure of Zika virus. *Science* 352, 467–470.

Tan, C. A., Topper, S., Ward Melver, C., Stein, J., Reeder, A., Arndt, K., et al. (2014). The first case of CDK5RAP2-related primary microcephaly in a non-consanguineous patient identified by next generation sequencing. *Brain Dev.* 36, 351–355.

Tang, H., Hammack, C., Ogden, S. C., Wen, Z., Qian, X., Li, Y., et al. (2016). Zika Virus infects human cortical neural progenitors and attenuates their growth. *Cell Stem Cell* 18, 587–590.

Ventura, C. V., Maia, M., Ventura, B. V., Van Der Linden, V., Araujo, E. B., Ramos, R. C., et al. (2016). Ophthalmological findings in infants with microcephaly and presumable intra-uterus Zika virus infection. *Arq. Bras. Oftalmol.* 79, 1–3.

Victora, C. G., Schuler-Faccini, L., Matijasevich, A., Ribeiro, E., Pessoa, A., Celso Barros, F., et al. (2016). Microcephaly in Brazil: how to interpret reported numbers? *Lancet Lond. Engl.* 387, 621–624.

Walker, C. L., Little, M.-T. E., Roby, J. A., Armistead, B., Gale, M., Rajagopal, L., et al. (2019). Zika virus and the nonmicrocephalic fetus: why we should still worry. *Am. J. Obstet. Gynecol.* 220, 45–56.

Walker, C. L., Merriam, A. A., Ohuma, E. O., Dighe, M. K., Gale, M., Rajagopal, L., et al. (2018). Femur-sparing pattern of abnormal fetal growth in pregnant women from New York City after maternal Zika virus infection. *Am. J. Obstet. Gynecol.* 219, 187.e1–187.e20.

Wang, J.-N., and Ling, F. (2016). Zika Virus infection and microcephaly: evidence for a causal link. *Int. J. Environ. Res. Public. Health* 13:1031.

Wang, Z., Wang, Z., Wu, T., Shi, L., Zhang, L., Zheng, W., et al. (2010). Conserved motif of CDK5RAP2 mediates its localization to centrosomes and the Golgi complex. *J. Biol. Chem.* 285, 22658–22665.

World Health Organization [WHO] (2016). *Director-General Summarizes the Outcome of the Emergency Committee Regarding Clusters of Microcephaly and Guillain-Barré syndrome*. Avialble at: https://www.who.int/news-room/detail/01-02-2016-who-director-general-summarizes-the-outcome-of-the-emergency-committee-regarding-clusters-of-microcephaly-and-guillain-barré-syndrome (accessed December 18, 2020).

World Health Organization (2019). *WHO | Zika Virus and Complications: 2016 Public Health Emergency of International Concern*. WHO. Available online at: http://www.who.int/emergencies/zika-virus-tmp/en/

WHO Child Growth Standards (2019). *Child Growth Standards*. Available online at: https://www.who.int/tools/child-growth-standards (accessed March 9, 2021).

Yockey, L. J., Jurado, K. A., Arora, N., Millet, A., Rakib, T., Hastings, A. K., et al. (2018). Type I interferons instigate fetal demise after Zika virus infection. *Sci. Immunol.* 3:eaao1680.

Zaqout, S., Bessa, P., Krämer, N., Stoltenburg-Didinger, G., and Kaindl, A. M. (2017). CDK5RAP2 is required to maintain the germ cell pool during embryonic development. *Stem Cell Rep*. 8, 198–204.

Conflict of Interest: The authors declare that the research was conducted in the absence of any commercial or financial relationships that could be construed as a potential conflict of interest.

frontiers in Genetics

ORIGINAL RESEARCH
published: 24 June 2021
doi: 10.3389/fgene.2021.566168

Long-Term Disturbed Expression and DNA Methylation of SCAP/SREBP Signaling in the Mouse Lung From Assisted Reproductive Technologies

*Fang Le[1], Ning Wang[1], Qijing Wang[1], Xinyun Yang[1], Lejun Li[1], Liya Wang[1], Xiaozhen Liu[1], Minhao Hu[1], Fan Jin[1,2] and Hangying Lou[1]**

[1] Center of Reproductive Medicine, Zhejiang University School of Medicine Women's Hospital, Hangzhou, China, [2] Key Laboratory of Reproductive Genetics, Ministry of Education, Hangzhou, China

Assisted reproductive technology (ART) has been linked to cholesterol metabolic and respiratory disorders later in life, but the mechanisms by which biosynthetic signaling remain unclear. Lung inflammatory diseases are tightly linked with the sterol regulatory element-binding protein (SREBP) and SREBP cleavage-activating protein (SCAP), but this has not been shown in an ART offspring. Here, mouse models from a young to old age were established including *in vitro* fertilization (IVF), intracytoplasmic injection (ICSI), and *in vivo* fertilized groups. In our results, significantly higher plasma levels of CRP, IgM, and IgG were identified in the aged ICSI mice. Additionally, pulmonary inflammation was found in four aged ART mice. At three weeks, ART mice showed significantly downregulated levels of *Scap*, *Srebp-1a*, *Srebp-1c*, and *Srebf2* mRNA in the lung. At the same time, significant differences in the DNA methylation rates of *Scap-Srebfs* and protein expression of nuclear forms of SREBPs (nSREBPs) were detected in the ART groups. Only abnormalities in the expression levels of *Srebp-1a* and *Srebp-1c* mRNA and nSREBP1 protein were found in the ART groups at 10 weeks. However, at 1.5 years old, aberrant expression levels and DNA methylation of SCAP, SREBP1, and SREBP2, and their associated target genes, were observed in the lung of the ART groups. Our results indicate that ART increases long-term alterations in SCAP/SREBP expression that may be associated with their aberrant methylation status in mouse.

Keywords: assisted reproductive technologies, SCAP/SREBP, mice, DNA methylation, chronic lung diseases

OPEN ACCESS

Edited by:
Daniel Enquobahrie, University of Washington, United States

Reviewed by:
Etienne Lefai, l'Alimentation et l'Environnement (INRAE), France
Valerie L. Sodi, Drexel University, United States

****Correspondence:***
Hangying Lou
louhangying888@zju.edu.cn

Specialty section:
This article was submitted to Epigenomics and Epigenetics, a section of the journal Frontiers in Genetics

Received: *27 May 2020*
Accepted: *24 May 2021*
Published: *24 June 2021*

Citation:
Le F, Wang N, Wang Q, Yang X, Li L, Wang L, Liu X, Hu M, Jin F and Lou H (2021) Long-Term Disturbed Expression and DNA Methylation of SCAP/SREBP Signaling in the Mouse Lung From Assisted Reproductive Technologies. Front. Genet. 12:566168. doi: 10.3389/fgene.2021.566168

INTRODUCTION

In vitro fertilization (IVF) and other assisted reproductive technologies (ARTs) offer hope to subfertile couples worldwide. To date, more than 7 million babies have been delivered by ART worldwide, and every year, there is a sign that this trend is increasing (Novakovic et al., 2019). Although most ART babies and children are healthy, some studies are still concerned on the effects ART procedures may have on the long-term health of these children (Berntsen et al., 2019). Researches into the "developmental origins of health and disease" (DOHaD) in humans have demonstrated that exposures during early development (pre-conceptional, *in utero*, and early post-natal periods) can increase the risk of disease, particularly cardiovascular, metabolic, and

respiratory disorders, later in life (Safi-Stibler and Gabory, 2020). Children born following ART may be at an increased risk of adult health problems, in part because of the laboratory techniques used, such as ovarian stimulation, embryo culture, embryo frozen, and intracytoplasmic sperm injection (ICSI) (Gluckman et al., 2008; Padhee et al., 2015; Feuer and Rinaudo, 2016). In addition to the possible risks posed by these techniques, studies have demonstrated adverse perinatal outcomes after ART (Dhalwani et al., 2016; Vrooman and Bartolomei, 2017; Maheshwari et al., 2018), which themselves can have consequences for adult heath. For instance, preterm birth, low birth weight, and being small for gestational age, which are well documented to be increased in children conceived by ART, have been associated with cardiometabolic disturbances in adulthood (Chen et al., 2012) and diminished lung function (Duijts, 2012).

Increased fasting glucose levels, blood lipid levels, adiposity, and blood pressure have been found in ART-conceived children (Valenzuela-Alcaraz et al., 2013; Lou et al., 2014; Meister et al., 2018). Moreover, in our recent and other long-term studies, ART induced the potential high risk of fatty liver in adulthood and resulted in an abnormal lipid metabolism in aged mice (Gu et al., 2018; Le et al., 2019). Emerging studies have indicated that dyslipidemia is often associated with lung disease (Yao et al., 2016). However, the long-term effects of ART on respiratory function remain poorly defined due to the relatively short time ART has been developed. Recent studies have suggested an association of IVF and ICSI with asthma in ART offsprings (Carson et al., 2013; Kuiper et al., 2015; Lewis et al., 2017). An increase in respiratory atopy was also reported in the IVF-conceived singletons compared with the controls (Halliday et al., 2014). Thus, there is a need to know whether adverse respiratory health outcomes later in life are associated with ART.

Persons with an impaired lung function have been found to have higher levels of cholesterol, suggesting a critical importance of alveolar cholesterol homeostasis in the normal lung physiology (Whitsett and Weaver, 2002). Cholesterol is essential for type II cell function; however, excessive amounts of cholesterol impair surfactant function. The transcriptional mechanisms regulating cholesterol synthesis have been shown to be dependent on the transcription factors sterol regulatory element-binding proteins (SREBPs) in the respiratory epithelium (Zhang et al., 2004; Bridges et al., 2014). Three distinct SREBP isoforms, SREBP-1a, -1c, and -2, are encoded by *Srebf1* and *Srebf2*. When intracellular cholesterol levels are abundant, SREBPs (SREBP1 and SREBP2) are held in the endoplasmic reticulum (ER) complexed to the sterol-sensing protein SREBP cleavage-activating protein (SCAP), which prevents the proteolytic generation of the transcriptionally active nuclear forms of SREBPs (nSREBPs), thereby limiting the transcription of SREBP target genes including the lipogenic and cholesterogenic genes, such as low density lipoprotein receptor (LDLR), acetoacetyl CoA synthetase (AACS), sterol 14α-demethylase (CYP51), farnesyl diphosphate synthase (FDPS), and 3-hydroxy-3-methyl-glutaryl-CoA reductase (HMGCR) (Ericsson et al., 1996; Horton et al., 2002; Harding et al., 2005). Deletion of *Scap* in the adult mouse lung inhibited SREBP activity in respiratory epithelial cells, resulting in an altered pulmonary lipid homeostasis (Besnard et al., 2009). Recent study reveals that, in addition to controlling cholesterol biosynthesis, SCAP-SREBP2 also serves as a signaling hub integrating cholesterol metabolism with inflammation in macrophages (Guo et al., 2018). Aberrant SREBP activity in respiratory epithelial cells was linked with lipotoxicity-related lung inflammation and tissue remodeling in adult mice (Plantier et al., 2012). Furthermore, an aberrant epigenetic profile may be the potential mechanism of adult disease risk in ART-conceived offspring (El et al., 2017; Safi-Stibler and Gabory, 2020). Data demonstrated that DNA methylation may be a part of the biological processes underlying lung function (Lepeule et al., 2012). Hence, we hypothesized that the periconception and early intrauterine exposures associated with ART lead to poorer physical health outcomes, perhaps through epigenetic changes in SCAP/SREBP, resulting in a higher prevalence of chronic lung illness.

Due to the improvement in respiratory function at a young age and dyslipidemia in ART-conceived individuals, there is a need to establish whether ART is associated with lung inflammation later in life. In our recent study, abnormalities in the blood lipids were identified in the ART-conceived elderly mice (Le et al., 2019). Thus, this present study was designed to ascertain whether conception by ART is associated with respiratory diseases later in life through the establishment of mouse models of conception including IVF, ICSI, and *in vivo*. Furthermore, given the mounting evidence for a role of the SCAP/SREBP pathway and epigenetic regulation in chronic lung disorders, we defined the dynamic roles of the SCAP/SREBP pathway and the methylation status of its components in the lungs of ART-conceived mice from a young to old age.

MATERIALS AND METHODS

Animals

C57BL/6J female (6–8 weeks) and male mice (10–12 weeks) were used as oocyte and sperm donors in this study. This study was approved by the Ethics Committee of Zhejiang University Animal Care. All of the animals were housed with a 12 h light/dark cycle at 25 ± 0.5°C and 50–60% humidity. The C57BL/6J female mice were randomly divided into the ICSI, IVF, and *in vivo* groups. All of the experiments were conducted between 09:00 and 17:00 to minimize the circadian influences.

Production of IVF-, ICSI-, and *in vivo*-Conceived Mice

IVF and ICSI Groups

First, C57BL/6J female mice were superovulated with an intraperitoneal injection of 7.5 IU of pregnant mare serum gonadotropin (PMSG), and 48 h later, with an intraperitoneal injection of 7.5 IU of human chorionic gonadotropin (hCG), as previously reported (Le et al., 2019). Then, the cumulus-oocyte complexes were collected after 15 h post-hCG administration in human tubal fluid (HTF) medium, which contained 10% synthetic serum substitute (SSS) (Irvin Scientific, United States) at 37°C. Lastly, cumulus-oocyte complexes were then either

transferred into a fertilization drop (for the IVF group) or into a dispersion drop (for the ICSI group). Before using for insemination or microinjection, sperm were capacitated for 1.5 h at 5% CO_2 in air at 37°C which were obtained from the epididymis of C57BL/6J males.

As previously described (Le et al., 2019), in the IVF group, oocyte-cumulus cell complexes were added into a drop in which the final sperm concentration was approximately 1–2.5 × 10^6 ml^{-1}. The embryos were cultured in fresh 10% SSS HTF at 5% CO_2 in air at 37°C after fertilization. Then, 24 h later, 2-cell-stage embryos were obtained from the IVF group. In the ICSI group, metaphase II (M II) oocytes were fertilized by ICSI. Sperm heads were singly injected into each oocyte as previously described (Le et al., 2019). Injected oocytes were cultured in 10% SSS fresh HTF in humidified 5% CO_2 at 37°C. Then, 24 h later, 2-cell-stage embryos were obtained from the ICSI group.

In vivo Group

In the *in vivo* group, C57BL/6J female mice were caged with male mice at a ratio of 1:1. The next day, we separated the female mice with vaginal plugs from the males. After 44 h, the 2-cell embryos for the *in vivo* group were obtained from the oviducts.

Embryo Transfer and Tissue Collection

ICR (Institute of Cancer Research) females (8–10 weeks old) were used as pseudopregnant recipients. After the females mated with the ICR vasectomized males (2:1), vaginal plugs were detected in the females which was considered day 0.5 of the pseudopregnancy. As previously shown (Le et al., 2019), 12–15 of 2-cell-stage embryos were transferred into the oviducts of a 0.5-d pseudo-pregnant foster mother in each group. The litters were redistributed on the day after birth to have litter sizes of six pups to ensure standardized nutrition and maternal care. In total, 36 *in vivo*-conceived, 32 IVF-conceived, and 32 ICSI-conceived mice were examined. The birth outcomes were shown in our recent published work (Le et al., 2019).

Serum Analysis

At 1.5 years old, after the mice were euthanized, venous blood of aged mice was withdrawn. Plasma levels of C-reactive protein (CRP), immunoglobulin (Ig) G, and IgM were determined using commercially available specific ELISA kits according to the instructions provided by the manufacturers (Cusabio Company, Wuhan, China).

Histological Analysis of Mouse Models

At 3 weeks (n = 10/group), 10 weeks (n = 10/group), and 1.5 years old (IVF, n = 12; ICSI, n = 12; *in vivo*, n = 16), lungs were excised and weighed. In addition, histopathological analyses were performed. Afterfixed in 4% paraform for 24 h, lungs were transfered to 70% ethanol. Individual lobes of biopsy material were placed in processing cassettes, dehydrated through a serial alcohol gradient, and embedded in paraffin wax. Lung tissue sections (5 μm) were stained with hematoxylin and eosin (HE). The slides were observed under a microscope, and five regions within the HE-stained sections were examined and scored at 200 × magnification. Morphological analysis of random fields from each section was performed by two experienced pathologists. Analysis of lung injury was scored on the basis of four parameters as previously described (Smith et al., 1997): (a) alveolar hemorrhage, (b) alveolar edema, (c) infiltration or aggregation of neutrophils in the airspace or the vessel wall, and (d) thickness of the alveolar wall.

Real-Time Quantitative PCR (RT-qPCR)

Total RNA was extracted from the lung (n = 10/group) by using the RNAiso Plus (TaKaRa, Tokyo, Japan). Then, RT-qPCR was conducted as previously described (Le et al., 2019). The quantification of gene transcripts was conducted by RT-qPCR by using the SYBR® Premix Ex Taq™ (TaKaRa, Tokyo, Japan) in an ABI 7900 thermocycler. The primers of *Scap*, *Srebf2*, and their associated genes are shown in **Supplementary Table 1**. The primers of *Srebp-1a* and *Srebp-1c* were used as shown in the previous study (Besnard et al., 2009). The housekeeping gene *Gapdh* was used as the reference gene and was stably expressed between our treatment groups. The fold-change was calculated by using the comparative Ct method.

Western Blotting Analysis

Western blot analysis of SCAP/SREBP was performed as previously described (Le et al., 2019). Briefly, aliquots (45 μg) of the nuclear and membrane fractions from three mice per group were subjected to SDS-PAGE on 8 or 10% gel. The separated samples were transferred to nitrocellulose membranes exposed to the rabbit anti-GAPDH antibody (1:1,000 dilution; Abcam, Inc.), mouse anti-SREBP1 antibody (1:1,000 dilution; Abcam, Inc.), and rabbit anti-SCAP/SREBP2 antibodies (1:1,000 dilution; Abcam, Inc.) for 2 h after electrophoresis. Then, the membranes were incubated in the DyLight™ 680-Labeled goat anti-rabbit or anti-mouse IgG (H–L) (1:5,000 dilution; KPL, Gaithersburg, United States) for 1 h at room temperature. Lastly, the images were visualized by an Odyssey® Imager (LI-COR, United States).

Methylation-Specific PCR (MSP) and Pyrosequencing Analysis

As described previously, DNA (1 μg) was processed from the lung (n = 10/group) for bisulfite sequencing analysis using the EpiTect Bisulfite kit (Qiagen, Valencia, CA, United States). Primers for *Scap*, *Srebf1*, and *Srebf2* are shown in **Supplementary Table 2**. By using the PSQ 96 ID system, the methylation-specific PCR and pyrosequencing were conducted (Le et al., 2019). The mean ± *SD* was calculated for DNA methylation rates.

Statistical Analyses

Data were analyzed using a software (SPSS, Version 16. Chicago, IL, United States). The mean ± *SD* was shown for data. Between-group comparisons were made by one-way analysis of variance (ANOVA). When required, non-parametric tests were used as indicated. The significance level was set at $P < 0.05$.

RESULTS

Organ Weight, Histological, and Plasma Analysis of the ART Mice

As shown in **Table 1**, there was no difference in the body weight and lung weight between the ART groups and the *in vivo* group at young (3 weeks), adult (10 weeks), and old (1.5 years) ages. However, as shown in **Table 2**, the aged ICSI mice showed significantly higher levels of CRP, IgG, and IgM than the *in vivo* mice ($P < 0.05$). Moreover, in our recent paper (Le et al., 2019), higher levels of cholesterol and low density lipoprotein-cholesterol (LDL-C) and lower levels of high-density lipoprotein-cholesterol (HDL-C) and apolipoprotein-A1 (Apo-A1) were found in the aged ICSI mice.

Histology analysis based on alveolar edema, hemorrhage, infiltration, or aggregation of neutrophils in the airspace or the vessel wall and thickness of the alveolar wall. Representative images of lung sections were analyzed (HE staining; **Figure 1**). At 3 and 10 weeks, we found no histological changes in the lungs of the ART-conceived mice compared to those in the *in vivo* mice. Although no statistical differences were found between the ART and *in vivo* groups, as shown in **Figures 1b–e**, lung architecture was compromised in two ICSI males and two IVF mice (one female and one male). In addition, infiltration of a large number of inflammatory cells was found in the alveolar interstitium of the ART group (**Figures 1b–e**) as compared with the *in vivo* group (**Figure 1a**).

TABLE 1 | Comparison body and organ weight of ART and *in vivo* mice at three growth stages.

	In vivo	IVF	ICSI	*P*
Numbers	36	32	32	>0.05
Sex ratio	1:1	1:1	1:1	>0.05
Body weight (g)				
3 weeks	11.33 ± 0.78	10.68 ± 1.09	11.15 ± 0.52	>0.05
10 weeks	26.16 ± 3.78	26.06 ± 2.85	26.20 ± 4.06	>0.05
1.5 years	26.03 ± 3.82	25.04 ± 3.56	25.27 ± 2.28	>0.05
Lung weight (g)				
3 weeks	0.11 ± 0.01	0.11 ± 0.02	0.12 ± 0.03	>0.05
10 weeks	0.15 ± 0.01	0.14 ± 0.01	0.14 ± 0.01	>0.05
1.5 years	0.21 ± 0.07	0.26 ± 0.15	0.23 ± 0.10	>0.05

TABLE 2 | Plasma analysis of the aged mice conceived by ART and *in vivo*.

	In vivo	IVF	ICSI	*P*
Numbers	16	12	12	>0.05
Sex ratio	1:1	1:1	1:1	>0.05
N (inflammation)	N/A	2	2	>0.05
CRP (mg/L)	3.81 ± 0.53	4.34 ± 0.68	4.59 ± 0.54	<0.01
IgG (mg/mL)	6.92 ± 0.12	7.09 ± 0.37	7.36 ± 0.53	<0.05
IgM (mg/mL)	1.05 ± 0.04	1.19 ± 0.14	1.25 ± 0.13	<0.01

N, Numbers of lung inflammation.
P < 0.05: ICSI vs. in vivo (ANOVA), P < 0.01: ICSI vs. in vivo (ANOVA).

Long-Term Changes in the mRNA Expression Levels of *Scap*/*Srebp* in the Lung

We assessed the effects of ART on the mRNA expression of *Scap*/*Srebp* in the lung from a young to an old age.

As shown in **Figures 2A–D**, at 3 weeks, significantly lower expression levels of *Scap*, *Srebp-1a*, *Srebp-1c*, and *Srebf2* mRNAs were found in the lung of IVF- and ICSI-conceived mice compared with that in the *in vivo* mice (0.5–0.8-fold, $P < 0.01$). At 10 weeks, compared with the expression levels in the *in vivo* mice, only the expression levels of *Srebp-1a* and *Srebp-1c* mRNAs were statistically lower in the IVF mice (0.7- and 0.8-fold, respectively, $P < 0.05$). However, at 1.5 years old, statistically lower expression levels of *Scap*, *Srebp-1a*, *Srebp-1c*, and *Srebf2* mRNA were found in the IVF- and ICSI-conceived aged mice compared with those in the *in vivo* group (0.5–0.7-fold, $P < 0.01$).

Long-Term Changes in the DNA Methylation Status of *Scap*/*Srebf* in the Lung

As shown in **Figures 3A–C**, at 3 weeks, the methylation rate of *Scap* was significantly higher in the IVF group (68.37 ± 3.49%) than in the *in vivo* group (61.80 ± 3.72%) and ICSI group (64.45 ± 2.99%). Moreover, compared with the *in vivo* group (17.36 ± 0.75%), the *Srebf1* showed a significantly higher methylation rate in the IVF (21.04 ± 2.46%) and ICSI (21.42 ± 2.04%) groups ($P < 0.01$). A higher methylation rate of *Srebf2* was also found in the ICSI group than in the *in vivo* group (81.76 ± 1.27% vs. 79.00 ± 0.83%, $P < 0.01$). At 10 weeks, only the methylation rate of *Srebf1* was significantly higher in the IVF group compared with that in the *in vivo* group (19.91 ± 0.64% vs. 18.91 ± 0.95%, $P < 0.05$). There were no significant differences in the methylation rate of *Scap* and *Srebf2* among the three groups. But at 1.5 years old, the methylation rate of *Scap* in the ICSI group (76.65 ± 5.68%) and IVF group (78.77 ± 3.76%) was significantly higher than that in the *in vivo* group (70.67 ± 1.40%) ($P < 0.05$). In addition, ICSI and IVF mice had a significantly higher methylation rate than the *in vivo* group at the *Srebf1* and *Srebf2* CpG sites ($P < 0.05$).

Long-Term Changes in the Protein Expression Levels of SCAP-SREBP in the Lung

At 3 weeks, IVF and ICSI mice showed a significant downregulation in the expression of nSREBP1 amounts compared with the *in vivo* group in the lung (**Figure 4A**, $P < 0.01$). There were no significant differences in other proteins, such as SCAP, the precursor of SREBP1 (pSREBP1) and SREBP2, among the groups (**Figure 4A**, $P > 0.05$). As shown in the **Figure 4B**, at 10 weeks, a significantly lower expression level of nSREBP1 amounts was found in the IVF mice compared to that in the *in vivo* mice ($P < 0.05$). There were no significant differences in the expression of other proteins among the three groups, such as SREBP2 and SCAP. At 1.5 years of age, significantly lower expressions of nSREBP1 and nSREBP2

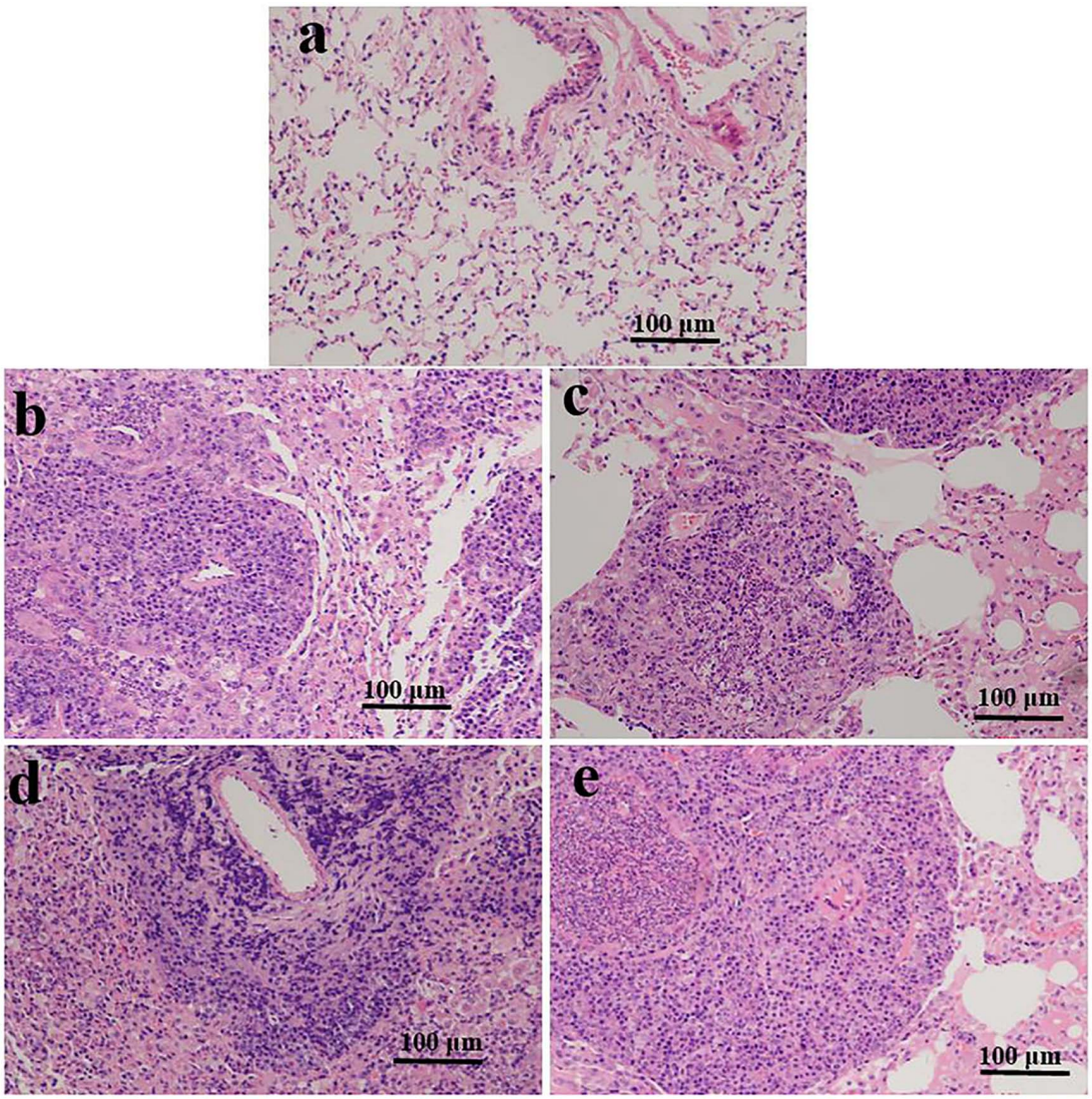

FIGURE 1 | Representative photomicrographs of HE-stained lung sections are shown for ART- and *in vivo*-conceived aged mice. The lungs of an *in vivo*-conceived female **(a)**, an IVF-conceived female **(b)**, an IVF-conceived male **(c)**, and an ICSI-conceived male **(d,e)**. Histology analysis are based on alveolar edema, hemorrhage, infiltration, or aggregation of neutrophils in the airspace or the vessel wall and thickness of the alveolar wall. Original magnification × 200. In **(b–e)**, lung architecture was compromised and a large number of inflammatory cells infiltrated in the alveolar interstitium.

amounts were found in the ICSI group when compared with the expression in other groups ($P < 0.05$). No expression differences were identified for SCAP and pSREBPs among the three groups (**Figure 4C**, $P > 0.05$).

The mRNA Expression Changes of the nSREBP Associated Genes in the Lung of Aged ART-Conceived Mice

From the above protein results, significantly lower expression levels of nSREBPs were found in the lung of ICSI-aged mice. Thus, we further assessed the mRNA expression of nSREBP target genes in the lung at 1.5 years old. As shown in **Supplementary Figure 1A**, statistically lower expression levels of *Ldlr*, *Cyp51*, and *Fdps* mRNAs were found in the ICSI-conceived aged mice compared with those in the *in vivo* and IVF groups (0.5–0.8-fold, $P < 0.01$). There were no significant differences in the expression of *Aacs* and *Hmgcr* in the ICSI group. In addition, only the expression levels of *Aacs* mRNA were found in the IVF group as compared with the other groups (0.6-fold, $P < 0.01$).

Furthermore, lower amounts of nSREBPs not pSREBPs protein was found in the ICSI mice in our work. Studies show that nSREBP is released from the membrane by two sequential proteolytic cleavages by Site-1 protease (S1P, MBTPS1) and Site-2 protease (S2P, MBTPS2) (Yang et al., 2002). Thus, the mRNA expression levels of *Mbtps1* and *Mbtps2* were analyzed in the lung at old age. As shown in **Supplementary Figure 1B**, the expression levels of *Mbtps1* and *Mbtps2* mRNAs were significantly lower

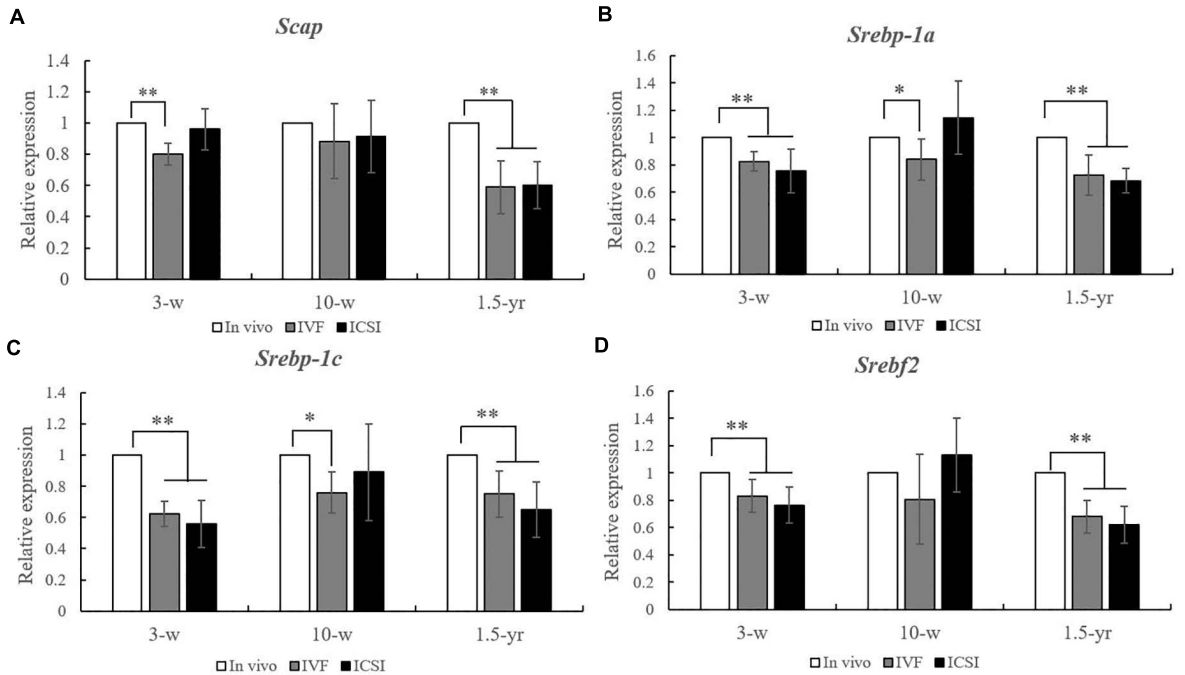

FIGURE 2 | Expression level analysis of *Scap*, *Srebp-1a*, *Srebp-1c*, and *Srebf2* mRNA in the lungs from the ICSI, IVF, and *in vivo* groups (n = 10/group). mRNA expression level analysis at 3, 10 weeks, and 1.5 years of age by real-time quantitative PCR (RT-qPCR). **(A)** mRNA expression level of *Scap*. **(B)** mRNA expression level of *Srebp-1a*. **(C)** mRNA expression level of *Srebp-1c*. **(D)** mRNA expression level of of *Srebf2*. The relative expression levels represent the amount of expression normalized to *Gapdh* expression. Data concerning the relative amount was calculated by the $2^{-\Delta\Delta Ct}$ method. Mean ± *SD* values are plotted. Between-group comparisons were made by one-way analysis of variance (ANOVA). $^{*}P < 0.05$, $^{**}P < 0.01$. 3-w, 3 weeks; 10-w, 10 weeks; 1.5-yr, 1.5 years old.

in the ICSI-conceived aged mice than in the IVF and *in vivo* conceived mice (0.3- and 0.7-fold, $P < 0.01$).

DISCUSSION

Given the increasing risk of respiratory disorders at a young age and dyslipidemia in an ART-conceived offspring (Lou et al., 2014; Kuiper et al., 2015; Lewis et al., 2017), there is a need to know whether these situations are associated with lung dysfunctions later in life. However, the long-term effects and the molecular mechanisms associated with respiratory disorders in ART-conceived individuals remain poorly defined. Thus, we sought to identify the role of the SCAP/SREBP pathway, a known signaling cascade associated with cellular lipid homeostasis, in the lung of ART-conceived mice from a young to an old age. In our study, pulmonary inflammation was found in four aged ART mice. In addition, significantly higher plasma levels of CRP, IgM, and IgG were identified in the aged ICSI mice. Our results detected that the SCAP/SREBP signaling expression was influenced by ART from a young age and was changed the most in the elderly. Moreover, we found that IVF and ICSI produced persistent changes in the SCAP/SREBP expression through the epigenetic regulatory mechanism of DNA methylation.

Impaired glucose tolerance, increased body fat and stiffness, and altered fatty acid composition have been reported in an IVF-conceived offspring (Ceelen et al., 2008; Scherrer et al., 2012; Feuer and Rinaudo, 2016; Vrooman and Bartolomei, 2017). Our recently and previously published papers also found that ART-conceived offspring, including IVF- or ICSI-conceived mice and human fetuses, had higher blood lipid levels across development, such as cholesterol, triglycerides, LDL, and apolipoproteins (Lou et al., 2014; Le et al., 2019). Previous data indicated that lipid storage diseases are often accompanied by chronic inflammation and fibrosing alveolitis (Minai et al., 2000). In our work, no histological changes in the lung were found in young or adult ART-conceived mice, but four aged ART mice showed a higher infiltration of inflammatory cells in the lung. Moreover, persons with an impaired lung function have been found to have higher levels of inflammatory markers, such as CRP and IL6. Inflammatory markers also may be correlated with inflammatory diseases in other organs, such as the liver, kidney, heart, pancreas, brain, and reproductive system. No inflammatory diseases were found in the liver, heart, and brain in our previously published work (Le et al., 2019). In the elderly, ICSI-conceived mice exhibited higher plasma levels of CRP, IgM, and IgG, which suggest that *in vitro* manipulations may be linked with an increased risk of chronic lung inflammation later in life. Additionally, a few recent studies of children indicated that those born after ART were more likely to be prescribed with anti-asthmatic medication, but the underlying duration of subfertility rather than an effect of treatment appeared to be the putative risk factor (Finnstrom et al., 2011; Kallen et al., 2013). In our mouse models, after excluding subfertility

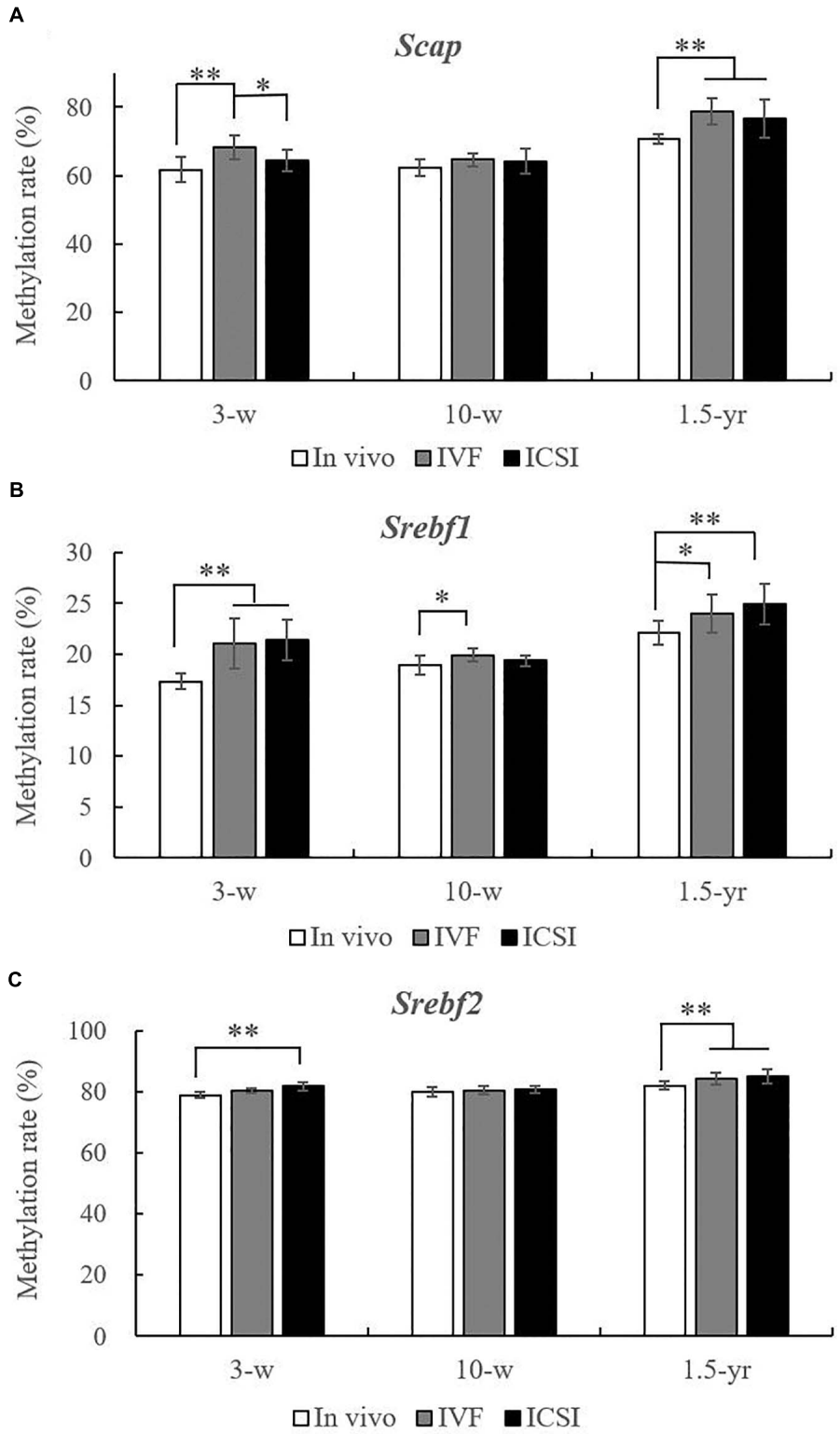

FIGURE 3 | Statistical methylation analysis of *Scap*, *Srebf1*, and *Srebf2* in the IVF, ICSI, and *in vivo* groups (n = 10/group). **(A)** DNA methylation rate of *Scap* at 3 weeks, 10 weeks, and 1.5 years of age. **(B)** DNA methylation rate of *Srebf1* at 3 weeks, 10 weeks, and 1.5 years of age. **(C)** DNA methylation rate of *Srebf2* at 3 weeks, 10 weeks, and 1.5 years of age. Mean ± SD values are plotted. Between-group comparisons were made by one-way analysis of variance (ANOVA).*$P < 0.05$, **$P < 0.01$. 3-w, 3 weeks; 10-w, 10 weeks; 1.5-yr, 1.5 years old.

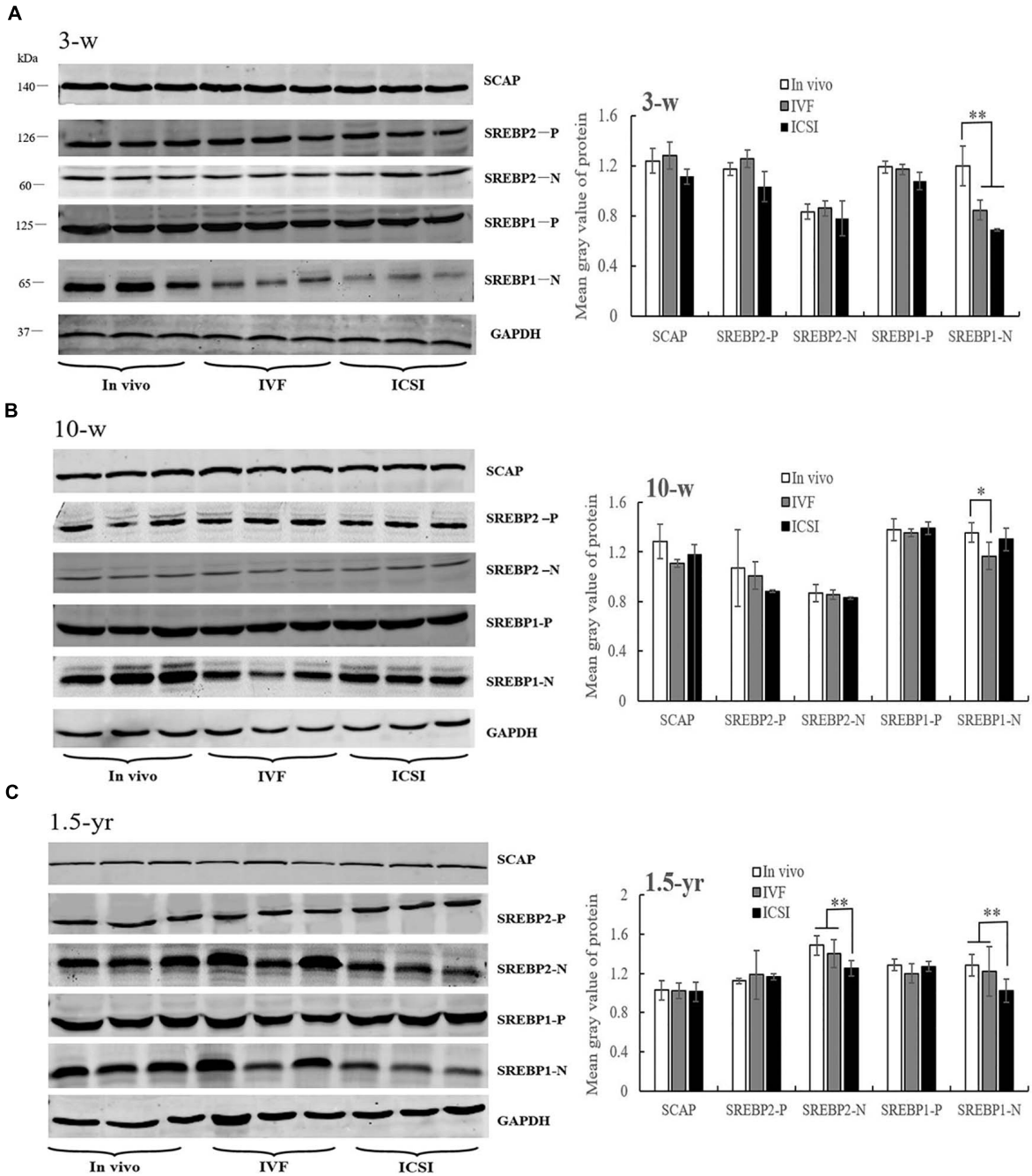

FIGURE 4 | Western blotting analysis of membrane (SCAP and SREBP1/2-P) and nuclear extract (SREBP1/2-N) fractions in the ICSI, IVF, and *in vivo* mice. Bands of SCAP, SREBPs, and GAPDH and the mean gray value at 3 weeks **(A)**, 10 weeks **(B)**, and 1.5 years of age **(C)**. N, nuclear extract of SREBP; P, precursor form of SREBP. Mean ± *SD* values are plotted. Between-group comparisons were made by one-way analysis of variance (ANOVA). $^{*}P < 0.05$, $^{**}P < 0.01$. 3-w, 3 weeks; 10-w, 10 weeks; 1.5-yr, 1.5 years old.

factors, we still observed higher inflammatory biomarker levels in the elderly ICSI mice, which may suggest that *in vitro* manipulations or ovarian stimulation could be the potential risk factors for the later occurrence of lung inflammation. Moreover, anatomopathological analysis of ICSI-conceived animals later in life showed an increase in the presence of solid tumors in the lungs compared to the analysis of the control animals (Fernandez-Gonzalez et al., 2008). Thus, as technology continues to improve, researchers will continue to uncover the effects of ART on later occurences of lung diseases.

The SCAP/SREBP pathway has previously been extensively studied in relation to cholesterol metabolism, lipogenesis, and

glucose homeostasis (Yang et al., 2002). Data from both bioinformatics and mouse models have demonstrated important roles for SCAP/SREBP signaling in lung lipid homeostasis (Besnard et al., 2009; Plantier et al., 2012). For the first time, abnormal expression levels of *Srebp-1a*, *Srebp-1c*, *Srebf2*, and *Scap* mRNA were found in the lungs of ART-conceived mice both at a young and an elderly age, which suggests that the periconceptual manipulations of ART have a long-term influence on the gene expressions of SCAP/SREBP signaling. However, ART-conceived mice in our study only showed a decreased level of nSREBP1 and nSREBP1 amounts in the lung, which may be due to the complicated post-transcriptional, translation, and post-translational modifications of SCAP/SREBP (Greenbaum et al., 2003). Previous evidence indicated that miRNAs are involved in the regulation of SCAP/SREBP post-transcriptionally (Bridges et al., 2014). Furthermore, the SCAP/SREBP is also regulated by various post-translational modifications, such as acetylation, phosphorylation, and sumoylation (Cheng et al., 2018). Recent reports demonstrated that SREBP1 activation was shown to induce lipotoxicity that consequently extended SREBP-related pathology to include inflammation and fibrosis in the lung (Zhou et al., 2015; Shichino et al., 2019). In our results, lower mRNA transcription and protein levels of nSREBP1 were found from young, to adult, and to elderly life, which further indicate that SREBP1 may be particularly vulnerable to differential expressions because of early life manipulation. SREBP-1a and SREBP-1c with a different exon 1 are known as two isoforms of SREBP1. SREBP-1c is involved in fatty acid synthesis and lipogenesis, whereas SREBP1a are mainly involved in cholesterol synthesis (Besnard et al., 2009). Recent publications indicate that SREBP-1a also plays a crucial role in the inflammatory response in macrophages (Lee et al., 2018). Activation of SCAP/SREBP enhances lipogenesis causing pulmonary lipotoxicity in both alveolar type II epithelial cells and alveolar macrophages (Besnard et al., 2009; Guo et al., 2018). In our work, not only *Srebp-1c* but also *Srebp-1a* expressions were lower in the lung of ART-conceived mice, suggesting that both alveolar macrophages and epithelial cells may be responsible for their reduction. However, additional *in vitro* studies about this topic should be conducted in the future.

The SREBPs are synthesized as precursors (pSREBP) located in the ER membrane where it forms a complex with SCAP and insulin induced gene (INSIG). Two proteases cleave pSREBP in the Golgi to release the transcriptionally active nSREBP (Yang et al., 2002). The nSREBPs then translocate into the nucleus where it binds to sterol regulatory element (SRE) binding sites in the regulatory region of target genes (Goldstein et al., 2006). Lower amounts of nSREBPs not pSREBPs protein were found in our ICSI-conceived mouse models. The reason for the result may from the lower expression of *Scap*, *Mbtps1*, and *Mbtps2*, which processed pSREBP in the Golgi leading to decreased levels of active nSREBPs. In our results, lower expression levels of the nSREBP target genes, such as *Ldlr*, *Cyp51*, *Aacs*, and *Fdps*, were found in the lung of ART-aged mice, especially in the ICSI group, which may be associated with an alveolar cholesterol imbalance in lung physiology and result in lung diseases. Furthermore, nSREBP is regulated by other post-translational mechanisms (Cheng et al., 2018). Together, these results indicate that ART induced long-term nSREBPs perturbation of their activity, which may cause a potentially higher risk of lung inflammation later in life.

Given the evidence for a strong influence of *in vitro* exposures on epigenetic regulation, epigenetic changes may be one of the factors that explain the increasing prevalence of asthma, chronic obstructive pulmonary disease, and interstitial lung disease (Lepeule et al., 2012; Safi-Stibler and Gabory, 2020). Experimental studies are beginning to point to the role of the SCAP/SREBP pathway in the development of lung diseases in animals (Bridges et al., 2014). Our group hypothesized that aberrant DNA methylation of the SCAP/SREBP pathway at different growth stages may link with the potentially higher risk of later lung inflammation in ART-conceived mice. Hence, we investigated the DNA methylation of SCAP/SREBP in the lung from a young to old age. At young, ART mice showed higher methylation rates of *Scap*, *Srebf1*, and *Srebf2*, which is in accordance with a decrease in the expression of each of these transcripts. However, in adult ART-conceived mice, only *Srebf1* showed a significantly higher methylation rate than those in the *in vivo* mice, which suggests that manipulation during embryo development may alter the methylation status of specific genes. With an advanced age, the ART mice showed higher methylation rate of all the genes, including *Scap*, *Srebf1*, and *Srebf2*, which indicates a specific epigenetic variability that is associated with aging. Consistent with our results, other studies have reported that DNA methylation is known to change throughout aging and has been associated with age-related diseases including cancer, cardiovascular diseases, and atherosclerosis (Nebbioso et al., 2018; Salameh et al., 2020).

When interpreting our work, the strengths and limitations need to be considered. Firstly, we showed the effects of ART on the respiratory health and associated molecular mechanisms from a young age to elderly life to provide insights into the long-term respiratory health of an ART offspring. In addition, we adjusted for embryo transfer and litter size in our study; these factors themselves have been detected to increase the risk of diseases in an ART-born offspring later in life. Although every effort has been made, there are still limitations in our work. One limitation is that our study cannot draw conclusions on how the methylation patterns of these genes relate to changes in lung function throughout life which still requires further investigation at the cytological level. Moreover, this is an animal model study. Long-term studies in humans who were conceived by ART are necessary to determine the effects of ART on respiratory diseases later in life. Finally, the small size is another limitation in our study. Taken together, there is still a need for more works to show the effects of ART on lung diseases later in life and the associated molecular mechanisms in ART-born individuals.

DATA AVAILABILITY STATEMENT

The raw data supporting the conclusions of this article will be made available by the authors, without undue reservation.

ETHICS STATEMENT

The animal study was reviewed and approved by the Zhejiang University Animal Care Committee.

AUTHOR CONTRIBUTIONS

FL and HL designed the study. FL, NW, and LW established the mouse models and performed the statistical analysis. XY and XL performed the gene expression analysis. QW, MH, and LL performed Western blot analysis and pyrosequencing. FJ revised the manuscript. All authors contributed to the article and approved the submitted version.

FUNDING

This work was supported by the National Key R&D Program of China (2018YFC1004900), the National Natural Science Foundation of China (81501321 and 81601336), and the Natural Science Foundation of Zhejiang Province (LGD19H040001).

ACKNOWLEDGMENTS

We thank all the members of our laboratory for their support and valuable suggestions.

SUPPLEMENTARY MATERIAL

The Supplementary Material for this article can be found online at: https://www.frontiersin.org/articles/10.3389/fgene.2021.566168/full#supplementary-material

Supplementary Figure 1 | Expression level analysis of nSREBP associated genes in the lungs from the ICSI, IVF, and *in vivo* groups (n = 10/group). mRNA expression level analysis at 1.5 years of age by real-time quantitative PCR (RT-qPCR). **(A)** mRNA expression level of nSREBP targets genes of *Ldlr*, *Cyp51*, *Aacs*, *Fdps*, and *Hmgcr*. **(B)** mRNA expression level of *Mbtps1* and *Mbtps2*. The relative expression levels represent the amount of expression normalized to Gapdh expression. Data concerning the relative amount was calculated by the $2^{-\Delta\Delta Ct}$ method. Mean ± *SD* values are plotted. Between-group comparisons were made by one-way analysis of variance (ANOVA). $^{**}P < 0.01$.

Supplementary Table 1 | The genes sequences for real-time quantitative PCR.

Supplementary Table 2 | The genes sequences for BSP and pyrosequencing.

REFERENCES

Berntsen, S., Soderstrom-Anttila, V., Wennerholm, U. B., Laivuori, H., Loft, A., Oldereid, N. B., et al. (2019). The health of children conceived by ART: 'the chicken or the egg?'. *Hum. Reprod. Update* 25, 137–158. doi: 10.1093/humupd/dmz001

Besnard, V., Wert, S. E., Stahlman, M. T., Postle, A. D., Xu, Y., Ikegami, M., et al. (2009). Deletion of Scap in alveolar type II cells influences lung lipid homeostasis and identifies a compensatory role for pulmonary lipofibroblasts. *J. Biol. Chem.* 284, 4018–4030. doi: 10.1074/jbc.M805388200

Bridges, J. P., Schehr, A., Wang, Y., Huo, L., Besnard, V., Ikegami, M., et al. (2014). Epithelial SCAP/INSIG/SREBP signaling regulates multiple biological processes during perinatal lung maturation. *PLoS One* 9:e91376. doi: 10.1371/journal.pone.0091376

Carson, C., Sacker, A., Kelly, Y., Redshaw, M., Kurinczuk, J. J., and Quigley, M. A. (2013). Asthma in children born after infertility treatment: findings from the UK millennium cohort study. *Hum. Reprod.* 28, 471–479. doi: 10.1093/humrep/des398

Ceelen, M., van Weissenbruch, M. M., Vermeiden, J. P., van Leeuwen, F. E., and Delemarre-van, D. W. H. (2008). Cardiometabolic differences in children born after in vitro fertilization: follow-up study. *J. Clin. Endocrinol. Metab.* 93, 1682–1688. doi: 10.1210/jc.2007-2432

Chen, W., Srinivasan, S. R., Yao, L., Li, S., Dasmahapatra, P., Fernandez, C., et al. (2012). Low birth weight is associated with higher blood pressure variability from childhood to young adulthood: the bogalusa heart study. *Am. J. Epidemiol.* 176, S99–S105. doi: 10.1093/aje/kws298

Cheng, X., Li, J. Y., and Guo, D. L. (2018). SCAP/SREBPs are central players in lipid metabolism and novel metabolic targets in cancer therapy. *Curr. Top. Med. Chem.* 18, 484–493. doi: 10.2174/1568026618666180523104541

Dhalwani, N. N., Boulet, S. L., Kissin, D. M., Zhang, Y., McKane, P., Bailey, M. A., et al. (2016). Assisted reproductive technology and perinatal outcomes: conventional versus discordant-sibling design. *Fertil. Steril.* 106, 710–716. doi: 10.1016/j.fertnstert.2016.04.038

Duijts, L. (2012). Fetal and infant origins of asthma. *Eur. J. Epidemiol.* 27, 5–14. doi: 10.1007/s10654-012-9657-y

El, H. N., Haertle, L., Dittrich, M., Denk, S., Lehnen, H., Hahn, T., et al. (2017). DNA methylation signatures in cord blood of ICSI children. *Hum. Reprod.* 32, 1761–1769. doi: 10.1093/humrep/dex209

Ericsson, J., Jackson, S. M., Lee, B. C., and Edwards, P. A. (1996). Sterol regulatory element binding protein binds to a cis element in the promoter of the farnesyl diphosphate synthase gene. *Proc. Natl. Acad. Sci. U. S. A.* 93, 945–950. doi: 10.1073/pnas.93.2.945

Fernandez-Gonzalez, R., Moreira, P. N., Perez-Crespo, M., Sanchez-Martin, M., Ramirez, M. A., Pericuesta, E., et al. (2008). Long-term effects of mouse intracytoplasmic sperm injection with dna-fragmented sperm on health and behavior of adult offspring. *Biol. Reprod.* 78, 761–772. doi: 10.1095/biolreprod.107.065623

Feuer, S., and Rinaudo, P. (2016). From embryos to adults: a DOHaD perspective on in vitro fertilization and other assisted reproductive technologies. *Healthcare* 4:51. doi: 10.3390/healthcare4030051

Finnstrom, O., Kallen, B., Lindam, A., Nilsson, E., Nygren, K. G., and Olausson, P. O. (2011). Maternal and child outcome after in vitro fertilization-a review of 25 years of population-based data from sweden. *Acta Obstet. Gynecol. Scand.* 90, 494–500. doi: 10.1111/j.1600-0412.2011.01088.x

Gluckman, P. D., Hanson, M. A., Cooper, C., and Thornburg, K. L. (2008). Effect of in utero and early-life conditions on adult health and disease. *N. Engl. J. Med.* 359, 61–73. doi: 10.1056/NEJMra0708473

Goldstein, J. L., DeBose-Boyd, R. A., and Brown, M. S. (2006). Protein sensors for membrane sterols. *Cell* 124, 35–46. doi: 10.1016/j.cell.2005.12.022

Greenbaum, D., Colangelo, C., Williams, K., and Gerstein, M. (2003). Comparing protein abundance and mrna expression levels on a genomic scale. *Genome Biol.* 4:117. doi: 10.1186/gb-2003-4-9-117

Gu, L., Zhang, J., Zheng, M., Dong, G., Xu, J., Zhang, W., et al. (2018). A potential high risk for fatty liver disease was found in mice generated after assisted reproductive techniques. *J. Cell Biochem.* 119, 1899–1910. doi: 10.1002/jcb.26351

Guo, C., Chi, Z., Jiang, D., Xu, T., Yu, W., Wang, Z., et al. (2018). Cholesterol homeostatic regulator SCAP-SREBP2 integrates NLRP3 inflammasome activation and cholesterol biosynthetic signaling in macrophages. *Immunity* 49, 842–856. doi: 10.1016/j.immuni.2018.08.021

Halliday, J., Wilson, C., Hammarberg, K., Doyle, L. W., Bruinsma, F., McLachlan, R., et al. (2014). Comparing indicators of health and development of singleton young adults conceived with and without assisted reproductive technology. *Fertil. Steril.* 101, 1055–1063. doi: 10.1016/j.fertnstert.2014.01.006

Harding, H. P., Zhang, Y., Khersonsky, S., Marciniak, S., Scheuner, D., Kaufman, R. J., et al. (2005). Bioactive small molecules reveal antagonism between the integrated stress response and sterol-regulated gene expression. *Cell Metab.* 2, 361–371. doi: 10.1016/j.cmet.2005.11.005

Horton, J. D., Goldstein, J. L., and Brown, M. S. (2002). SREBPs: activators of the complete program of cholesterol and fatty acid synthesis in the liver. *J. Clin. Invest.* 109, 1125–1131. doi: 10.1172/JCI15593

Kallen, B., Finnstrom, O., Nygren, K. G., and Otterblad, O. P. (2013). Asthma in swedish children conceived by in vitro fertilisation. *Arch. Dis. Child.* 98, 92–96. doi: 10.1136/archdischild-2012-301822

Kuiper, D. B., Seggers, J., Schendelaar, P., Haadsma, M. L., Roseboom, T. J., Heineman, M. J., et al. (2015). Asthma and asthma medication use among 4-year-old offspring of subfertile couples-association with IVF?. *Reprod. Biomed. Online* 31, 711–714. doi: 10.1016/j.rbmo.2015.08.002

Le, F., Lou, H. Y., Wang, Q. J., Wang, N., Wang, L. Y., Li, L. J., et al. (2019). Increased hepatic INSIG-SCAP-SREBP expression is associated with cholesterol metabolism disorder in assisted reproductive technology-conceived aged mice. *Reprod. Toxicol.* 84, 9–17. doi: 10.1016/j.reprotox.2018.12.003

Lee, J. H., Phelan, P., Shin, M., Oh, B. C., Han, X. L., Im, S. S., et al. (2018). SREBP-1a–stimulated lipid synthesis is required for macrophage phagocytosis downstream of TLR4-directed mTORC1. *Proc. Natl. Acad. Sci. U. S. A.* 115, E12228–E12234. doi: 10.1073/pnas.1813458115

Lepeule, J., Baccarelli, A., Motta, V., Cantone, L., Litonjua, A. A., Sparrow, D., et al. (2012). Gene promoter methylation is associated with lung function in the elderly: the normative aging study. *Epigenetics* 7, 261–269. doi: 10.4161/epi.7.3.19216

Lewis, S., Kennedy, J., Burgner, D., McLachlan, R., Ranganathan, S., Hammarberg, K., et al. (2017). Clinical review of 24-35 year olds conceived with and without in vitro fertilization: study protocol. *Reprod. Health* 14:117. doi: 10.1186/s12978-017-0377-3

Lou, H., Le, F., Zheng, Y., Li, L., Wang, L., Wang, N., et al. (2014). Assisted reproductive technologies impair the expression and methylation of insulin-induced gene 1 and sterol regulatory element-binding factor 1 in the fetus and placenta. *Fertil. Steril.* 101, 974–980. doi: 10.1016/j.fertnstert.2013.12.034

Maheshwari, A., Pandey, S., Amalraj, R. E., Shetty, A., Hamilton, M., and Bhattacharya, S. (2018). Is frozen embryo transfer better for mothers and babies? Can cumulative meta-analysis provide a definitive answer?. *Hum. Reprod. Update* 24, 35–58. doi: 10.1093/humupd/dmx031

Meister, T. A., Rimoldi, S. F., Soria, R., von Arx, R., Messerli, F. H., Sartori, C., et al. (2018). Association of assisted reproductive technologies with arterial hypertension during adolescence. *J. Am. Coll. Cardiol.* 72, 1267–1274. doi: 10.1016/j.jacc.2018.06.060

Minai, O. A., Sullivan, E. J., and Stoller, J. K. (2000). Pulmonary involvement in niemann-pick disease: case report and literature review. *Respir. Med.* 94, 1241–1251. doi: 10.1053/rmed.2000.0942

Nebbioso, A., Tambaro, F. P., Dell'Aversana, C., and Altucci, L. (2018). Cancer epigenetics: moving forward. *PLoS Genet.* 14:e1007362. doi: 10.1371/journal.pgen.1007362

Novakovic, B., Lewis, S., Halliday, J., Kennedy, J., Burgner, D. P., Czajko, A., et al. (2019). Assisted reproductive technologies are associated with limited epigenetic variation at birth that largely resolves by adulthood. *Nat. Commun.* 10:3922. doi: 10.1038/s41467-019-11929-9

Padhee, M., Zhang, S., Lie, S., Wang, K. C., Botting, K. J., McMillen, I. C., et al. (2015). The periconceptional environment and cardiovascular disease: does in vitro embryo culture and transfer influence cardiovascular development and health?. *Nutrients* 7, 1378–1425. doi: 10.3390/nu7031378

Plantier, L., Besnard, V., Xu, Y., Ikegami, M., Wert, S. E., Hunt, A. N., et al. (2012). Activation of sterol-response element-binding proteins (SREBP) in alveolar type II cells enhances lipogenesis causing pulmonary lipotoxicity. *J. Biol. Chem.* 287, 10099–10114. doi: 10.1074/jbc.M111.303669

Safi-Stibler, S., and Gabory, A. (2020). Epigenetics and the developmental origins of health and disease: parental environment signalling to the epigenome, critical time windows and sculpting the adult phenotype. *Semin. Cell Dev. Biol.* 97, 172–180. doi: 10.1016/j.semcdb.2019.09.008

Salameh, Y., Bejaoui, Y., and El, H. N. (2020). DNA methylation biomarkers in aging and age-related diseases. *Front. Genet.* 11:171. doi: 10.3389/fgene.2020.00171

Scherrer, U., Rimoldi, S. F., Rexhaj, E., Stuber, T., Duplain, H., Garcin, S., et al. (2012). Systemic and pulmonary vascular dysfunction in children conceived by assisted reproductive technologies. *Circulation* 125, 1890–1896. doi: 10.1161/CIRCULATIONAHA.111.071183

Shichino, S., Ueha, S., Hashimoto, S., Otsuji, M., Abe, J., Tsukui, T., et al. (2019). Transcriptome network analysis identifies protective role of the LXR/SREBP-1c axis in murine pulmonary fibrosis. *JCI Insight* 4:e122163. doi: 10.1172/jci.insight.122163

Smith, K. M., Mrozek, J. D., Simonton, S. C., Bing, D. R., Meyers, P. A., Connett, J. E., et al. (1997). Prolonged partial liquid ventilation using conventional and high-frequency ventilatory techniques: gas exchange and lung pathology in an animal model of respiratory distress syndrome. *Crit. Care Med.* 25, 1888–1897. doi: 10.1097/00003246-199711000-00030

Valenzuela-Alcaraz, B., Crispi, F., Bijnens, B., Cruz-Lemini, M., Creus, M., Sitges, M., et al. (2013). Assisted reproductive technologies are associated with cardiovascular remodeling in utero that persists postnatally. *Circulation* 128, 1442–1450. doi: 10.1161/CIRCULATIONAHA.113.002428

Vrooman, L. A., and Bartolomei, M. S. (2017). Can assisted reproductive technologies cause adult-onset disease? Evidence from human and mouse. *Reprod. Toxicol.* 68, 72–84. doi: 10.1016/j.reprotox.2016.07.015

Whitsett, J. A., and Weaver, T. E. (2002). Hydrophobic surfactant proteins in lung function and disease. *N. Engl. J. Med.* 347, 2141–2148. doi: 10.1056/NEJMra022387

Yang, T., Espenshade, P. J., Wright, M. E., Yabe, D., Gong, Y., Aebersold, R., et al. (2002). Crucial step in cholesterol homeostasis: sterols promote binding of SCAP to INSIG-1, a membrane protein that facilitates retention of SREBPs in ER. *Cell* 110, 489–500. doi: 10.1016/s0092-8674(02)00872-3

Yao, X., Gordon, E. M., Figueroa, D. M., Barochia, A. V., and Levine, S. J. (2016). Emerging roles of apolipoprotein E and apolipoprotein A-I in the pathogenesis and treatment of lung disease. *Am. J. Respir. Cell Mol. Biol.* 55, 159–169. doi: 10.1165/rcmb.2016-0060TR

Zhang, F., Pan, T., Nielsen, L. D., and Mason, R. J. (2004). Lipogenesis in fetal rat lung: importance of C/EBPalpha, SREBP-1c, and stearoyl-CoA desaturase. *Am. J. Respir. Cell Mol. Biol.* 30, 174–183. doi: 10.1165/rcmb.2003-0235OC

Zhou, Z., Wang, F., Ren, X., Wang, Y., and Blanchard, C. (2015). Resistant starch manipulated hyperglycemia/hyperlipidemia and related genes expression in diabetic rats. *Int. J. Biol. Macromol.* 75, 316–321. doi: 10.1016/j.ijbiomac.2015.01.052

Conflict of Interest: The authors declare that the research was conducted in the absence of any commercial or financial relationships that could be construed as a potential conflict of interest.

Advantages of publishing in Frontiers

OPEN ACCESS
Articles are free to read for greatest visibility and readership

FAST PUBLICATION
Around 90 days from submission to decision

HIGH QUALITY PEER-REVIEW
Rigorous, collaborative, and constructive peer-review

TRANSPARENT PEER-REVIEW
Editors and reviewers acknowledged by name on published articles

Frontiers
Avenue du Tribunal-Fédéral 34
1005 Lausanne | Switzerland

Visit us: www.frontiersin.org
Contact us: frontiersin.org/about/contact

REPRODUCIBILITY OF RESEARCH
Support open data and methods to enhance research reproducibility

DIGITAL PUBLISHING
Articles designed for optimal readership across devices

FOLLOW US
@frontiersin

IMPACT METRICS
Advanced article metrics track visibility across digital media

EXTENSIVE PROMOTION
Marketing and promotion of impactful research

LOOP RESEARCH NETWORK
Our network increases your article's readership